PIG MUCUS AS AN INHIBITORY AGENT OF HIV-1

Santhoshan Thiagaraj Pillay

Thesis presented for the degree of

DOCTOR OF PHILOSOPHY

In the Department of

General Surgery

UNIVERSITY OF CAPE TOWN

Supervised by

Professor Anwarul Haq Suleman Mall

TABLE OF CONTENTS

DECLARATION ..... **IX**

ACKNOWLEDGEMENTS ..... **X**

LIST OF ABBREVIATIONS ..... **XII**

ABSTRACT ..... **XVII**

CHAPTER 1: LITERATURE REVIEW **1**

1.1 The Human Immunodeficiency Virus Epidemic 1

1.2 Characterization of HIV-1 1

1.3 Sexual Transmission of HIV 2

1.4 Anti-HIV Vaginal Microbicides 4

1.5 Mucus and Mucins 5

1.5.1 Secreted gel forming mucins 7

1.5.1.1 MUC2 8

1.5.1.2 MUC5AC 8

1.5.1.3 MUC5B 8

1.5.1.4 MUC6 9

1.5.1.5 MUC19 9

1.5.2 Soluble mucins 9

1.5.2.1 MUC7 9

1.5.2.2 MUC8 10

1.5.2.3 MUC9 10

1.5.3 Transmembrane mucins 10

1.5.3.1 MUC1 10

1.5.3.2 MUC3A and MUC3B 11

1.5.3.3 MUC4 11

1.5.3.4 MUC12 12

1.5.3.5 MUC13 12

1.5.3.6 MUC15 12

1.5.3.7 MUC16 12

1.5.3.8 MUC17 12

1.5.3.9 MUC18 13

1.5.3.10 MUC20 13
1.5.3.11 MUC21 13
1.5.3.12 MUC22 13
1.5.4 Difficulties when working with mucin glycoproteins 17
1.5.5 Mucin Research 18
1.5.6 Rationale for using pig and horse mucins as an alternative for human mucin research 21
1.6 Aims and Objectives 23
CHAPTER 2: MATERIALS AND METHODS 24
2.1 Ethics Approval 24
2.2 Materials 24
2.3 Sample Collection 25
2.3.1 Pig gastric mucus collection 25
2.3.2 Pig saliva collection 25
2.3.3 Pig cervical mucus collection 26
2.3.4 Horse saliva collection 26
2.4 First Ultracentrifugation of samples 27
2.4.1 Glycoprotein and Protein detection of ultracentrifugation samples 27
2.4.2 Periodic Acid Schiff (PAS) assay for glycoprotein detection 27
2.4.3 BIO-RAD Quick Start™ Bradford assay for protein detection 28
2.4.4 Second Ultracentrifugation of samples 28
2.5 Dialysis of samples 28
2.6 Freeze drying 29
2.7 Column Chromatography 29
2.7.1 Sepharose 2B Column Chromatography 29
2.7.2 Sepharose 4B Column Chromatography 29
2.7.2.1 Sepharose 4B Column Chromatography Separation of Pig Salivary Muc19 30
2.7.2.2 Sepharose 4B Column Chromatography Separation of Horse Salivary Muc19 30

2.8 Chemical Treatments....31
2.8.1 DTT Treatment....31
2.8.2 Trypsin Treatment....31
2.9 Gel electrophoresis....31
2.9.1 Gradient (4 – 20%) Sodium dodecyl sulphate polyacrylamide gel electrophoresis (SDS-PAGE)....31
2.9.2 Protein Staining of SDS-PAGE gel....32
2.9.3 PAS staining of SDS-PAGE gel....32
2.10 Slot Blot Analysis....33
2.11 Pig Mucin Derived Anti-HIV-1 Gels for in vitro Analysis....33
2.12 Pseudoviral Assay....33
2.13 Toxicity Assay....37
2.14 Nanoparticle and Pseudoviral Analysis of Mucin-Derived Gel....39
2.14.1 Non Muco-adhesive Particles....39
2.14.2 Probing of the Mucus Gel Mesh to Determine Structural Arrangement....40
2.14.3 Preparation of Fluorescent Labelled HIV-1 Pseudovirus....40
2.15 Referencing....41
CHAPTER 3: THE PURIFICATION OF PGM....42
3.1 Results....42
3.1.1 First Ultracentrifugation of Pig Gastric Mucus....42
3.1.2 Second Ultracentrifugation of Pig Gastric Mucus....43
3.1.3 Size Exclusion Sepharose 2B Column Chromatography of PGM....44
3.1.4 SDS-PAGE 4 – 20% Gradient Gel Electrophoresis....45
3.1.5 PAS Stained Gradient Gel Electrophoresis....48
3.1.6 Slot Blot Analysis of PGM....49
3.2 Discussion....51
CHAPTER 4: THE EFFECT OF PGM DERIVATIVES ON HIV-1 IN VITRO....54

4.1 Results 54
4.1.1 PGM derivatives Inhibit HIV-1 on the Pseudoviral Assay 54
4.1.2 Gastric Region-Specific PGM Inhibition of HIV-1 on Pseudoviral Assay 56
4.1.3 Toxicity Assay for Pig Gastric Mucin 57
4.2 Discussion 58
4.2.1 PGM inhibits HIV-1 in vitro 58
4.2.2 Mucins from four regions of the pig stomach inhibit HIV-1 in vitro 60
CHAPTER 5: THE EFFECT OF PIG SALIVARY MUCIN (PSM) DERIVATIVES ON HIV-1 IN VITRO 65
5.1 Results 65
5.1.1 The Purification of PSM 65
5.1.1.1 Sepharose 4B Column Chromatography of Pig Saliva 65
5.1.1.2 Ultracentrifugation of PSM V_0 66
5.1.1.3 Sepharose 4B separation of PSM V_0 Muc19 67
5.1.1.4 Ultracentrifugation of PSM V_0 Muc19 68
5.1.1.5 SDS-PAGE 4 – 20% Gradient Gel Electrophoresis 69
5.1.1.6 PAS Stained SDS-PAGE 4 – 20% Gradient Gel Electrophoresis 72
5.1.1.7 Slot Blot Analysis of PSM 73
5.1.2 PSM derivatives Inhibits HIV-1 on a Pseudoviral Assay 73
5.1.3 Toxicity Assay for PSM 75
5.2 Discussion 76
5.2.1 Purification and Treatment of PSM derivatives 76
5.2.2 PSM derivatives as an Anti-Viral Agent 82
5.2.3 Toxicity Assay of PSM Derivatives 84
CHAPTER 6: THE EFFECT OF PIG CERVICO-VAGINAL MUCINS (PCM) ON HIV-1 IN VITRO 86
6.1 Results 86
6.1.1 First Ultracentrifugation of Pig Cervico-vaginal Mucus 86
6.1.2 Second Ultracentrifugation of Pig Cervico-vaginal Mucus 87

6.1.3 Size Exclusion Sepharose 2B Column Chromatography of PCM 88
6.1.4 SDS-PAGE Gradient Gel Electrophoresis 89
6.1.5 Slot Blot Analysis of PCM 92
6.1.6 PCM Derivatives Inhibits HIV-1 on a Pseudoviral Assay 92
6.1.7 Toxicity Assay for PCM 94
6.2 Discussion 94
6.2.1 Purification and Treatment of PCM 94
6.2.2 Pseudoviral Assay of PCM Derivatives 96
6.2.3 Toxicity Assay of PCM Derivatives 98
CHAPTER 7: THE EFFECT OF HORSE SALIVARY MUCIN (HSM) ON HIV-1 IN VITRO 99
7.1 Results 99
7.1.1 Sepharose 4B Column Chromatography of Horse Saliva 99
7.1.2 Ultracentrifugation of HSM V_0 100
7.1.3 Slot Blot of HSM V_0 101
7.1.4 Ultracentrifugation of HSM V_0 Muc19 102
7.1.5 HSM Derivatives Inhibits HIV-1 on a Pseudoviral Assay 102
7.1.6 Toxicity Assay of HSM Derivatives 104
7.2 Discussion 105
7.2.1 Purification and Treatment of HSM 105
7.2.2 HSM Inhibits HIV-1 in vitro 107
7.2.3 Toxicity of HSM Derivatives 108
CHAPTER 8: THE ANALYSIS OF MUCIN DERIVED GELS ON HIV-1 IN VITRO 110
8.1 Results 110
8.1.1 Investigation of Gel Solutions on Pseudoviral Assay 110
8.1.2 Investigation of Mucin-Derived Gels on Pseudoviral Assay 112

8.1.3 Probing of the Mucus Gel Mesh to Determine Structural Arrangement and Tracking of Fluorescently Labelled HIV 114
8.2 Discussion 115
8.2.1 The Inhibition of HIV-1 by Mucin-Derived Gels 115
8.2.2 Structural Arrangement and HIV Particle Tracking of PGM in Simulated Vaginal Fluid 119
CHAPTER 9: CONCLUSION 122
APPENDIX 124
1 Buffers 124
1.1 Collection Buffer 1 124
1.2 Collection Buffer 2/Column Chromatography Elution Buffer 124
1.3 Ultracentrifugation Buffer 124
1.4 5% DMEM 124
1.5 10% DMEM 125
1.6. Gradient (4 – 20%) Sodium Dodecyl Sulfate-Polyacrylamide Gel Electrophoresis (SDS-PAGE) Gel Buffers: 125
1.6.1. 30% Bis/Acrylamide 125
1.6.2. Running gel buffer 125
1.6.3. Spacer gel Buffer 125
1.6.4. Tank Buffer 125
1.6.5. Sample Application Buffer 126
2. Ammonium Persulphate (AMPS) 126
3. Gradient (4 – 20%) SDS-PAGE Gels 126
3.1. 4% running gel 126
3.2. 20% running gel 126
3.3. 3% stacking gel 126
4. Periodic acid Schiff (PAS) gel staining 127
4.1. Schiff's reagent 127
4.2. 50% ethanol 127

4.3. 0.1% periodic acid and 3% acetic acid 127
4.4. 0.1% SDS 127
5. Periodic acid Schiff (PAS) assay for in vitro glycoprotein detection 127
5.1. Schiff's reagent 127
5.2. Periodic acid solution 127
5.3. Decolourised Schiff's reagent 128
6. BIO-RAD assay for in vitro protein detection 128
7. Saline-Sodium Citrate (SSC) 128
REFERENCES 130

DECLARATION

I, Santhoshan Thiagaraj Pillay, hereby declare that the research on which this dissertation/thesis is based on is my original work (except where acknowledgements indicate otherwise) and that neither the whole work nor any part of it has been, is being, or is submitted for another degree in this or any other university.

I empower the university to reproduce for research either the whole or any portion of the contents in any manner whatsoever.

Signature ……

Date……

ACKNOWLEDGEMENTS

I dedicate my work to the people that have had faith in me throughout my life and to those my research may benefit.

I thank my family, who have stood by me through all my adversities. Thank you to my parents for their sacrifices over the years. I hope to make you and all those before you, proud with my accomplishments. To the Joseph family (Kameshrie, Neil, Olivia and Caitlin), thank you for your love and support, and keeping my sanity through this PhD.

To the Govindasamy family (Kamila, Thavasthri and to the late Dan), thank you for letting me be a part of your lives and my sincerest gratitude for the encouragement you have given me these past years.

To the Mall Laboratory (Ms. Marilyn Tyler, Ms. Zoe Lotz, Ms. Julia Peacocke, Ms. Refiloe Mofokeng, Ms. Rufaro Chivaura, Ms. Yolanda Mthembu, Mr. Baxolele Mhlekude, Ms. Isla McQuaid and Ms. Kathleen Kehoe), thank you for all your help. When I changed from immunology to biochemistry I needed a lot of training and patience and I was fortunate to be in a laboratory that had both in abundance. It has been a pleasure to work alongside you all, and I thank you for your friendship.

To my partner, Ms. Darshini Govindasamy, thank you for your love and support. This doctoral journey has been fraught with difficulties, uncertainties and wrong turns, but despite my misplaced negativity you saw me though the best and the worst. I hope to someday repay your kindness, your unwavering belief in me, belief I sometimes lost. Words cannot describe how much you mean to me and I look forward to our future endeavours.

To my supervisor, Professor Anwar-ul-Haq Suleman Mall, thank you for your faith in me, your expert guidance and patience. My sincerest gratitude for making me a better scientist and seeing my PhD through the turbulent environment we faced.

Thank you to the funding organizations (Poliomyelitis Research Foundation (through my Honour, Masters and Doctoral degrees), National Research Foundation - German Academic Exchange Service (DAAD), University of Cape Town postgraduate Bursary) for funding my research. It is no exaggeration to state that without these funding entities my scientific career would not have made it past an undergraduate level.

Thank you to Ms. Henrietta Lacks for your contribution to science and my work.

LIST OF ABBREVIATIONS

3-(4,5-dimethylthiazol-2-yl)2,5-diphenyl tetrazolium bromide	MTT
4-(2-hydroxyethyl)-1-piperazineethanesulfonic acid	HEPES
Acceleration caused by gravity	g
Aldehyde groups	-CHO
Ammonium persulphate	AMPS
Animal Unit	AU
Bovine submaxillary mucin	BSM
Caesium chloride	CsCl
Carbon Dioxide	CO_2
Centimetre	cm
Cluster of Differentiation 4	CD4
Coomassie brilliant blue	CBB
Daltons	Da
Degrees Celsius	^oC
Dendritic cells	DCs
Dendritic cell-specific intercellular adhesion molecule-3-grabbing non-integrin	DC-SIGN
Diethylaminoethyl	DEAE
Diffusive transport rates	$\Delta r^2(\Delta t)$
Disodium hydrogen orthophosphate	Na_2HPO_4
Disulphide	S–S
Dithiothreitol	DTT

Domain for panbronchiolitis	DPB
Dulbecco's modified Eagle's medium	DMEM
Effective diffusivities	D_{eff}
Elapsed time	*t*
Envelope protein	Env
Ethylenediaminetetra-acetic acid disodium salt	Na_2-EDTA
Faculty of Health Sciences	FHS
Foetal bovine serum	FBS
Gas Chromatography Mass Spectrometry	GC-MS
Glycoprotein 120	gp120
Glycosylated	gly
Grams per millilitre	g/ml
Green fluorescent protein	GFP
Guanidine hydrochloride	GuHCl
Half maximal Inhibitory Concentration	IC_{50}
Herpes simplex virus-1	HSV-1
Horse radish peroxidise	HRP
Horse salivary mucin	HSM
Human cervical mucus	CVM
Human Immunodeficiency Virus	HIV
Human Immunodeficiency Virus-1	HIV-1
Human Immunodeficiency Virus-2	HIV-2
Human Papilloma Virus – 16	HPV-16
Human T lymphoblastoid cell line	CEM SS cells

Hydrochloric Acid	HCl
Hydroxyl groups	-OH
Immunoglobulin A	IgA
Immunoglobulin A neuropathy	IgAN
Immunoglobulin G	IgG
International Centre for Genetic Engineering and Biotechnology	ICGEB
Iodoacetamide	IAA
KiloDaltons	kDa
KwaZulu-Natal	KZN
Litre	L
Major	M
Matrix-Assisted Laser-Desorption Mass Spectrometry	MALDI-MS
Median lethal dose	LD_{50}
Merkel cell polyoma-virus	MCV
Microlitres	µl
Millibars	mBar
Millilitres	ml
Millimetres	mm
MilliMolar	mM
Milliseconds	ms
Minutes	mins
Molar	M
N,*N*′-Methylenebisacrylamide	Bis/Acrylamide
N-Ethylmaleimide	NEM

Nanometres	nm
Non-essential Amino acids	NEAA
Non-major and non-outlier	N
Non- (or weakly) N-glycosylated	non-gly
Normal	N
Nucleotide reverse transcriptase inhibitor	NTRI
Nucleotides	nt
Outlier	O
Panbronchiolitis-related mucin-like protein 1	PBMUCL1
Partially fractioned mucins sourced from human saliva	MG1
Peripheral Blood Mononuclear Cells	PBMCs
Periodic acid Schiffs	PAS
Phenylmethanesulfonyl Fluoride	PMSF
Pig Cervicovaginal Mucin	PCM
Pig Gastric Mucin	PGM
Pig Salivary Mucin	PSM
Poly-Ethylene Glycol	PEG
Pre-exposure prophylaxis	PrEP
Pro-von Willebrand factor	pro-vWF
Relative Light Units	RLU
Revolutions Per Minute	rpm
Saline-sodium citrate	SSC
Seconds	s
Serine-Threonine-Proline	STP

Sodium azide	NaN_3
Sodium chloride	NaCl
Sodium dodecyl sulphate	SDS
Sodium dodecyl sulphate polyacrylamide gel electrophoresis	SDS-PAGE
Sodium metabisulphite	$Na_2S_2O_5$
Tenofovir	TFV
Thymus cells	T cells
Tris(Hydroxymethyl)aminomethane	Tris
Tetramethylethylenediamine	TEMED
Time-averaged mean squared displacements	MSDs
Time scale or time lag	τ
United Nations Joint Programme on Human Immunodeficiency Virus/Acquired Immune Deficiency Syndrome	UNAIDS
University of Cape Town	UCT
Variable number of tandem repeats	VNTR
Vaginal and Oral Interventions to Control the Epidemic	VOICE
Volume per volume	v/v
Volts	V
von Willebrand Factor	vWF
Weight per Volume	w/v

ABSTRACT

The Human Immunodeficiency Virus (HIV) epidemic still poses a problem with approximately 2 million new infections reported worldwide in 2014. New strategies are required to alleviate this burden. Our laboratory has previously shown that crude saliva and purified mucins from cervical plug mucin, saliva and breast milk inhibit HIV-1 infection *in vitro.* This project investigates purified mucins sourced from pig and horse mucus, as an alternative and abundant source of material for anti-HIV-1 research.

Pig gastric and cervico-vaginal mucus was collected and stirred overnight in 6M guanidine hydrochloride with 10mM Na_2HPO4, 10mM EDTA, 1mM PMSF and 5mM NEM. Gastric and cervicovaginal mucus was purified by density gradient ultracentrifugations in CsCl at 105 000g for 48 hours, twice, and mucin rich fractions were separated by size exclusion column chromatography. Mucin-rich materials eluting in the void volume (V_0) were reduced with 10mM dithithreitol (DTT) or subjected to proteolysis with trypsin. Pig saliva was collected in 0.2M NaCl:0.02% sodium azide and horse saliva (due to its viscous nature) was collected and stirred overnight in 6M guanidine hydrochloride with 10mM Na_2HPO4, 10mM EDTA, 1mM PMSF and 5mM NEM. Pig and horse saliva samples underwent size exclusion column chromatography, where the V_0 fractions of both were purified with one density gradient ultracentrifugation and then dialysed and freeze dried, after which aliquots were treated with either DTT or trypsin. At every stage of purification, lyophilized aliquots of all mucin sources were tested on a luciferase based replication defective HIV neutralization assay on a CD4 expressing HeLa cell line. Luciferase expression quantified as relative light units by a luminometer was used to calculate percentage neutralization. Log dose response curves were constructed to extrapolate the half maximal inhibitory concentrations (IC_{50}) on GraphPad Prism. Samples were tested on an MTT cell toxicity assay. Pig gastric and cervicovaginal mucins were added to a simulated vaginal fluid to make gels (at a concentration of 30mg of mucin per ml of buffer). These gels were tested on the neutralization, MTT assays and the pig gastric mucin gel then underwent particle tracking and nanoparticle diffusion assays at varying pH.

Pig gastric and cervicovaginal mucin showed good inhibition and low toxicity, with pig gastric mucin V_0 having the best IC_{50} (1.668µg/ml). Pig and horse saliva showed inhibition but low cell viability. Pig gastric and cervicovaginal mucin gels exhibited good IC_{50}'s but pig gastric

mucin had the best neutralization and lowest toxicity (PGM in Gel Solution 4 IC_{50}: 20.23μg/ml). HIV particle tracking and nanoparticle diffusion assays showed that the pig gastric mucin gel inhibited HIV-1 at low pH and existed as a soft gel. This project shows the efficacy of pig gastric mucin to possibly being a component of an anti-HIV-1 vaginal microbicide.

CHAPTER 1: LITERATURE REVIEW

1.1 The Human Immunodeficiency Virus Epidemic

In 2015, the United Nations Joint Programme on Human Immunodeficiency Virus/Acquired Immune Deficiency Syndrome (UNAIDS) released a global report detailing Human Immunodeficiency Virus (HIV) statistics for 2014 (UNAIDS, 2015). This report indicated that ~36.9 million people were living with HIV worldwide and that approximately 2 million people acquired new infections. In 2014, there were 1.2 million deaths resulting from AIDS-related diseases, globally (UNAIDS, 2015).

Sub-Saharan Africa was the most affected region that year, accounting for 25.8 million persons living with HIV. Over half of the 25.8 million were women. Sub-Saharan Africa accounted for 1.4 million new infections and ~790 000 people died of AIDS-related illnesses (UNAIDS, 2015). In 2014, South Africa had ~6.8 million people living with HIV and deaths due to AIDS were approximately 140 000. In 2012, the UNAIDS report highlighted an increase in unsafe sexual practices in South Africa (e.g. no condom use, multiple partners etc.) (UNAIDS, 2013).

In 2015, the South African National Department of Health released HIV provincial data for the year end 2013 (National Department of Health, 2015). This report indicated that the province with the highest prevalence was KwaZulu-Natal (KZN), with an increase of 37.4% in 2012 to 40.1% in 2013 (National Department of Health, 2015).

1.2 Characterization of HIV-1

There are 2 types of Human Immunodeficiency Virus namely HIV-1 and HIV-2. Both HIV-1 and HIV-2 infection lead to disease, but type 1 has higher transmission rates and faster clinical progression (Nyamweya et al., 2013). HIV-1 represents most of the AIDS burden and is thought to have originated from the simian virus, SIV_{cpz} (Nyamweya et al., 2013; Taylor et al., 2008). This virus infected several chimpanzee communities in southern Cameroon (Nyamweya et al., 2013; Taylor et al., 2008). This progenitor most likely passed from chimpanzees to human hunters through blood borne transmission. Phylogenetic analysis performed on HIV-1 and its related progenitor viruses show that there have been three transmission events in the early parts of the 20^{th} century. These three transmission events gave rise to three HIV-1 groups, viz. Major (M), Outlier (O) and non-major and non-outlier (N) (Keele et al., 2006; Korber et al., 2000). The predominant circulating HIV-1 group is group M, and can be further divided

into phylogenetically linked subtypes (or clades) A1, A2, A3, A4, B, C, D, F1, F2, G, H, J and K. Researchers suggests that the infecting subtype can influence Cluster of Differentiation 4 (CD4) thymus cell (T cell) decline (Novitsky et al., 2010; Touloumi et al., 2013). Studies in East Africa showed that there is a shorter median time of progression to AIDS in people infected with subtype D than subtype A (Baeten et al., 2007; Kaleebu et al., 2002; Kiwanuka et al., 2008). Research in Sub Saharan Africa suggest that despite subtype C having a less efficient replication process than subtype B (Ball et al., 2003), individuals with subtype C infection have a faster disease progression (Amornkul et al., 2013; Neilson et al., 1999). Subtype C is the predominant clade in countries with over 80% of HIV-1 infections worldwide such as southern Africa and India (Buonaguro et al., 2007; Hemelaar et al., 2006). The most predominant subtype in South Africa (as well as countries with the largest epidemics like Zimbabwe and Zambia) is subtype C which accounts for 48% of infections, worldwide (Lihana et al., 2012). A study carried out in 2003 showed that 95% of HIV-1 samples from the province of KwaZulu-Natal were subtype C (Gordon et al., 2003).

1.3 Sexual Transmission of HIV

The HI virus infects any cells bearing CD4 glycoprotein receptor and co-receptors CCR5 or CXCR4 (both are members of a seven-transmembrane chemokine-receptor family) (Levy, 2007). HIV can also attach to miscellaneous cell surface receptors like dendritic cell-specific intercellular adhesion molecule-3-grabbing non-integrin (DC-SIGN) and lectins on dendritic cells, heparan-sulphate moieties (these interact with positively charged side chains present on the viral Env) or natural receptors for cellular host proteins present in its viral envelope (Klasse, 2012). Susceptible cells residing in the genital and colorectal mucosae include CD4 T cells, macrophages and dendritic cells (DCs) (Haase, 2011). Typically, HIV infection involves binding of the viral envelope glycoprotein 120 (gp120) to the host cell CD4 receptor (Klasse, 2012). This results in a conformational change that exposes co-receptors CXCR4 or CCR5 that interacts with the viral gp120 (Klasse, 2012). This interaction of gp120 with a co-receptor exposes another viral envelope protein, gp41, which fuses the viral envelope with the cell membrane. After viral entry, the viral core is released into the cytoplasm and disassembled. Viral RNA is then converted into viral DNA, via viral reverse transcriptase, and transported to the cell nucleus, where it integrates into the host genome, by means of viral integrase. At this stage, the infection is irreversible and the cell can release progeny virions (Klasse, 2012).

Sexual transmission of HIV usually occurs when semen infected with HIV encounters the cervico-vaginal or colorectal mucous membranes. At this stage the virus may be transmissible

in a free form or cell associated form (e.g. infected macrophages). The latter seems to act as the viral reservoir at mucosal surfaces (Collins et al., 2000). Before breaching the epithelium, the virus must overcome the non-specific mucus defence layer, the cervico-vaginal mucus. Vaginal fluids also have natural defences (for example lactic acid, antibodies, cytokines, chemokines, secretory leukocyte protease inhibitor, defensins) to protect from HIV infection. These are produced either by the host or microbiota (Cole et al., 2008; Hirbod et al., 2007). Even the physiochemical properties of the mucus fluids (e.g. pH, content, external fluids present) covering the sites of infection can effect HIV/leukocyte infection (Cone, 2009; Olmsted et al., 2005). For example, lactic acid produced by lactobacilli, lowers the pH of the vagina in healthy women (of reproductive age) to 3.5 – 4.5 (Owen et al., 1999) and this low pH can strongly inhibit HIV (Aldunate et al., 2013). Conversely an increase in pH of vaginal fluid has been shown to increase the ability of HIV to cross this barrier (Erickson et al., 2015; Lai et al., 2009).

There are less recognized roles in rectal fluids to HIV infection, and the mucin network present may slightly decrease viral transmission but its neutral pH is thought to offer no protection against HIV (Alexander et al., 2007; Evans et al., 1988; Mestecky et al., 2005).

There have been many mechanisms proposed as to how HIV sexual transmission can occur via the cervico-vaginal route, for example the role semen plays. Semen induces naturally formed amyloid fibrils that enhances HIV from infected semen to target cells and epithelial cells (Church, 2008). Semen also causes an upregulation in pro-inflammatory chemokines and cytokines that recruit HIV target cells (Doncel et al., 2014). Infected leukocytes can cross disrupted stratified squamous epithelium or through the simple columnar epithelia of the endocervix and colorectum (Anderson et al., 2010) via intercellular gaps or transcytosis to establish an infection in the lamina propria (Hladik et al., 2009; Meng et al., 2002).

The colorectal epithelium is easily damaged during sexual intercourse, facilitating viral transmission as well as uptake of microfold cells and infected dendritic cells (Fotopoulos et al., 2002; Gurney et al., 2005) which may also be a pathway to HIV infection. The presence of multiple lymphoid nodules in the rectum aids viral replication in the rectum (Cameron et al., 2006). These criteria may in part explain the higher transmission rates of anal intercourse (0.65% to 1.7% higher during anal intercourse) when compared to the vaginal route (Baggaley et al., 2010; Boily et al., 2009; Jin et al., 2010).

Once HIV has reached the vaginal lamina propria, the initial infection can occur within an hour in either "resting" or activated CD4+ T cells, due to their sheer abundance (Haase, 2005; Keele et al., 2006; Zhang et al., 1999). After amplification, free or cell associated virus can be transported to nearby lymphoid tissue where extensive replication takes place leading to systemic distribution (Haase, 2005).

In the colorectal mucous membrane CD4+ T cells play the same role as the vaginal counterparts, with one marked difference, namely the colorectal lymphocytes are constitutively activated (Lapenta et al., 1999). HIV transmission at the colorectal mucosal membrane is further exacerbated by the presence of lymphoid cells and follicles in the lamina propria as well as direct access to blood circulation (Brenchley et al., 2008).

1.4 Anti-HIV Vaginal Microbicides

Topically applied vaginal microbicide gels are products first thought of in the early 1990s to provide women with protection against sexual transmission of HIV-1 (Stein, 1990; Voelker, 2006). The goal was to create an HIV prevention landscape (along with oral pre-exposure prophylaxis(PrEP)) that allowed women to have different antiretroviral (ARV) drug-based formulations for HIV prevention with or without their partners' agreement (Doggett et al., 2015). The 2013 statistics showed ~16 million women (aged 15 and above) living with HIV worldwide and 80% of which reside in sub-Saharan African (UNAIDS, 2014). In this region the primary contributor to the HIV epidemic is heterosexual transmission among female adolescents and young women (UNAIDS, 2014). This emphasizes the need for an effective non-toxic microbicide.

The first generation of vaginal microbicide gels were not effective at preventing HIV infection but actually induced genital inflammation and subsequent cytokine responses that enhanced HIV-1 infection in the women that used them (Fichorova et al., 2001; Mesquita et al., 2009). These early microbicides were surfactants that either non-specifically disrupted cellular and microbial membranes or altered the pore size of the mucus coating the genital mucosal surfaces (Lai et al., 2010a). Banerjee and Puniyani showed that different formulations of surfactants altered mucus gel simulants by lowering its viscosity (Banerjee et al., 2000; Banerjee, 1999). In the past 20 years, no candidate microbicides (viz. N-9, C31G [Savvy®], sodium laurel sulphate, cellulose sulphate, Carraguard® containing carrageenan and PRO-2000® showed significant protection against HIV in clinical trials (Ariën et al., 2011; Doncel et al., 2010; Karim et al., 2010).

Unlike the previous non-specific inhibitors of HIV-1, Karim *et al* (2010, 2012) developed an antiretroviral microbicide, Tenofovir (TFV) gel providing proof of concept that such formulations are possible in the fight against the AIDS pandemic and the empowerment of women whose vulnerability to infection in this situation is obvious. This gel consisted of a 1% TFV (a nucleotide reverse transcriptase inhibitor (NTRI)) and showed 39% protection against male-to-female sexual transmission of HIV (Karim et al., 2010; Karim et al., 2012). Despite this data, the ongoing Vaginal and Oral Interventions to Control the Epidemic (VOICE) clinical trial showed poor efficacy of the 1% TFV vaginal gel. This gel as well as an oral TFV tablet (Viread) were halted as they showed poor efficacy compared to placebo products (Cost et al., 2012; Microbicide Trials Network, 2011).

1.5 Mucus and Mucins

There has been recent interest in mucins with respect to detection and treatment of carcinomas (Devine et al., 1992; Mall, 2008) and also in particular in their role as diagnostic and therapeutic agents (Graham et al., 1996). Crude mucus secretions form gels on the epithelial surfaces of the auditory, gastrointestinal, respiratory, urogenital systems, lacrimal gland, apical cells of the cornea and the conjunctiva of the eyes (Hodges et al., 2013; Perez-Vilar et al., 2007). These gels hydrate and protect the epithelial surfaces from physical or chemical injury, dehydration and infection as well as help the movement of materials through internal tracts. (Allen, 1981b; Perez-Vilar et al., 1999).

Mucins are large molecular weight glycoproteins and are the major component of the mucus gels coating the epithelial tracts of the body, and are secreted by the epithelial cells lining these tracts (Perez-Vilar & Hill, 1999). Members of the mucin family can differ in their size spans from a few hundred to several thousand amino acid residues and are some of the largest known proteins (Perez-Vilar & Hill, 1999). Mucins are heavily O-glycosylated glycoproteins that fall into three broad categories: i) gel forming, that coat and protect the epithelial surfaces of the internal tracts of the body (Allen, 1981b), ii) secreted and non-gel forming (Bobek et al., 1996) and iii) membrane-bound (Pratt et al., 2000). All mucin peptide chains contain tandem repeats of serine and/or threonine rich domains, whose hydroxyl groups form *O*-glycosidic linkages with oligosaccharides. Carbohydrates make up to 90% of mucins. The physiochemical and biological properties of mucus are due to mucins. Mucins are large glycoproteins responsible for the viscoelastic properties of normal mucus gels (Allen, 1981b). Figure 1.1 shows the general structure of mucins (Bansil et al., 2013).

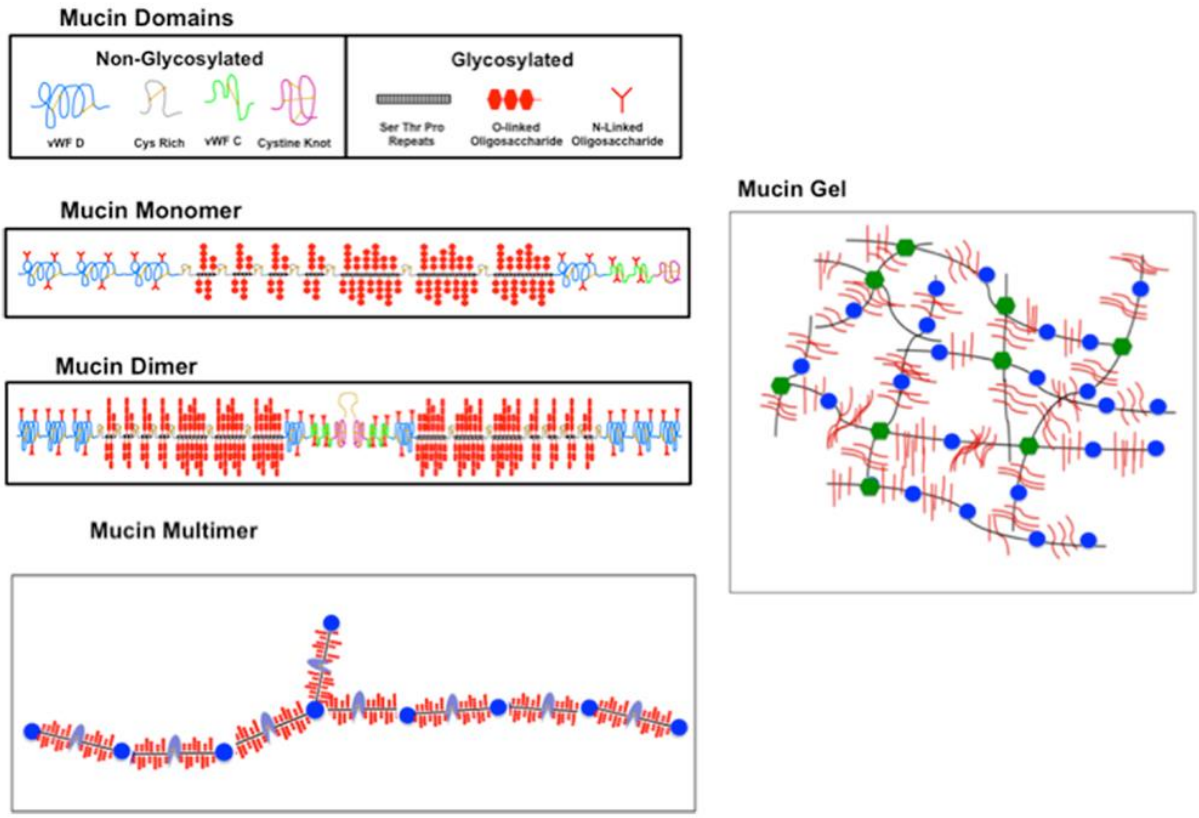

Figure 1.1 Illustration of the general structure of mucins. This diagram shows the structure of MUC2, but the general arrangement is displayed by all mucins. The top most panel highlights the glycosylated (gly) and non- (or weakly) N-glycosylated (non-gly) domains of mucin represented by symbols as shown in the picture. The second panel shows the gly and non-gly domains associated to form the mucin monomer, with von Willebrand Factor (vWF) domains at the N terminal, cysteine rich and cysteine knot domains at the C terminal, intermingled with the O-glycosylated Serine-Threonine-Proline (STP) repeats creating the gly domain. The third panel shows how mucin dimers are formed by disulphide (S–S) linking of two monomers via a bond linking the C-terminal cysteine knot domains. The bottom panel shows the branched structure of a mucin multimer with alternating gly (black with red brush) and non-gly (blue) domains. The N-terminal branch can be seen. The right panel shows how a mucin gel is formed by hydrophobic grouping of unfolded non-gly domains of the multimer. The crosslinking of non-gly domains is represented by the colour green instead of blue (Bansil et al., 2013).

Thus far, five secreted polymeric gel-forming (MUC2, MUC5AC, MUC5B, MUC6 and MUC19), three secreted non-polymeric non gel-forming (MUC7, MUC8 and MUC9), fourteen membrane bound (MUC1, MUC3A, MUC3B, MUC4, MUC9, MUC12, MUC13, MUC15, MUC16, MUC17, MUC18, MUC20, MUC21 and MUC22) and one unclassified mucin (MUC14) have been identified (Baños-Lara et al., 2015; Rose et al., 2006; Thornton et al., 2008). Every human mucin has a homologous mucin in other animals, for example, pig submaxillary mucin has similar tissue distribution and structure to MUC5B (Eckhardt et al., 1997; Perez-Vilar & Hill, 1999). Human mucins are represented as capital letters (e.g. MUC5B) whereas animal homologues start with a capital letter (e.g. Muc5b). Another similarity between human and pig mucin is the size of native and reduced MUC6 subunits being larger than MUC5AC (Nordman et al., 1997; Nordman et al., 1998). The conformation of gel forming mucins has been disputed as the conformational changes with the purification methods used to investigate mucins. Researchers who extracted mucins in 0.2M NaCl: 0.02% NaN_3 in the absence of proteolytic inhibitors proposed a "windmill" model that described gel-forming mucins as four high molecular weight subunits (2 x 10^6 Daltons (Da)) being linked by the naked, non-glycosylated regions to a low molecular weight linker protein (70 000 – 90 000Da) via disulphide bonds (Pearson et al., 1981). Researchers extracting gel-forming mucins in 6 Molar (M) guanidine hydrochloride (GuHCl) and protease inhibitors proposed a different model as their buffer was not subjected to endogenous proteolysis (Carlstedt et al., 1983c; Carlstedt et al., 1984). They suggested a linear, flexible, random coil model that linked subunits by disulphide bridges (Carlstedt & Sheehan, 1983c; Carlstedt & Sheehan, 1984).

1.5.1 Secreted gel forming mucins

The genes coding for MUC2, MUC5AC, MUC5B, and MUC6 have been mapped to chromosome 11p15.5, localized in a 400kb cluster that is rich on CpG islands (Pigny et al., 1996). These genes are located between HRAS and IGF2, and share the common ancestor gene comparable to the human von Willebrand factor (vWF) gene (Desseyn et al., 2000; Desseyn et al., 1998a). The last gel forming mucin MUC19 has its genes localized to chromosome 12q12. Secreted gel forming mucins are created by the oligomerization of the mucus backbone's tri-dimensional network, giving mucus its viscoelastic properties. All gel forming mucins share some structural characteristics, like a large central tandem repeat region flanked by a non-repeating region. These tandem repeats vary in length from 24 nucleotides (nt) for MUC5AC (Duperat et al., 1995) to 507nt for MUC6 (Toribara et al., 1993). These tandem repeat domains encompass several sub-domains that are rich in cysteine residues. The number

of sub-domains varies between mucin, which allows dimerization of mucins (Ambort et al., 2011). The amino and carboxy regions share structural similarities with the B, C, D and CK domains of the pro-von Willebrand factor (pro-vWF). The N and C- regions also allow for mucin polymers to form (Desseyn et al., 1997a; Desseyn et al., 1998b; Desseyn et al., 1997b; Duperat et al., 1995; Gum et al., 1992; Gum et al., 1994; Toribara et al., 1997).

1.5.1.1 MUC2

This mucin was first characterized by Gum *et al* in 1989, when its cDNA was identified from the cDNA library of human small intestine (Gum et al., 1994; Williams et al., 1999b). MUC2 is mostly expressed in the goblet cells of the intestine, colon and rectum (Escande et al., 2004; Gum et al., 1989; Toribara et al., 1991; Tytgat et al., 1994) and mature MUC2 has a molecular mass of 550 kiloDaltons (kDa) (Tytgat et al., 1996). MUC2 expression is associated with the pathogenesis of colorectal neoplasia and furthermore, downregulation of MUC2 is detected in colorectal cancer, gastric cancer as well as ovarian tumours (Blank et al., 1994; Dong et al., 1997; Reis et al., 2000; Utsunomiya et al., 1998). Adenomas and mucinous carcinomas also express MUC2 (Blank et al., 1994).

1.5.1.2 MUC5AC

MUC5AC is primarily secreted from tracheobronchial goblet cells of gastric epithelia (Audie et al., 1993; Vandenhaute et al., 1997), conjunctiva and lacrimal gland tissues (Yu et al., 2008). DTT reduction of glycosylated MUC5AC produced subunits with a molecular mass of 2.2 megaDaltons (MDa) (Sheehan et al., 2004). Aberrant expression of MUC5AC can be seen in colorectal adenomas (Bartman et al., 1999; Buisine et al., 1996) and pancreatic cancers (Aubert et al., 1994; Kim et al., 2002). MUC5AC expression levels are associated with the stage of cellular dysplasia.

Patients suffering with cystic fibrosis, asthma, bronchitis, Sjögren syndrome and advanced cholangiocarcinoma express higher levels of MUC5AC (Hughes et al., 2001; Mall et al., 2010; Park et al., 2009; Temann et al., 1997). Contrary to the previous examples, a reduction in MUC5AC expression is an indicator of declining survival in colorectal carcinoma patients (Kocer et al., 2006; Kocer et al., 2002).

1.5.1.3 MUC5B

MUC5B is composed of 5 000 amino acids and is the second largest gel-forming mucin (Desseyn et al., 1997a; Desseyn et al., 1997b). It’s glycosylated structure has a high molecular

mass of 14 – 40MDa (Piras et al., 2011). MUC5B is found in human saliva, salivary glands, tracheobronchial and oesophageal epithelia, endocervical and pancreatobiliary epithelial cells (Audie et al., 1993; Thornton et al., 1999; Vandenhaute et al., 1997). MUC5B isolated from human saliva has been shown to have anti-HIV-1 activity (Habte et al., 2006; Peacocke et al., 2012). MUC5AC and MUC5B mucin proteins are present in healthy and diseased human airway secretions (Sheehan et al., 2000; Sheehan et al., 1999; Thornton et al., 1996; Thornton et al., 1997; Thornton et al., 2008).

1.5.1.4 MUC6

MUC6 proteins are expressed in the gastric mucosa as well as the mucopeptic cells of the neck region in the body (Bartman et al., 1998; Byrd et al., 1997; De Bolós et al., 1995; Ho et al., 1995; Reis et al., 1999). MUC6 is also produced by gastric and duodenal mucous glands, endocervical and pancreatobiliary epithelial cells (Bartman et al., 1998). Abnormal expression of MUC6 can be seen in gastric carcinomas and significant levels are detected in well-differentiated cholangiocarcinomas (Park et al., 2009), breast cancer (De Bolós et al., 1995), and colonic sessile serrated adenoma (Owens et al., 2008).

1.5.1.5 MUC19

The human MUC19 gene has a size of 180kb, making it the largest gel-forming mucin. It's peptide sequence consists of over 7 000 amino acids and is located at chromosome 12q12 (Chen et al., 2004). The MUC19 apoprotein has a molecular mass of 693.4kDa (Culp et al., 2004). It is expressed in the middle ear, mucous cells of sublingual and submandibular glands, corneal and conjunctival epithelial cells, submucosal gland of tracheal tissue as well as the lacrimal gland tissues (Chen et al., 2004; Kerschner et al., 2009; Yu et al., 2008). MUC19 is not present in human salivary glands and there is a decreased expression in the conjunctiva of patients with Sjögren syndrome (Rousseau et al., 2008).

1.5.2 Soluble mucins

1.5.2.1 MUC7

The MUC7 gene is 10kb long and is situated on chromosome 4q13.3 (Bobek et al., 1993a). gene has a low molecular mass of 150 – 200kDa and encodes a 39kDa protein. MUC7 is secreted by the sublingual and submandibular salivary glands (Gururaja et al., 1998). It acts as an antimicrobial agent in the oral cavity, and has been shown to agglutinate HIV-1 thus inhibiting infection (Bergey et al., 1994; Bergey et al., 1993b; Habte et al., 2006;

Nagashunmugam et al., 1998; Peacocke et al., 2012). This may be a result of the MUC7 structure, namely the two cysteine residues located in the N-terminal region (Liu et al., 1999). MUC7 also has anti-candidal activity via the histatin-like domain it possesses (Bing et al., 2000). MUC7 is expressed in the oral cavity, minor salivary gland, respiratory tract, healthy conjunctiva, pancreas, submucosal glands of the bronchus and in cholangiocarcinomas (Jumblatt et al., 2003; Li et al., 2006; Sasaki et al., 1998; Sharma et al., 1998; Zhang et al., 1998). In diseased states, the MUC7 gene is expressed in bladder cancer specifically during malignant transformation of the bladder urothelium in pre-invasive carcinoma *in situ* but is not expressed in superficial non-invasive bladder tumours (Retz et al., 1998).

1.5.2.2 MUC8

The MUC8 gene is located on chromosome 12 at position q24.3. This mucin is expressed in the nasal epithelial cells, the epithelium of the middle ear as well as middle ear effusions (Kerschner, 2007; Kim et al., 2005; Takeuchi et al., 2003). MUC8 expression is upregulated in nasal polyp epithelium and is thought to play a role in pathogenesis of chronic sinusitis with polyps (Seong et al., 2002).

1.5.2.3 MUC9

MUC9 is expressed from late follicular development through to the early cleavage stage in embryonic development, middle ear epithelia, and middle ear effusions (Kerschner, 2007; Takeuchi et al., 2003). MUC9 exists as incompletely glycosylated non-sulphated molecules with a molecular mass of 90 – 120kDa (Zaretsky et al., 2013). MUC9 may also be membrane-bound in the fallopian tubes (Parham, 2014).

1.5.3 Transmembrane mucins

Membrane bound mucins are linked to cells via a unique transmembrane domain. It is the cytoplasmic tail of these mucins that facilitates their association with cytosolic adaptor proteins and cytoskeletal elements (Carraway et al., 2003). In this way transmembrane mucins play an important role in signal transduction (Carraway et al., 2003).

1.5.3.1 MUC1

MUC1 spans about 4-7kb of genomic DNA (depending on the size of the central domain) and is located on chromosome 1q21-24 (Gendler et al., 1990; Lan et al., 1990; Lancaster et al., 1990; Ligtenberg et al., 1990; Peat et al., 1992; Siddiqui et al., 1988; Swallow et al., 1987a; Wreschner et al., 1990). Mature glycosylated MUC1 has a molecular mass of 250 – 500kDa

(Brayman et al., 2004). MUC1 is expressed by nearly all glandular epithelial surfaces of the female reproductive, respiratory and gastrointestinal tracts, middle ear; salivary and mammary glands and healthy pancreatic intralobular ducts (Brayman et al., 2004; Buisine et al., 2000; Gendler, 2001; Lee et al., 2003; Masaki et al., 1998; Ringel et al., 2003; Terada et al., 1996). MUC1 expression is highly upregulated in breast, colorectal, lung, ovarian, pancreatic and prostate cancers (Ajioka et al., 1996; Burdick et al., 1997; Girling et al., 1989; Zhang et al., 1998; Zotter et al., 1987). One function of MUC1 proteins is to maintain luminal integrity of the lining epithelium by acting as an anti-adhesive protein, thereby aiding in the metastasis of tumour cells (Kim et al., 1996; Taylor-Papadimitriou et al., 2002).

1.5.3.2 MUC3A and MUC3B

The MUC3 gene is large and located on chromosome 7 in the q22 region (Fox et al., 1992; Gum et al., 1990). MUC3A and MUC3B are expressed by gastrointestinal epithelia. The alternative splicing of the central domain results in four variants that may be membrane bound or secretory (Crawley et al., 1999; Hattrup et al., 2008; Williams et al., 1999b).

1.5.3.3 MUC4

The MUC4 gene was first isolated from tracheobronchial cDNA and then from colon mucosa and pancreatic tumour cell lines (Khorrami et al., 2002; Moniaux et al., 1999; Porchet et al., 1991). The gene has been mapped to chromosome 3q29 (Gross et al., 1991). MUC4 proteins are expressed in various healthy tissues like the respiratory tract, colon, eye, lung, salivary glands, stomach, vagina, ectocervix, uterus, and the prostate (Audie et al., 1993; Gendler et al., 1995; Gipson, 2001; Gipson et al., 2004; Juusola et al., 2005; Liu et al., 1998; Reid et al., 1997). MUC4 has a molecular mass of 550 – 930kDa (Moniaux et al., 2007). Aberrant MUC4 expression can be seen in inflammatory conditions and cancers like Crohn's disease, dysplasia and adenocarcinoma of the oesophagus, gall bladder carcinomas, lung adenocarcinoma, salivary gland mucoepidermoid carcinoma, pancreatic ductal adenocarcinoma, prostate cancer, epithelial ovarian carcinomas, breast cancer, cystic fibrosis and chronic obstructive pulmonary disease (Andrianifahanana et al., 2001; Arul et al., 2000; Balagué et al., 1995; Buisine et al., 2000; Buisine et al., 2001; Buisine et al., 1999; Chauhan et al., 2006; Copin et al., 2001; Handra-Luca et al., 2005; Lamblin et al., 2001; Leikauf et al., 2002; Llinares et al., 2004; Moniaux et al., 2004; Rakha et al., 2005; Singh et al., 2007; Swartz et al., 2002; Tsutsumida et al., 2007).

1.5.3.4 MUC12

The MUC12 gene has been mapped to chromosome 7q22 (Williams et al., 1999a). MUC12 (also known as MUC11) is expressed mostly in healthy colons and stomachs, and to a lesser extent in the pancreas, prostate and uterus ([Internet], 2017; Hattrup & Gendler, 2008; Packer et al., 2004; Williams et al., 1999a).

1.5.3.5 MUC13

The MUC13 gene is located on chromosome 3q13.3 and encodes a cell surface membrane-anchored mucin that is expressed in healthy gastrointestinal tracts, respiratory tracts, tracheas, middle ears and kidneys (Hattrup & Gendler, 2008; Kerschner, 2007; Walsh et al., 2007; Williams et al., 2001). Glycosylated MUC13 has a molecular mass between 54.7 – 175kDa (Milman, 2006). In diseased states it is abnormally expressed in gastric, colorectal, oesophageal, lung and pancreatic cancers (Packer et al., 2004; Walsh et al., 2007).

1.5.3.6 MUC15

The MUC15 gene has been mapped to chromosome 11p14.3. MUC15 expression is abundant in placenta, kidney, testis, oesophagus, salivary glands, thyroid glands and trachea. It is moderately expressed in the pancreas, foetal kidney, foetal lung, lymph nodes, foetal and adult thymus (Pallesen et al., 2002; Pallesen et al., 2008). Glycosylated MUC15 has a molecular mass between 33.3 – 110kDa (Milman, 2006). Aberrant MUC15 expression can be seen in colorectal tumours and its expression may enhance the invasive potential of colorectal cells (Huang et al., 2009).

1.5.3.7 MUC16

The MUC16 gene is located on chromosome 19p13.2. MUC16 is a transmembrane-bound molecule that is also known as CA125 and was cloned from an ovarian cancer cell line OVCAR-3 (Gipson et al., 2004). Glycosylated MUC16 has a molecular mass of 1 519.2kDa (www.proteinatlas.org). It is mainly expressed in the female reproductive tract, the middle ear, the ocular surface and the respiratory tract (Bast et al., 2005; Blalock et al., 2007; Kerschner, 2007).

1.5.3.8 MUC17

The MUC17 gene is mapped to the same chromosomal locus as MUC3A/B, MUC11 and MUC12, viz. 7q22 (Gum et al., 2002; Williams et al., 1999a). The MUC17 apoprotein has a molecular mass of 36kDa (Moniaux et al., 2006). MUC17 is expressed in the gastrointestinal

tract, stomach, foetal kidney and conjunctival epithelium (Corrales et al., 2003; Gum et al., 2002; Malmberg et al., 2008). The overexpression of MUC17 can be seen in pancreatic cancer cells (Moniaux et al., 2004).

1.5.3.9 MUC18

MUC18 is a membrane bound glycoprotein, and in its mature form is 113kDa. The gene encoding MUC18 resides on chromosome 4. It is expressed in lung and breast tissue. MUC18 is expressed on primary melanomas and is found on 80% of advanced metastases ad primary tumours (Lehmann et al., 1989; Parham, 2014).

1.5.3.10 MUC20

MUC20 has been mapped to chromosome 3q29 and is expressed mostly in the kidney, but is moderately expressed in the placenta, prostate, lung, liver, colon, oesophagus, middle ear and rectum (Higuchi et al., 2004; Kerschner, 2007). Glycosylated MUC20 has a molecular mass between 76 – 78kDa (Higuchi et al., 2004). There is an up-regulation of MUC20 in immunoglobulin A neuropathy (Higuchi et al., 2004; Li et al., 2005).

1.5.3.11 MUC21

The MUC21 gene is an epiglycanin and is located on chromosome 6, neighbouring the MHC class I, and is within the vulnerability domain for panbronchiolitis (DPB) (Keicho et al., 2000). MUC21 expression is abundant in the colon, lung, normal bronchi, bronchioles, bronchial glands, thymus, large intestine and testis (Itoh et al., 2008).

1.5.3.12 MUC22

The MUC22 gene, much like MUC21, resides on chromosome 6 (6p21.3) (Azuma et al., 2017). MUC22 mucin is also known as Panbronchiolitis-related mucin-like protein 1 (PBMUCL1). MUC22 is expressed in lung tissue and is the mature protein is 173.478kDa (GeneCards; Matsuzaka et al., 2002).

The summarized distribution of various mucins can be seen below in Table 1.

Table 1. The distribution of mucins in human tissue

Mucin	**Type of Mucin**	**Expression site**	**Reference**
MUC1	Transmembrane	Stomach, breast, gallbladder, cervix, pancreas, respiratory tract, duodenum, colon, kidney, eye, B cells, T cells, dendritic cells, middle ear epithelium	(Gipson et al., 1997b; Ho et al., 1995; Kerschner, 2007; Linden et al., 2008; Pinkus et al., 1985; Swallow et al., 1987b; Wreschner et al., 1990; Wykes et al., 2002)
MUC2	Secreted and Gel forming	Small intestine, colon, respiratory tract, eye, middle ear epithelium	(Berry et al., 2004; Dohrman et al., 1994; Gum et al., 1989; Kerschner, 2007; Linden et al., 2008; Ogata et al., 1992)
MUC3A/B	Transmembrane	Small intestine, colon, gall bladder, duodenum, middle ear epithelium	(Ho et al., 1993; Kerschner, 2007; Linden et al., 2008; Pratt et al., 2000; Vandenhaute et al., 1997)
MUC4	Transmembrane	Respiratory tract, colon, stomach, cervix, eye, middle ear epithelium	(Gipson & Inatomi, 1997b; Gipson et al., 1999; Kerschner, 2007; Linden et al., 2008; Moniaux et al., 2000; Porchet et al., 1991)

MUC5AC	Secreted and Gel forming	Respiratory tract, stomach, cervix, eye, middle ear epithelium	(Gipson et al., 1997a; Inatomi et al., 1996; Kerschner, 2007; Linden et al., 2008; Porchet et al., 1995; Spurr-Michaud et al., 2007)
MUC5B	Secreted and Gel forming	Respiratory tract, salivary glands, cervix, gallbladder, seminal fluid, middle ear epithelium	(Davies et al., 2002; Escande et al., 2002; Gipson et al., 2001; Kerschner, 2007; Linden et al., 2008; Porchet et al., 1995; Russo et al., 2006; Vandenhaute et al., 1997)
MUC6	Secreted and Gel forming	Stomach, duodenum, gallbladder, pancreas, seminal fluid, cervix, middle ear epithelium	(Bartman et al., 1998; De Bolós et al., 1995; Kerschner, 2007; Linden et al., 2008; Toribara et al., 1993; Vandenhaute et al., 1997)
MUC7	Secreted and non-gel forming	Salivary glands, respiratory tract, middle ear epithelium	(Bobek et al., 1993b; Kerschner, 2007; Linden et al., 2008; Sharma et al., 1998)
MUC8	Not known if it is secreted and/or gel forming	Respiratory tract	(Rose et al., 1997)

MUC9	Secreted and Gel forming	Fallopian tube	(Levanon et al., 2010)
MUC12 (also known as MUC11)	Transmembrane	Colon, small intestine, stomach, pancreas, lung, kidney, prostate, uterus	(Linden et al., 2008; Packer et al., 2004; Williams et al., 1999a)
MUC13	Transmembrane	Colon, small intestine, trachea, kidney, appendix, stomach, middle ear epithelium	(Kerschner, 2007; Linden et al., 2008; Packer et al., 2004; Williams et al., 2001)
MUC15	Transmembrane	spleen, thymus, prostate, testis, ovary, small intestine, colon, peripheral blood leukocyte, bone marrow, lymph node, tonsil, breast, foetal liver, lungs, middle ear epithelium	(Kerschner, 2007; Linden et al., 2008; Pallesen et al., 2002)
MUC16	Transmembrane	Peritoneal mesothelium, reproductive tract, respiratory tract, eye, middle ear epithelium	(Andersch-Björkman et al., 2007; Gipson et al., 2008; Hori et al., 2004; Kerschner, 2007; Linden et al., 2008; Yin et al., 2001)

MUC17	Transmembrane	Small intestine, colon, duodenum, stomach, middle ear epithelium	(Gum et al., 2002; Kerschner, 2007; Linden et al., 2008)
MUC18	Transmembrane	Lung and breast	(Lehmann et al., 1989; Parham, 2014)
MUC19	Secreted and Gel forming	Sublingual gland, submandibular gland, respiratory tract, eye, middle ear epithelium	(Chen et al., 2004; Kerschner, 2007; Linden et al., 2008; Yu et al., 2008)
MUC20	Secreted and Gel forming	Kidney, placenta, colon, lung, prostate, liver, middle ear epithelium	(Higuchi et al., 2004; Kerschner, 2007; Linden et al., 2008)
MUC21	Transmembrane	Colon, lung, normal bronchi, bronchioles, bronchial glands, thymus, large intestine and testis	(Itoh et al., 2008)
MUC22	Transmembrane	Lung	(Matsuzaka et al., 2002)

1.5.4 Difficulties when working with mucin glycoproteins

There are many problems when working with native gel-forming mucins, the first issue being the size of mucins. For example, human MUC5B is composed of 5000 – 6000 amino acid residues of which ~3000 are in the highly glycosylated mucin domains (i.e. serine and threonine rich sequences) (Perez-Vilar & Mabolo, 2007). *O*-glycosylated mucins can reach an average molecular weight of over 1 MegaDalton (MDa) and this is further increased when disulphide-linked species are assembled. This varied range of molecular weights, renders resolution via classical techniques inadequate (Perez-Vilar & Mabolo, 2007). The copious amount of *O*-

linked oligosaccharide chains causes mucins to have aberrant results in common size exclusion techniques like size-exclusion chromatography or sodium dodecyl sulphate polyacrylamide gel electrophoresis (SDS-PAGE) (Tytgat et al., 1995). Another problem is the molecular polydispersity that is brought on by genetic polymorphism, proteolysis and/or the level of glycosylation, all of which are characteristic of gel-forming mucins (Veerman et al., 2003; Vinall et al., 2000; Wickstrom et al., 2001).

The next problem is the viscosity of gel forming mucins as they can range from a viscous fluid (e.g. saliva) to a strongly viscoelastic gel (e.g. gastric mucins). These viscous gels are not readily dispersible in non-denaturing buffers (Bansil et al., 1995; Bansil et al., 2006).

One method to overcome these issues is to extract the mucins in a solution containing chaotropic agents (e.g. guanidine hydrochloride) to reduce the stability of the native proteins by reducing the hydrophobic effect (Perez-Vilar & Mabolo, 2007; Salvi et al., 2005) or the reduction of disulphide bonds. Guanidine hydrochloride has been shown to cause proteins to adopt a randomly coiled structure, unfold proteins, break non-covalent bonds and the disassembly of gels (Georgiades et al., 2014). The drawback to using these chemicals is the disappearance of structural information and may hamper functional studies (Bansil et al., 1995; Raynal et al., 2003). It is possible to extract mucins in non-denaturing conditions but there is the risk of contamination from cellular and bacterial proteins which may alter properties of mucin (Perez-Vilar and Mabolo, 2007). An example of a non-denaturing compound that retards bacterial growth and preserves human salivary markers is sodium azide (NaN_3) (Whembolua et al., 2006).

1.5.5 Mucin Research

Mucins are an integral part of innate immunity and with the advancement of new research technologies; there are many novel directions that mucin research can take. As mentioned in section 1.5.3, the correlation between inflamed or diseased states and dysregulation of mucin expression has been well documented (Blank et al., 1994; Dong et al., 1997; Reis et al., 2000; Utsunomiya et al., 1998; Yu et al., 2008; Bartman et al., 1999; Buisine et al., 1996; Aubert et al., 1994; Kim et al., 2002; Hughes et al., 2001; Park et al., 2009; Temann et al., 1997; Kocer et al., 2006; Kocer et al., 2002; Henke et al., 2004; De Bolós et al., 1995; Owens et al., 2008; Rousseau et al., 2008; Retz et al., 1998; Seong et al., 2002; Ajioka et al., 1996; Burdick et al., 1997; Girling et al., 1989; Zhang et al., 1998; Zotter et al., 1987; Andrianifahanana et al., 2001; Arul et al., 2000; Balagué et al., 1995; Buisine et al., 2000; Buisine et al., 2001; Buisine et al.,

1999; Chauhan et al., 2006; Copin et al., 2001; Handra-Luca et al., 2005; Lamblin et al., 2001; Leikauf et al., 2002; Llinares et al., 2004; Moniaux et al., 2004; Rakha et al., 2005; Singh et al., 2007; Swartz et al., 2002; Tsutsumida et al., 2007; Williams, et al., 1999a; Hattrup & Gendler, 2008; Packer et al., 2004; Packer et al., 2004; Walsh et al., 2007; Huang et al., 2009; Higuchi et al., 2004; Li et al., 2005; Keicho et al., 2000). Mucin expression is a valuable marker to determine normal versus diseased conditions. Prognoses can be made on the development and progression of malignant diseases based on mucin expression and alterations in glycosylation (Rachagani et al., 2009). The changes in glycosylation give rise to several epitopes in oligosaccharide side chains which can be exploited as diagnostic or prognostic markers. These carcinoma markers are also used therapeutically in cancer immunotherapy (Devine & McKenzie, 1992; Hollingsworth et al., 2004). An example of this immunotherapy was published in 2006, where stage II breast cancer patients were vaccinated with an oxidized mannan-MUC1 (Apostolopoulos et al., 2006). Immunized patients showed T cell populations directed towards MUC1 variable number of tandem repeats (VNTR) and there was no recurrence of the disease over a 5 year period after immunization (Apostolopoulos et al., 2006).

A Korean research group recently reported that inflammatory airway disease in a patient with diabetes, high glucose concentrations increased MUC5B expression and pro-inflammatory factors in human airway epithelial cells (Ye et al., 2016). Previous research has shown that changes in the amount, glycoform and structure of MUC5B are associated with airway obstruction (Kirkham et al., 2008; Kirkham et al., 2002; Sheehan et al., 1999; Sheehan et al., 1995). These alterations in MUC5B assembly and processing may play a role in the abnormal properties of mucins in disease. Ye *et al* (2016) found that the addition of pro-inflammatory factor inhibitors (p38 inhibitor or epidermal growth factor receptor inhibitor) reduced inflammation and high glucose induced MUC5B expression.

In 2009, Sandberg *et al* proposed that partially fractionated mucins sourced from bovine submaxillary gland (BSM), pig gastric mucin (PGM) and human saliva (MG1) could be used as biomaterial coatings (Sandberg et al., 2009). They suggested that an ideal implanted biomaterial would perform its intended function over a long period with minimal repercussions. They further stated that such an implant would control non-specific adsorption of human host proteins to the material surface while at the same time allowing necessary integration for extensive contact with the implant. To maintain this balance, they decided to look at mucins as they are the central components of epithelial mucosa forming an anti-adhesive barrier preventing interactions with the epithelium while acting as a selective mediator between the

external environment and the host (Van Klinken et al., 1995). Their previous work showed how commercially available mucin from the bovine submaxillary gland adsorbed to polymeric materials, PMMA, silicone, Tecoflex® polyurethane and polystyrene; and reduced the risk of infection from *Staphylococcus aureus* and CNS S. *epidermis* (Shi, 2000; Shi et al., 2000a; Shi et al., 2000b). Their 2009 study showed that stable mucin coatings were formed on polymers of different wettability. They noted that there was batch-to-batch variability in commercially bought BSM, and that using mucins from animal sources was better with rigorous purification procedures. This may indicate valuable non-mucin components being lost during commercial purification. This study outlined two important areas, viz. the ability of animal sourced mucins in microbial protection and the importance of using non-commercially sourced animal mucins.

In 2012 Lieleg *et al*, published a paper in which they incorporated animal sourced mucins into a broad-spectrum antiviral agent. They suggested that because of the increased mutation rates and high level of variation between viruses, that there is a need for a broad-spectrum antiviral agent (Lieleg et al., 2012). An antiviral agent is crucial when the immune system cannot repel infection, or when vaccinations are not available or inadequate. They then decided to look at the innate immune system's anti-microbial biopolymer-based hydrogel also known as mucus (Linden et al., 2008; Thornton et al., 2004). Previous studies on native human cervical mucus (CVM) have shown that even though the average pore size of CVM matrix is 340 ± 70nm, viral particles smaller than that can be trapped at low pH, most notably herpes simplex virus-1 (HSV-1: ~180 nm) and human immunodeficiency virus-1 (HIV-1: ~120 nm) via mucoadhesion (Cu et al., 2008; Lai et al., 2009; Lai et al., 2007; Lai et al., 2010b). Human salivary mucins have also been suggested to reduce HSV-1 infectivity (Bergey et al., 1993a), and isolated gastrointestinal mucins have shown to inhibit rotaviruses and noroviruses (Tian et al., 2005; Yolken et al., 1992). Lieleg *et al* (2012) hypothesized that with the range of microbes that mucins already inhibit, it would be an effective supplement for hygiene and health products, or lubricants to enhance the natural immune system (Lieleg et al., 2012). They also addressed a key problem in human mucin research, in that, the quantity of human mucins obtained for investigation is very small, relative to the purified yield required for experimentation. Their study looked at pig gastric mucin, as these have been previously used as a component for artificial saliva in the treatment for patients salivary deficiency (xerostomia) (Blixt-Johansen et al., 1992; Duxbury et al., 1989). Lieleg *et al* (2012) used partially purified pig gastric mucins reconstituted in a buffered solution which was then layered onto human cervical cells. Thereafter they added fluorescently labelled Human Papilloma Virus-16 (HPV-

16) and Merkel cell polyoma-virus (MCV) reporter vectors. Infection was determined by green fluorescent protein (GFP) expression under flow cytometry. They also looked at the effect their mucin in buffered solution would have against Influenza A virus on a modified canine kidney cell line. Their results showed efficient infection prevention from the small diameter viruses HPV-16, MCV and Influenza A.

In the past our laboratory has worked on human mucins and HIV-1 *in vitro*, specifically crude and purified saliva, breast-milk and cervical plug mucins (Habte et al., 2010; Habte et al., 2008; Habte et al., 2007; Habte et al., 2006; Mthembu et al., 2014; Peacocke et al., 2012). In 2008, our laboratory showed that purified pregnancy plug mucins (consisting of MUC1, MUC2, MUC5AC and MUC5B), incubated on human T lymphoblastoid cell line (CEM SS cells), inhibited HIV-1 activity by ~97.5%, whereas crude cervical plug mucus did not (Habte et al., 2008). The results were based on a p24 ELISA assay. In 2012, the same assay was utilized to illustrate the effect of crude and purified salivary mucins (consisting of MUC5B and MUC7) on HIV-1 from patients with and without HIV. Our results showed that crude and purified human saliva, independent of status, inhibited HIV-1 *in vitro* (Peacocke et al., 2012). Mthembu *et al* (2014) tested crude and purified breast milk mucins from HIV positive and negative patients, on an *in vitro* HIV-1 p24 assay. She showed that crude breast milk did not inhibit HIV-1 *in vitro* but purified breast milk mucins did inhibit HIV-1 (Mthembu et al., 2014). These studies are ongoing and to be able to further develop our ideas we require large volumes of crude mucus to perform detailed studies on purified mucins and other components of mucus and their effect on the HI virus. One possible solution to this problem, as outlined by Lieleg *et al* (2012), is to work with an animal model for mucin research, primarily the pig model for antiviral research.

1.5.6 Rationale for using pig and horse mucins as an alternative for human mucin research

An animal model, in general is established to appropriately replicate the condition under investigation. This is based on the evidence and inferred similarities between the animal model and humans (Meurens et al., 2012). In terms of anatomy, genetics and physiology, pigs are very like humans (Mall et al., 1997b; Meurens et al., 2012; Nordman et al., 1998). Several surgical procedures in human medicine are typically practiced on pigs, including catheterization, heart surgery, endoscopy, valve manipulation and broncho-alveolar lavages. Furthermore, the size and composition of the pig genome are comparable to that of humans (Hart et al., 2007). There are also high protein and genome sequence homologies in pigs and humans. Researchers have shown that the domestic pig (*Sus scrofa*) is 84.1% homologous to

the human genome (Fang et al., 2012). It is thought that the pig and human genomes diverged 97 million years ago, but the pig genome still has many similarities to the human genome (e.g. genes related to cardiovascular function), making the pig model an intriguing disease model for researchers (Groenen et al., 2012).

The effect of animal and human saliva on HIV was previously investigated by Fultz (1986). Fultz (1986) mixed 0.2ml of HIV-1 subtype B virus (then termed HIV, LAV strain) with 0.2ml of human saliva and chimpanzee saliva (1:1 dilution) (Folks et al., 1986). Samples were then either passed through a filter undiluted or diluted with phosphate buffered saline (1:2) and then filtered (Fultz, 1986). The virus and saliva mixtures were incubated for either 1 minute, 1 hour, 5 hours, and 24 hours at 37 degrees Celsius (^{o}C). Virus and saliva mixtures were then added to phytohaemagglutinin-stimulated human adult white blood cells for 18 hours. Supernatant was collected every 3 – 4 days. The cells were then washed and tested for HIV reverse transcriptase activity. This assay was then repeated on HIV infected phytohaemagglutinin-stimulated human adult white blood cells. This study showed that whole saliva and filtered saliva from a chimpanzee and a human inhibited HIV-1 subtype B virus *in vitro* (Fultz, 1986). Fultz (1986) hypothesised that saliva inactivates the virus but inhibition was not due to saliva constituents like lysozymes, lactoferrin, lactoperoxidase or low pH.

In 2008, Rousseau *et al* published proteomic data on human saliva in comparison to horse, pig, cow and rat saliva (Rousseau et al., 2008). They collected saliva in a denaturing buffer and after purification, analysed the resulting products. They found that in human saliva the predominant polymeric mucin is MUC5B and while humans have the MUC19 gene (the largest gel-forming mucin), MUC19 is not expressed by the salivary glands in humans (Chen et al., 2004; Rousseau et al., 2008; Thornton et al., 1999). In contrast, they found that gel-forming mucins in horse, pig, cow and rat saliva existed as a heterogeneous mixture Muc5b and Muc19, of which, Muc19 has similar structures to other human gel-forming mucins (Chen et al., 2004).

In 1997, Nordman *et al*, purified mucins from pig gastric mucosa. They trypsin digested the reduced subunits of glycoproteins, and they found two populations of high molecular mass mucins, the fragmentation pattern of which, were like those of human cervical and tracheobronchial mucins (Carlstedt et al., 1983a; Carlstedt & Sheehan, 1984; Davies et al., 1996; Nordman et al., 1997; Thornton et al., 1990). In 1998, the same research group used antibodies to show that the pig gastric mucosa had the same tissue distribution as the human stomach (Bara et al., 1991; Nordman et al., 1998; Turner et al., 1995). They also noted the

work of Turner and colleagues who constructed a cDNA library from the pig stomach and found that mucin expression was similar to that of human gastric mucosa, where MUC5AC was secreted by the surface epithelium and MUC6 by the glands (Carlstedt et al., 1995; De Bolós et al., 1995; Ho et al., 1995). Nordman *et al* (1998) also highlighted that gland mucins were less sensitive to proteolytic degradation in comparison to those from the surface, and hence play a vital role in protecting the cell surface epithelia from stomach acid (Nordman et al., 1998).

It has been well documented how cow, sheep and sow arborisation peaks correspond to those of humans, but the duration of ovulation is greater in animals (Alliston et al., 1958; Betteridge et al., 1962; Polge, 1965; Raeside, 1963; Ullery et al., 1959). The longer period of mucus production coupled with the ease of sample collection highlights the benefits of using the pig model (Haynes, 1971).

It is our firm belief that our future work will benefit in many ways from sourcing and working with animal mucins.

1.6 Aims and Objectives

1.6.1 To find an abundant and effective animal sourced alternative for human mucin research. Animal mucus sources are from pig saliva, gastric, cervico-vaginal mucus and horse saliva.

1.6.2 To investigate the animal model mucins effect on cell free HIV infectivity on an *in vitro* pseudo-viral assay and determine which is the most effective for further studies.

1.6.3 To create a candidate animal mucin derived anti-HIV gel that keeps its anti-HIV-1 activity.

CHAPTER 2: MATERIALS AND METHODS

2.1 Ethics Approval

This project was granted ethical approval by the University of Cape Town, Faculty of Health Sciences Animal Ethics Committee, FHS AEC REF No: 013/027.

2.2 Materials

Disodium hydrogen orthophosphate (Na_2HPO_4), guanidine hydrochloride (GuHCl), phenylmethanesulfonyl fluoride (PMSF), N-ethylmaleimide (NEM), solid caesium chloride (CsCl), Sepharose 2B beads, Sepharose 4B beads, pararosaniline hydrochloride, pararosaniline chloride, potassium metabisulphite, Periodic acid, acetic acid, 3-(4,5-dimethylthiazol-2-yl)2,5-diphenyl tetrazolium bromide (MTT), sodium chloride (NaCl), dithiothreitol (DTT), iodoacetamide (IAA), glycerol, 4-(2-hydroxyethyl)piperazine-1-ethanesulfonic acid, N-(2-hydroxyethyl)piperazine-N′-(2-ethanesulfonic acid) (HEPES), sodium azide (NaN_3), ethylenediaminetetra-acetic acid disodium salt (Na_2-EDTA), *N*,*N*′-Methylenebisacrylamide (Bis/Acrylamide), trypsin-EDTA and diethylaminoethyl (DEAE) dextran were purchased from Sigma-Aldrich® Co, St Louis, MO, USA. The Bradford assay reagent was obtained from Quickstart, BioRad (Bio-Rad Laboratories Inc., Hercules, California, United States of America). Nitrocellulose membranes, dialysis tubing, sodium metabisulphite ($Na_2S_2O_5$), Tris(Hydroxymethyl)aminomethane (Tris) were supplied by Kimix (South Africa). The ECL™ Western Blotting Detection Kit was bought from Amersham Biosciences (Amersham, United Kingdom). Luciferase substrate was purchased from Promega (Anatech Analytical Technology, Bellville, South Africa). Polyclonal rabbit anti-human MUC5AC (1 in 5000 dilution) and rabbit anti-human MUC5B (1 in 2000 dilution) antibodies were provided by the Thornton Lab from the University of Manchester, United Kingdom. Monoclonal mouse anti-human MUC6 (CLH5) (1 in 100 dilution) was from Novocastra Laboratories Ltd (Newcastle, United Kingdom). Monoclonal mouse anti human MUC7 (1 in 1500 dilution) antibody was from Santa Cruz Biotechnology, Inc (Santa Cruz, California, United States of America). Polyclonal goat anti-rabbit (1 in 5000 dilution) and polyclonal rabbit anti-mouse horse radish peroxidise (HRP) linked secondary antibodies were from Dako, Denmark. Foetal bovine serum (FBS), Pen-Strep, L-Glutamine, non-essential amino acids (NEAA), Dulbecco modified Eagle medium (DMEM) with 4-(2-hydroxyethyl)-1-piperazineethanesulfonic acid (HEPES) were

from Gibco (Massachusetts, United States of America). Trypan blue solution, glycine, sodium dodecyl sulfate (SDS), bromophenol blue, hydrochloride chloride (HCl), ammonium persulphate (AMPS) and tetramethylethylenediamine (TEMED) were obtained from Merck (Germany). TZM-bl/JC53 cells (a HeLa cell line engineered with CCR5, CXCR4 co-receptors and CD4 receptors) were provided by the International Centre for Genetic Engineering and Biotechnology (ICGEB), University of Cape Town (UCT), South Africa. Thermo Scientific PageRuler Prestained Protein Ladder was purchased from Thermo Scientific, Lithuania. Vacutec Acqua Stain was purchased from Vacutec, Johannesburg, South Africa.

2.3 Sample Collection

2.3.1 Pig gastric mucus collection

Twenty-one pig stomachs were collected from Winelands Pork Abattoir, La Belle Rd, Stikland, Cape Town, 7530. The stomachs were transported in a closed bucket to our laboratory at the University of Cape Town (UCT), Faculty of Health Sciences (FHS), Groote Schuur Hospital, Old Main Building, J-Floor, J50 room 30, Main Road, Observatory, 7925, Cape Town, R.S.A. On average, transportation of stomachs took 30 minutes. Pig stomachs were opened with a pair of scissors along the greater curvature and gently washed with water. Ulcerated stomachs were excluded. Mucus was lightly scraped from the pars oesophagea, body, cardiac gland and pyloric antrum regions using 2 sterile glass slides. At least 50ml of mucus was collected form pig stomachs. The scraped mucus was placed into pre-weighed specimen jars kept on ice. The jars contained 10 milliMolar (mM) Na_2HPO_4, 6 Molar (M) GuHCl, 10mM EDTA, 1mM PMSF and 5mM NEM (see Collection Buffer 1, Appendix section 1.1) in a ratio of 3 millilitres (ml) 10mM Na_2HPO_4, 6M GuHCl, 10mM EDTA, 1mM PMSF and 5mM NEM at pH6.5 to every 1ml of gastric mucus. Pig gastric mucus was then pooled and stirred slowly overnight at 4 degrees Celsius (^oC). Thereafter, the sample was homogenized to separate any mucus coupled with insoluble contaminants with an ultra-turrax T25 (IKA Laboratory, Staufen, Germany) at 24 000 revolutions per minute (rpm) for 60 seconds (s). Homogenized samples were then centrifuged at 3000rpm for 60 minutes (mins) and the supernatant was stored in a -20^oC freezer.

2.3.2 Pig saliva collection

Pig saliva was collected from 20 pigs by the UCT Animal Unit (AU), Faculty of Health Sciences, Chris Barnard Building, Falmouth Road, Observatory, Cape Town, 7935. The saliva was collected on site by staff from local pig farms. Approximately 100ml of saliva was

collected for each pig. Samples were collected in 0.2M NaCl:0.02% sodium azide (see Sample Collection Buffer 2, Appendix section 1.2) in a ratio of, 4ml buffer 0.2M NaCl:0.02% sodium azide to every 1ml of pig saliva. Pig saliva was not collected in guanidine hydrochloride as a cost saving measure. Saliva samples were brought to our laboratory where the saliva was pooled and stirred slowly overnight at 4^{o}C. Samples had low viscosity and solubilized easily in the overnight stir. Thereafter, the sample was centrifuged at 3000rpm for 60 mins and the supernatant was stored in a -20^{o}C freezer.

2.3.3 Pig cervical mucus collection

Pig cervical mucus was collected from 10 pigs by Sister M. Botes, UCT Animal Unit (AU), Faculty of Health Sciences, Chris Barnard Building, Falmouth Rd, Observatory, Cape Town, 7935. The cervical mucus was collected on site by their staff from local pig farms. Pigs were in the oestrus cycle of ovulation. Approximately 5ml of cervical mucus was collected from each pig. Pig cervical mucus samples were collected in 10mM Na_2HPO_4, 6M GuHCl, 10mM EDTA, 1mM PMSF and 5mM NEM at pH6.5 (see Collection Buffer 1, Appendix section 1.1) in a ratio of 9ml buffer for every 1ml of pig cervical mucus. Samples were collected from the UCT AU and brought to our lab. Pig cervical mucus was pooled and stirred slowly overnight at 4^{o}C. No homogenization was required as there were no insoluble contaminants in the sample that could not be removed by centrifugation. Thereafter, samples were centrifuged at 3000rpm for 60 mins and supernatant was stored in a -20^{o}C freezer.

2.3.4 Horse saliva collection

Horse saliva was collected from 1 horse by Ms Heather Epstein who runs a farm and is an acquaintance of Professor A. S. Mall. Approximately 50ml of saliva was collected. The sample was collected in 10mM Na_2HPO_4, 6M GuHCl, 10mM EDTA, 1mM PMSF and 5mM NEM at pH6.5 (see Collection Buffer 1, Appendix section 1.1) in a ratio of 4ml buffer for every 1ml of horse saliva. This buffer was selected as the sample had to be stored for a long period (at 4^{o}C) as Ms. Epstein lived far away. Samples were collected from the UCT AU and brought to our lab. The mucus in buffer was slow stirred for overnight at 4^{o}C. Thereafter, the sample was centrifuged at 3000rpm for 60 mins and the supernatant was dialysed against distilled water over three changes for a minimum of 6 hours each at 4^{o}C and then freeze dried (see section 2.6).

2.4 First Ultracentrifugation of samples

Supernatant collected from sections 2.3.1 and 2.3.3 after the initial 3 000rpm centrifugation were subjected to a density gradient ultracentrifugation. Supernatant from sections 2.3.2 and 2.3.4 underwent a density gradient ultracentrifugation after Sepharose 4B gel filtration. Density gradient ultracentrifugation is a separation technique that works on the Archimedes' principle which states that a particle settling in a simple fluid is subjected to its own weight and an upward density force that is based on the weight of the displaced fluid (Piazza et al., 2012).

Supernatant was prepared for caesium chloride (CsCl) density gradient ultracentrifugation to separate mucins and proteins in a solution of 4M GuHCl (see Ultracentrifugation Buffer, Appendix, section 1.3). During density gradient ultracentrifugation, CsCl molecules dissociate and Caesium ions (Cs^+) downward movement opposed by a diffusion force results in a density gradient from CsCl molecules within the tube. The lower density fractions migrate to the top of the tube, with the density gradient moving down the tube. Mucins and proteins in the tube move to a fraction corresponding to their density (Creeth et al., 1970).

The density of supernatants was adjusted to 1.39 grams per millilitre (g/ml), by adding CsCl and 4M GuHCl (see Ultracentrifugation Buffer, Appendix, section 1.3). These were injected with disposable syringes into ultracentrifuge tubes and heat sealed with a tube topper. Tubes were placed in a Ti70 rotor and then into a Beckman L45 ultra-centrifuge for 48 hours at 40 000rpm at a temperature of 4^{o}C.

Tubes were divided into 9 fractions spaced 1 centimetre (cm) apart. Fractions were pipetted into 10ml glass tubes using sterile disposable syringes. The densities of each fraction were recorded by weighing a volume of 1ml on an analytical balance.

2.4.1 Glycoprotein and Protein detection of ultracentrifugation samples

2.4.2 Periodic Acid Schiff (PAS) assay for glycoprotein detection

This assay detects glycoproteins once their hydroxyl groups (-OH) are oxidized to aldehyde groups (-CHO) in the presence of periodic acid. Decolourised Schiff's reagent reacts with the aldehyde group to give a pink/purple colour (Thornton et al., 1996).

Ten microlitres (µl) of each sample from each fraction was plated into a 96-well microtiter plate. One hundred microlitres of periodic solution (7% acetic acid with 50% periodic acid) was added to 20µl of sample and incubated at 37^{o}C for 1 hour. After incubation, 100µl of decolourised Schiff's reagent (see Appendix, section 5.1) was added to each well and incubated

at room temperature for 30 mins. Thereafter, the absorbance was read on an Anthos HTII Plate Reader (GoIndustry DoveBid, Lancashire, United Kingdom) at 585nm. While the optimum wavelength for this assay is 555nm, our plate reader had 585nm filter which was close enough to read the relevant absorbance.

2.4.3 BIO-RAD Quick Start™ Bradford assay for protein detection

The Bradford assay utilises a protein-binding dye that exists in 3 forms: cationic, neutral and anionic (Compton et al., 1985). The anionic form is not present at the dye reagent pH, but this forms complexes primarily with arginine via Van der Waals forces and hydrophobic interactions. It also binds slightly to basic amino acids Histidine and Lysine as well as aromatic residues Tryptophan, Tyrosine and Phenylalanine (Compton & Jones, 1985).

Twenty microlitres from each fraction was plated into a 96-well microtiter plate. Two hundred microlitres of diluted BIO-RAD Quick Start™ Bradford dye (see Appendix section 6) were added to the samples and incubated at room temperature for 5 mins. Thereafter the plate was read on an Anthos HTII Plate Reader (GoIndustry DoveBid, Lancashire, United Kingdom) at 585nm.

2.4.4 Second Ultracentrifugation of samples

Fractions containing glycoproteins were pooled and had their densities adjusted to 1.41 g/ml, by adding CsCl and 4M GuHCl (see Ultracentrifugation Buffer, Appendix, section 1.3). These were injected with disposable syringes into ultracentrifuge tubes and heat sealed. Tubes were placed in a Ti70 rotor and then into a Beckman L45 ultra-centrifuge for 48 hours at 40 000rpm at a temperature of 4°C.

Tubes were divided into 9 fractions spaced 1 centimetre (cm) apart. Fractions were collected into centrifuge tubes using sterile disposable syringes. The densities of each fraction were recorded by weighing a volume of 1ml on an analytical balance.

Fractions then underwent PAS and Bradford Assays to determine the glycoprotein and protein rich fractions, respectively. Thereafter, samples underwent dialysis.

2.5 Dialysis of samples

To remove salts and small soluble molecular weight impurities, samples were dialysed against distilled water. Dialysis tubing (nitrocellulose membrane, average flat width 25 millimetres (mm)) was boiled in a beaker of water (at 100^{o}C) in the presence of 2% weight per volume

(w/v) sodium bicarbonate solution in 1mM EDTA solution until the membranes opened and floated to the top. Pooled fractions and/or supernatant of each sample were pipetted into the opened dialysis tubing. Thereafter, the tubing was placed into a 12 Litre (L) bucket and dialysed against at least three changes of distilled water (at 6 hour intervals) with continuous stirring on a Fried Electric Magnetic Stirrer (Haifa, Israel), at 4°C.

2.6 Freeze drying

Empty centrifuge tubes had holes made in their lids, using a heated needle (using the flame of a Bunsen burner). They were weighed and had the dialysed contents, emptied into them (15ml or 50ml, depending on the volume of dialysed sample). Tubes were left overnight in a -80°C freezer. Samples were then placed in the vacuum chamber of a Freeze Zone 6 Freeze Dry System (Labconco, Kansas City, United States) and freeze dried at -50°C under a vacuum of 0.021 millibars (mBar). Samples were left in the freeze dryer until all the ice in the sample had undergone sublimation leaving behind lyophilized protein and/or glycoprotein.

2.7 Column Chromatography

2.7.1 Sepharose 2B Column Chromatography

Sepharose 2B beads were degassed to remove bubbles and then packed into a glass column (100cm x 2cm, volume of 300ml). Zero point two Molar NaCl:0.02% sodium azide was eluted through the column via a Peristaltic Pump (MINIPULS® 3, Gilson, Inc. USA). The column was connected to a chromatography fraction collector (FC 204 Fraction Collector, Gilson, Inc. USA) that eluted each fraction at 1ml per minute. Fractions were tested for glycoproteins and proteins using the PAS Assay (see Appendix section 5) and BIO-RAD Assay (see section 2.4.3. and Appendix section 6). Data was graphically viewed on Microsoft Excel, the resulting peaks that were of interest were pooled and dialysed (see Section 2.5. above) and freeze dried (see Section 2.6. above).

2.7.2 Sepharose 4B Column Chromatography

Sepharose 4B beads were degassed to remove bubbles and then packed into a glass column (30cm x 2.5cm, volume of 140ml). Zero point two Molar NaCl:0.02% sodium azide was eluted through the column via a Peristaltic Pump (MINIPULS® 3, Gilson, Inc. USA). The column was connected to a chromatography fraction collector (FC 204 Fraction Collector, Gilson, Inc. USA) that eluted each fraction at 1ml per tube. Every second fraction was tested for glycoproteins and proteins using the PAS Assay (see Appendix section 5) and BIO-RAD Assay

(see section 2.4.3 and Appendix section 6). Data was graphically viewed on Microsoft Excel, the resulting peaks that were of interest were pooled and dialysed (see Section 2.5 above) and freeze dried (see Section 2.6 above).

2.7.2.1 Sepharose 4B Column Chromatography Separation of Pig Salivary Muc19

Zero point two Molar NaCl:0.02% sodium azide was eluted through the previously prepared Sepharose 4B column (see section 2.7.2) via a Peristaltic Pump (MINIPULS® 3, Gilson, Inc. USA) at a volume that was three times the bed volume of the column to ensure it was cleared of any previously run samples. While Sepharose 4B separation may not have the optimal resolution to separate the two similarly sized mucins Muc5b and Muc19, it was the best exclusion chromatography that was available to us and it was decided to change the flow rate to see if this could help separate the mucins. The column was connected to a chromatography fraction collector (FC 204 Fraction Collector, Gilson, Inc. USA). Aliquots of pig saliva collected in 0.2M NaCl:0.02% sodium azide were eluted through the Sepharose 4B column at 0.5ml per tube rather than the 1ml per tube seen in section 2.7.2. This was to ensure broader peaks for the void volume (V_0). Fractions were tested for glycoproteins and proteins using the PAS Assay (see Appendix section 5) and BIO-RAD Assay (see section 2.4.3 and Appendix section 6). Data was graphically viewed on Microsoft Excel. The fractions making up the V_0 (i.e. the large molecular weight fraction) were individually investigated under Slot Blot for Muc5b and Muc19. It is important to note that there still may be Muc5b present in the Muc19 sample as antibodies raised to human mucins were used and Muc5b may also be present at lower than detectable limits. Fractions that were Muc19 positive and Muc5b negative were pooled and dialysed (see Section 2.5 above) against 4M GuHCl over three changes for a minimum of 6 hours each at 4^{o}C. The volume of 4M GuHCl was at least 20 times the volume of pooled Muc19 fractions.

2.7.2.2 Sepharose 4B Column Chromatography Separation of Horse Salivary Muc19

Zero point two Molar NaCl:0.02% sodium azide was eluted through the previously prepared Sepharose 4B column (see section 2.7.2) via a Peristaltic Pump (MINIPULS® 3, Gilson, Inc. USA) at a volume that was three times the bed volume of the column to ensure it was cleared of any previously run samples. While Sepharose 4B separation may not have the optimal resolution to separate the two similarly sized mucins Muc5b and Muc19, it was the best exclusion chromatography that was available to us and it was decided to change the flow rate to see if this could help separate the mucins. The column was connected to a chromatography

fraction collector (FC 204 Fraction Collector, Gilson, Inc. USA). Lyophilized crude horse saliva was dissolved in 0.2M NaCl:0.02% sodium azide and eluted on a Sepharose 4B column (eluting buffer was also 0.2M NaCl:0.02% sodium azide). Fractions were collected at 0.5ml per tube. This was to ensure broader peaks for the V_0. Fractions were tested for glycoproteins and proteins using the PAS Assay (see Appendix section 5) and BIO-RAD Assay (see section 2.4.3. and Appendix section 6). Data was graphically viewed on Microsoft Excel. Aliquots of fractions making up the V_0 (i.e. the large molecular weight fraction) were individually investigated under Slot Blot for Muc5b and Muc19. It is important to note that there still may be Muc5b present in the Muc19 sample as antibodies raised to human mucins were used and Muc5b may also be present at lower than detectable limits. Aliquots that were Muc19 positive and Muc5b negative were pooled and dialysed (see Section 2.5 above) against 4M GuHCl over three changes for a minimum of 6 hours each at 4^{o}C. The volume of 4M GuHCl was at least 20 times the volume of pooled Muc19 fractions.

2.8 Chemical Treatments

2.8.1 DTT Treatment

DTT (10mM) was added to Sepharose (2B or 4B) eluted V_0 samples (pig saliva, gastric and cervico-vaginal mucin) in 0.2M NaCl:0.02% sodium azide. The sample was then incubated in a water bath at 37^{o}C for 5 hours. To ensure there was no re-association of disulphide bonds, 25mM IAA was added. The sample tube was covered in foil and incubated in the dark overnight. Samples were then dialysed (see Section 2.5. above) and freeze dried (see Section 2.6. above).

2.8.2 Trypsin Treatment

Trypsin from pig pancreas was added to Sepharose (2B or 4B) eluted V_0 samples (pig saliva, gastric and cervico-vaginal mucin) in 0.2M NaCl:0.02% sodium azide at a dilution of 1:100. This was incubated at 37^{o}C for 5 hours. Samples undergoing trypsin treatment were not pH controlled so the optimal trypsin treatment may not have occurred. Samples were then dialysed (see Section 2.5. above) and freeze dried (see Section 2.6. above).

2.9 Gel electrophoresis

2.9.1 Gradient (4 – 20%) Sodium dodecyl sulphate polyacrylamide gel electrophoresis (SDS-PAGE)

SDS-PAGE was used to detect mucins and proteins in all samples as well as to estimate their molecular weights. Due to the large sizes of mucins a gradient SDS-PAGE gel was preferred

for this analysis, to ensure maximum movement into the gel. The gels were prepared as per Laemmli *et al* (1970). The components of the gels are outlined in Appendix sections 1.6 to 3.3 (Laemmli, 1970).

The structure of mucins poses a problem for SDS-PAGE gel analysis. Dense O-linked glycans and multimerization (due to intra- and inter-molecular disulphide bonds) results in mucins having a range of molecular weights. The high molecular weight mucins (e.g. MUC16 has a molecular weight of 1 519.2kDa) are prevented from electrophoretic migration in standard SDS-PAGE gels. The inability of these high molecular weight mucins to penetrate the gels result in the mucins remaining on the gel surface (Paszkiewiczgadek et al., 1995; Ramsey et al., 2016; www.proteinatlas.org).

Freeze-dried pellets (1mg) were brought up in 100µl SDS sample application buffer (see Appendix section 1.6.5), and heated for 1 min in boiling water at 100°C. Fifteen microlitre aliquots of each sample and protein ladder were added to the appropriate wells. The BIO-RAD Mini-PROTEAN® Tetra Cell, 4-Gel system electrophoresis tank was filled with tank buffer and attached to a Consort E844 400 Volts (V) – 400 milliAmperes (mA) Electrophoresis Power Supply. The gels were run at the manufacturers recommended Volts, Amperes and time depending on the number of gels in the tank.

2.9.2 Protein Staining of SDS-PAGE gel

SDS-PAGE gel was placed in a glass container and stained with Vacutec Acqua Stain Protein Gel Stain for 10 mins at room temperature (per manufacturer's instruction). The gel was scanned on a Hewlett Packard desktop scanner and saved to a computer.

2.9.3 PAS staining of SDS-PAGE gel

Glycoproteins were visualized using the PAS staining method as used by Dubray and Bezard (1982) (see Appendix section 4). Briefly, the gel was immersed in 50% ethanol for 30 mins at room temperature. After washing the gel with distilled water for 10 mins, the gel was incubated in 3% acetic acid with 1% periodic acid for 30 mins. Thereafter, the gel was washed and left in distilled water overnight at 4°C. The gel was then washed in a solution of 0.1% sodium metabisulphite in 10mM HCl twice for 10 mins. The gel was then incubated with decolourised Schiff's reagent in the dark for 1 hour, followed by 1 hour in 0.1% sodium metabisulphite in 10mM hydrochloric acid (Dubray et al., 1982). The resulting glycoprotein stained gel was scanned and saved on a computer.

2.10 Slot Blot Analysis

Mucins were identified via Slot blotting. One Nitrocellulose membrane and three pieces of blotting paper were cut to the appropriate size and immersed in 4x saline-sodium citrate (SSC) buffer (see Appendix section 7) for 10 mins. The wet nitrocellulose membrane was placed on three pieces of blotting paper and sandwiched in a Minifold® II, Schleicher & Schuell, Inc. 72-well Slot Blot Manifold (New Hampshire, United States). Samples (50µl for each) were pipetted into wells and transferred under vacuum to a nitrocellulose membrane (BioTrace^{TM} NT membrane, Pall Corporation, New York, United States) treated with poly-L-lysine (1:50 dilution with SSC buffer). The bands were vacuum-transferred for 1 hour at 40mBar using a Pharmacia LKB Vacugene XL vacuum blotter (Kalamazoo, United States). Membranes were incubated with 5% (w/v) low-fat milk powder in 1x TBST (Tris saline buffer with 0.05% Tween-20) for 30 mins at room temperature to block non-specific binding sites. The primary antibody was diluted accordingly (see Appendix Table 1) in 5% (w/v) low-fat milk powder in 1x TBST and incubated for 3 hours on a shaker or overnight at 4°C. Membranes were then washed with 1x TBST, 4 times for 3 mins each. Secondary antibodies (see Appendix Table 1) were appropriately diluted in 5% (w/v) low-fat milk powder in 1x TBST and incubated for 30 mins at room temperature. Membranes were washed thrice with 1x TBST, for 10 mins, followed by a quick rinse with distilled water. To view the mucins, the membranes were developed using ChemiFast Chemiluminescent Substrate kit (Vacutec). Briefly, equal parts of reagent A and reagent B were mixed and an appropriate amount was added to cover the membrane before being dried by blotting with filter paper. The membrane was then viewed in a Syngene G-box (Syngene, Haryana, India).

2.11 Pig Mucin Derived Anti-HIV-1 Gels for *in vitro* Analysis

Buffers were constructed from previous work done by Allen *et al* (1976) and Owen *et al* (1999). Four buffers were constructed using the components seen in Appendix Table 2. Per Allen *et al* (1976) for an effective mucin gel there should be 30mg of mucin for 1ml of buffer. Gels were constructed by adding 30mg of either purified pig gastric mucin or purified pig cervical mucin to each buffer (Allen et al., 1976; Owen & Katz, 1999). The buffers were adjusted to neutral pH (~7.0 – 7.2) to successfully run on pseudoviral and MTT assays.

2.12 Pseudoviral Assay

Antiviral properties of mucins were tested on a modified HIV neutralization luciferase-based reporter gene assay (Montefiori, 2009). This assay originally assessed neutralizing antibodies

for HIV, to study the immune response in infected individuals (Montefiori, 2009). The Montefiori (2009) assay was modified by the Dorfman laboratory (from the International Centre for Genetic Engineering and Biotechnology (ICGEB)) to test mucins instead of antibodies against HIV infection. This pseudoviral assay, uses TZM-bl/JC53 cells (a Hela cell line with CCR5, CXCR4 coreceptors and CD4 receptors). This assay was carried out in a P2 facility at the Dorfman laboratory situated in ICGEB, Faculty of Health Sciences, UCT. These cell lines were engineered, frozen, thawed and cultured by the Dorfman laboratory. The cells have been transfected with an LTR (long translational repeat) promoted luciferase and ß-galactosidase gene sequence. The virus is made from plasmid SG3*env transcribing all viral genes except for a dysfunctional env and a plasmid containing env. The functional env can be varied to represent different viral strains. The viral tat gene initiates the LTR promoter and thus luciferase and ß-galactosidase production (see Figure 2.1 and Figure 2.2). This study used a moderately infective virus derived from a Durban (KwaZulu-Natal, South Africa) strain, viz. Du422.1. This too, was cultured, titrated and supplied by the Dorfman laboratory.

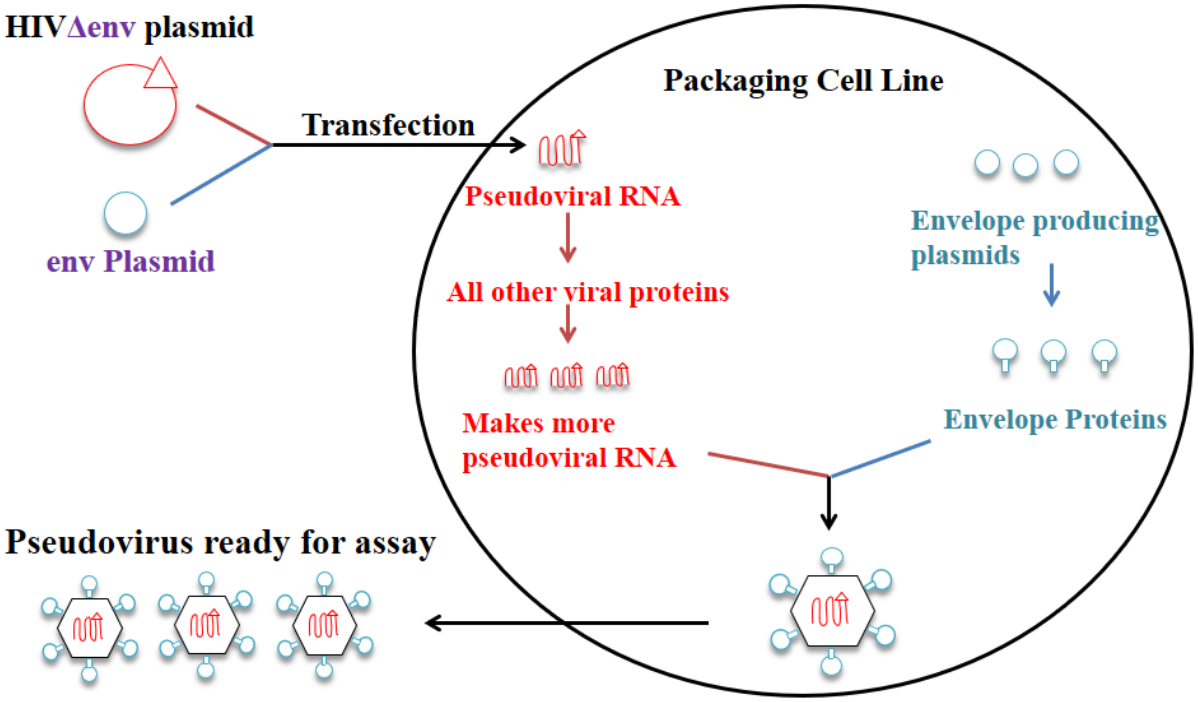

Figure 2.1 Engineering of HIV pseudovirus. Packaging cells are transfected with an LTR (long translational repeat) promoted luciferase and ß-galactosidase gene sequence. The HI virus is made from plasmid SG3*env transcribing all viral genes except for a dysfunctional env and a plasmid containing env. The functional env and/or pseudoviral RNA can be varied to represent different viral strains. This study used the RNA of a HIV-1 subtype C isolated from the Kwa-Zulu Natal province.

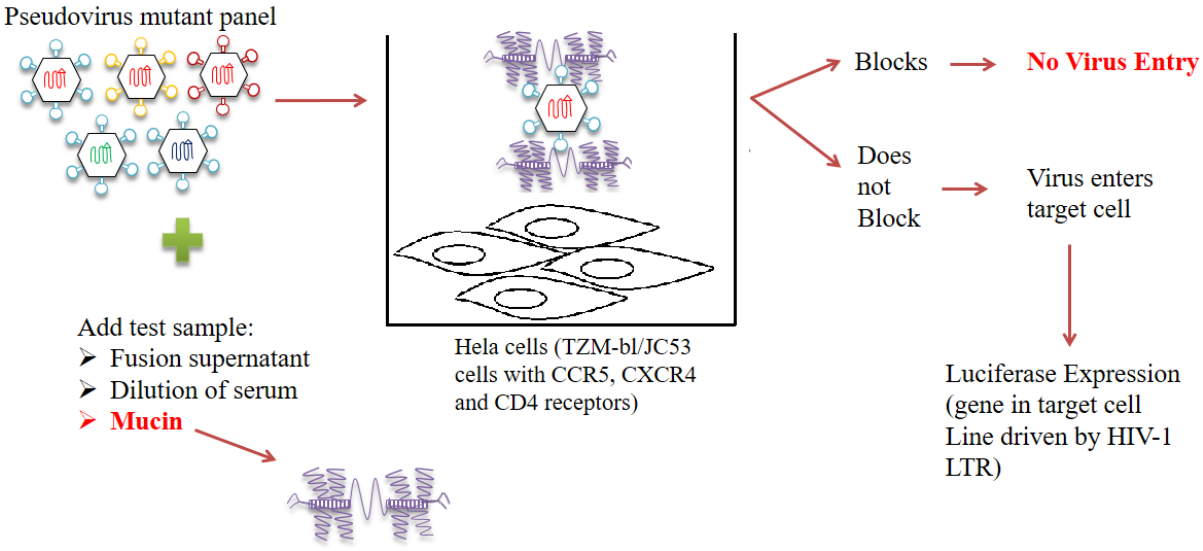

Figure 2.2 The HIV pseudoviral assay. Previously engineered HIV pseudovirus is incubated with mucin for an hour at room temperature. Thereafter, the HIV pseudoviral and mucin mixture is added to TZM-bl/JC53 cells (a Hela cell line with CCR5, CXCR4 coreceptors and CD4 receptors). If the mucins fail to block HIV pseudoviral infection, the viral tat gene initiates the LTR promoter and thus luciferase and ß-galactosidase production. If mucin blocks viral entry, there is no luciferase and ß-galactosidase production.

Pig and horse mucin derivatives were tested on the pseudoviral assay to assess how different treatments enhanced or retarded HIV-1 infection *in vitro*. Samples were prepared in growth media (at 500 – 1000 micrograms (µg) per 1ml of buffer) 10% Dulbecco's Modified Eagle's Medium (DMEM) (see Appendix section 1.5), (a 5% DMEM solution is used for normal cell maintenance (see Appendix section 1.4)). Confluent cells on day 1 of the assay were trypsin treated (0.8ml trypsin EDTA added to cell culture petri dish) for 4 mins. Thereafter, the cells were transferred in 6ml 10% DMEM to a centrifuge tube and centrifuged in an Eppendorf 5810 R Centrifuge (USA Scientific, Inc, USA) at 1000rpm for 5min at 21ºC. Cells were then dissolved in an appropriate amount of 10% DMEM and counted on a haemocytometer (30µl Trypan Blue and 10µl cells in media). DEAE Dextran (7.5mg/ml) was added to the cells to remove any natural charge repulsion between virus and cells. Cell concentration was adjusted to give 1 million cells per plate (approximately 10 416 cells per well) and plated on 96 well flat-bottomed plates. Plates were placed in a 37ºC incubator (5% carbon dioxide (CO_2)) overnight. On day 2, a separate plate was used to serially dilute the samples by half the volume (done 7 times from the starting concentration of 500 – 1000µg/ml), and in duplicate, but leaving wells for negative (cells in media only) and positive controls (cells in media plus virus) media. The starting volumes for dilution were either 300µl or 350µl. To a new tube, replication

defective pseudovirus HIV-1 subtype C Du422.1 virus was diluted in 10% DMEM (the dilution was dependant on the virus concentration which was determined by the Dorfman laboratory). Briefly, the starting concentration of the virus was mathematically divided by four (as the virus would make a quarter of the components of the well i.e. 1 part cells, 2 parts mucin and 1 part virus) the total volume of virus required (i.e. number of wells multiplied by the volume of virus per well) was divided by the previous quotient to give the volume of pure virus that must be diluted up to the total volume needed. Seventy-five microliters or 82.5µl (depending on whether the dilutions started at 300µl or 350µl respectively) of virus was added to the appropriate wells and incubated for an hour at room temperature, after which, 150µl of well contents from the dilution plate was added to the corresponding well of the cell culture plate. The previous steps highlight another deviation from the Montefiore (2009) neutralization assay. In the Montefiore (2009) based neutralization assay, antibodies under investigation were incubated with a replication defective virus for 1 hour, to which TZM-bl/JC53 cells were added for 48 hours (Montefiori, 2009). During the optimization of the pseudovirus assay, it was shown that adding the cells last to a virus and mucin mixture stopped cells from adhering to the bottom of microtitre wells (data not shown) impairing TZM-bl/JC53 cell growth and the success of the assay.

In the virus control, virus was added to wells in the absence of mucin, where luciferase activity was detected as 50 000 Relative Light Units (RLU). Plates were then incubated in a 37^{o}C incubator (5% CO_2) for 48 hours. Thereafter, 100µl of media was removed from each well and replaced with an equal amount of Luciferase and incubated in the dark for 2 mins. Results were measured and recorded using a GloMax®-96 Luminometer (Promega, France). Data was extracted to Microsoft Excel to calculate the percentage Neutralization of each sample at every dilution, using the following equation:

(AverageRLUVC - AverageRLU[Sample]) / (AverageRLUVC-AverageRLUCC) x 100%

Where

AverageRLUVC = Average Relative Light Units of the Virus Controls

AverageRLU[Sample] = Average Relative Light Units of the Sample

AverageRLUCC = Average Relative Light Units of the Cell Controls

The readout with no mucin was assigned the output value of 0% neutralization and the sample readout with no virus was assigned the output value of 100% neutralization. The percentage neutralization and corresponding concentration of samples was exported to GraphPad Prism Version 6 to calculate the half maximal Inhibitory Concentration (IC_{50}). The IC_{50} was calculated from a nonlinear regression (curve fit) Dose-response - Inhibition curve, using a Log[inhibitor] vs normalized response-variable slope graph, where

$$Y = 100/(1+10^{((LogIC_{50}-X)*Hillslope)})$$

The percentage neutralization previously calculated on Microsoft Excel was imported as the inhibitor in the above equation. The solid lines seen in the dose response curves correspond to the best model of an inhibition curve. Ninety-five percent confidence intervals were based upon curve fit of inhibition curves. A 95% confidence interval is a range where there is a 95% probability that the true effect lies within it. Tighter or narrower confidence intervals indicate more reliable data (Higgins et al., 2011). In this study that would translate to the effect of mucin specific HIV-1 inhibition. The log dose response curves were reported in this assay with the X-axis showing the non-logged concentration to better visualize the relationship between concentration and HIV-1 neutralization. Data was expressed in 4 significant figures.

2.13 Toxicity Assay

An MTT (3-(4,5-dimethylthiazol-2-yl)2,5-diphenyl tetrazolium bromide) assay (Śliwka et al., 2016) was used to assess the toxicity of our purified mucin products, including any associated proteins, on the same cell line as the pseudoviral assay. The pseudoviral assay method was mimicked here but with no HIV addition. This assay relies on the ability of mitochondrial enzymes of viable cells to change the MTT tetrazolium salt into its purple formazan derivative (Ferrari et al., 1990). This colour change is measured on a microplate reader at 585nm to determine the percentage of viable cells relative to the control cells that have no sample just media.

Samples were prepared in growth media 10% DMEM (see Appendix section 1.5), (a 5% DMEM solution is used for normal cell maintenance (see Appendix section 1.4). Confluent cells on day 1 of the assay were treated with trypsin (0.8ml trypsin-EDTA solution added to cell culture petri dish) for 4 mins. Thereafter, the cells were transferred in 6ml 10% DMEM to a centrifuge tube and centrifuged at 1000rpm for 5 mins at 21^{o}C. Cells were then resuspended in an appropriate amount of 10% DMEM and counted on a haemocytometer (30µl Trypan Blue

and 10µl cells in media). DEAE Dextran (7.5mg/ml) was added to the cells to remove any natural charge repulsion between virus and cells. Cell concentration was adjusted to give 1 million cells per plate (approximately 10 416 cells per well) and plated on 96-well flat-bottomed plates. Plates were placed in a 37ºC incubator (5% CO_2) overnight. On day 2, a separate plate was used to serially dilute the samples by half the volume (done 7 times from the starting concentration of 1mg/ml), and in duplicate, but leaving wells for negative (cells in media only) and positive controls (cells in media plus virus) media. The contents of wells (150µl) from the dilution plate were added to the corresponding wells of the cell culture plate. Plates were then incubated in a 37ºC incubator (5% CO_2) for 44 hours. Thereafter, 20µl MTT (5mg/ml in 10% DMEM) was added to all the wells and incubated for 4 hours at 37ºC. Following incubation, 100µl of wells contents were removed and replaced with 0.1 Normal (N) HCl in isopropanol and incubated at room temperature for 5 mins on a shaker, then read on a microplate reader at 585nm. Data was extrapolated to Microsoft Excel to determine percentage viability using the following formula:

$$\text{Percentage Viability} = \frac{\text{(Absorbance Value of Sample – Absorbance of Media)}}{\text{(Average of Cell Control Absorbance values – Absorbance of Media)}} \times 100\%$$

The percentage viability and corresponding concentration of samples were exported to GraphPad Prism V6 to calculate the medium lethal dose (LD_{50}) (Manage et al., 2013; Trevan, 1927). The LD_{50} was calculated from a nonlinear regression (curve fit) Dose-response - Inhibition curve, using a Log[inhibitor] vs normalized response- variable slope graph, where

$$Y = 100/(1+10\text{^}((\text{Log}IC_{50}-X)*\text{Hillslope}))$$

Here, the percentage viability previously calculated on Microsoft Excel was imported as the inhibitor in the above equation. In cases where an LD_{50} could not be calculated for a sample (due to non-convergence of dose response curve), the percentage viability closest to that sample's corresponding IC_{50} was quoted. Ninety-five percent confidence intervals were based upon curve fit of cell viability curves (curves not shown). A 95% confidence interval is a range where there is a 95% probability that the true effect lies within it. Tighter or narrower confidence intervals indicate more reliable data (Higgins & Green, 2011). In this part of the

study that would translate to the effect of mucin toxicity on TZM-bl cells (Higgins & Green, 2011).

2.14 Nanoparticle and Pseudoviral Analysis of Mucin-Derived Gel

To assess the thermal motions of particles in our gels, we collaborated with Associate Professor Sam Lai, University of North Carolina Eshelman School of Pharmacy, Division of Molecular Pharmaceutics. His research centres on particle diffusion analysis of native mucus gels with minimal perturbation of the sample.

2.14.1 Non Muco-adhesive Particles

Associate Professor Lai's laboratory uses fluorescent carboxyl-modified polystyrene particles sized at 100 nanometres (nm), 200nm, 500nm and 1000nm (purchased from Molecular Probes, Eugene, OR, USA). These particles were covalently modified with 2 – 3.4kDa amine-modified polyethylene glycol (PEG) (purchased from Nektar Therapeutics, San Carlos, CA, USA). The particles were coated with PEG to ensure a reduction in intrinsic forces play a role in the motion of the particles. In this way, only steric hindrance would play a role in the retardation of particle movement.

To record the trajectories of the particles, they used a silicon-intensified target camera (VE-100, Dage-MTI, Michigan, IN, USA) mounted on an inverted epifluorescence microscope with a 100x oil-immersion objective (numerical aperture 1.3). In 8-well glass chambers (Labtek, Campbell, CA, USA) ~10^{10} particles/ml were added to 250 – 500µl of our mucin gel mixture, to a final concentration of <2% volume per volume (v/v). This mixture was incubated for 2 hours and then viewed under a microscope. Thereafter, 10% (w/v) (nonylphenoxy)polyethylene oxide (Igepal CO-630, Rhône-Poulenc, Courbevoie, France) was added to a final concentration of 1% (v/v), gently stirred, incubated for 2 hours and viewed under a microscope. Movies of the trajectories were captured with Metamorph software (Universal Imaging Corp., Downingtown, PA) at a temporal resolution of 66.7 milliseconds (ms) for 20s. With the tracking resolution set at 10nm (Apgar et al., 2000), the coordinates of nanoparticles were transformed into time-averaged mean squared displacements (MSDs) and were calculated as

$$\langle \Delta r^2(\tau) \rangle = [x(t + \tau) - x(t)]^2 + [y(t + \tau) - y(t)]^2$$

τ represents time scale or time lag, from which the distributions of MSDs and effective diffusivities (D_{eff}) were calculated (Dawson et al., 2003; Lai et al., 2007; Suh et al., 2005). The resulting MSD of nanoparticles vs τ also fit the equation $MSD = 4D_0\tau^{\alpha}$ where α is the slope of the curve on a log-log scale. This is a measure of the extent of obstruction to particle diffusion (Suh, Dawson et al. 2005).

2.14.2 Probing of the Mucus Gel Mesh to Determine Structural Arrangement

To calculate the pore sizes of our mucin derived gel, the Lai group used an obstruction-scaling model for covalently cross-linked hydrogels, developed by Amsden *et al* (Amsden, 1998, 1999; Olmsted et al., 2001; Shen et al., 2006). The rationale behind using this method is that Amsden's equation is applicable to the physical entanglement cross-links found in mucus as long there is no chemical interaction between the solute particles, the gel mesh and that the particles traveling through the pores of the gel undergo the viscous drag of water. This model describes the ratio of particle diffusion in a gel mesh and its diffusion in water as

$D_g/D_0 = \exp((-\pi/4)((r_s+r_f)/(r_g+r_f))^2)$

Where D_g = the diffusion coefficient of a particle in a polymer gel;

D_0 = the diffusion coefficient of the same particle in water;

r_s = the particle radius;

r_f = the gel fibre radius (this was set at 3.5nm) (Olmsted et al., 2001; Shen et al., 2006)

r_g = the effective radius of the pore

The average effective pore size ($2r_g$) was calculated by entering measured transport data via the maximum likelihood method.

2.14.3 Preparation of Fluorescent Labelled HIV-1 Pseudovirus

Replication-defective HIV-1, labelled internally with an mCherry-Gag construct to ensure minimal alteration of the viral surface, was prepared by transfecting 293T cells with plasmids encoded with NL4-3Luc$^+$Vpr$^-$Env$^-$, Gag-mCherry, and YU2 Env in a 4:1:1 ratio. The cell supernatant was collected 48 hours later, and fluorescently tagged virions from the cell supernatant was purified by centrifugation through 25% sucrose at 160,000*g* for 2.5 hours. The virions were washed, and resuspended in phosphate-buffered saline (PBS). Thereafter it was divided into aliquots, and stored at -80°C (Nunn et al., 2015).

2.15 Referencing

Journal articles, websites, books etc. used in this thesis were referenced using Endnote® X7.7 Thomson Reuters, US. The referencing style is in accordance with the American Psychological Association, 6th edition.

CHAPTER 3: THE PURIFICATION OF PGM

3.1 Results

3.1.1 First Ultracentrifugation of Pig Gastric Mucus

Aliquots taken from pooled pig gastric mucus samples shared similar profiles to each other after the first density gradient ultracentrifugation process. Figure 3.1 shows the protein, glycoprotein and density profiles of a representative sample.

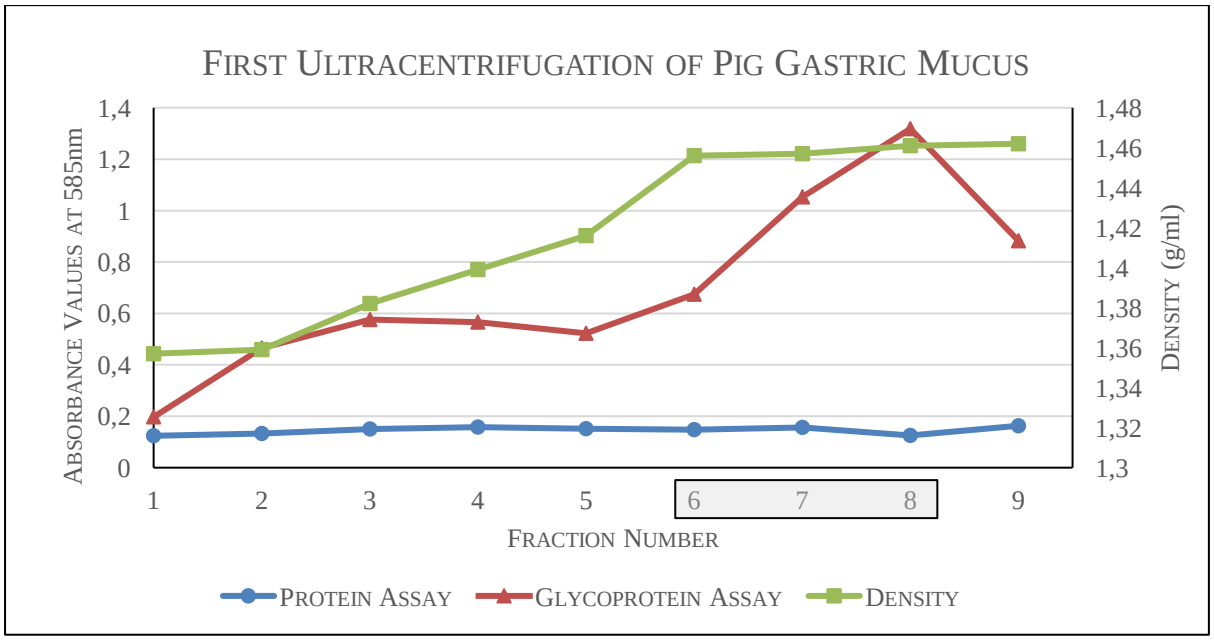

Figure 3.1 First ultracentrifugation profile of pig gastric mucus. Pig gastric mucus was slowly stirred overnight in 6M guanidine hydrochloride with 10mM Na_2HPO_4, 10mM EDTA, 1mM PMSF and 5mM NEM. The densities of samples were adjusted to 1.39g/ml with caesium chloride and 4M GuHCl. They were then subjected to a 48-hour ultracentrifugation at 105 000g at 4°C. Protein content was determined using Bradford Reagent assay (—●—); glycoprotein content was identified using a PAS assay (—▲—) and the densities (—■—) were recorded on the secondary axis. The box on the X-axis represents the fractions collected for a second round of ultracentrifugation enrichment.

Fractions that had glycoprotein rich densities of 1.39g/ml to 1.41g/ml were pooled. In Figure 3.1 the glycoprotein rich fraction were 6 – 8. These samples were then prepared for a second round of density gradient ultracentrifugation.

3.1.2 Second Ultracentrifugation of Pig Gastric Mucus

The pooled fractions from section 3.1.1 had their densities adjusted to 1.41g/ml with caesium chloride and 4M GuHCl. They underwent a second ultracentrifugation under the same conditions as the first. Protein and glycoprotein content as well as densities were all recorded in the same way as the first density gradient ultracentrifugation. The second density gradient ultracentrifugation profiles of pig gastric mucus all shared a similar pattern. Figure 3.2 shows the pattern of a representative sample.

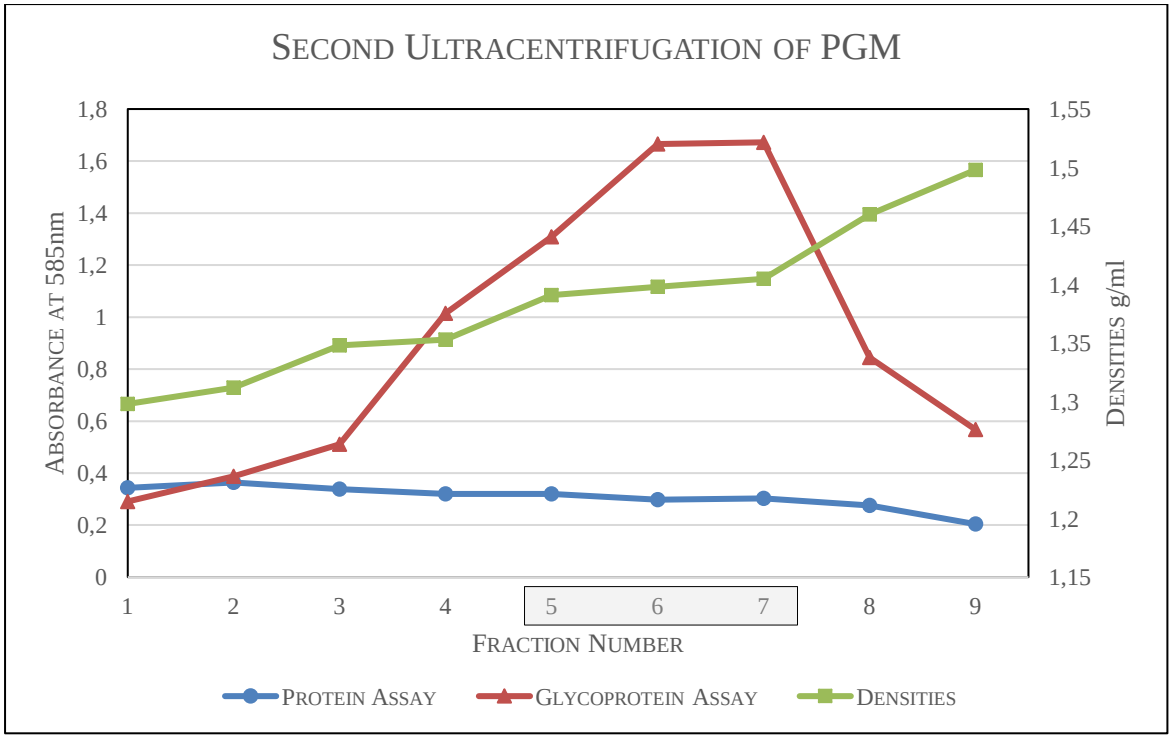

Figure 3.2 Profile of second ultracentrifugation of pig gastric mucus. Glycoprotein rich fractions from the first ultracentrifugation were pooled and had their densities adjusted to 1.41g/ml with caesium chloride and 4M GuHCl. The fractions then underwent ultracentrifugation for 48 hours at 105 000g at 4ºC. Protein content was determined using Bradford Reagent assay (); glycoprotein content was identified using a PAS assay () and the densities () were recorded on the secondary axis. The box on the X-axis enclosing numbers 5 – 7 represents the fractions collected, pooled, dialysed against distilled water and freeze dried.

Samples that had high glycoprotein content and a density of 1.40 – 1.41g/ml were pooled, dialysed against over three changes of distilled water for a minimum of 6 hours each at 4ºC and then freeze dried.

3.1.3 Size Exclusion Sepharose 2B Column Chromatography of PGM

Aliquots of lyophilized mucin were run on a Sepharose 2B column to separate mucins based on size. Protein and glycoprotein profiles stayed consistent throughout the many chromatography runs. Figure 3.3 is a representative sample of protein and glycoprotein distribution after PGM was run on the Sepharose 2B column.

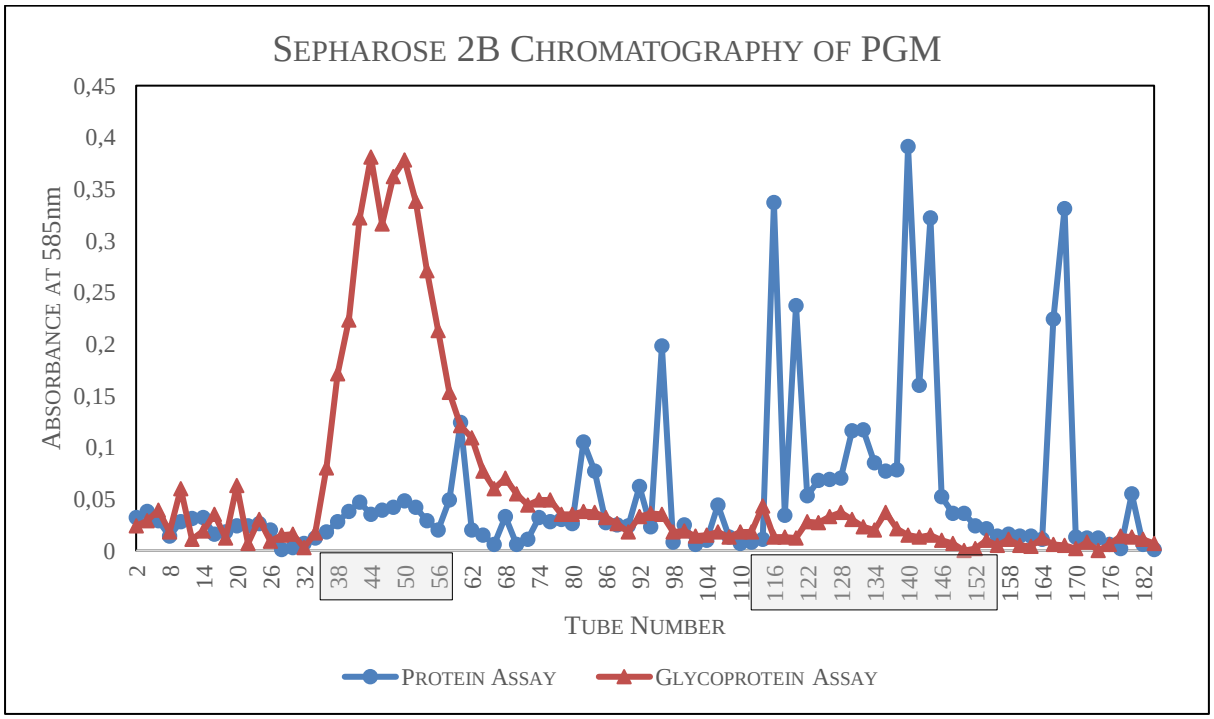

Figure 3.3 Sepharose 2B separation profile of PGM in 0.2M NaCl:0.02% sodium azide. Purified lyophilized pig gastric mucin was resuspended in 10ml 0.2M NaCl:0.02% sodium azide and eluted through a Sepharose 2B glass column under peristaltic pressure. Every second fraction was tested for proteins and glycoproteins. Protein content was determined using Bradford Reagent assay (); and glycoprotein content was identified using a PAS assay (). The box on the X-axis represents fractions that were pooled.

A clear PAS positive peak eluted in the V_0 of the column (fractions 38 – 56), suggesting the presence of polymeric mucin in the purified sample, together with some subunit trailing into the included volume (V_i) (Figure 3.3). The protein positive material under this V_0 peak denotes the protein of the mucin (Mall et al., 1997b; Pearson et al., 1981). Interestingly a fair amount of protein eluted as a series of peaks in the V_i of the column suggestive of reactivity to glycoprotein (Allen, 1978; Mall et al., 1988) or possibly the removal of contaminating proteins from the preparation. Fractions 116 – 152 were pooled and designated V_i. The V_0 and V_i fractions were then dialysed against distilled water over three changes for a minimum of 6 hours each at 4ºC and freeze dried.

3.1.4 SDS-PAGE 4 – 20% Gradient Gel Electrophoresis

Aliquots of samples were run on an SDS-PAGE gradient gel (4 – 20%) following reduction with DTT and proteolysis with trypsin treatments of PGM. Figure 3.4 shows the results of the samples run on the SDS-PAGE stained for proteins (see section 2.9.2) and Figure 3.5 shows PAS glycoprotein staining (see section 2.9.3).

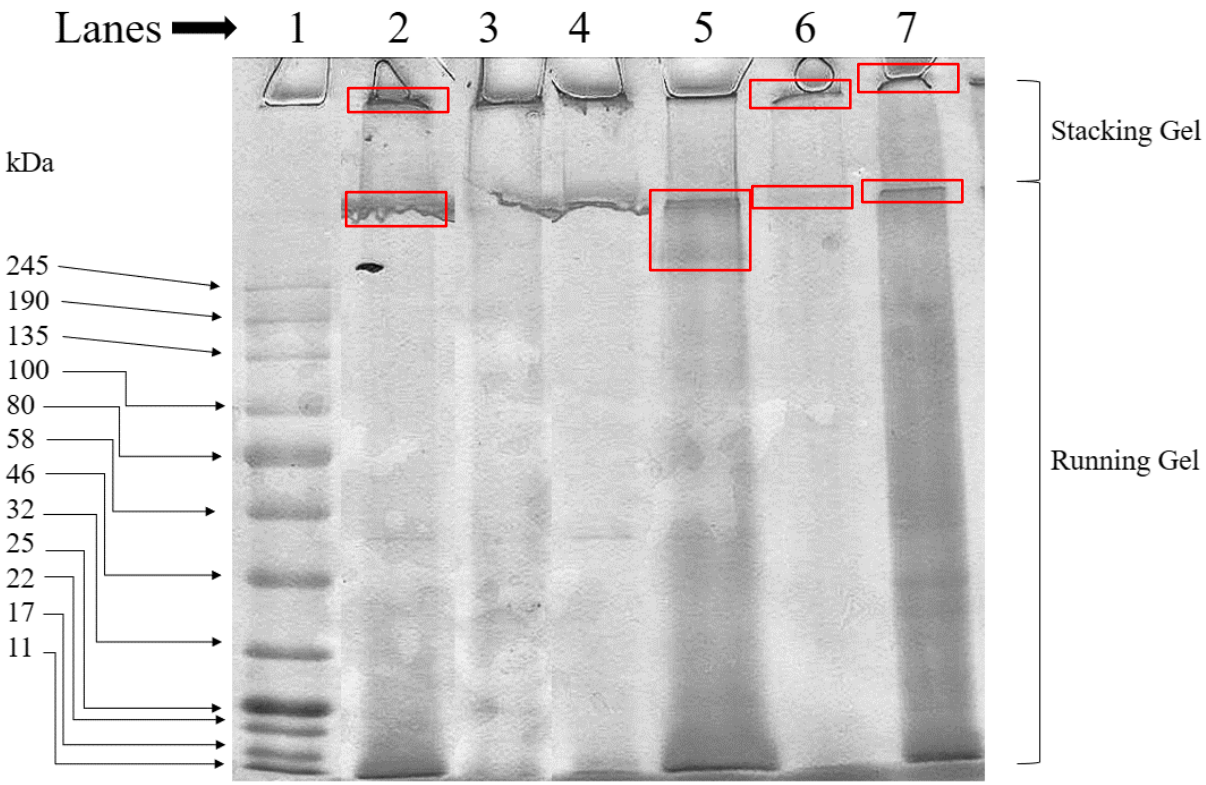

Figure 3.4 Protein stained 4 – 20% gradient SDS-PAGE gel of PGM derivatives. At different stages of pig gastric mucin purification and treatment, 1mg lyophilized aliquots were dissolved in 100µl 2% SDS, 1% glycerol and 0.01% bromophenol blue for SDS-PAGE gel investigation. Lane 1, 10µl of Thermo Scientific PageRuler Prestained Protein Ladder; Lane 2, crude pig gastric mucus; Lane 3, purified pig gastric mucin after purification after two density gradient ultracentrifugations; Lane 4, the Sepharose 2B V_0 fraction (Muc5ac and Muc6); Lane 5, the Sepharose 2B V_i fraction; Lane 6, DTT treatment of the Sepharose 2B V_0 fraction (Muc5ac and Muc6) and in Lane 7, trypsin treatment of the Sepharose 2B V_0 fraction (Muc5ac and Muc6). The red circles denote distinct visible bands (in some cases, partially visible).

Protein staining revealed a few bands of interest (outlined by red boxes). Upon gel electrophoresis, the crude pig gastric mucus (Figure 3.4, lane 2) showed a strong band that could not penetrate the running gel and appeared on the top of the well (first red box). This represents the high molecular weight mucin that cannot get into the gel (first red box from the top in Figure 3.4, lane 2). There is also a second band of protein (possibly mucin) that lies between the stacking and running gel (second red box from the top). Figure 3.4 lane 3 shows the effect of purification by two rounds of density gradient ultracentrifugation in CsCl, there being less mucin or possible *in vivo* degradation of mucin in the same position as the previous band in Figure 3.4, lane 2 (second red box). It is important to note that this is a protein stain

and protein makes up a very small amount of the mucin. There may have been mucin loss during the density gradient ultracentrifugation as only 2 – 3 fractions are collected out of a total of 9. Previous work in our laboratory had shown all 9 ultracentrifugation fractions contained mucin (data not shown). The 2 – 3 fractions chosen had the least protein contamination. Figure 3.4, lane 4 shows the eluted V_0 fraction from a Sepharose 2B column after two density gradient ultracentrifugations. This was the purest of all the samples and was highlighted by the faint protein banding pattern in lane 4. Figure 3.4, lane 5 shows the eluted V_i fraction from a Sepharose 2B column after two density gradient ultracentrifugations containing most of the smaller mucins and impurities. Figure 3.4, lane 5 shows the subunit at the beginning of the stacking gel and an intense protein smear in the top of the running gel (see red box). The same subunit material appears at the same spot when purified mucin is treated with DTT (Figure 3.4, lane 6), again suggesting that the reduction of disulphide bonds produces a subunit in pig gastric mucin (Mall et al., 1999; Pearson et al., 1981). DTT treatment of the V_0 fraction (Figure 3.4, lane 6) showed mucin bands in red boxes, these were smaller than the corresponding bands in Figure 3.4, lane 2 (red boxes). This suggests that with disulphide bond breakage the large mucins could move further down the gel as is evident by the mucin smear. Figure 3.4, lane 7 shows the effect of trypsin on the non-glycosylated sections of the mucin. There is an increase in the mucin smear effect but also the appearance of more bands all the way down the gel, together with a stronger background. Identification of bands lay outside the scope of this study and may be looked at in future studies with the aid of proteomics.

3.1.5 PAS Stained Gradient Gel Electrophoresis

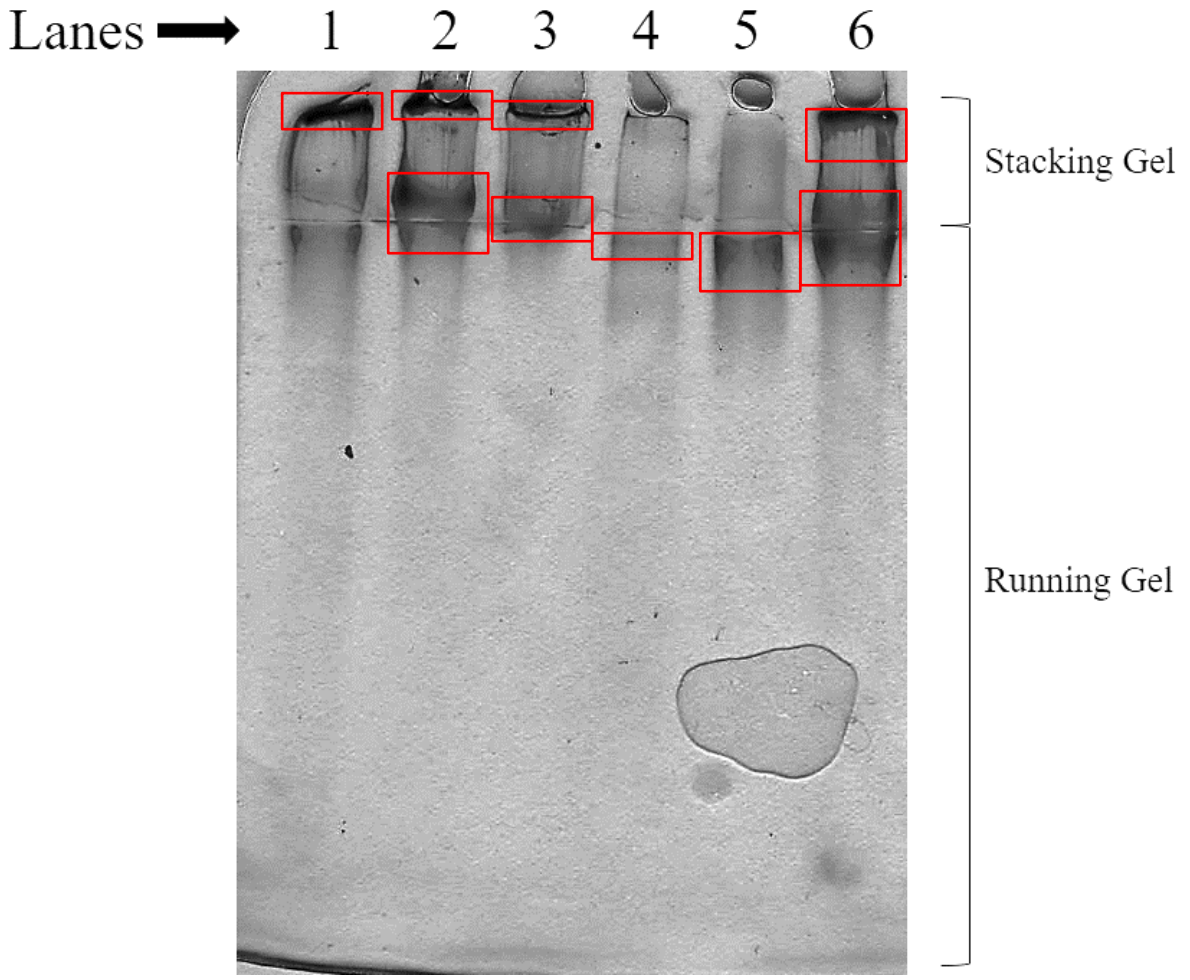

Figure 3.5 Glycoprotein stained 4 – 20% gradient SDS-PAGE gel of PGM derivatives. At different stages of pig gastric mucin purification and treatment, 1mg lyophilized aliquots were dissolved in 100µl of 2% SDS, 1% glycerol and 0.01% bromophenol blue for SDS-PAGE gel investigation. Lane 1, crude pig gastric mucus; Lane 2, purified pig gastric mucin after purification after the second density gradient ultracentrifugation; Lane 3, the Sepharose 2B V_0 fraction (Muc5ac and Muc6); Lane 4, the Sepharose 2B V_i fraction; Lane 5, DTT treatment of the Sepharose 2B V_0 fraction (Muc5ac and Muc6) and Lane 6, trypsin treatment of the Sepharose 2B V_0 fraction (Muc5ac and Muc6).

Figure 3.5 illustrates the PAS stained distribution of PGM and its derivatives through an SDS-PAGE (for method see Section 2.9.2). The result of the staining showed a similar pattern to the protein staining (Figure 3.4). Figure 3.5, lane 1 shows crude pig gastric mucus appearing as a dark band at the top of the gel (see red box). A large amount of mucin did not enter the stacking gel for the crude mucus material (Figure 3.5, lane 1), and stained as a 'blob' with PAS, indicating the presence of mucin in the crude material. As the purification steps continued,

there was some loss of mucin (Figure 3.5, lanes 2 – 3). The bigger mucins stayed in the stacking gel or stayed in the top of the well (see red boxes) unless treated with DTT or trypsin. After two density gradient ultracentrifugations, the mucin had moved further into the stacking gel (Figure 3.5, lane 2) (see second red box) more than the crude mucus (Figure 3.5, lane 1). There was less of this 'blob' after mucin purification (Figure 3.5, lane 2) and some mucin positive material is shown to have migrated into the stacking gel. In fact there is some staining at the beginning of the running gel (Figure 3.5, lane 2), suggesting the presence of subunit in the original crude material (see second red box), as described previously for pig gastric mucin (Mall et al., 1999; Pearson et al., 1981). Figure 3.5, lane 3 shows the PGM V_0 fraction eluted through a Sepharose 2B column after two density gradient ultracentrifugations. The V_0 shows the larger mucins did not readily move into the gel (see red boxes). Figure 3.5, lane 4 (PGM V_i) contrasted with Figure 3.5, lane 3 which showed smaller mucins that moved further down the gel (see red box). DTT treatment (Figure 3.5, lane 5) allowed more mucin subunits to enter the well and increased migration down the gel (see red box). Trypsin treatment (Figure 3.5, lane 6) allowed more subunit material into the stacking gel and into the top of the running gel (see red boxes). It is possible that bands seen at the interface of the stacking gel and running gel may be due to the presence of cell surface mucins.

3.1.6 Slot Blot Analysis of PGM

Antibodies used for this study (see Appendix A, Table 1 for antibody type and dilutions) were mostly raised against human gastric proteins. The antibody supplier's website confirmed sequence similarity and binding would occur between antibodies raised against human gastric mucins and pig gastric mucins. At the time of the study the availability of antibodies to South Africa, raised to pig gastric mucins were limited and extremely expensive. Figure 3.6 shows the slot blot detection of Muc5ac and Muc6 performed on PGM extracted from this study.

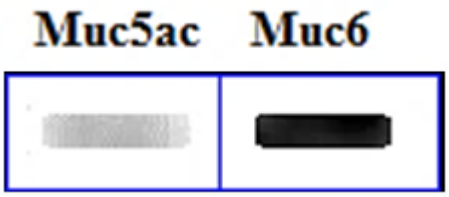

Figure 3.6 Slot Blot analysis of PGM. The left panel shows pig gastric mucins (having undergone 2 density gradient ultracentrifugations, dialysis against distilled water and freeze drying) dissolved in 100ml 2% SDS, 1% glycerol and 0.01% bromophenol blue. Samples were then transferred under

vacuum to a nitrocellulose membrane and split. The membrane in the left block was probed first with rabbit anti-human Muc5ac antibody (1in 5000 dilution) then goat anti-rabbit secondary antibody conjugated to horse radish peroxidase (HRP) (1in 5000 dilution). The membrane in the right block was probed first with rabbit anti-human Muc6 antibody (1in 1000 dilution) then goat anti-rabbit secondary antibody conjugated to HRP (1in 5000 dilution).

PGMs tested positive for both Muc5ac and Muc6. To assess the regional expression of Muc5ac and Muc6 in pig stomach, mucus from four histologically different sections (see Figure 3.7) were collected and separately underwent purification with two rounds of density gradient ultracentrifugation (Chapter 2, sections 2.4 to 2.6).

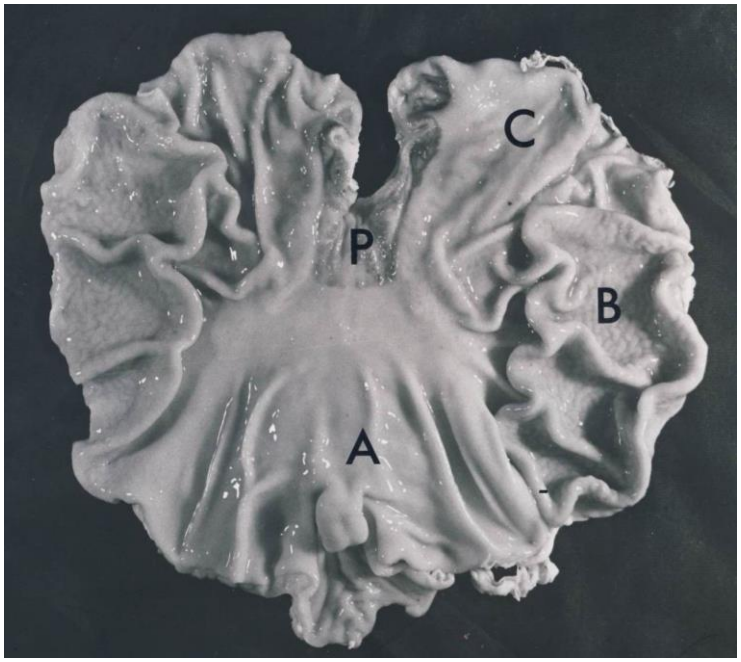

Figure 3.7 Diagram of the pig stomach opened along the greater curvature stomach (Mall, 1984). P, pars oesophagea; C, the cardiac gland; B, body and A, pyloric antrum.

Pigs and humans both have a monogastric or simple single-chambered stomach. Figure 3.7 illustrates the general regions shared by all monogastric stomachs (Colville et al., 2008). The regions under investigation are the pars oesophagea, the cardiac gland area, the body area, the pyloric antrum. Figure 3.8 shows the slot blot analysis of these regions.

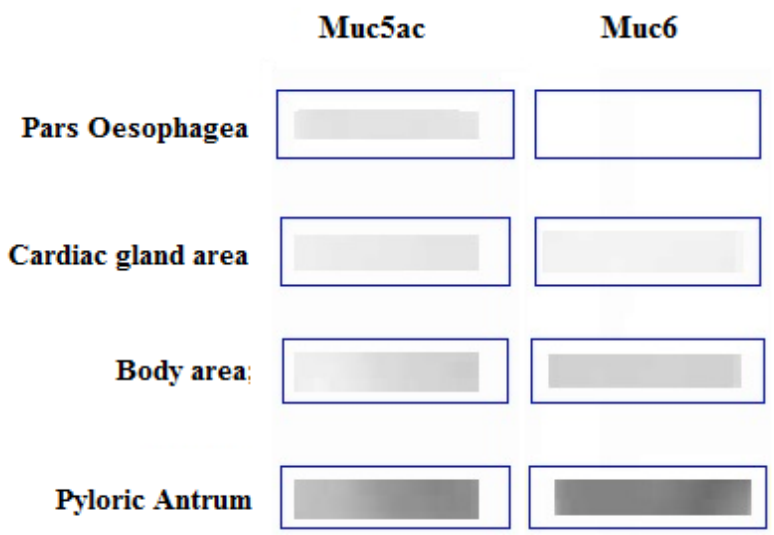

Figure 3.8 Regional expression of Muc5ac and Muc6 in pig stomach

Muc5ac is present throughout the regions but is present at high concentrations in the pyloric antrum, whereas Muc6 is present mostly in the body and antrum regions. It is partially expressed in the cardiac and absent in the pars oesophagea.

3.2 Discussion

In the past, our laboratory has done significant work on the effect of human mucins on HIV-1 *in vitro* (Habte et al., 2010; Habte et al., 2008; Habte et al., 2007; Habte et al., 2006; Mthembu et al., 2014; Peacocke et al., 2012). This included saliva, breast-milk and cervico-vaginal material. From that preliminary data, the importance of mucins and their inhibitory effects on HIV-1 could be seen. However, sourcing human material has its limitations, partly because human material is difficult to obtain and the amount of mucin retrieved after purification was minute (depending on the source and time of day) (Dawes, 1972; Hardt et al., 2005; Koh et al., 2007). Our research into the effects of mucin on HIV-1 began with human salivary studies. Collecting saliva was difficult partly because many individuals were uncomfortable about donating saliva. There was huge variability in the amount of sample from different individuals due to diurnal variations in secretions and the difficulty of collection from all volunteers at a specific time. The mucin yield could be negligible after purification if the original volume of saliva was low. However, the importance of a study such as this was noted from the preliminary data. To further our research, we required an abundant source of mucins that were like human mucins and would have a similar inhibitory effect on HIV-1. This study bridged that gap by

investigating the effect animal sourced mucins and its derivatives had on pseudo-HIV-1 subtype C *in vitro*. The chosen animal sources were pig (gastric, salivary, cervico-vaginal mucus) and horse (salivary) mucus. The rationale for our pig model was derived from previous experiments performed by our laboratory and other groups (Carlstedt et al., 1995; De Bolós et al., 1995; Ho et al., 1995; Mall et al., 1997b; Meurens et al., 2012; Nordman et al., 1998). Horse saliva was sought after the study by Rousseau *et al* (2008).

The derivatives of pig gastric mucin tested in this experiment were commercially bought pig gastric mucin Type II from Sigma-Aldrich® Co (St Louis, MO, USA), and mucin derived from crude mucus scrapings of pig stomachs obtained from the local abattoir. Stomachs were opened along the greater curvature, gently rinsed with running water, and the mucus scraped off the mucosal surface with a glass slide (Figure 3.7). This crude PGM was purified by density gradient ultracentrifugation in CsCl and called purified PGM. It was further eluted through column chromatography and the V_0 collected as purified PGM V_0 (Muc5ac and Muc6) (Nordman et al., 2002; Nordman et al., 1998); the same went for the V_i material, also eluted from a Sepharose 2B column. Finally, we had untreated mucin, DTT treated and trypsin treated aliquots of purified PGM V_0.

After the two density gradient ultracentrifugations, aliquots of pig gastric mucin were eluted through a Sepharose 2B column. Our laboratory has previously used Sepharose 2B gel filtration to separate human gastric mucin so we theorized Sepharose 2B to be the best gel filtration for PGM (Mall et al., 1992). The glycoprotein and protein profile of the Sepharose 2B chromatography is shown in Figure 3.3. The protein content of mucins is approximately 13 – 20% (Allen, 1981b). This low protein content can be seen in Figure 3.3 peak 1 fractions 38 – 56 but the V_i fraction (second peak of Figure 3.3: fractions 116 – 152) appears to have a high protein content. The high protein staining may be due to smaller glycoproteins that have been fractionated with the mucins during density gradient ultracentrifugation in CsCl. These smaller glycoproteins might have a lower carbohydrate to protein ratio than in the larger mucins. Protein peaks are sensitive to the higher protein ratio and show an interference pattern rather than the presence of lingering protein contamination in the sample (Mall et al., 1988). Mucin purification by CsCl density gradient ultracentrifugation is an established method (Creeth & Denborough, 1970) and in this study an additional step of gel filtration was used to ensure that all possible contaminants were separated from the sample (Figure 3.7).

In Figure 3.4, the "smeared" effect across the lanes is attributed to the heterogeneity and polydispersity of glycoproteins (Harding, 1984). Briefly, heterogeneity describes several distinct species in which there is no single molecular weight for the solute species due to (in this case) polydispersity which is defined by the presence of non-interacting constituents of a macromolecular system of different densities or molecular weights (Harding, 1984). Figure 3.5, lane 2 shows a subunit that has moved down form the top of the well (see second red box) after 2 density gradient ultracentrifugations. The relative sizes of mucins that are immobilized at the top of the wells and running gels are in line with the predicted size of subunits (2 – 3MDa) conforming to the linear model of mucin (Carlstedt & Sheehan, 1984). Carlstedt and Sheehan (1984) researched the polymeric structures of mucins from cervical, gastric and respiratory mucus. Carlstedt and Sheehan (1984) extracted mucins in the same buffer that we used for pig gastric mucus (i.e. 6M GuHCl at pH6.5). Pearson *et al* (1981) also found mucin subunits of 2MDa which may suggest windmill conformation, but they also found a 70 – 72kDa linker subunit which is not present in our samples. The key difference of the Pearson *et al* (1981) findings and our study is the extraction buffer. Pearson *et al* (1981) extracted gastric mucins in 0.2M NaCl:0.02% sodium azide whereas we used 6M GuHCl with protease inhibitors (10mM Na_2HPO_4, 10mM EDTA, 1mM PMSF and 5mM NEM) at pH6.5. Removing mucins from 6M GuHCl with the above protease inhibitors causes aggregation resulting in the appearance of larger mucin subunits (Mall et al., 1988).

The slot blot analysis of our mucins was carried out with antibodies raised against human mucins MUC5AC and MUC6 (Appendix, Table 1). This was primarily due to the suppliers lacking antibodies raised to pig mucins of interest (i.e. Muc5ac, Muc5b, Muc6, Muc7 and Muc19). There were also logistic issues as suppliers who did have pig mucin antibodies did not ship to South Africa. Muc5ac is present throughout the regions whereas Muc6 is present mostly in the body and antrum regions. It has partial expression in the cardiac and not (or possibly at lower than the detectable limit) in the pars oesophagea. Our results confirm the immunohistological findings of Nordman *et al* (2002). They showed that MUC5AC was present in surface epithelia of the stomach regions (cardiac, body and antrum regions) and Muc6 was present in the glands of those regions (Nordman et al., 2002). Glandular restricted expression of MUC6 explains why we did not find any Muc6 in the pars oesophagus as this section represents the non-glandular region.

CHAPTER 4: THE EFFECT OF PGM DERIVATIVES ON HIV-1 *IN VITRO*

4.1 Results

4.1.1 PGM derivatives Inhibit HIV-1 on the Pseudoviral Assay

To assess the value of pig gastric mucin derivatives as a potential component of an anti-HIV-1 gel, samples were tested on a pseudoviral assay. Pseudoviral data (see section 2.12 for method) was put into Graphpad Prism Version 6 to construct Log Dose Response Curves (see Figure 4.1). From these curves the half maximal inhibitory concentration was calculated.

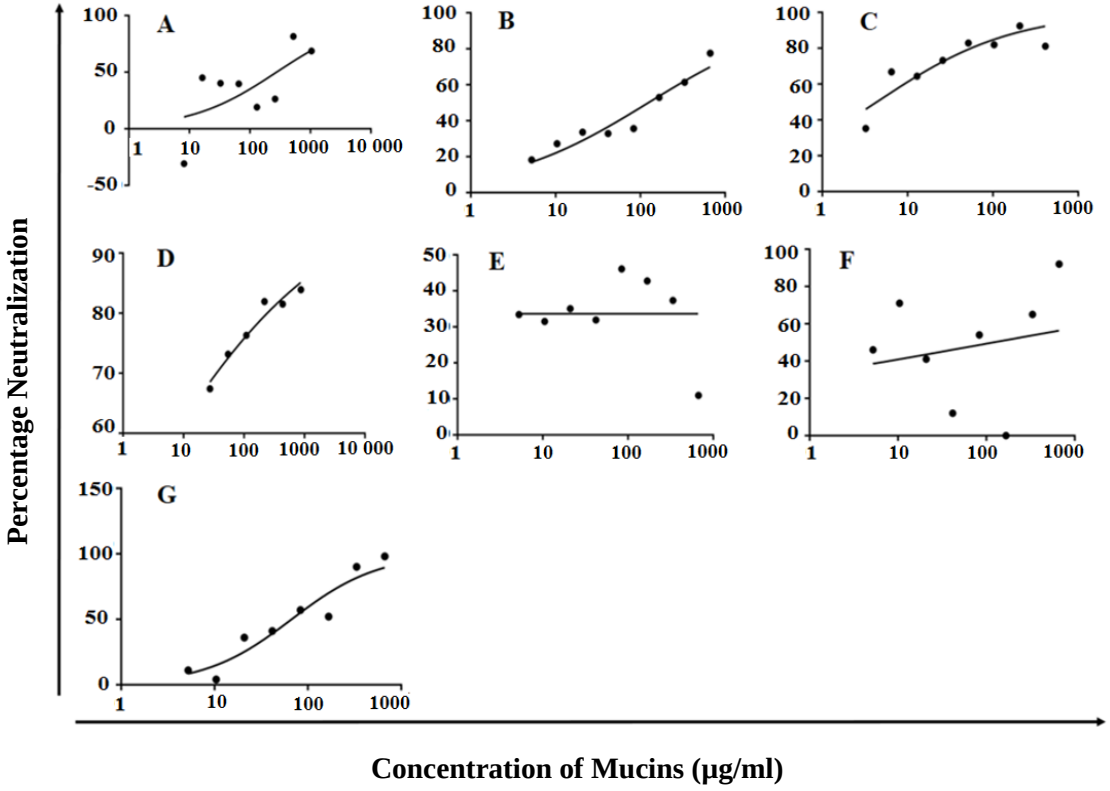

Figure 4.1 Dose response curves of PGM derivatives. A, commercially bought pig gastric mucin from Sigma Aldrich; B, crude pig gastric mucin; C, purified PGM after two density gradient ultracentrifugations; D, PGM V_0 (Muc5ac and Muc6) eluted from Sepharose 2B column chromatography after two density gradient ultracentrifugations; E, PGM V_i eluted from Sepharose 2B column chromatography density gradient ultracentrifugations; F, DTT treatment of PGM V_0 (Muc5ac and Muc6) and G, trypsin treatment of the intact PGM V_0 (Muc5ac and Muc6).

Reliability of the log dose response curves can be assessed visually by how close the points of the curve lie to the solid trend line. Commercial pig gastric mucin (Figure 4.1 A), PGM V_i (Figure 4.1 E) and DTT treated PGM V_0 (Figure 4.1 F) had the least reliable curves. From the curves in Figure 4.1, an IC_{50} was calculated for each sample. The IC_{50} for this study is defined as the concentration of mucin required to inhibit HIV infection by 50% (Montefiori, 2009). Table 4.1 show the summary of Graphpad Prism calculations and the effectiveness of the treatments on PGM in retarding HIV-1 infection.

Table 4.1 The calculated PGM IC_{50}'s and 95% Confidence Intervals

Pig Gastric Mucin Derivative	**IC_{50} (µg/ml)**	**95% Confidence Intervals (µg/ml)**
Commercial Pig Gastric Mucin	276.1	35.16 to 2168
Crude PGM	124.2	75.83 to 203.5
Purified PGM	10.50	7.065 to 15.60
PGM post-CsCl V_0 (Muc5ac and Muc6)	1.668	0.4136 to 6.725
PGM V_i	No Inhibition	
DTT treated PGM V_0 (Muc5ac and Muc6)	110.1	46.52 to 260.6
Trypsin treated PGM V_0 (Muc5ac and Muc6)	66.95	37.72 to 118.8

Results were deemed reliable if the IC_{50} was within 3 orders of the 95% Confidence Intervals' lower and upper limits. From that calculation, the above data suggests non-gel forming commercially bought PGM (Schömig et al., 2016) was not as reliable as our other data. PGM V_i did not inhibit HIV-1 as the graph did not converge in Graphpad Prism. Crude pig mucus did inhibit the pseudovirus (IC_{50}: 124.2µg/ml) and inhibition was increased over ten-fold after purification (IC_{50}: 10.50µg/ml). Once the PGM components were separated on size the best inhibition was seen in the PGM V_0 fraction (gel filtration after purification) (IC_{50}: 1.668µg/ml). From this V_0 fraction, disulphide bonds were cleaved with DTT and this drastically reduced inhibition to almost the IC_{50} of crude mucus (IC_{50}: 110.1µg/ml). When the V_0 fraction had the naked protein removed, there was also a reduction in HIV inhibition (IC_{50}: 66.95µg/ml) but not as extensive as the DTT treatment.

4.1.2 Gastric Region-Specific PGM Inhibition of HIV-1 on Pseudoviral Assay

Crude and purified PGM from different regions of the pig stomach were also tested on the pseudoviral assay. Figure 4.2 shows the log dose response curves of the assay.

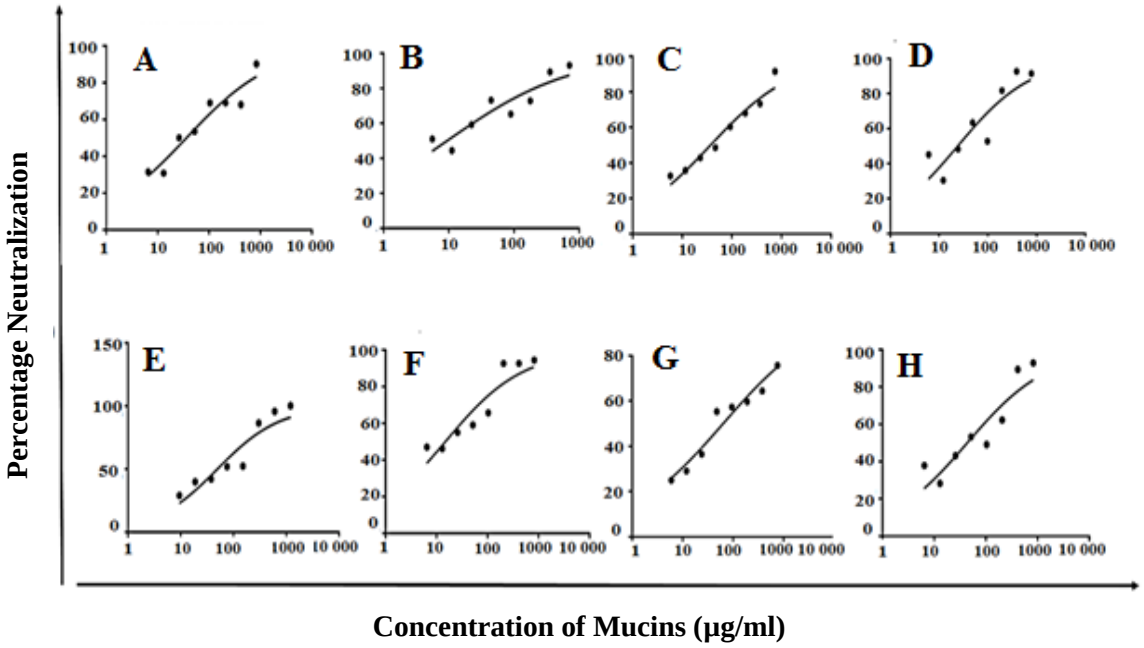

Figure 4.2 Dose response curves of PGM from different regions of the pig stomach. Scraping from different regions of pig stomachs were kept separate, purified and run on the HIV-1 pseudoviral assay. A, crude pars oesophagea mucus; B, purified pars oesophagea mucin; C, crude cardiac gland mucus; D, pure cardiac gland mucin; E, crude body mucus; F, purified body mucin; G, crude pyloric antrum mucus and H, purified pyloric antrum mucin.

All points in the curves adhered to the trend line and were reliable. Table 4.2 shows the summary of Graphpad Prism calculations and the effectiveness of PGM from different regions of the pig stomach on halting HIV-1 infection.

Table 4.2 Showing the calculated regional PGM IC_{50}'s and 95% Confidence Intervals

Mucins from Gastric Regions	**IC_{50} (µg/ml)**	**95% Confidence Intervals (µg/ml)**
Crude Pars Oesophagea Mucus (Muc5ac)	37.12	25.18 to 54.74
Purified Pars Oesophagea Mucin (Muc5ac)	24.09	10.31 to 56.29
Crude Cardiac Gland Mucus (Muc5ac and Muc6)	36.14	21.51 to 60.73
Purified Cardiac Gland Mucin (Muc5ac and Muc6)	9.392	3.772 to 23.38
Crude Body Mucus (Muc5ac and Muc6)	49.24	25.68 to 94.44
Purified Body Mucin (Muc5ac and Muc6)	14.89	7.065 to 31.38
Crude Pyloric Antrum Mucus (Muc5ac and Muc6)	63.67	42.83 to 94.65
Purified Pyloric Antrum Mucin (Muc5ac and Muc6)	43.60	20.34 to 93.46

Both the crude and purified regions of PGMs inhibited HIV-1 *in vitro* suggesting that all regions have anti-HIV-1 potential. The lowest mucin IC_{50}'s and hence best HIV-1 inhibition came from purified mucins of the cardiac gland and body area.

4.1.3 Toxicity Assay for Pig Gastric Mucin

Toxicity was assessed by running the samples on the same cell line as the pseudoviral assay (TZM-bl/JC53, Hela cell line). Use of the same cell line assured that any cytotoxic effects of mucin did not interfere with inhibition data. LD_{50} values were calculated from percentage cell viability data. LD_{50} in this study is defined as the lethal dose of mucin derivative that results in 50% cell death. Commercial PGM, crude PGM, purified PGM, PGM V_0 (Muc5ac and Muc6), DTT treated PGM V_0 (Muc5ac and Muc6), trypsin treated PGM V_0 (Muc5ac and Muc6) samples were tested for cell toxicity using an MTT assay (see section 2.13). Table 4.3 shows the results of the MTT assay.

Table 4.3 The Results of PGM derivatives on an MTT Assay

PGM Derivative	**LD_{50} (µg/ml)**	**Concentration (µg/ml)**	**% Cell Viability**
Commercially bought PGM	Curve did not converge	196.25	100
Crude PGM (Muc5ac and Muc6)	2 428		
Purified PGM (Muc5ac and Muc6)	29 727		
PGM post-CsCl V_0 (Muc5ac and Muc6)	363		
PGM V_i	Curve did not converge	153.75	60.64
DTT treated PGM V_0 (Muc5ac and Muc6)	~8.351		
Trypsin treated PGM V_0 (Muc5ac and Muc6)	293.6		

There were high LD_{50}s for crude PGM, Purified PGM, PGM V_0 and trypsin treated PGM V_0 indicating that higher doses of these mucins are required to be lethal. DTT treated PGM V_0 had a low LD_{50} calling into question the validity of the DTT treated PGM V_0 IC_{50} data. Further analysis is required to determine the reason for this. Commercially bought PGM and PGM V_i did not produce curves from which LD_{50} values could be calculated. The percentage cell viabilities quoted for these samples were at a concentration closely related to their corresponding IC_{50} (from section 4.1.2). Commercially bought PGM showed good percentage cell viability (100%) at 196.25µg/ml which is close to its IC_{50} (IC_{50}: 276.1µg/ml). This suggests that commercially bought PGM IC_{50} data is trustworthy. In contrast, PGM V_i had low percentage cell viability (60.64%) at 153.75µg/ml, suggesting that the toxicity of PGM V_i may have contributed to PGM V_i having no HIV inhibitive properties. Therefore, it appears that toxicity of PGM derivatives (excluding PGM V_i and DTT treated PGM V_0) does not substantially interfere with measurement of HIV-1 inhibitory activity.

4.2 Discussion

4.2.1 PGM inhibits HIV-1 *in vitro*

In 2012, Lieleg *et al* (2012) investigated pig gastric mucin as an anti-viral agent but unlike our study which looked at HIV-1, they tested pig gastric mucin against HPV-16, MCV and H1N1 Influenza Virus. They purchased non-gel forming commercial pig gastric mucins from Sigma-Aldrich® Co, St Louis, MO, USA. They combined this mucin with HEPES buffer and commercial Matrigel to form a biolpolymer on the surface of human cervical cell lines (for

fluorescently labelled HPV-16) and kidney cell lines (for fluorescently labelled MCV and H1N1 influenza virus) to test viral inhibition. They found inhibition of MCV, H1N1 and HPV-16 using 0.25 – 1% mucin gels (Lieleg et al., 2012). This result showed the ability of PGM to act as an antiviral agent. Lieleg *et al* (2012) did not look at HIV as their laboratory was not certified to work with HIV (personal communication with Dr. Katharina Ribbeck). We hypothesized that the inhibitory potential may be higher in gel forming pig gastric mucin purified from pig stomachs rather than the use of commercial non-gel forming PGM in the Lieleg *et al* (2012) study. Since studies in our laboratory have shown that human salivary, breast milk and cervical plug mucins have inhibitory activity against HIV-1, we proposed pig gastric mucins would have similar effects because of suggested biological similarities between pig and human (Mall et al., 1997b; Nordman et al., 1997; Nordman et al., 1998) against HIV-1. This was worth testing and the study of Lieleg *et al* (2012) was encouraging in this regard.

PGM derivatives in our study were tested on a pseudoviral assay at neutral pH (~6.5 – 7.2). At this pH PGM Hong *et al* (2005) predicted PGM to exist as an extended fibre-like conformation (400nm) in a dilute solution. This was proven by utilizing atomic force microscopy (Hong et al., 2005). Our study measured inhibition by calculating the IC_{50} from log dose response curves. Inhibition of HIV-1 was seen in all derivatives but one, the PGM V_i fraction. The commercial mucin (like the commercial mucin used by Lieleg *et al* (2012)) had the highest IC_{50} (276.1µg/ml, see Table 4.1) from the inhibiting mucins and the widest range of 95% Confidence Intervals. Wider confidence intervals of mucin derivatives indicate there is little knowledge of the true inhibitory effect of commercial pig gastric mucin on HIV-1 (Higgins & Green, 2011). After performing two density gradient ultracentrifugations and dialysing against three changes of distilled water, native pig gastric mucus yielded the second lowest IC_{50} (10.50µg/ml, see Table 4.1) which was over 20 times more effective than commercial PGM. After eluting this purified PGM through a Sepharose 2B column, the larger fraction containing Muc5ac and Muc6, the PGM V_0 had an IC_{50} of 1.668µg/ml (see Table 4.1). When this experiment with the same material was repeated a year later it gave an IC_{50} of 4.35µg/ml (data not shown) indicating the low IC_{50} is reproducible. Once the PGM V_0 underwent disulphide bond cleavage (DTT treated PGM V_0) or proteolysis (trypsin treated PGM V_0) the inhibitory potential dropped (110.1 and 66.95µg/ml respectively, see Table 4.1). Reduction of disulphide bridges of mucin polymer results in the production of ~500kDa subunits (Allen, 1981a; Mall et al., 1988; Pearson et al., 1981) or ~2MDa (Carlstedt et al., 1983a; Mall et al., 1988; Mall et al., 1987), suggesting that polymer is required for effective inhibition of HIV-1. The differences

in size between mucins extracted in non-denaturing versus denaturing medium (Carlstedt et al., 1983a; Mall et al., 1988) are significant. Mucins in this study were prepared in 6M GuHCl with protease inhibitors 10mM Na_2HPO_4, 10mM EDTA, 1mM PMSF and 5mM NEM, perhaps resulting in a more effective inhibition of HIV-1, if this inhibition is by aggregation due to the oligosaccharide components of the mucins. Georgiades *et al* (2014) showed that in the conditions of denaturation with the use of a chaotrophic agent (GuHCl) and DTT, PGM exists as an untangled polyelectrolyte comb (Georgiades et al., 2014). This is indicative of the importance size and entanglement plays on the HIV-1 inhibitory activity of PGM V_0. Entanglement or aggregation of HIV-1 by mucins has been reported to be a possible mechanism for inhibition of HIV-1 by mucins (Bergey et al., 1994; Bergey et al., 1993b) A cell viability assay was necessary to show the effect of mucins on the cervical cell line and that the calculated IC_{50} values were not due to false inhibition because of mucin induced cell death (this would lower the luminescence emission). There were generally good cell viability data for PGM derivatives (see Table 4.3) apart from PGM V_i (cell viability at 153.75µg/ml was 60.64%), DTT treated PGM V_0 (LD_{50}: ~8.351µg/ml). Cell viabilities were good for commercially bought PGM (at 196.25µg/ml, percentage cell viability: 100%; IC_{50}: 276.1µg/ml), crude PGM (LD_{50}: 2 428µg/ml; IC_{50}: 124.2µg/ml), purified PGM (LD_{50}: 29 727µg/ml; IC_{50}: 10.50µg/ml), PGM V_0 (LD_{50}: 363µg/ml; IC_{50}:1.668 µg/ml) and trypsin treated PGM V_0 (LD_{50}: 293.6µg/ml; IC_{50}: 66.95µg/ml) thus their corresponding IC_{50} values were deemed reliable. Trypsin treated PGM V_0 (IC_{50}: 66.95µg/ml) showed a lower IC_{50} than DTT treated PGM V_0 (IC_{50}: 110.1µg/ml) indicating that the size of the mucin is not the full explanation of PGM inhibiting HIV-1 in vitro. Further studies need to be done on this point to decipher what other mechanisms may be contributing to inhibition.

4.2.2 Mucins from four regions of the pig stomach inhibit HIV-1 *in vitro*

Our next experiment assessed the effect of mucins from four different regions (namely the pars oesophagea, cardiac gland area, body area, pyloric antrum) of the pig stomach on HIV-1 *in vitro*. The results of this investigation would streamline mucus collection for future pig gastric research. Mucins from all regions of pig stomach showed inhibition with narrow 95% confidence intervals. The tight 95% confidence intervals are indicative that the mucin specific inhibition of HIV-1 was a real effect and not a false positive. Differential mucin inhibition of HIV-1 was seen after purification by two density gradient ultracentrifugations. The two lowest IC_{50} values were seen in the purified mucins of the cardiac gland (IC_{50}: 9.392µg/ml, see Table 4.2) and purified body regions (IC_{50}: 14.89µg/ml, see Table 4.2). This is interesting because

the cardiac gland area of the pig stomach is adjacent to the non-glandular pars oesophagea, an extension of the oesophagus into the pig stomach (see Figure 3.7)**,** a region of keratinized squamous epithelium. Pigs spontaneously ulcerate in this region through stress (change of pens, transport to abattoir and human contact etc.) and with 100% reproducibility after the ligation of the bile-duct (Mall et al., 1997b). The region is protected by the flow of mucus from the cardiac gland area and so it would be expected that this region would produce significant amounts or a different kind of mucus (Mall et al., 1997b). These findings have made the pig a very suitable model for the study of gastric ulceration (Mall et al., 1997a), especially for the role of mucus in the context of the use of anti-ulcer preparations (Mall et al., 1991) and *H. pylori* and its role in gastric ulceration (Mall et al., 2004).

In 1997, Karlsson *et al* performed high temperature gas chromatography mass spectrometry (GC-MS) and matrix-assisted laser-desorption mass spectrometry (MALDI-MS) to investigate oligosaccharides from different regions of pig gastric mucosa (Karlsson et al., 1997). Oligosaccharides present in mucins are mostly linked by a Ser(Thr)-GalNAc bond to the polypeptide chain (Allen, 1981a; Chantler, 2012). The most common sugars occurring in mucins are GalNAc, Gal, Fuc, GlcNAc and sialic acid (Chantler, 2012). Many mucins are sulphated at either Gal or GlcNAc. Mucin oligosaccharide structures are divided into four groups: Type 1 core (Galβ1-3GalNAc-), Type 2 core (Galβ1-3[GlcNAcβ1-6]GalNAc), Type 3 core (GlcNAcβ1-3GalNAc1) and Type 4 core (GlcNAcβ1-3-[GlcNAcβ1-6]GalNAc) (Chantler, 2012). Chantler *et al* (2012) found significant differences between the regions, for instance, oligosaccharides containing Galβ1-3GalNAcα1- and Galβ1-3(GlcNAcβ1-6)GalNAcα1- were widely distributed. The cardiac gland area and body region are the only sections that express GlcNAβ1-3GalNAα1- structures. Chantler *et al* (2012) noted that GlcNAcβ1-3(GlcNAcβ1-6)GalNAcα1- oligosaccharides were restricted to the cardia region. They also reported that GlcNAc addition in β1-linkage to both the C-3 and C-6 of protein bound GalNAc is limited to the cardia of the stomach. This substitution results in mucins from the cardiac gland region to undergo additional glycosylation. The most characteristic difference they found was that the oligosaccharides present in the body region were larger in size (7 to 18 residues) than any other region of the gastric mucosa. This was the result of an increased number of *N*-acetyl-lactosamine units in linear arrangement. Karlsson *et al* (1997) noted that the core mucin structures (type 1 core, type 2 core, type 3 core and type 4 core) present in the pig stomach are the same as human gastric mucins (Hanisch et al., 1993). Karlsson *et al* (1997) rationalized that the presence of both shorter and longer oligosaccharides in gastric mucosa

offer modified structure and protection. Karlsson et al (1997) hypothesized that shorter, less complex oligosaccharides promote highly glycosylated domains to an extended conformation, whereas the longer glycans may offer protection by acting as interactive binding sites for bacterial surface proteins mucosa. This finding may highlight the importance of preserving the polymeric structure when studying mucin specific inhibition of HIV. Our study showed that the differential mucin structures gave rise to varied regional IC_{50}'s on the Pseudoviral assay. The more glycosylated cardiac gland region (purified cardiac mucin), showed the best inhibition (IC_{50}: 9.392µg/ml, see Table 4.2). This data may highlight the importance of mucin glycosylation in viral inhibition. Purified mucin from the body region of the stomach (as previously mentioned, had the longest oligosaccharides) show the second lowest IC_{50}'s (14.89µg/ml, see Table 4.2) compared to the unseparated purified PGM (10.50µg/ml). A summary of this can be seen below in Table 4.4.

Table 4.4 Shows the IC_{50} data and oligosaccharide types of pig gastric regions

Mucins from Gastric Regions	**IC_{50} in µg/ml**	**Oligosaccharides (Karlsson et al., 1997)**
Crude Pars Oesophagea Mucus (Muc5ac)	37.12	The mucus here is a combination of mucus from other regions of the stomach. The pars oesaphageal does not secrete mucus. It is made of keratinizing squamous epithelial cells (Orlando, 1991).
Purified Pars Oesophagea Mucin (Muc5ac)	24.09	The mucus here is a combination of mucus from other regions of the stomach. The pars oesaphageal does not secrete mucus. It is made of keratinizing squamous epithelial cells (Orlando, 1991).
Crude Cardiac Gland Mucus (Muc5ac and Muc6)	36.14	Galβ1-3GalNAcα1- (Type 1 core), Galb1-3(GlcNAcβ1-6)GalNAcα1- (Type 2 core), GlcNAcβ1-3GalNAcα1- (Type 3 core) GlcNAcβ1-3(GlcNAcβ1-6)GalNAcα1- (Type 4 core)
Purified Cardiac Gland Mucin (Muc5ac and Muc6)	9.392	Galβ1-3GalNAcα1- (Type 1 core), Galb1-3(GlcNAcβ1-6)GalNAcα1- (Type 2 core), GlcNAcβ1-3GalNAcα1- (Type 3 core) GlcNAcβ1-3(GlcNAcβ1-6)GalNAcα1- (Type 4 core)
Crude Body Mucus (Muc5ac and Muc6)	49.24	Galβ1-3GalNAcα1 (Type 1 core) Galβ1-3(GlcNAcβ1-6)GalNAcα1 (Type 2 core) GlcNAβ1-3GalNAα1 (Type 3 core)
Purified Body Mucin (Muc5ac and Muc6)	14.89	Galβ1-3GalNAcα1 (Type 1 core) Galβ1-3(GlcNAcβ1-6)GalNAcα1 (Type 2 core) GlcNAβ1-3GalNAα1 (Type 3 core)
Crude Pyloric Antrum Mucus (Muc5ac and Muc6)	63.67	Gal-3GalNAcol (Type 1 core) Gal-3(GlcNAc-6)GalNAcol (Type 2 core)
Purified Pyloric Antrum Mucin (Muc5ac and Muc6)	43.60	Gal-3GalNAcol (Type 1 core) Gal-3(GlcNAc-6)GalNAcol (Type 2 core)

Our data show that PGM derivatives are effective in inhibiting HIV-1 *in vitro* and would be a good candidate for an anti-HIV-1 vaginal gel to be used prior to sexual intercourse, as an additional barrier against HIV transmission (Lai et al., 2009).

Lai *et al* (2009) showed that cervicovaginal mucus, obtained from donors with normal lactobacillus-dominated vaginal flora, efficiently traps HIV, causing it to diffuse more than 1000-fold more slowly than it does in water. This is due to the acidification of the mucus by Lactobacilli, which produce lactic acid which acts by abolishing the negative surface charge on HIV without lysing the virus membrane, and facilitating its entrapment in the mucus (Lai et al., 2009). The surface charge of HIV at pH 7 lactic acid showed a negative charge but that negative charge was lost when the lactic acid solution was lowered to pH 4 where lactate ions are negatively charged themselves. Pig gastric mucus, like human gastric mucus, forms a mucus gel barrier on the mucosal surface of the stomach and protects it from the shear forces associated with digestion and the potency of hydrochloric acid and pepsin (Allen et al., 1983; Mall et al., 1997b; Rees et al., 1982). A vaginal anti-HIV-1 gel, acidic in nature (Lai et al., 2009) would have the right properties to act as a barrier against transmission of the virus during sexual intercourse.

CHAPTER 5: THE EFFECT OF PIG SALIVARY MUCIN (PSM) DERIVATIVES ON HIV-1 *IN VITRO*

5.1 Results

5.1.1 The Purification of PSM

5.1.1.1 Sepharose 4B Column Chromatography of Pig Saliva

Pig saliva was collected in 0.2M NaCl:0.02% sodium azide (see Appendix section 1.2). Samples were pooled and centrifuged to eliminate contaminants. Thereafter, saliva in 0.2M NaCl:0.02% sodium azide was eluted on a Sepharose 4B column (eluting buffer was also 0.2M NaCl:0.02% sodium azide). Aliquots of pooled pig saliva samples shared a similar profile to each other after Sepharose 4B column chromatography. Figure 5.1 is a representative sample of protein and glycoprotein distribution after PSM was run on the Sepharose 4B column.

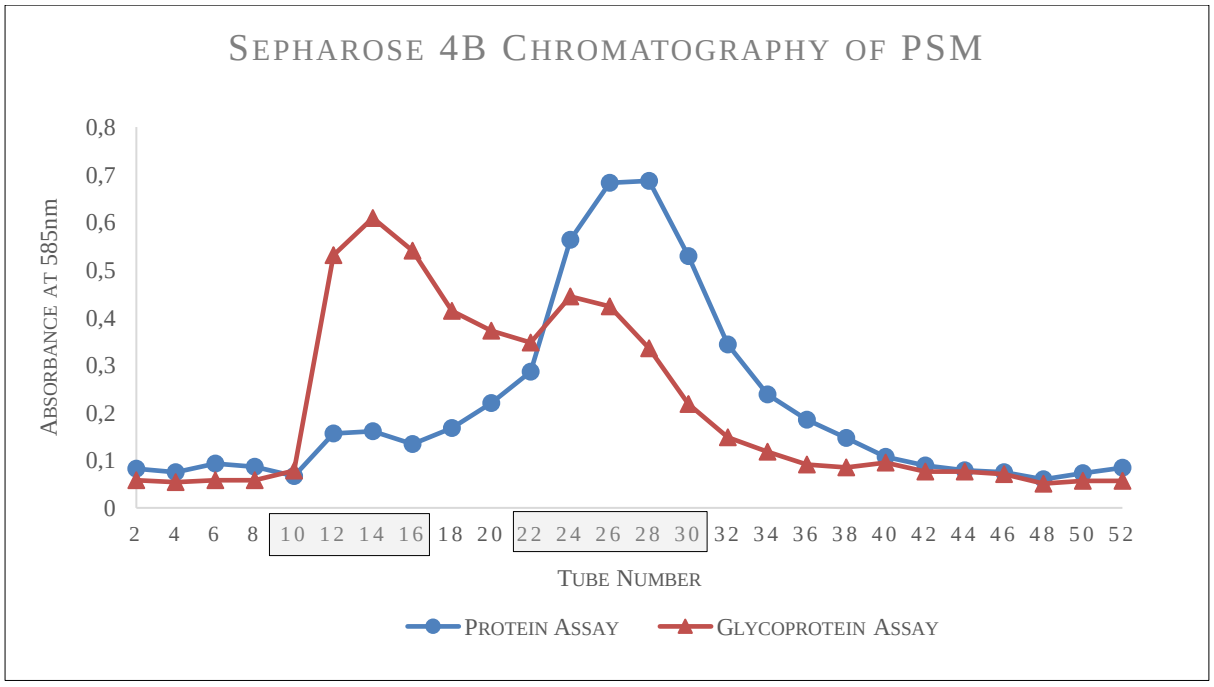

Figure 5.1 Sepharose 4B separation profile of PSM in 0.2M NaCl:0.02% sodium azide. Pig saliva was diluted with 0.2M NaCl:0.02% sodium azide (4:1), centrifuged and eluted through a Sepharose 4B glass column under peristaltic pressure. Every second fraction was tested for proteins and glycoproteins. Protein content was determined using Bradford Reagent assay (—●—); and glycoprotein content was identified using a PAS assay (—▲—). The box on the X-axis represents fractions that were pooled.

A distinct PAS positive peak eluted in the V_0 of the column (Figure 5.1, fractions 10 – 16), suggesting the presence of large polymeric mucin in the purified sample. Another PAS positive peak can be seen in the V_i (Figure 5.1, fractions 22 – 30). The PAS positive V_i peak is indicative of a smaller mucin or other glycoproteins present in saliva. The V_0 and V_i fractions were then dialysed against distilled water over three changes for a minimum of 6 hours each at 4ºC and then freeze dried. For this study, we were interested in the mucins present in the V_0. Thus, the V_0 fractions were set up for further purification.

5.1.1.2 Ultracentrifugation of PSM V_0

Aliquots of lyophilized V_0 were dissolved in 4M GuHCl (see Appendix section 1.3). The density was adjusted and samples ultracentrifuged as stated in section 2.4. Figure 5.2 shows the protein, glycoprotein and density profiles of a representative sample.

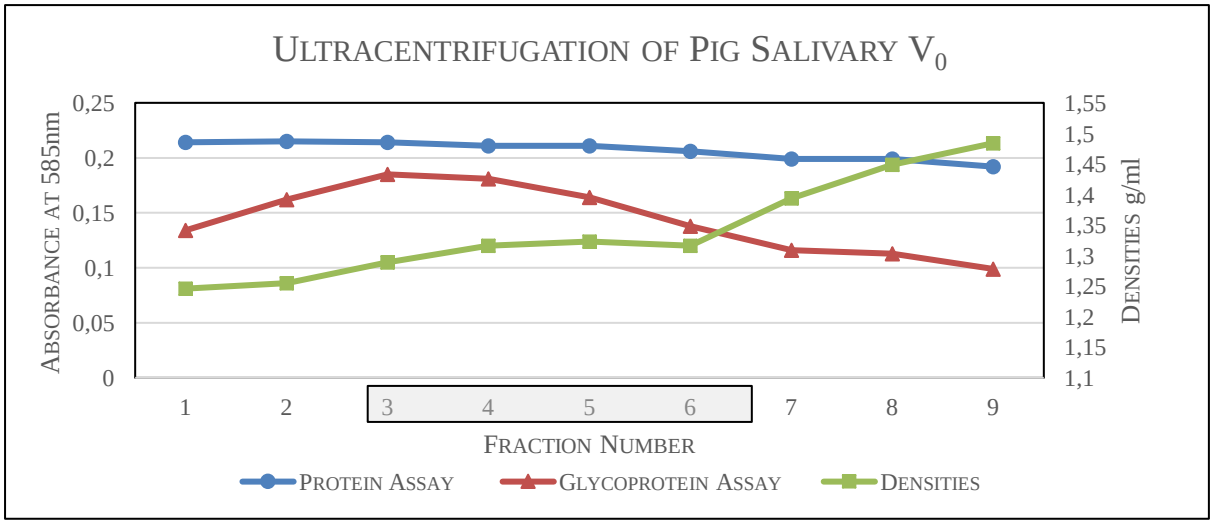

Figure 5.2 Ultracentrifugation profile of PSM V_0. Lyophilized aliquots of PSM V_0 were dissolved in 4M GuHCl. Samples then had their densities adjusted to 1.39g/ml with caesium chloride and 4M GuHCl. They were then subjected to a 48-hour ultracentrifugation at 105 000g at 4ºC. Protein content was determined using Bradford Reagent assay (—●—); glycoprotein content was identified using a PAS assay (—▲—) and the densities (—■—) were recorded on the secondary axis. The box on the X-axis represents the fractions collected for dialysis against distilled water over three changes of a minimum of 6 hours each at 4ºC and freeze dried.

Samples that had high glycoprotein content and a density of 1.40 – 1.41g/ml were pooled. In Figure 5.2 fractions 3 – 6 were pooled. They were then dialysed against distilled water over three changes for a minimum of 6 hours each at 4°C and freeze dried.

5.1.1.3 Sepharose 4B separation of PSM V_0 Muc19

Proteomic analysis carried out by Rousseau *et al* (2008) showed the presence of Muc19 and Muc5b in pig saliva. To separate Muc19 and Muc5b, new pig saliva samples collected in 0.2M NaCl:0.02% sodium azide were eluted through a Sepharose 4B column. Unlike the Sepharose 4B column in section 5.1.1, the fraction collector was set to collect 500µl per tube instead of the previous 1ml per tube. This was done to elicit broader V_0 peaks to better separate Muc19 and Muc5b. Figure 5.3 is a representative sample of protein and glycoprotein distribution after PSM was eluted through a Sepharose 4B column.

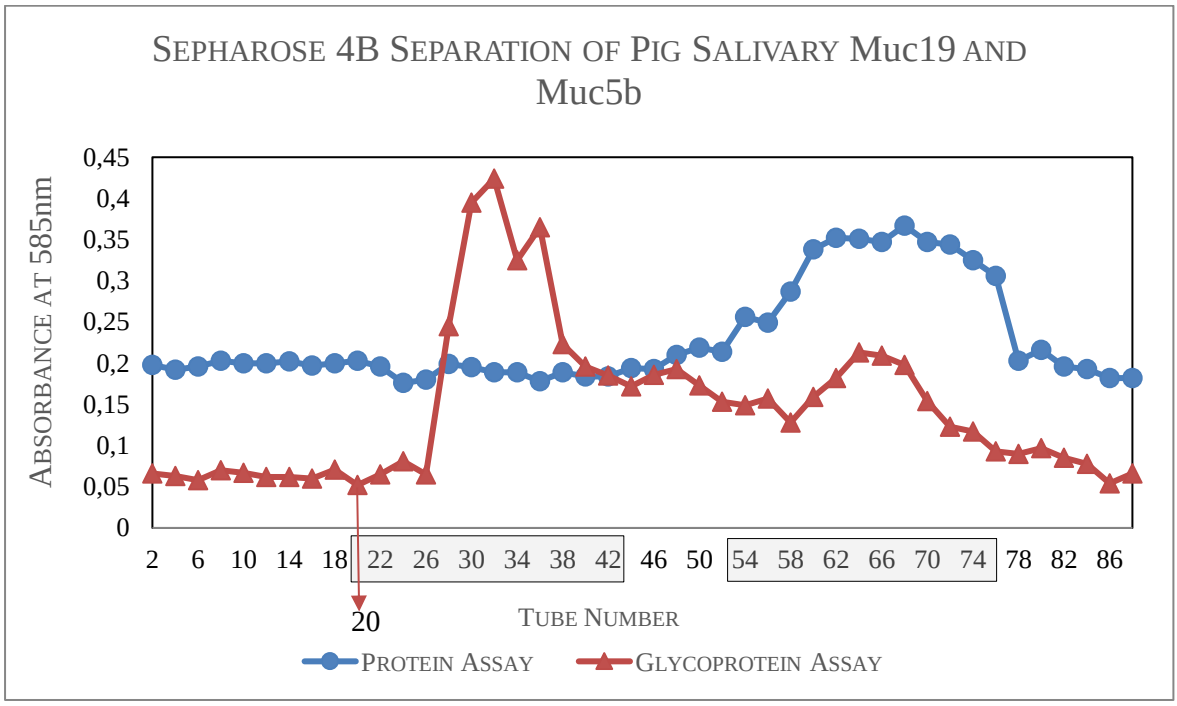

Figure 5.3 Sepharose 4B separation of pig salivary Muc19 and Muc5b in salt azide. Pig saliva was diluted with 0.2M NaCl:0.02% sodium azide (4:1), centrifuged and eluted through a Sepharose 4B glass column under peristaltic pressure. Fractions were collected at 500µl per tube. Every second fraction was tested for proteins and glycoproteins. Protein content was determined using Bradford Reagent assay (); and glycoprotein content was identified using a PAS assay (). The box on the X-axis represents fractions that were pooled.

In Figure 5.3, fractions 20 to 42 were designated the V_0 and fractions 54 to 74 were designated the V_i. Due to limiting amounts of Muc19 antibody, only the fractions corresponding to the V_0 peak was assessed under slot blot analysis. The V_0 fractions were kept separate and set up for slot blot analysis (see section 2.10). Information on the Muc5b and Muc19 antibodies used for the slot blot can be seen in Appendix, Table 1. Figure 5.4 shows the results of slot blot analysis on the V_0 fractions in Figure 5.3. They have been aligned with their fraction number to show the presence of Muc5b and Muc19.

Fractions →	20	22	24	26	28	30	32	34	36	38	40	42
Muc19	positive 	positive 	positive 	positive 	positive 	positive 	positive 	positive 	positive 	positive 	positive 	positive 
Muc5b	negative	positive	positive	positive	positive	positive	positive	positive	positive	negative	negative	negative

Figure 5.4 Slot blot analysis of Muc19 and Muc5b in PGM V_0. PSM was run on a Sepharose 4B column collecting 500µl per tube. The V_0 fractions then underwent slot blot analysis to determine the presence of Muc19 and Muc5b. Figure 5.4 is divided into three panels. The top panel shows the fraction number. The second panel from the top shows the expression of Muc19. The bottom panel shows the presence of Muc5b. The antibodies used for this slot blot were anti-horse Muc19 (1:1000 dilution) and anti-human MUC5B (1:2000 dilution).

In Figure 5.4, fractions 20 and 38 – 42 stained positive for Muc19 in the absence of Muc5b. These fractions were pooled and then dialysed against 4M GuHCl over three changes for a minimum of 6 hours each at 4°C. The volume of 4M GuHCl was at least 20 times the volume of V_0.

5.1.1.4 Ultracentrifugation of PSM V_0 Muc19

In Figure 5.4, Muc19 positive fractions (fractions 20 and 38 – 42) were pooled and prepared for a density gradient ultracentrifugation. The density of the sample was adjusted to 1.41g/ml and subjected to a 48-hour ultracentrifugation at 105 000g at 4°C. Figure 5.5 shows the protein, glycoprotein and density profiles of a representative sample.

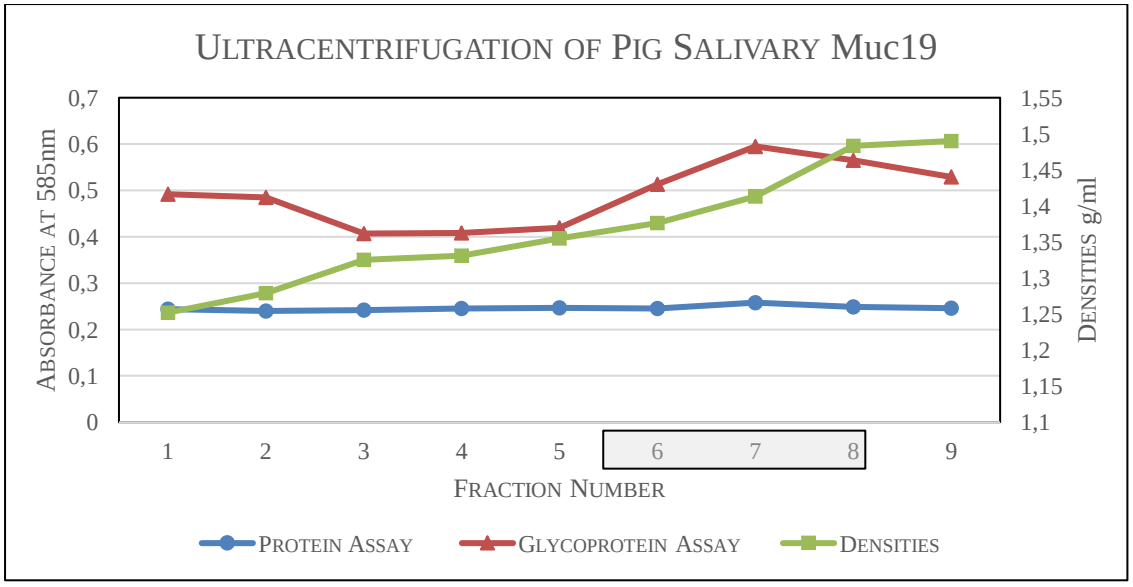

Figure 5.5 Ultracentrifugation profile of pig salivary Muc19. Pig salivary mucus was passed through a Sepharose 4B column and the V_0 fractions containing Muc19 only were pooled. They were then dialysed against 4M GuHCl over three changes for a minimum of 6 hours each at 4ºC. Samples densities were adjusted to 1.41g/ml with caesium chloride and 4M GuHCl, before undergoing ultracentrifugation for 48 hours at 105 000g at 4ºC. Protein content was determined using Bradford Reagent assay (—●—); glycoprotein content was identified using a PAS assay (—▲—) and densities (—■—) were recorded on the secondary axis. The box on the X-axis represents the fractions collected for dialysis against distilled water and freeze dried.

Fractions that had glycoprotein rich densities of 1.39g/ml to 1.41g/ml were pooled. In Figure 5.5 fractions 6 – 8 were pooled. These samples were dialysed against 3 changes of distilled water for 6 hours each, then freeze dried for further investigation.

5.1.1.5 SDS-PAGE 4 – 20% Gradient Gel Electrophoresis

Aliquots of samples were run on an SDS-PAGE gradient gel (4 – 20%) before and after reduction with DTT and proteolysis with trypsin of PSM. Figures 5.6 and 5.7 are SDS-PAGE gels stained for protein (see section 2.9.2) and PAS (see section 2.9.3) respectively.

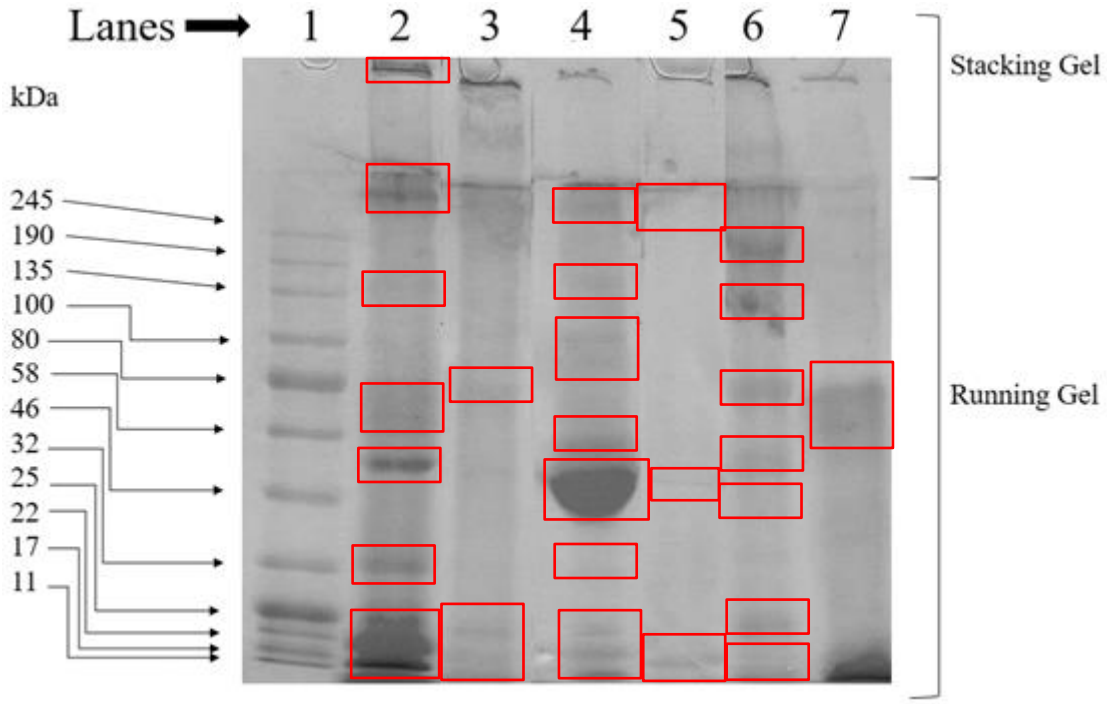

Figure 5.6 Protein stained 4 – 20% gradient SDS-PAGE gel of PSM derivatives. At different stages of pig gastric mucin purification and treatment, 1mg lyophilized aliquots were dissolved in 100µl 2%SDS, 1% glycerol and 0.01% bromophenol blue for SDS-PAGE gel investigation. Lane 1, 10µl of Thermo Scientific PageRuler Prestained Protein Ladder; Lane 2, crude pig saliva; Lane 3, purified Sepharose 4B V_0 fraction density gradient ultracentrifugation (from section 5.1.2, Figure 5.2) (Muc5b and Muc19); Lane 4, Sepharose 4B V_i fraction (from section 5.1.1, Figure 5.1) (Muc7), Lane 5, purified PSM V_0 Muc19 fraction density gradient ultracentrifugation (from section 5.1.4, Figure 5.5); Lane 6, DTT treatment of the Sepharose 4B V_0 fraction (Muc5b and Muc19) and in Lane 7 was trypsin treated Sepharose 4B V_0 fraction (Muc5b and Muc19).

Gel electrophoresis showed that all samples had varying amounts of large material that remained in the stacking gel (Figure 5.6, lanes 2 – 7). Bands or regions of interest were highlighted as red boxes. More visible material was also present in the form of a smear at the beginning of the running gel, which is very likely subunit material of the larger mucin, an expected behaviour of mucins on gels (Mall et al., 1999; Mall et al., 1997b; Newton et al., 1998; Pearson et al., 1981) (Figure 5.6, lanes 2 – 4 and 6). Untreated crude pig saliva (Figure 5.6 lane 2) showed several protein bands visible at varying sizes (red boxes). Figure 5.6 lane 3 shows the purification of Sepharose 4B V_0 fraction by density gradient ultracentrifugation in CsCl (from section 5.1.2, Figure 5.2). Ultracentrifugation (Figure 5.6, lane 3) resulted in proteins moving down the gel (red boxes) that were previously immobilised at the top of the

running gel in Figure 5.6 lane 2. Protein bands were seen at 80, 22, 17 and 11kDa (red boxes in Figure 5.6, lane 3). The smaller proteins present in Figure 5.6 lane 2 were eluted in the V_i fraction (Figure 5.6 lane 4, red boxes). The Muc19 eluted material from the V_0 of the Sepharose 4B column (from section 5.1.4, Figure 5.5) (Figure 5.6, lane 5) and the trypsin treated V_0 carrying both Muc5b and Muc19 (lane 7) showed very little subunit material. In fact, treatment with trypsin (lane 7) showed a strong band in the region of 40 – 50kDa (red box). Figure 5.6, lane 6 shows the density gradient ultracentrifugation purified V_0 fraction after DTT treatment. Here it can be seen that the bands previously present at the top of the stacking and running gel (Figure 5.6 lane 3) have moved down the gel. Most notably bands appeared at 190, 135, 80, 58, 32, 22, 17 and 11kDa (Figure 5.6, lane 6, red boxes). Figure 5.6, lane 7 shows the effect trypsin had on the naked regions of the mucin. In this lane, there is an increase in the mucin smear effect from 80 to 11kDa.

5.1.1.6 PAS Stained SDS-PAGE 4 – 20% Gradient Gel Electrophoresis

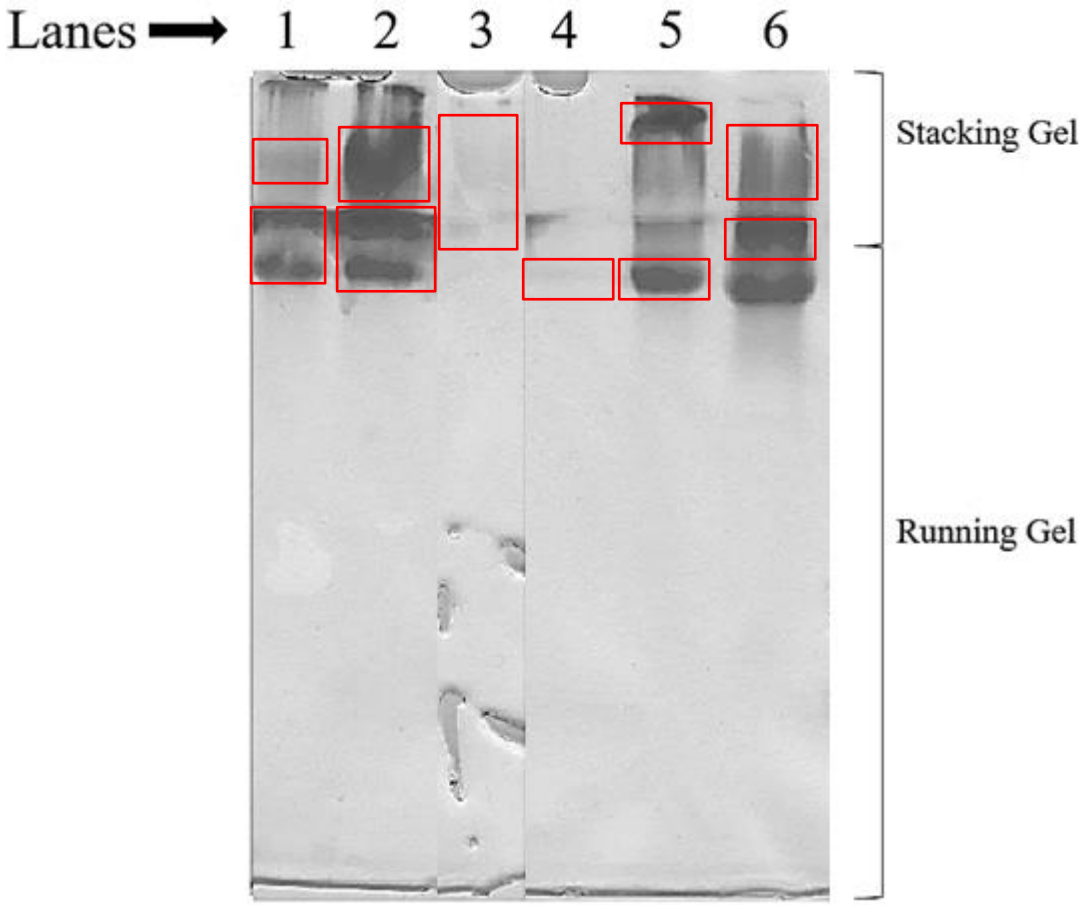

Figure 5.7 Glycoprotein stained 4 – 20% gradient SDS-PAGE gel of PSM. At different stages of pig saliva purification and treatment, 1mg aliquots were dissolved in 100ml Sample Application Buffer for SDS-PAGE gel investigation. Lane 1, crude pig saliva; Lane 2, Sepharose 4B V_0 fraction purified after density gradient ultracentrifugation (from section 5.1.2, Figure 5.2) (Muc5b and Muc19); Lane 3, Sepharose 4B V_i fraction; Lane 4, ultracentrifugation purified Sepharose 4B separated Muc19 (from section 5.1.4, Figure 5.5); Lane 5, DTT treatment of the Sepharose 4B V_0 fraction (Muc5b and Muc19) and Lane 6, trypsin treatment of the Sepharose 4B V_0 fraction.

Figure 5.7 illustrates the PAS stained distribution of PSM and its derivatives through an SDS-PAGE (for method see Section 2.9.2). The result of the staining showed prominent bands of mucin present in the top of the stacking gel and running gel (Figure 5.7, lanes 1, 2, 5 and 6). Figure 5.7 lane 1 shows crude mucus partially in the stacking gel and immobilised in the top of the running gel (see red boxes). Figure 5.7, Lane 2 shows the density gradient

ultracentrifugation of PSM Sepharose 4B V_0 fraction (from section 5.1.1.2, Figure 5.2). Lane 2 shows a band in the stacking gel (see first red box) and two distinct bands at the top of the running gel (see second red box) (similar to Lane 1). Figure 5.7, lane 3 shows the V_i of PSM eluted through a Sepharose 4B column. This lane shows faint mucin smearing banding pattern in the stacking gel and at the top of the running gel (see red box). Figure 5.7, lane 4 shows ultracentrifugation purified Sepharose 4B separated Muc19 (from section 5.1.1.4, Figure 5.5). There was a loss of mucin going through purification, and this is reflected by the faint staining but there is a very faint band that moved a little into the running gel (see red box). Figure 5.7, lane 5 shows DTT treatment of the Sepharose 4B V_0 fraction (from section 5.1.1.2, Figure 5.2). DTT treatment resulted in the disappearance of bands previously seen in the stacking gel (Figure 5.7, lane 2, first red box) and in the start of the running gel (Figure 5.7, lane 2, first band in the second red box). DTT treatment also resulted in a thick band at the top of the stacking gel. Trypsin treatment (Figure 5.7, lane 6) allowed more subunit material into the stacking gel (see first red box) and into the top of the running gel (see second red box).

5.1.1.7 Slot Blot Analysis of PSM

Figure 5.4 shows the Muc5b and Muc19 slot blot of PSM but the MUC7 antibody available to us (see Appendix Table 1.) did not work for both the PSM V_0 and V_i (data not shown).

5.1.2 PSM derivatives Inhibits HIV-1 on a Pseudoviral Assay

We measured the ability of pig salivary mucin isolates to inhibit HIV-1 entry into a model target cell line, TZM-bl (Montefiori, 2009). PSM derivatives were assessed on a pseudoviral assay. Data recorded from a luminometer was analysed on Microsoft Excel where percentage neutralizations were calculated based on negative and positive controls. This data was put into Graphpad Prism Version 6 to construct Log Dose Response Curves (Figure 5.8). From these curves IC_{50} values were calculated.

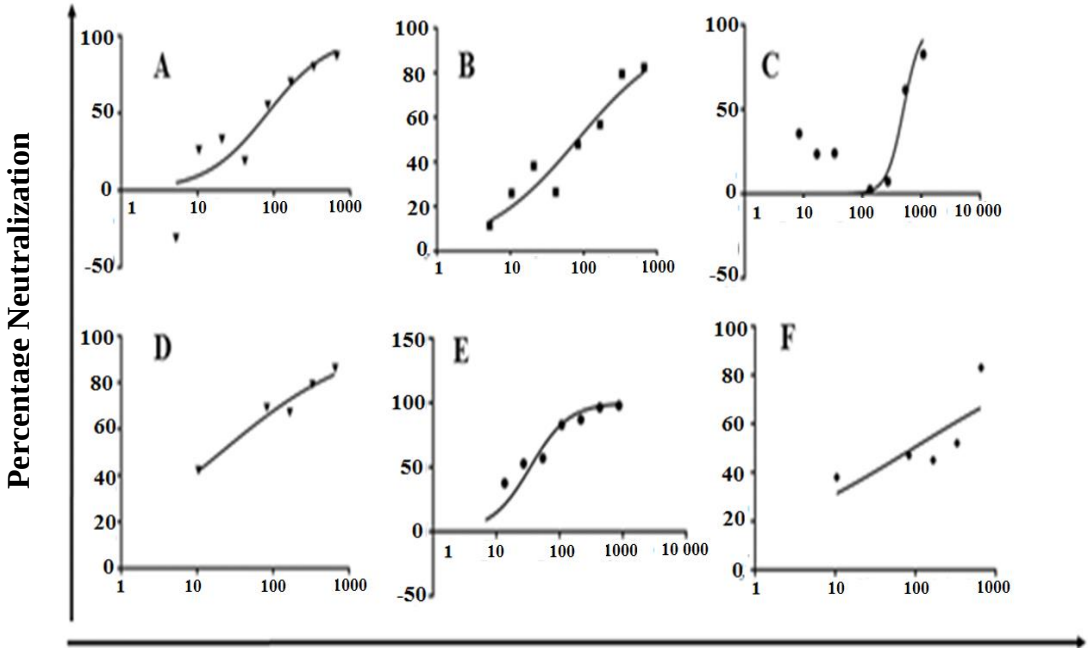

Figure 5.8 Log dose response curve of PSM derivatives. A, crude pig saliva; B, PSM V_0 eluted from Sepharose 4B column chromatography and subjected to density gradient ultracentrifugation (Muc5b and Muc19); C, PSM V_i eluted from Sepharose 4B column chromatography (Muc7); D, DTT treatment of PSM V_0 (Muc5b and Muc19); E, trypsin treated PSM V_0 (Muc5b and Muc19) and F, PSM V_0 Muc19 eluted from Sepharose 4B column chromatography.

Reliability of the log dose response curves can be assessed visually by how close the points of the curve lie to the solid line, which corresponds to the best model of an inhibition curve. Points on the curve for PSM V_i (Figure 5.8 C) showed substantial deviation for the modelled inhibition curve and PSM Muc19 (Figure 5.8 F) also showed deviation to a lesser extent. Table 5.1 shows the calculated 95% confidence interval of the IC_{50} value based upon the level of deviation of the points from the modelled inhibition curve.

Table 5.1 The calculated PSM IC_{50}'s and 95% Confidence Intervals

Pig Salivary Mucin Derivative	**IC_{50} (µg/ml)**	**95% Confidence Intervals (µg/ml)**
Crude PSM	83.67	50.17 to 139.6
PSM V_0 (Muc5b and Muc19)	23.61	13.89 to 40.13
PSM V_i	498.9	277.0 to 898.6
DTT treated PSM V_0 (Muc5b and Muc19)	20.79	9.100 to 47.48
Trypsin treated PSM V_0 (Muc5b and Muc19)	34.44	16.35 to 72.54
PSM Muc19	94.43	9.829 to 907.2

All PSM derivatives showed HIV-1 inhibition *in vitro*. The PSM Muc19 IC_{50} (IC_{50}: 94.43µg/ml) was the only one to lie outside three times the upper and lower limits of its 95% Confidence Intervals. The IC_{50} for Crude PSM (IC_{50}: 83.67µg/ml) improved almost 4-fold after elution through a 4B Sepharose column and undergoing one round of density gradient ultracentrifugation (PSM V_0 IC_{50}: 23.61 µg/ml). The PSM V_i showed the least inhibition (IC_{50}: 498.9µg/ml), more so than the crude (IC_{50}: 83.67µg/ml). This may have been due to gel filtration removing Muc7 and contaminants from the crude PSM. DTT treatment of PSM V_0 did not change the IC_{50} by much (PSM V_0 IC_{50}: 23.61 µg/ml, DTT treated PSM V_0 IC_{50}: 20.79 µg/ml). Trypsin treatment decreased inhibition of HIV-1 by almost half (IC_{50}: 34.44µg/ml). Muc19 had an IC_{50} above that of crude PSM, but as stated the data was not as reliable as other data (IC_{50}: 94.43µg/ml).

5.1.3 Toxicity Assay for PSM

Crude PSM, PSM V_0 having undergone density gradient ultracentrifugation (Muc5b and Muc19), PSM V_i, DTT treated PGM V_0 (Muc5b and Muc7), trypsin treated PGM V_0 (Muc5b and Muc19) and PSM V_0 Muc19 (having undergone density gradient ultracentrifugation), were tested for cell toxicity using an MTT assay (see section 2.13). It was necessary to run our samples on this toxicity assay to ensure the inhibition seen in the pseudoviral assay was not the result of mucin derivatives killing TZM-bl cell targets. Table 5.2 shows the results of this MTT assay.

Table 5.2 The Results of PSM Derivatives on an MTT Assay

Pig Salivary Mucin Derivative	**LD_{50} (µg/ml)**	**Concentration (µg/ml)**	**% Cell Viability**
Crude PSM	Curve did not converge	62.50	64.36
PSM V_0 (Muc5b and Muc19)	3 446		
PSM V_i (Muc7)	943.9		
PSM V_0 treated with DTT (Muc5b and Muc19)	1 247		
PSM V_0 treated with Trypsin (Muc5b and Muc19)	127.2		
PSM V_0 Muc19	Curve did not converge	83.33	180.2

LD_{50} values were calculated for most samples. Dose response curves did not converge for crude PSM and PSM V_0 Muc19, in these instances the percentage viability of mucin close to the calculated IC_{50} was reported. The highest LD_{50} values were seen in PSM V_0 (LD_{50}: 3 446µg/ml) and DTT treated PSM V_0 (LD_{50}: 1 247µg/ml). Crude PSM did not show good cell viability (at 62.50µg/ml there was 64.36% cell viability). PSM Muc19 showed a higher than 100% cell viability at 83.33µg/ml, this may have been due to the constituents of the samples that promote cell division over and above the cell control or interference by cellular enzyme activity (Pozzolini et al., 2003).

5.2 Discussion

5.2.1 Purification and Treatment of PSM derivatives

This part of our project investigated the potential of using PSM as an alternative to human salivary mucin. Previous researchers have shown that there are similarities in tissue distribution and structure between pig and human salivary MUC5B (Eckhardt et al., 1997). *O*-glycan side chains make up ~60 – 70% of PSM mucins' mass. It is believed that these *O*-glycan side chains are responsible for PSM mucins extended structure, resistance to proteases and play an important role in the protective property of PSM mucins (Jentoft, 1990; Shorgen et al., 1989). These extended structures are possible due to intra- and interchain disulphide bonds between half-cysteine residues present in the D-domains (D1, D2 and D3) of PSM von Willebrand factor

domain. Unlike other mucins, the D1-, D2- and D3-domains of PSM are N-glycosylated when expressed in COS-7 cells (Perez-Vilar et al., 1996; Sadler, 1998).

Pig saliva was not collected in guanidine but 0.2M NaCl: 0.02% sodium azide, as a cost saving measure. There were saliva samples collected from 20 pigs and large mucin subunits could still be extracted from 0.2M NaCl. This buffer may have allowed mucins to undergo endogenous proteolysis but this extraction still yields 2MDa subunits (Carlstedt & Sheehan, 1984). Our laboratory has previously eluted human saliva through gel filtration (Sepharose 4B) with 0.2M NaCl: 0.02% sodium azide (Peacocke et al., 2012). A Sepharose 4B column was chosen for PSM as our laboratory had previously separated human salivary mucins by using the same Sepharose 4B gel filtration (Habte et al., 2010; Habte et al., 2006; Peacocke, 2011; Peacocke et al., 2012). Figure 5.1 shows the Sepharose 4B profile of PSM eluted with the same buffer i.e. 0.2M NaCl: 0.02% sodium azide. The Sepharose gel filtration profile of PSM is similar to human saliva showing two mucin rich peaks, one present in the V_0 and the other in the V_i (Habte et al., 2006; Peacocke et al., 2012). The mucin rich peak in the V_0 was smaller than the V_i and contained less protein much like that of human salivary mucins eluted through a Sepharose 4B column (Peacocke et al., 2012).

Figure 5.6 shows the protein staining pattern of PSM derivatives under SDS-PAGE (4 – 20%) gradient gel electrophoresis. Crude pig saliva (Figure 5.6 lane 2) showed many bands especially at the lower end of the gel (last red box). Crude PSM (Figure 5.6 lane 2) showed more protein bands than crude PGM (Figure 3.4, lane 2). After gel filtration (on a Sepharose 4B column) and ultracentrifugation, crude pig saliva the V_0 fraction (Figure 5.6, lane 3) showed no bands below 190kDa. This staining pattern was similar to PGM V_0 (Figure 3.4, lane 4) apart from PSM V_0 (Figure 5.6, lane 3) having a more intense stain in the upper running gel indicating the presence of high molecular weight proteins. The V_i fraction (from section 5.1.1, Figure 5.1) contained the bands below 190kDa (Figure 5.6, lane 4) that were also present in the crude saliva (Figure 5.6, lane 2). The banding patterns displayed by PSM V_0 (purified by ultracentrifugation from section 5.1.2, Figure 5.2) and V_i (Figure 5.6 lanes 3 and 4 respectively) share similar features to human saliva eluted through a Sepharose CL-4B column after two density gradient ultracentrifugations (Habte et al., 2006). The main difference is the presence of more protein bands in the PSM V_0 and V_i (see red boxes). It is important to note that the PSM V_0 underwent just one round of density gradient ultracentrifugation in contrast to the two ultracentrifugations that human saliva had undergone in that study (Habte et al., 2006). The PSM V_i did not undergo a density gradient ultracentrifugation so any contaminating proteins in the V_i had not been

removed and these contaminating proteins are visible in Figure 5.6 lane 4. Previous work done on human saliva by Habte *et al* (2006) also showed multiple bands in the V_i. Habte *et al* (2006) collected human saliva in 6M GuHCl with protease inhibitors (10mM EDTA, 5mM NEM and 0.05% CHAPS at pH6.5) and eluted it on a Sepharose CL-4B gel column with 4M GuHCl. The comparison of our PSM V_i and human saliva V_i from Habte *et al* (2006) is shown in Figure 5.9.

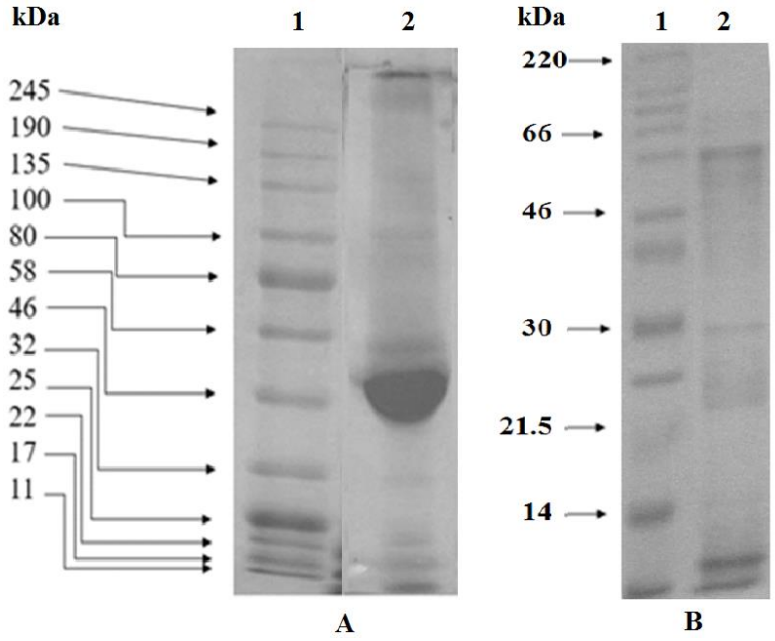

Figure 5.9 Comparison of PSM V_i and human saliva V_i. A, PSM collected in 0.2M NaCl:0.02% sodium azide was eluted through a Sepharose 4B column with the same buffer, then run on a 4 – 20% gradient SDS-PAGE gel and stained for proteins; Lane 1, 10µl of Thermo Scientific PageRuler Prestained Protein Ladder and Lane 2, PSM V_i from the Sepharose 4B column. B, Human saliva collected in 6M GuHCl with protease inhibitors (10mM EDTA, 5mM NEM and 0.05% CHAPS at pH6.5) was eluted on a Sepharose CL-4B column with a buffer made up of 4M GuHCl plus protease inhibitors (10mM EDTA, 5mM NEM and 0.05% CHAPS at pH6.5) and run on a 10% SDS-PAGE gel then stained for proteins; Lane 1, Molecular weight marker; Lane 2, human saliva V_i (Habte et al., 2008).

Human saliva V_i (Figure 5.9, B, Lane 2) showed multiple bands, much like PSM V_i (Figure 5.9, A, Lane 2). PSM V_i (Figure 5.9, A, Lane 2) showed higher molecular weight protein bands than human saliva V_i (Figure 5.9, B, Lane 2). Human saliva V_i (Figure 5.9, B, Lane 2) did not show the protein blob seen at ~46kDa in PSM V_i (Figure 5.9, A, Lane 2). PGM V_i (Figure 3.4, lane 5) showed far less protein bands but a more intense smearing effect than PSM V_i (Figure 5.6, lane 4). Figure 5.6, lane 5 shows Muc19 present in the Sepharose 4B V_0 fraction (from section 5.1.4, Figure 5.5). Muc19 is the largest gel forming mucin (Chen et al., 2004) but from

where our Muc19 samples were eluted off the Sepharose 4B column we may be testing the smallest gene product. The presence of Muc19 has been verified in pig saliva but not in human saliva (Rousseau et al., 2008). This lane (Figure 5.6, lane 5) shows very little protein staining with bands at the start of the running gel, a band just below 58kDa and a band at 17kDa (see red boxes). Low protein staining is expected as very few fractions of the V_0 were taken for Muc19 enrichment. DTT treatment of PSM V_0 fraction (Figure 5.6, lane 6) allowed protein bands to travel further down the lane. Bands in this lane were seen at 245, 190, 135, <80, 58, 46, 32, 22 and 11kDa (see red boxes). The protein band seen below 80kDa (third red box from the top, Figure 5.6, lane 6) may be the 70kDa low molecular weight "link" protein described by Pearson *et al* (1981). The presence of the other bands may be due to degradation. DTT treated PSM V_0 (Figure 5.6, lane 6) showed more protein bands than DTT treated PGM V_0 (Figure 3.4, lane 6). Trypsin treatment of V_0 fraction (Figure 5.6, lane 7) created a protein smear from 80kDa to 11kDa. This contrasted with trypsin treated PGM V_0 that showed a protein smear throughout the lane (Figure 3.4, lane 7).

Figure 5.7 shows the PAS staining pattern of PSM derivatives under SDS-PAGE (4 – 20%) gradient gel electrophoresis. In Figure 5.6, the smear effect, characteristic of mucins, can be seen in lanes 2 – 4, 6 and 7, but when the corresponding derivatives are PAS stained (Figure 5.7, lanes 1, 2, 4 – 6) the smear effect is limited to the top of the running gel and in the stacking gel. One possible explanation is that the amount of mucins present is below the limit of detection for PAS, another reason could be the presence of mucin-like proteins in pig saliva similar to those found in bovine saliva (Bhargava et al., 1990). Figure 5.7, lanes 1, 2 and 6 (lane 1, crude pig saliva; lane 2, Sepharose 4B V_0 fraction purified after density gradient ultracentrifugation (from section 5.1.2, Figure 5.2) and lane 6, trypsin treatment of the Sepharose 4B V_0 fraction show two bands at the top of the running gel. Habte et al (2006) found the same banding pattern present in the V_0 of human saliva eluted through a Sepharose CL-4B column. Kirkham *et al* (2002) performed Western blot analysis on the V_0 of human sputa eluted through a Sepharose CL-2B column and found both bands at the top of the running gel to be MUC5B. A comparison of these bands is shown in Figure 5.10.

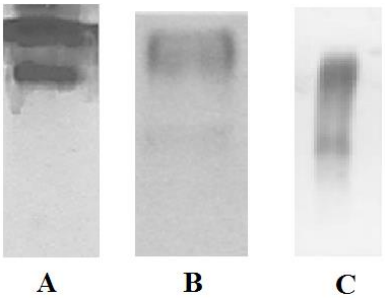

Figure 5.10 Comparison of PAS stained PSM V_0 from this study versus human salivary V_0 from Habte *et al* (2006) and Kirkham *et al* (2002). A, PAS stained bands from the top of the 4 – 20% SDS-PAGE running gel from PSM V_0 Figure 5.7 lane 2; B, PAS stained human salivary V_0 eluted from a Sepharose CL-4B column and run on a 10% SDS-PAGE gel (Habte et al., 2006); C, human saliva V_0 after ultracentrifugation and elution on a Sepharose CL-2B column then reduced, alkylated and run on a 1% w/v agarose gel and transferred to a nitrocellulose membrane for PAS staining (Kirkham et al., 2002).

Kirkham *et al* (2002) proposed that the presence of these two bands is due to the two glycoforms of MUC5B. They suggested MUC5B exists as a high-charge and low-charge glycoform, where the top band was a low-charge MUC5B glycoform that underwent less migration under the influence of an electric current and the lower band was the high-charge MUC5B glycoform that migrated further due to charge (Kirkham et al., 2002). Another contributing factor to the two bands is the presence of Muc19 in pig saliva (Rousseau et al., 2008). Mucins lay in the stacking gel or moved minimally into the running gel, regardless of the treatment. Purifying the PSM Sepharose 4B V_0 fraction (from section 5.1.2, Figure 5.2) with a density gradient ultracentrifugation showed a darker band in the stacking gel and two bands at the top of running gel (Figure 5.7, lane 2). This contrasted with PGM V_0 (Figure 3.5 lane 3, second red box) where a small amount of mucin that had moved into the running gel with no bands present but had a smear effect. Bands in the PSM V_0 (purified through gradient density ultracentrifugation) (Figure 5.7, lane 2) showed darker PAS staining than human saliva eluted through a Sepharose CL-4B column after two density gradient ultracentrifugations (Habte et al., 2006). This may be indicative of more mucin present in pig saliva after purification steps. The V_i fraction of PSM Sepharose 4B gel filtration (Figure 5.7, lane 3) showed very faint smearing of mucins in the stacking gel and a faint band just entering the running gel. The PAS staining of PSM V_i fraction was fainter than the V_i fraction of human saliva eluted through a Sepharose CL-4B column after two density gradient ultracentrifugations (Habte et al., 2006). Human saliva V_i did show patient variability but there was the presence

of two bands, much like our PSM V_i (Habte et al., 2006). A comparison of these results can be seen in Figure 5.11.

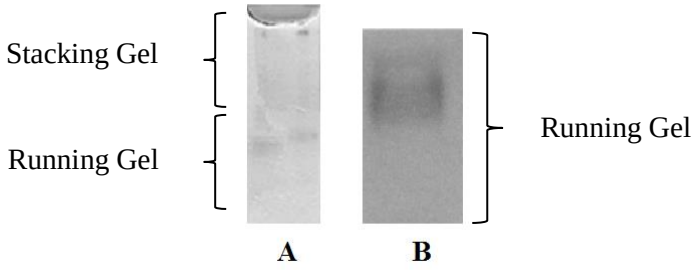

Figure 5.11 Comparison of PSM V_i and human salivary V_i. A, PAS stained bands from the top of the 4 – 20% SDS-PAGE gel from PSM V_i Figure 5.7 lane 3; B, PAS stained human salivary V_i eluted from a Sepharose CL-4B column and run on a 10% SDS-PAGE gel (Habte et al., 2006).

In Figure 5.11, lane A PSM V_i shows two faint bands, the first in the stacking gel and the second in the running gel. Lane B (Figure 5.11) the two bands lie at the top of the running gel. This may be due to two differentially charged glycoforms of Muc7 present in PSM V_i and MUC7 in human salivary V_i. Mucins present in the PGM V_i moved further into the running gel than PSM V_i indicating the mucins present in PGM V_i may have been smaller in size. Muc19 (from section 5.1.4, Figure 5.5) showed faint staining (Figure 5.7, lane 4), with a partially visible band in the top of the running gel (see red box). The location of the band coincides with the lower of the two bands present in Figure 5.7, lanes 1, 2, 5, 6 (lane 1, crude pig saliva; lane 2, Sepharose 4B V_0 fraction purified after density gradient ultracentrifugation (from section 5.1.2, Figure 5.2); lane 5, DTT treatment of the Sepharose 4B V_0 fraction and lane 6, trypsin treatment of the Sepharose 4B V_0 fraction) which indicates that Muc19 may lie in the same region as the high-charge Muc5b glycoform. DTT treatment of the PSM V_0 fraction (Figure 5.7, lane 5) resulted in less banding in the stacking gel and one distinct band in the running gel. It is possible the DTT treatment lowered the charge of one of the Muc5b glycoforms resulting in the immobilized band present at the top of the well in Figure 5.7, lane 5. This difference in migration between the two bands is similar to the DTT treatment of human saliva V_0 (Figure 5.10 lane C (Kirkham et al., 2002)). DTT treated PGM V_0 (Figure 3.5, lane 5) resulted in just one band in the top of the running gel (see red box) and unlike DTT treated PSM V_0 (Figure 5.7, lane 5) there was no band in the stacking gel only a smear of glycoproteins. Trypsin treatment of the PSM V_0 fraction (Figure 5.7, lane 6) showed movement of mucins from the top of the wells into the stacking gel and two thick bands at the top of the running gel. In comparison to the trypsin treatment of PGM V_0 (Figure 3.5, lane 6), PGM V_0 which showed

no bands but intense smearing at the bottom of the stacking gel and the top of the running gel. This may indicate that PSM V_0 (Figure 5.7, lane 6) contained more trypsin sensitive glycoproteins (PSM Muc5b and Muc19) than PGM V_0 (Muc5ac and Muc6).

Slot blot analysis on PSM derivatives was carried out with antibodies raised to human MUC5B and MUC7 (Appendix Table 1). Muc19 antibodies were raised against horse Muc19 (Appendix Table 1). Figure 5.4 confirms the presence of Muc5b and Muc19 in the V_0 fraction. These findings are in line with previous research done by Rousseau et al (2008). They performed proteomic analysis of pig and human saliva and found that Muc19 is present in pig but not human. They could not confirm the presence of Muc5b in pig saliva as there was too little pig *Muc5b* genome sequence data to perform analysis on (Rousseau et al., 2008). The presence of Muc5b in our PSM V_0 fraction (Figure 5.4) was similar to Western blot work done in our laboratory on human saliva MUC5B present in the V_0 of Sepharose 2B and Sepharose CL-4B columns (Habte et al., 2010; Peacocke, 2011; Peacocke et al., 2012). Antibodies raised to pig Muc7 were not available for the duration of this study so the presence of Muc7 was based on previous work on Sepharose gel filtration Vi fractions of human saliva, in our lab and elsewhere (Bobek et al., 1996; Habte et al., 2010; Peacocke, 2011; Peacocke et al., 2012; Thornton et al., 1999). Habte et al (2010) and Peacocke et al (2012) had purified human saliva by subjecting them to density gradient ultracentrifugation. They then eluted the purified products through a Sepharose CL-4B column followed by SDS-PAGE and Western blot analysis on the void and included volumes. MUC7 was shown to be present in human saliva Vi fraction (Bobek et al., 1996; Habte et al., 2010; Peacocke, 2011; Peacocke et al., 2012; Thornton et al., 1999). Multiple methods (within our budget and with the available equipment) were used to try and separate Muc5b and Muc19 from the PSM V_0, but our attempts were unsuccessful (data not shown).

5.2.2 PSM derivatives as an Anti-Viral Agent

Our results showed that PSM derivatives (crude PSM, PSM V_0, PSM V_i, DTT treated PSM V_0, trypsin treated PSM V_0 and PSM Muc19) all inhibited HIV-1 *in vitro*. In 1994, Bergey *et al* (1994) investigated the interaction between salivary mucins and HIV-1. This was the first study to demonstrate mucin induced inhibition of HIV-1 by showing the inhibitory activity of human submandibular-sublingual (HSMSL) gland secretions on viral particles using electron micrographs. After subjecting HSMSL saliva to Sephadex G-200 chromatography, they incubated the mucin rich components with HIV-1 (~100 particles) then filtered the mixture through a low protein binding cellulose acetate 0.22 micrometre filter. The filtrate was added

to HeLa CD4+ cell monolayers for 90 mins of adsorption, thereafter monolayers were fixed with methanol and incubated with anti-HIV antibody (AIDS Research Reference Program, catalogue #192). Plaques were counted on an inverted microscope following the addition of amioethyl carbazol. They found that the mucin-rich fractions reduced the number of infectious units by 75% (Bergey et al., 1994). They then immobilized salivary components onto latex beads and monitored their interaction with HIV particles (including recombinant gp120) with low molecular weight mucin (MUC7). Their electron microscopic data suggested inhibition was due to aggregation of virus particles by the mucin-rich fractions.

Recently, our laboratory also performed experiments investigating how human saliva MUC5B and MUC7 affect HIV-1 infectivity. In 2012 Peacocke *et al* (2012) collected human saliva from HIV negative and positive volunteers and eluted them on a Sepharose CL-4B column. After purifying MUC5B and MUC7 mucins from each cohort, they were individually incubated with HIV-1 subtype C virus. The individual mucins were added to virus and incubated with CD4+ human T cell line (CEM SS) at three different time points. Thereafter the supernatant was collected after 4 days. The supernatant was tested on a qualitative p24 assay to assess viral replication. Peacocke *et al* (2012) showed that both the high and low molecular weight mucin fractions (MUC5B and MUC7) inhibited HIV-1 infection. These findings contrasted with the results of Bergey *et al* (1994), by showing MUC5B had better pseudovirus HIV-1 inhibition than MUC7 (Peacocke, 2011; Peacocke et al., 2012). This study confirmed the importance of salivary mucins in inhibiting HIV-1 *in vitro*.

Our study showed that, much like Peacocke et al (2012), both the high and low molecular weight mucin fractions (MUC5B and MUC7) inhibited HIV-1 infection. From our data, we have shown that all PSM derivatives (crude PSM, PSM V_0, PSM V_i, DTT treated PSM V_0, trypsin treated PSM and PSM Muc19) inhibited an HIV-1 subtype C pseudovirus *in vitro*. The lowest inhibition from our PSM derivatives was seen in the low molecular weight mucin rich fraction of PSM eluted through a Sepharose 4B column (PSM V_i IC_{50}: 498.9µg/ml, see Table 5.1). The PSM derivatives that showed the best HIV-1 inhibition were large molecular weight mucin rich fractions of PSM eluted through a Sepharose 4B column and purified by density gradient ultracentrifugation (PSM V_0 IC_{50}: 23.61µg/ml, see Table 5.1) and PSM V_0 with disulphide bond cleavage (DTT treated PSM V_0 IC_{50}: 20.79µg/ml, see Table 5.1). Both PSM V_0 and DTT treated PSM V_0 have a good 95% confidence interval indicating that this inhibitory effect is reliable. In contrast to the good inhibition shown by DTT treated PSM V_0 (IC_{50}: 20.79µg/ml, see Table 5.1), DTT treated PGM V_0 (IC_{50}: 110.1µg/ml, see Table 4.1) showed

low inhibition which may be due to the collection buffer. PSM was extracted in 0.2M NaCl:0.02% sodium azide which unlike the PGM extraction buffer viz. GuHCl with protease inhibitors, may have rendered PSM susceptible to protease activity. It is possible DTT treatment reduced PSM mucins that were already smaller due to endogenous protease activity, whereas GuHCl and protease inhibitors kept the structural integrity of PGM before DTT treatment. The effect of DTT treatment of PSM collected in GuHCl with protease inhibitors and DTT treated PGM collected in 0.2M NaCl:0.02% sodium azide needs further investigation. This data also indicates PSM V_0 with a mixture of Muc5b and Muc19 subunits inhibit HIV-1 best. This part of our study shows that PSM V_0 and DTT treated PSM V_0 are the best candidates to be components of an anti-HIV-1 gel. When these results are compared to PGM pseudoviral data, we can see that PGM (IC_{50}: 10.50µg/ml, see Table 4.1) and PGM V_0 (IC_{50}: 1.668µg/ml, see Table 4.1) showed better inhibition than our PSM data, making purified PGM the better candidate for an anti-HIV-1 gel.

5.2.3 Toxicity Assay of PSM Derivatives

PSM V_0 (LD_{50}: 3 446µg/ml, see Table 5.2), PSM V_i (LD_{50}: 943.9µg/ml, see Table 5.2), DTT treated PSM V_0 (LD_{50}: 1 247µg/ml, see Table 5.2) and trypsin treated PSM V_0 (LD_{50}: 127.2µg/ml, see Table 5.2) all gave high LD_{50} values. This indicates that their respective IC_{50} values were a true reflection of anti-HIV-1 activity and not a consequence of the mucin being toxic to TZM-bl target cells. LD_{50} values for crude PSM and PSM V_0 Muc19 could not be constructed but the former showed poor percentage cell viability (62.50µg/ml crude PSM showed 64.36%, see Table 5.2) and in contrast the latter showed good percentage cell viability (at 83.30µg/ml PSM V_0 Muc19 showed 180.2%, see Table 5.2).

Our results show that pig salivary mucins can be used for in vitro anti-HIV-1 studies with good inhibition and toxicity data that proves the reliability for our purified PSM derivatives. If an anti-HIV-1 gel were to be constructed from a PSM derivative it would be PSM V_0 (Muc5b and Muc19) as this derivative had good sample yield and showed promising inhibition with a tight 95% confidence interval (increasing the chances that we see a true inhibitory effect from PSM V_0 on pseudoviral HIV-1).

These findings are encouraging because collecting human saliva can be problematic and inconvenient. People are reluctant to donate samples and in most cases, even when they do, the amounts donated are negligible. Pigs produce large amounts of saliva whilst feeding and a minimal number of animals are required to meet our needs for purification of mucins and HIV

assays. There is a possible suggestion here that a mucin does not have to be large and polymeric to inhibit HIV-1. It could be that a mucin fragment with the required number of oligosaccharides or perhaps even the type of sugar side-chain of a specific sequence and composition, could inhibit HIV-1 by aggregation. Further studies are required to accurately determine what role size plays on HIV inhibition.

As far as we know there has not been any work done on the specific interaction between mucins and HIV-1. Our research (Habte et al., 2010; Habte et al., 2008; Habte et al., 2007; Habte et al., 2006; Lieleg et al., 2012; Mthembu et al., 2014; Peacocke, 2011; Peacocke et al., 2012), together with Lieleg *et al* (2012) suggests that inhibition of HIV-1 is by aggregation. This needs further investigation.

CHAPTER 6: THE EFFECT OF PIG CERVICO-VAGINAL MUCINS (PCM) ON HIV-1 *IN VITRO*

6.1 Results

6.1.1 First Ultracentrifugation of Pig Cervico-vaginal Mucus

Aliquots taken from pooled pig gastric mucus samples shared similar profiles to each other after the first density gradient ultracentrifugation process. Figure 6.1 shows the protein, glycoprotein and density profiles of a representative sample.

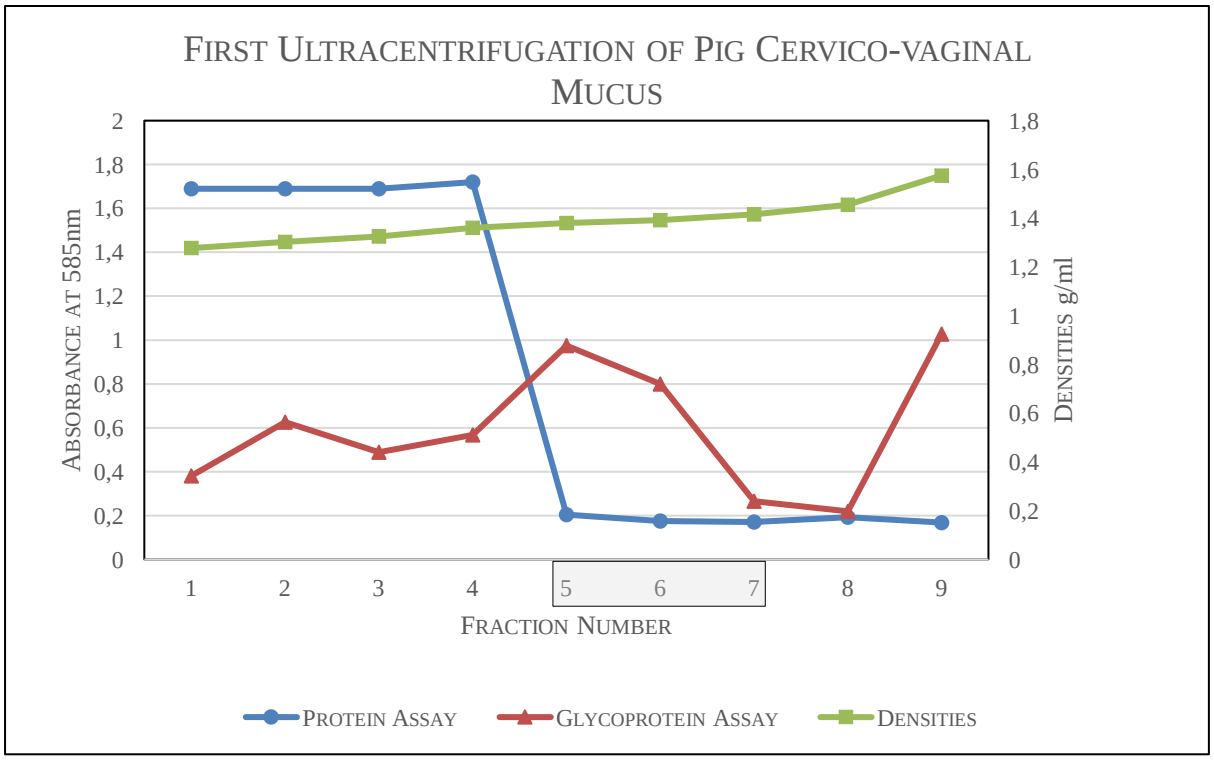

Figure 6.1 First ultracentrifugation profile of pig cervico-vaginal mucus in caesium chloride. Pig cervico-vaginal mucus was slowly stirred overnight in 6M guanidine hydrochloride with 10mM Na_2HPO_4, 10mM EDTA, 1mM PMSF and 5mM NEM. Samples then had their densities adjusted to 1.39g/ml with caesium chloride and 4M GuHCl. They were then subjected to a 48-hour ultracentrifugation at 105 000g at 4℃. Protein content was determined using Bradford Reagent assay (); glycoprotein content was identified using a PAS assay () and the densities () were recorded on the secondary axis. The box on the X-axis represents the fractions collected for a second round of ultracentrifugation enrichment.

Fractions that had glycoprotein rich densities of 1.39g/ml to 1.41g/ml were pooled. In Figure 6.1 fractions 5 – 7 were pooled. These samples were then prepared for a second round of density gradient ultracentrifugation.

6.1.2 Second Ultracentrifugation of Pig Cervico-vaginal Mucus

The densities of the pooled mucin fractions were adjusted to 1.41g/ml by the addition of caesium chloride and 4M GuHCl. Samples were ultracentrifuged under the same conditions as the first ultracentrifugation process. Protein and glycoprotein content as well as densities were all recorded in the same way as the first density gradient ultracentrifugation. The second density gradient ultracentrifugation profiles of pig cervico-vaginal mucus all shared a similar pattern to each other. Figure 6.2 shows the pattern of a representative sample.

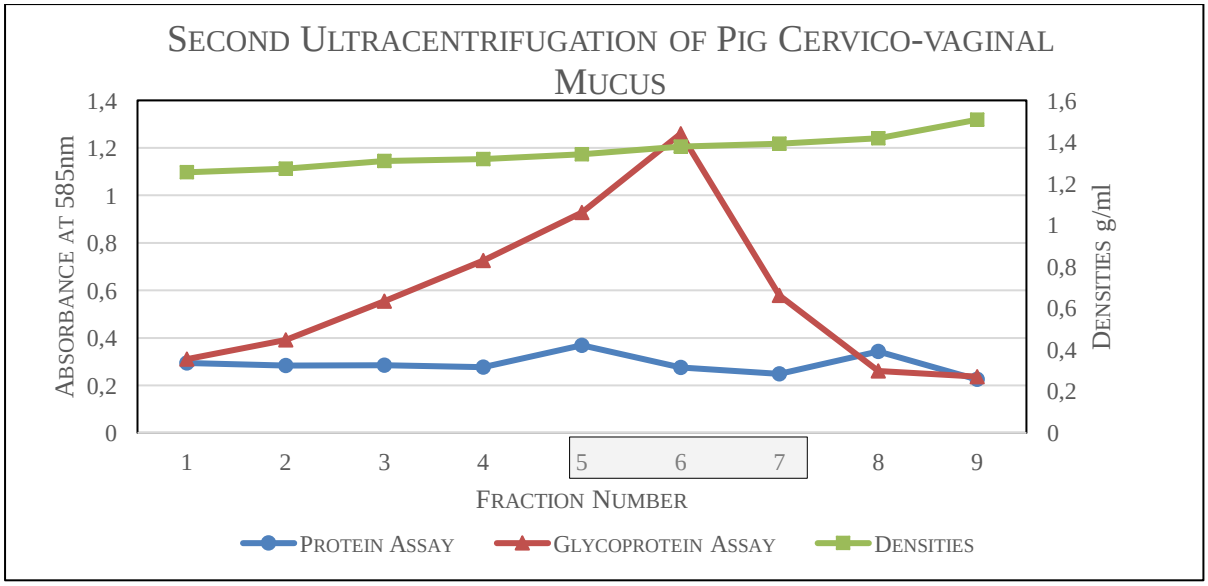

Figure 6.2 Profile of second ultracentrifugation of pig cervico-vaginal mucus. Glycoprotein rich fractions from the first ultracentrifugation were pooled and had their densities adjusted to 1.41g/ml with caesium chloride and 4M GuHCl. The fractions then underwent ultracentrifugation for 48 hours at 105 000g at 4°C. Protein content was determined using Bradford Reagent assay (—●—); glycoprotein content was identified using a PAS assay (—▲—) and the densities (—■—) were recorded on the secondary axis. The box on the X-axis represents the fractions collected, pooled, dialysed against distilled water and freeze dried.

Samples that had high glycoprotein content and a density of 1.40 – 1.41g/ml were pooled. In Figure 6.2 fractions 5 – 7 were pooled. They were then dialysed against distilled water over three changes for a minimum of 6 hours each at 4°C and then freeze dried.

6.1.3 Size Exclusion Sepharose 2B Column Chromatography of PCM

Aliquots of lyophilized PCM were run on a Sepharose 2B column to separate mucins based on size. Protein and glycoprotein profiles stayed consistent throughout the many chromatography runs. Figure 6.3 is a representative sample of protein and glycoprotein distribution after PCM was run on the Sepharose 2B column.

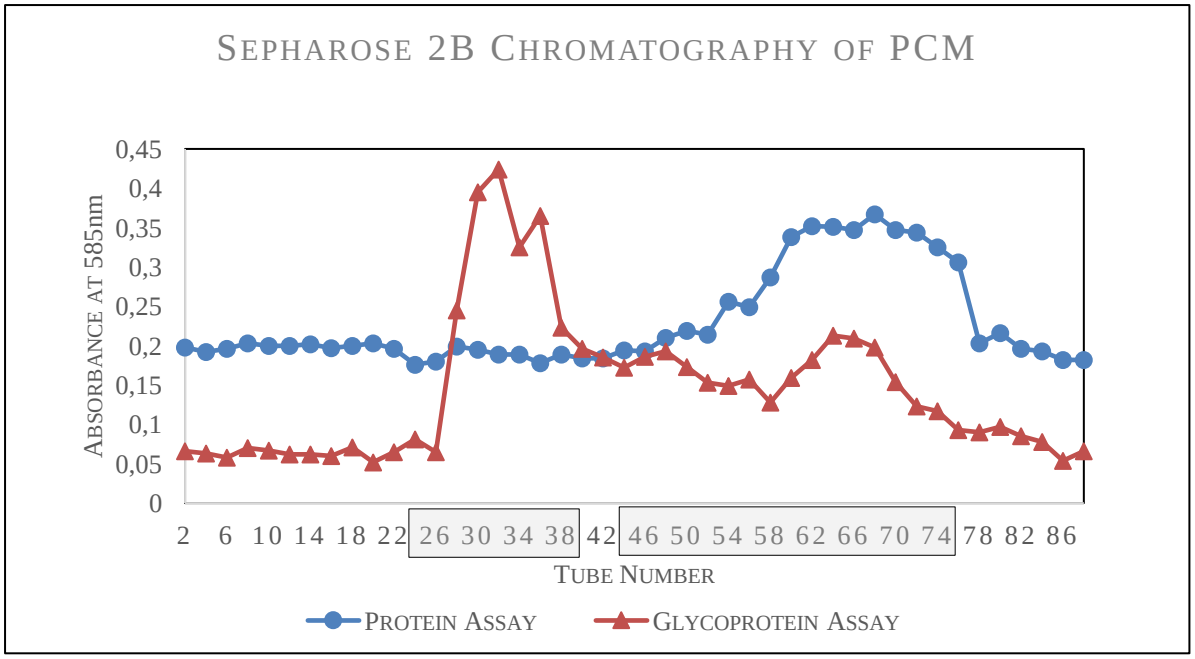

Figure 6.3 Profile of Sepharose 2B separation of PCM in 0.2M NaCl:0.02% sodium azide. Purified lyophilized PCM was dissolved in 10ml 0.2M NaCl:0.02% sodium azide. It was then eluted through a Sepharose 2B glass column under peristaltic pressure. Every second fraction was tested for proteins and glycoproteins. Protein content was determined using Bradford Reagent assay (); and glycoprotein content was identified using a PAS assay (). The box on the X-axis represents fractions that were pooled. Fractions 26 – 38 were pooled and designated V_0. Fractions 46 – 74 were pooled and designated V_i.

There was a clear PAS positive peak from fractions 26 – 38. These fractions were pooled and designated V_0 and is known to contain polymeric mucins (Pearson et al., 1981). There was still

some protein in the V_0, this may have been the result of the protein stain detecting mucin interference. The second PAS positive peak (V_i) (fractions 46 – 74) extended into the included volume of the column and would represent degraded or subunit mucin, as opposed to polymer (Mall et al., 1999; Mall et al., 1988; Pearson et al., 1981). The V_0 and V_i fractions were then dialysed against distilled water over three changes of a minimum of 6 hours each at 4°C and then freeze dried.

6.1.4 SDS-PAGE Gradient Gel Electrophoresis

Aliquots of crude untreated PCM were run on an SDS-PAGE gradient gel (4 – 20%) following reduction with DTT or proteolysis with trypsin treatments of PCM. Figure 6.4 shows the results of the samples run on the SDS-PAGE under protein staining (see section 2.9.2) and Figure 6.5 shows the gel under PAS glycoprotein staining (see section 2.9.3).

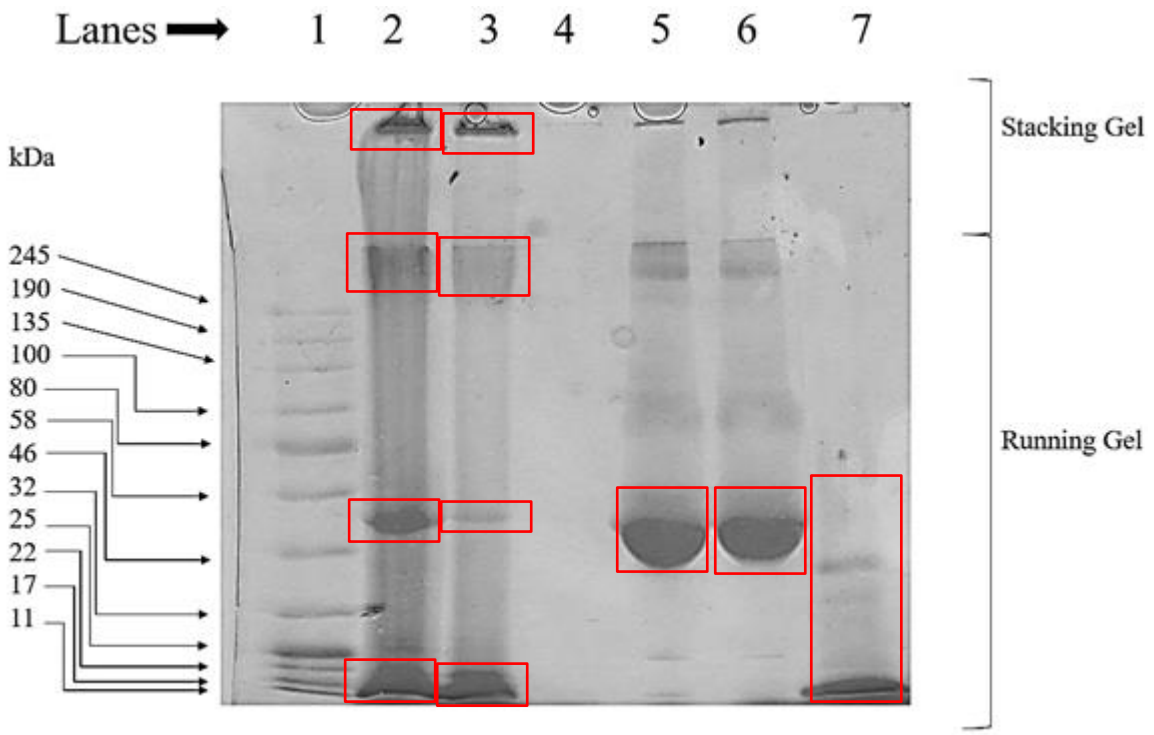

Figure 6.4 Protein stained 4 – 20% gradient SDS-PAGE gel of PCM derivatives. 1mg lyophilized aliquots, of crude and differentially treated samples were dissolved in 100µl 2% SDS, 1% glycerol and 0.01% bromophenol blue for SDS-PAGE gel investigation. Lane 1, 10µl of Thermo Scientific PageRuler Prestained Protein Ladder; Lane 2, crude pig cervico-vaginal mucus; Lane 3, purified PCM after purification in two density gradient ultracentrifugations; Lane 4, the PCM Sepharose 2B V_0 fraction; Lane 5, the PCM Sepharose 2B V_i fraction; Lane 6, DTT treatment of the PCM Sepharose 2B V_0 fraction and in Lane 7, trypsin treatment of the PCM Sepharose 2B V_0 fraction.

In Figure 6.4, the crude pig cervico-vaginal mucus (lane 2) showed bands at the top of the well, the top of the running gel, just below 58kDa and a thick band from 22 – 11kDa (see red box). There were visibly less proteins after two density gradient ultracentrifugations (Figure 6.4, lane 3). The bands were still present at the previously mentioned sizes for crude mucin, but the bands were smaller (see red boxes). Figure 6.4, lane 4 shows the eluted V_0 fraction from a Sepharose 2B column after two density gradient ultracentrifugations. The lane was very lightly stained as there was very little sample left to run on an SDS-PAGE gel. The reason for this was that the pseudoviral and MTT assays were a high priority leaving very little sample for gel electrophoresis. PCM V_i (Figure 6.4, lane 5) had an abundance of protein around the 46 – 58kDa range (see red box). DTT treatment of PCM V_0 (Figure 6.4, lane 6) showed the same profile as PCM V_i (Figure 6.4, lane 5). Trypsin treatment of PCM V_0 (Figure 6.4, lane 7) allowed the movement of glycoproteins farther down the gel. Bands present in lane 7 were seen from 46kDa and below (see red box).

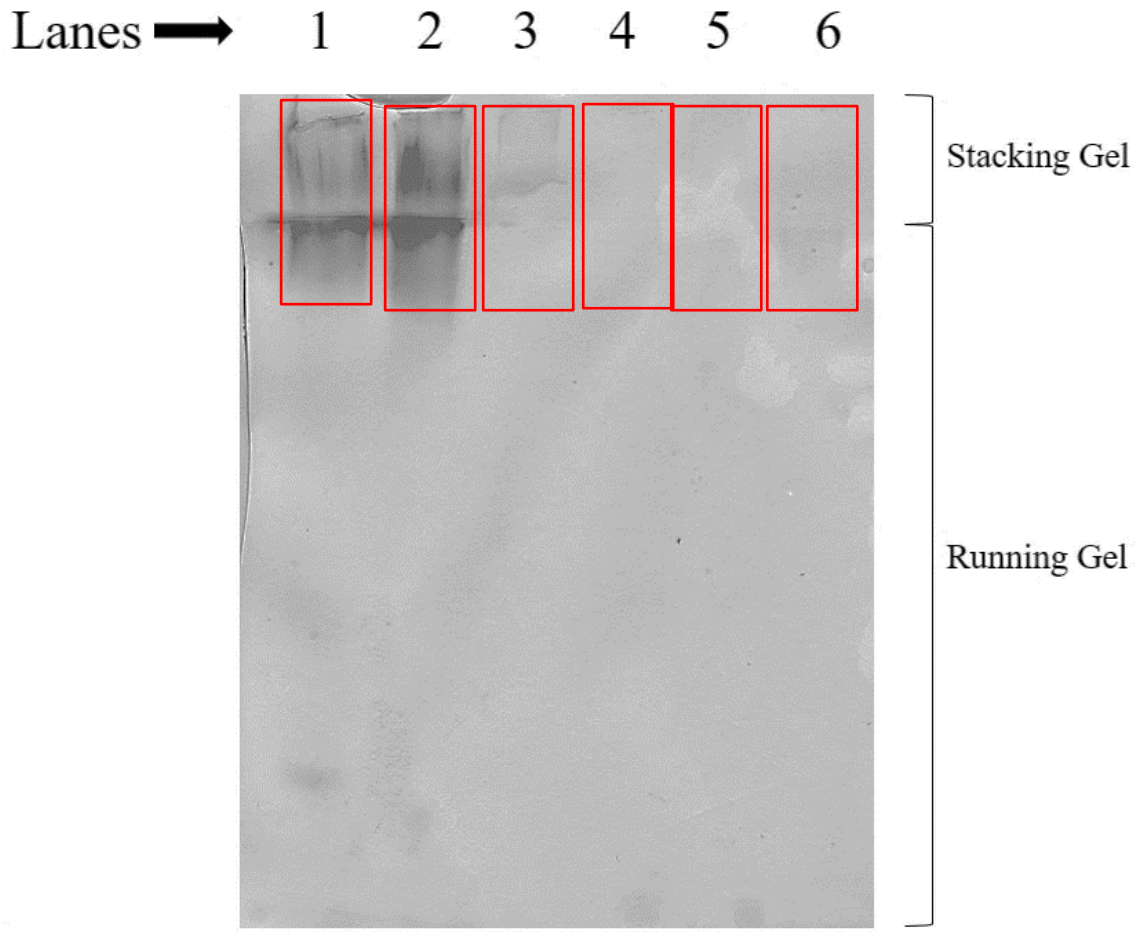

Figure 6.5 Glycoprotein stained 4 – 20% gradient SDS-PAGE gel of PCM derivatives. One milligram lyophilized aliquots, of crude and differentially treated samples were dissolved in 100µl 2% SDS, 1% glycerol and 0.01% bromophenol blue for SDS-PAGE gel investigation. Lane 1, crude pig cervico-vaginal mucus; Lane 2, purified PCM after two density gradient ultracentrifugations; Lane 3, the PCM Sepharose 2B V_0 fraction; Lane 4, the PCM Sepharose 2B V_i fraction; Lane 5, DTT treatment of the PCM Sepharose 2B V_0 fraction and Lane 6, trypsin treatment of PCM Sepharose 2B V_0 fraction.

Figure 6.5 illustrates the PAS stained distribution of PCM and its derivatives through an SDS-PAGE (for method see Section 2.9.2). As previously mentioned the bulk of the PCM samples went to the pseudoviral assay and MTT assay, this accounts for the faint staining in Figure 6.5, lanes 3 – 6. It is possible the mucin in these gels are present lower than the detectable limit for the assay. Lane 1 shows the crude PCM mucin distribution. There is smearing in the stacking gel and at the top of the running gel (see red box). After two density gradient ultracentrifugations (Figure 6.5, lane 2), PCM showed a darker smear effect in the same regions

(see red box) as seen in crude PCM (Figure 6.5, lane 1). Lanes 3 – 6 shows faint smearing in the stacking gel and with a very faint band at the top of the wells (see red boxes).

6.1.5 Slot Blot Analysis of PCM

Antibodies used for this study (see Appendix Table 1 for antibody type and dilutions) were mostly raised against human mucins. None of the antibodies gave a positive signal to PCM derivatives on slot blot analysis (data not shown). At the time of the study there weren't suppliers who stocked or shipped antibodies raised to PCM that were within our budget.

6.1.6 PCM Derivatives Inhibits HIV-1 on a Pseudoviral Assay

We measured the ability of PCM derivatives to inhibit HIV-1 entry into a model target cell line, TZM-bl (Montefiori, 2009). Aliquots of PCM were taken from every stage of purification and chemical treatment and run on a pseudoviral assay. Data was recorded from a luminometer onto Microsoft Excel where percentage neutralizations were calculated based on negative and positive controls. This data was put into Graphpad Prism Version 6 to construct Log Dose Response Curves (see Figure 6.6). From these curves the IC_{50} was calculated.

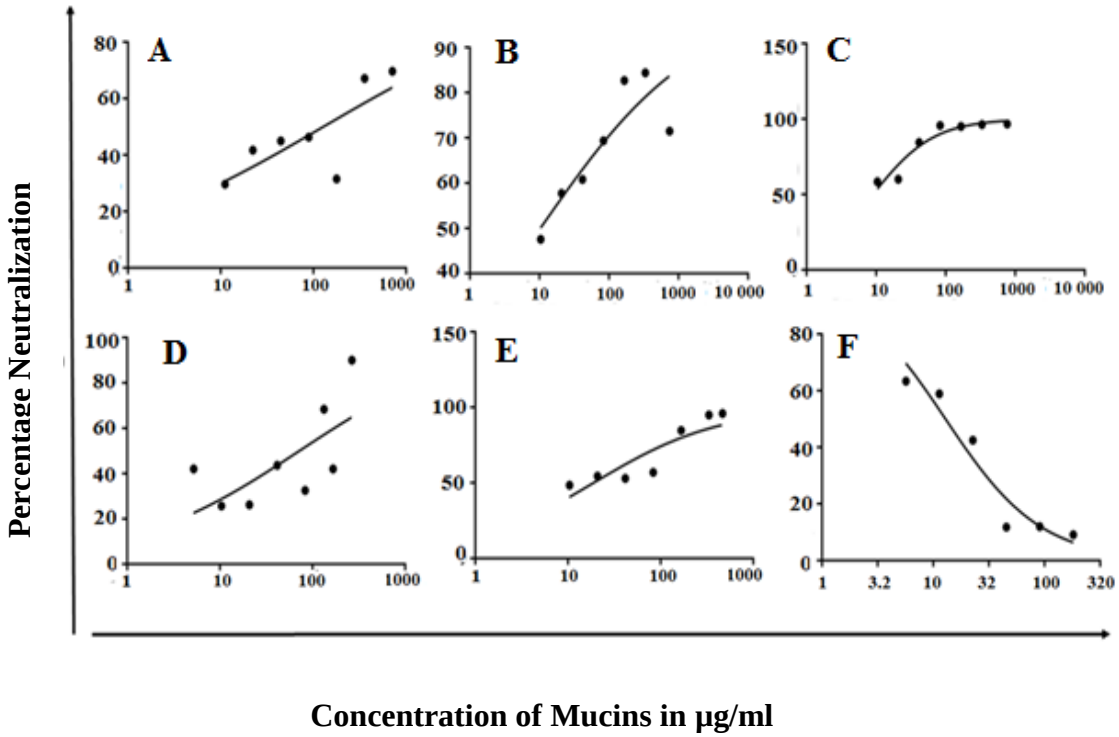

Figure 6.6 Log dose response curve of PCM. A shows the dose response curve for crude PCM; B shows purified PCM after two rounds of ultracentrifugation; C shows PCM V_0 after Sepharose 2B column chromatography; D shows the PCM V_i after Sepharose 2B column chromatography; E shows the effect

DTT treatment of PCM V_0 had on HIV-1 inhibition and F shows the effect Trypsin treatment of PCM V_0 had on HIV-1 inhibition.

Reliability of the log dose response curves can be assessed visually by how close the points of the curve lie to the solid line, which corresponds to the best model of an inhibition curve. The most reliable curves came from PCM V_0 (Figure 6.6 C) and DTT treatment of PCM V_0 (Figure 6.6 E). Points on the curve for PCM V_i (Figure 6.6 D) showed substantial deviation for the modelled inhibition curve. Table 6.1 shows the calculated 95% confidence interval of the IC_{50} value based upon the level of deviation of the points from the modelled inhibition curve.

Table 6.1 The summary of PCM IC_{50} values and 95% confidence intervals

PCM Derivative	**IC_{50} (µg/ml)**	**95% Confidence Intervals (µg/ml)**
Crude PCM	128.4	31.95 to 515.8
Purified PCM	10.32	2.520 to 42.23
PCM V_0	8.974	5.055 to 15.93
PCM V_i	72.12	16.55 to 314.3
DTT treated PCM V_0	18.92	7.014 to 51.01
Trypsin treated PCM V_0	12.90	8.036 to 20.71

Our data shows that all PCM derivatives (crude PCM, PCM having undergone two ultracentrifugations, the large (V_0) and smaller molecular weight (V_i) PCM fractions eluted from a Sepharose 2B column, PCM V_0 with DTT reduction and PCM with trypsin digested naked regions) tested on the pseudoviral assay inhibited HIV-1 *in vitro*. The most reliable data (in terms of 95% confidence intervals) came from the PCM V_0 (5.055 to 15.93µg/ml), DTT treated PCM V_0 (7.014 to 51.01µg/ml), trypsin treated PCM V_0 (8.036 to 20.71µg/ml). Trypsin treated PCM V0 showed a dose response curve in he opposite direction as the others and this needs to be investigated further. The least reliable data came from the crude PCM (31.95 to 515.8µg/ml). The purified PCM was almost within 4 orders of the upper and lower 95% Confidence intervals (2.520 to 42.23µg/ml). The lowest IC_{50} values were shown by PCM V_0 (8.974µg/ml) and purified PCM (10.32µg/ml). The highest IC_{50} value was exhibited by crude PCM (128.4µg/ml). Cleaving of disulphide bonds (with DTT) changed PCM V_0's inhibition potential over two-fold (18.92µg/ml).

6.1.7 Toxicity Assay for PCM

PCM derivatives (crude PCM, purified PCM, PCM V_0, PCM V_i, DTT treated PCM V_0 and trypsin treated PCM V_0) were run on an MTT assay (see section 2.13) to authenticate the HIV-1 inhibition seen in section 6.1.5. If the PCM derivatives were toxic and subsequently killed target cells it would have resulted in luminescence reduction giving false inhibition data. Table 6.2 shows the results of this MTT assay.

Table 6.2 Results of PCM Derivatives on MTT Assay

PCM Derivative	**LD_{50} (µg/ml)**	**Concentration (µg/ml)**	**% Cell Viability**
Crude PCM	Curve did not converge	168.13	66.93
Purified PCM	4 060		
PCM V_0	186.2		
PCM V_i	1 303		
DTT treated PCM V_0	1 071		
Trypsin treated PCM V_0	396.8		

All PCM derivatives, excluding crude PCM, showed high LD_{50} values which indicates that a high concentration of those PCM derivatives are needed to kill 50% of the target cells. The highest LD_{50} was seen in purified PCM (4 060µg/ml) and the lowest LD_{50} was shown by PCM V_0 (186.2µg/ml). An LD_{50} for crude PCM could not be calculated so a cell viability was quoted that was at a concentration close to crude PCM IC_{50} (IC_{50}: 128.4µg/ml, percentage cell viability: 66.93% at 168.13µg/ml). There were poor percentage cell viability values for crude PCM, which lowers the integrity of its inhibition data.

6.2 Discussion

6.2.1 Purification and Treatment of PCM

Cervico-vaginal mucus regulates sperm transport to the upper reproductive tract and fertilization (Carlstedt et al., 1983b; Carlstedt et al., 1982). Cervico-vaginal mucus also prevents desiccation by enhancing lubrication, impedes cervical enzymatic degradation and protects against pathogenic infection (Gipson et al., 1995; Idris et al., 1999; Venegas et al., 1995). Cervical mucus of farm animals may contain endometrial, follicular, oviductal and

peritoneal fluids; leukocytes, proteins, trace elements, enzymes as well as cellular debris from the cervical, vaginal and uterine epithelia (Hafez et al., 2013). The cervical mucus of farm animals is a hydrogel composed of water, low- and high-viscosity components (Hafez & Hafez, 2013). Cervical mucus have low molecular weight components such as amino acids, and free simple sugars (mannose, maltose and glucose) (Hafez & Hafez, 2013). The female human reproductive tract contains 6 mucins, namely MUC1, MUC2, MUC4, MUC5AC, MUC5B and MUC6 (Gipson et al., 1997a). To our knowledge there have been no studies on the mucins present in pig cervico-vaginal mucus.

Our laboratory has previously performed experiments on crude and purified human pregnancy plugs (Habte et al., 2008). Habte *et al* (2008) purified pregnancy plug mucins by two caesium chloride density gradient ultracentrifugations and characterized the products by Western blot analysis. Figure 6.1 showed the first caesium chloride density gradient ultracentrifugation profile of PCM as more protein was present in the first three fractions. The PCM profile was different from the first human pregnancy plug ultracentrifugation. The second PCM ultracentrifugation followed the same pattern as the second human pregnancy plug ultracentrifugation in that there was a distinct mucin rich peak and low protein content (Habte et al., 2008).

After two caesium chloride density gradient ultracentrifugations, aliquots of cervico-vaginal mucin were eluted through a Sepharose 2B column. Previous researchers have used Sepharose 2B gel filtration for human cervical pregnancy mucus so Sepharose 2B was assessed to be adequate to separate high and low molecular weight PCM mucins (Carlstedt et al., 1983b). The glycoprotein and protein profile of the Sepharose 2B chromatography is shown in Figure 6.3. The V_0 has a distinct mucin rich peak and the high protein stain in the V_i may again (as seen previously in Figure 3.3) be explained by mucin interference pattern of the protein stain detecting mucins rather than the presence of lingering protein contamination in the sample (Mall et al., 1988).

Figure 6.4 shows the protein staining pattern of PCM derivatives under SDS-PAGE (4 – 20%) gradient gel electrophoresis. Crude pig cervico-vaginal mucus (Figure 6.4, lane 2) showed bands at the top of the gel, at the start of the running gel, just below 58kDa and at the bottom of the gel (see red boxes). After two density gradient ultracentrifugations (Figure 6.4, lane 3), there were lighter bands in the same positions as Figure 6.4, lane 2 (see red boxes). After the ultracentrifugations (Figure 6.4, lane 3) PCM showed more bands and a darker protein smear

than purified PGM (Figure 3.4, lane 3) Figure 6.4, lane 4 shows the eluted V_0 fraction from a Sepharose 2B column. The faint banding is due to very little sample being present in the lane as the bulk of PCM V_0 was used for the neutralization assay and MTT assay. PCM V_0 was also subjected to repeat analysis on neutralization and MTT assays, this contributed to sample depletion. The smaller mucins and proteins eluted in the V_i (Figure 6.4, lane 5) shared the same banding pattern as DTT treated PCM V_0 (Figure 6.4, lane 6). This indicates that larger mucins may have undergone degradation before being eluted in the V_i (Figure 6.4, lane 5) and when the V_0 underwent disulphide bond breakage (Figure 6.4, lane 6) the same pattern was observed. The red boxes in Figure 6.4 lanes 5 and 6 show protein bands (between 46 – 58kDa) typically seen by the presence of albumin. In human crude cervical mucus, albumin is present at ~68kDa; the α-chain of IgA present just below 68kDa and the γ-chain of IgG is present at ~56kDa (Van Kooij et al., 1983). A similar protein blob was seen in PSM V_i at ~46kDa (Figure 5.6, lane 4). The proteins present in red boxes of Figure 6.4 lanes 5 and 6 were not identified as this lay outside the scope of our study. Trypsin treatment of the naked regions of PCM V_0 (Figure 6.4, lane 7) resulted in the appearance of protein bands from 11 – 80kDa (see red box) and the absence of mucins at the top of the running gel (previously seen in Figure 6.4 lanes 1, 2, 5 and 6). This may suggest that there were more naked regions and PCM V_0 had little glycosylation to protect the mucin from the proteolytic action of trypsin. Trypsin treatment of PCM V_0 (Figure 6.4, lane 7) resulted in a fainter protein smear than trypsin treated PGM (Figure 3.4, lane 7) and PSM (Figure 5.6, lane 7). The glycoprotein stain of PCM derivatives showed mucin smears in the stacking gel and at the start of the running gel (Figure 6.5, lanes 1 – 6). This was a pattern seen in PGM (Figure 3.5, lanes 1 – 6) and PSM (Figure 5.7, lanes 1 – 6) PAS stains, but PCM derivatives (Figure 6.5, lanes 1 – 6) showed no bands like those exhibited by PSM (Figure 5.7, lanes 1 – 2, 4 – 6). Our slot blots were unsuccessful as the antibodies available to us were raised against human mucins. Pig antibodies were unavailable due to logistic issues as suppliers who did have pig mucin antibodies did not ship to South Africa.

6.2.2 Pseudoviral Assay of PCM Derivatives

We tested the anti-HIV-1 potential of PCM derivatives on a pseudoviral assay and all derivatives showed inhibition. The affect cervico-vaginal mucus had on HIV-1 was previously studied by Lai *et al* (2009). In 2009, Lai *et al* (2009) performed experiments on cell free HIV diffusion through normal human cervico-vaginal mucus (CVM). They then mixed an HIV virus-like particle (VLP) incorporated with a green fluorescent protein (GFP) fused Vpr (Campbell et al., 2007) with undiluted CVM and tracked the virions with high-resolution

multiple-particle tracking (Lai et al., 2007; Suh et al., 2005). Their results showed that not only did healthy CVM slow HIV diffusion over a 1000-fold when compared to water, but HIV diffusion was better at low pH rather than neutral (Lai et al., 2009).

Habte *et al* (2008) previously tested the anti-HIV-1 Subtype D activity of crude and purified human pregnancy plug mucins by incubating them (0.9mg of each) with HIV-1 for an hour and then incubated on a human T lymphoblastoid cell line (CEM SS cells). HIV-1 infection was measured by the p24 antigen assay. Our study tested PCM derivatives on replication defective HIV-1 Subtype C. Crude PCM had the highest IC_{50} (128.4µg/ml, see Table 6.1) followed by the low molecular weight fraction eluted off the Sepharose 2B column (PCM V_i IC_{50}: 72.12µg/ml, see Table 6.1). Purifying PCM with two density ultracentrifugations enhanced HIV-1 inhibition almost 13-fold from crude PCM (IC_{50}: 10.32µg/ml, see Table 6.1). Isolating the larger mucin fraction eluted off a Sepharose 2B column (PCM V_0: 8.974µg/ml, see Table 6.1) gave the lowest IC_{50} which was marginally better than purified PCM (purified PCM IC_{50}: 10.32µg/ml, see Table 6.1). Removing disulphide bonds from the PCM V_0 lowered inhibition by over 50% (PCM V_0: 8.974µg/ml; DTT treated PCM V_0: 18.92µg/ml, see Table 6.1) indicating the importance of PCM V_0 keeping a longer structure to ensure maximum inhibition. A similar effect was seen in trypsin treated PCM V_0 (12.90µg/ml, see Table 6.1) i.e. the shorter PCM structure lowered HIV-1 inhibition but Figure 6.6, F shows the gradient of the dose response curve to be in the opposite direction of the other curves. If this is not the result of experimental error the it would suggest trypsin treated PCM V_0 increased infection at higher concentration. This requires further investigation. Habte *et al* (2008) reported 97.5% inhibition by 0.9mg purified human pregnancy plug mucins on HIV-1 Subtype D infection whereas we showed 1.04mg of purified PCM inhibited HIV-1 Subtype C by 97.78% (data not shown). The larger mucin components had the better IC_{50} values but removing the disulphide bonds and naked proteins had little effect on the IC_{50}. The 95% confidence intervals for purified PCM (2.520 to 42.23µg/ml, see Table 6.1), PCM V_0 (5.055 to 15.93µg/ml, see Table 6.1), DTT (7.014 to 51.01µg/ml, see Table 6.1) PCM V_0 were narrow and this can be interpreted as true inhibitory effect of HIV-1. Purified PCM (IC_{50}: 10.32µg/ml, see Table 6.1) and PCM V_0 (IC_{50}: 8.974µg/ml, see Table 6.1) showed lower IC_{50} values than the best inhibitors from PSM derivatives (PSM V_0 IC_{50}: 23.61µg/ml; DTT treated PSM V_0 IC_{50}: 20.79µg/ml, see Table 5.1) and were comparable to purified PGM (IC_{50}: 10.50µg/ml, see Table 4.1) but higher than PGM V_0 (IC_{50}: 1.668µg/ml, see Table 4.1).

6.2.3 Toxicity Assay of PCM Derivatives

To assess the validity of our inhibition data, PCM derivatives were run on an MTT assay to determine if the PCM derivatives were toxic to the TZM-bl target cells. All PCM derivatives apart from crude PCM, had high LD_{50} values. The highest LD_{50} was shown by purified PCM (4 060µg/ml, see Table 6.2) and crude PCM showed poor percentage cell viability values (crude PCM at 168.13µg/ml showed 66.93% cell viability (see Table 6.2)). The toxicity data from this part of the study shows that the inhibition data from all PCM derivatives (apart from crude PCM) can be trusted.

The results from this chapter indicate that PCM derivatives can be used for HIV-1 research and have the potential to inhibit HIV-1 *in vitro*. If a PCM derivative were to be used for an anti-HIV-1 gel, the most likely candidates (based on IC_{50} and LD_{50} values) would be purified PCM and PCM V_0. From these two derivatives (purified PCM and PCM V_0) purified PCM was chosen to progress to the anti-HIV-1 gel part of our study as the sample yield was higher, and that was crucial as gels were created at a concentration of 30mg of mucin per 1ml of buffer.

CHAPTER 7: THE EFFECT OF HORSE SALIVARY MUCIN (HSM) ON HIV-1 *IN VITRO*

7.1 Results

7.1.1 Sepharose 4B Column Chromatography of Horse Saliva

Horse saliva was collected in 6M guanidine hydrochloride with protease inhibitors (viz. 10mM Na_2HPO_4, 10mM EDTA, 1mM PMSF and 5mM NEM) (see Appendix section 1.1) as the sample had to be stored by Ms Heather Epstein (who runs a farm) and lived far away. Samples were pooled and centrifuged to eliminate contaminants. Thereafter, the supernatant was dialysed against distilled water over three changes for a minimum of 6 hours each at 4°C and then freeze dried. Aliquots of lyophilized crude saliva were dissolved in 0.2M NaCl:0.02% sodium azide and eluted on a Sepharose 4B column (eluting buffer was also 0.2M NaCl:0.02% sodium azide). Horse saliva samples shared a similar profile with each other after Sepharose 4B column chromatography. Figure 7.1 is a representative sample of protein and glycoprotein distribution after HSM was run on the Sepharose 4B column.

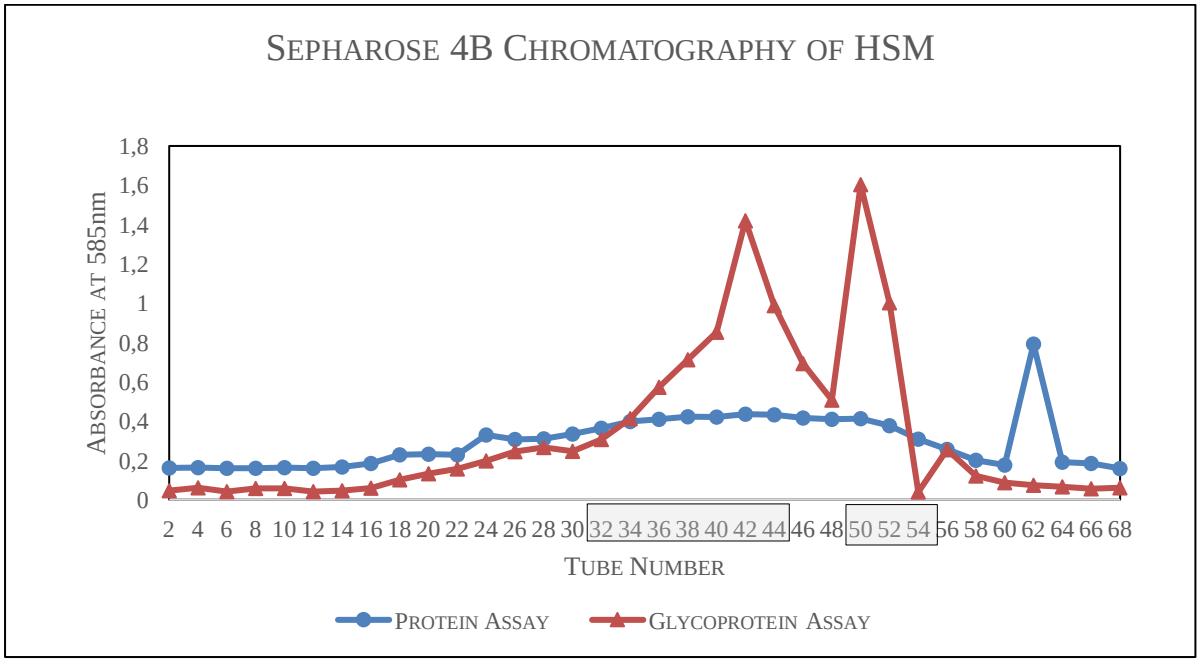

Figure 7.1 Sepharose 4B separation profile of HSM in 0.2M NaCl:0.02% sodium azide. Lyophilized crude horse saliva was dissolved in 0.2M NaCl:0.02% sodium azide (4:1) and eluted through a Sepharose 4B glass column under peristaltic pressure. Every second fraction was tested for proteins and glycoproteins. Protein content was determined using Bradford Reagent assay (—●—); and glycoprotein

content was identified using a PAS assay (). The box on the X-axis represents fractions that were pooled.

The samples had two distinct peaks denoting the presence of two sizes of mucins present in the sample. The first PAS positive peak eluted in the V_0 of the column (fractions 32 – 44), suggesting the presence of large polymeric mucins in the purified sample. These fractions were where the void volume usually eluted. The second PAS positive peak was observed in the V_i (fractions 50 – 54). The PAS positive V_i peak is indicative of some smaller mucins present in saliva. The V_0 and V_i fractions were then dialysed against distilled water over three changes for a minimum of 6 hours each at 4°C and then freeze dried. For this study, we were interested in the large mucins present in the V_0. Thus, the V_0 fractions were set up for further purification.

7.1.2 Ultracentrifugation of HSM V_0

Aliquots of V_0 were dialysed against 3 changes of 4M GuHCl (see Appendix section 1.3) at 6 hour intervals. The volume of 4M GuHCl was at least 20 times the volume of V_0. The density was adjusted and samples ultracentrifuged as stated in section 2.4. Figure 7.2 shows the protein, glycoprotein and density profiles of a representative sample.

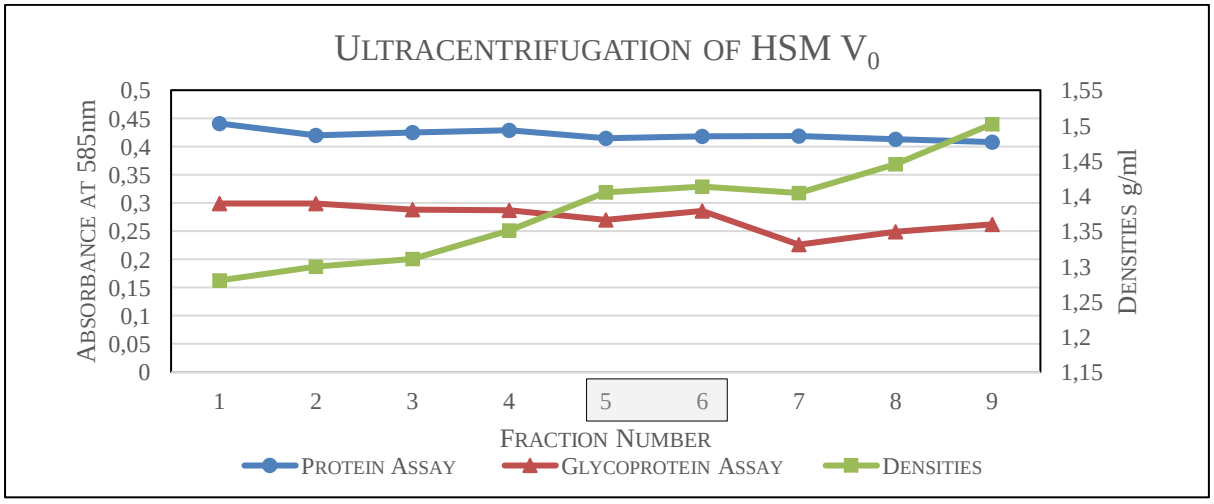

Figure 7.2 Ultracentrifugation profile of HSM. PSM V_0 was dialysed against 4M GuHCl. Samples then had their densities adjusted to 1.39g/ml with caesium chloride and 4M GuHCl. They were then subjected to a 48-hour ultracentrifugation at 105 000g at 4°C. Protein content was determined using Bradford Reagent assay (); glycoprotein content was identified using a PAS assay () and the densities () were recorded on the secondary axis. The box on the X-axis represents the fractions

collected for dialysis against distilled water over three changes of a minimum of 6 hours each at 4ºC and freeze dried.

Fractions that had high glycoprotein content and a density of 1.40 – 1.41g/ml were pooled. In Figure 7.2 fraction 5 and 6 were pooled. They were then dialysed against distilled water over three changes for a minimum of 6 hours each at 4ºC and then freeze dried. There was a high protein content throughout all the fractions.

7.1.3 Slot Blot of HSM V_0

The presence of Muc19 in horse saliva was confirmed by proteomic analysis carried out by Rousseau *et al* (2008). Aliquots of the Sepharose 4B column V_0 from Figure 7.1 (fractions 32 – 44) were set up for Muc5b and Muc19 slot blot analysis (see section 2.12). Due to limiting amounts of anti-horse Muc19 antibody, only the fractions corresponding to the V_0 peak was assessed under slot blot analysis. Information on the Muc5b and Muc19 antibodies used for the dot blot can be seen in Appendix Table 1. Figure 7.3 shows the results of slot blot analysis on the V_0 fractions.

Fractions	32	33	34	35	36	37	38	39	40	41	42	43	44
Muc19	positive	positive	positive	positive	positive	positive	positive	positive	positive	positive	positive	positive	positive
Muc5b	negative	negative	negative	positive	positive	positive	positive	positive	positive	positive	negative	negative	negative

Figure 7.3 Slot blot analysis of Muc19 and Muc5b in HSM V_0. HSM was run on a Sepharose 4B column under peristaltic pressure (see Figure 7.1). The V_0 fractions then underwent slot blot analysis to determine the presence of Muc19 and Muc5b. Figure 8.3 is divided into three panels. The top panel shows the fraction number. The second panel from the top shows the expression of Muc19. The bottom panel shows the presence of Muc5b.

Figure 7.3 shows fractions 32 to 44 analysed by Slot blot. Fractions containing Muc19 only were 32 – 34 and 42 – 44 were pooled for a total Muc5b-Muc19+ representation. They were then dialysed against distilled water over three changes for a minimum of 6 hours each at 4ºC and then freeze dried.

7.1.4 Ultracentrifugation of HSM V_0 Muc19

Aliquots of freeze dried HSM Muc19 mucin were dissolved in 4M GuHCl. The density of the sample was adjusted to 1.41g/ml and subjected to a 48-hour ultracentrifugation at 105 000g at 4ºC. Figure 7.4 shows the protein, glycoprotein and density profiles of a representative sample.

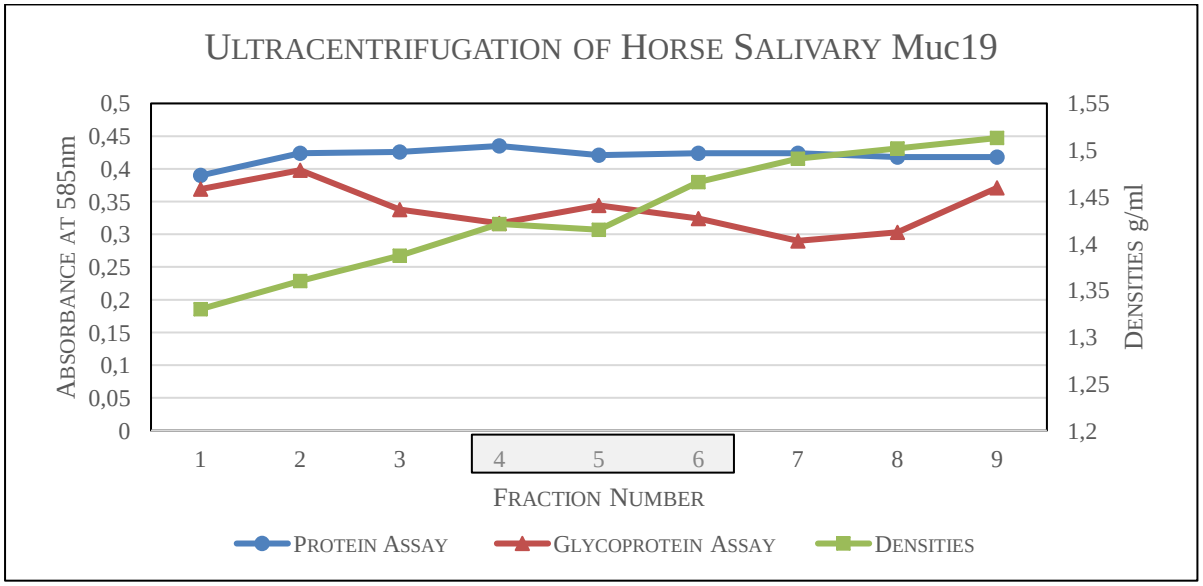

Figure 7.4 Ultracentrifugation profile of horse salivary Muc19. Pig salivary mucus was passed through a Sepharose 4B column and the V_0 was pooled and dialysed against distilled water over three changes for a minimum of 6 hours each at 4ºC. Freeze dried HSM Muc19 was dissolved in 4M GuHCl. Samples then had their densities adjusted to 1.39g/ml with caesium chloride and 4M GuHCl, before undergoing ultracentrifugation for 48 hours at 105 000g at 4ºC. Protein content was determined using Bradford Reagent assay (—●—); glycoprotein content was identified using a PAS assay (—▲—) and densities (—■—) were recorded on the secondary axis. The box on the X-axis represents the fractions collected and dialysed against distilled water and freeze dried.

Fractions that had glycoprotein rich densities of 1.39g/ml to 1.41g/ml were pooled. In Figure 7.4 fractions 4 – 6 were pooled. These samples were dialysed against 3 changes of distilled water for 6 hours each, then freeze dried for further investigation.

7.1.5 HSM Derivatives Inhibits HIV-1 on a Pseudoviral Assay

We measured the ability of HSM derivatives to inhibit HIV-1 entry into a model target cell line, TZM-bl on a pseudoviral assay (Montefiori, 2009). Data recorded from a luminometer was analysed on Microsoft Excel where percentage neutralizations were calculated based on

negative and positive controls. This data was put into Graphpad Prism Version 6 to construct Log Dose Response Curves (Figure 7.5). From these curves IC_{50} values were calculated.

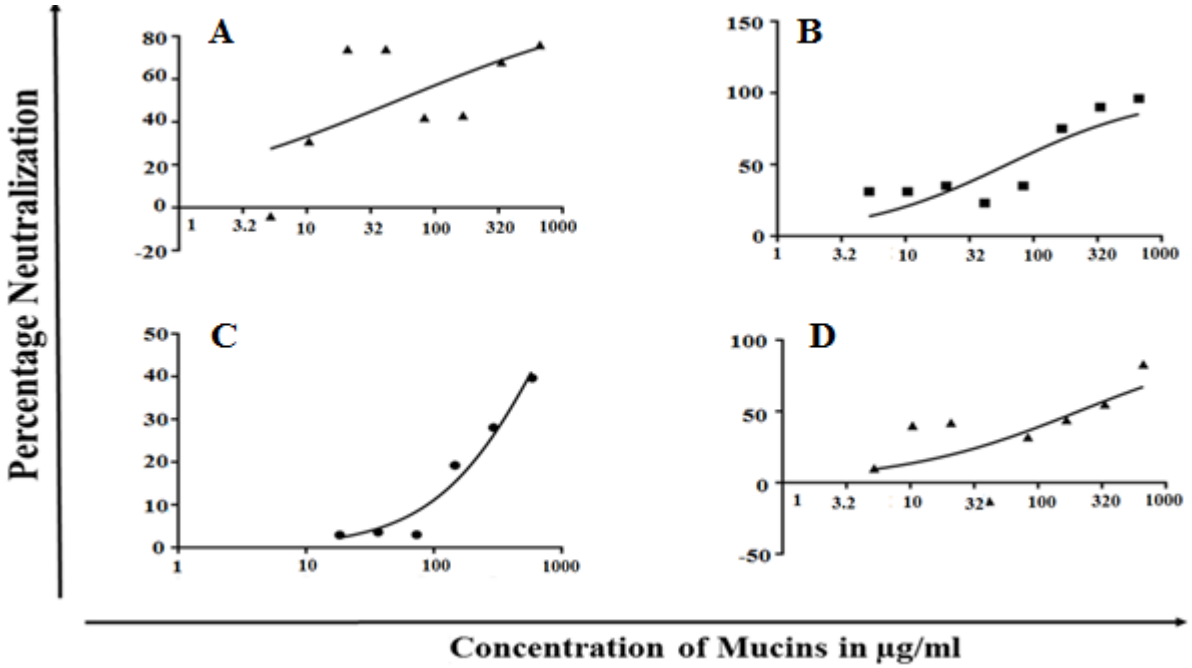

Figure 7.5 Dose response curves of HSM derivatives. A, crude horse saliva; B, HSM V_0 eluted from Sepharose 4B column chromatography and subjected to density gradient ultracentrifugation (Muc5b and Muc19); C, HSM V_i eluted from Sepharose 4B column chromatography (Muc7) and D, HSM V_0 Muc19 eluted from Sepharose 4B column chromatography.

.

Crude HSM (Figure 7.5 A) showed substantial deviation from the modelled inhibition curve. HSM V_0, HSM V_i and HSM Muc19 showed points close to the solid line which corresponds to the best model of an inhibition curve. Table 7.1 shows the calculated 95% confidence interval of the IC_{50} value based upon the level of deviation of the points from the modelled inhibition curve.

Table 7.1 Showing the calculated HSM IC_{50}'s and 95% Confidence Intervals

Horse Salivary Mucin Derivative	**IC_{50} (µg/ml)**	**95% Confidence Intervals (µg/ml)**
Crude HSM	51.32	6.060 to 434.7
HSM V_0 (Muc5b and Muc19)	76.35	40.27 to 144.8
HSM V_i	841.8	516.4 to 1372
HSM Muc19	131.9	35.03 to 496.8

All HSM derivatives showed HIV-1 inhibition *in vitro*. The most reliable data came from the HSM V_0 (95% Confidence intervals: 40.27 to 144.8µg/ml) and V_i (95% Confidence intervals: 516.4 to 1372µg/ml). The least reliable data was seen in crude HSM (95% Confidence intervals: 6.060 to 434.7µg/ml) and HSM Muc19 (95% Confidence intervals: 35.03 to 496.8µg/ml). Crude HSM showed the best inhibition (IC_{50}: 51.32µg/ml) but it's wide 95% confidence intervals indicated that the true inhibitory effect of crude HSM could not be seen in this experiment. HSM V_0 showed the second-best inhibition (IC_{50}: 76.35µg/ml) but showed tighter 95% confidence intervals (40.27 to 144.8µg/ml) indicating that the inhibition shown by HSM V_0 was reliable. The IC_{50} of the HSM V_i, presumably Muc7, (IC_{50}: 841.8µg/ml) showed the least inhibitive potential, in fact the IC_{50} was over 16 times that of crude HSM IC_{50} (crude HSM IC_{50}: 51.32µg/ml). The IC_{50} of HSM Muc19 (IC_{50}: 131.9µg/ml) was almost twice the IC_{50} of HSM V_0 (HSM V_0 IC_{50}: 76.35µg/ml) and almost three times that of the crude (crude HSM IC_{50}: 51.32µg/ml).

7.1.6 Toxicity Assay of HSM Derivatives

Crude HSM, HSM V_0 having undergone density gradient ultracentrifugation (Muc5b and Muc19), HSM V_i (Muc7) and HSM V_0 Muc19 (having undergone density gradient ultracentrifugation) were tested for cell toxicity using an MTT assay (see section 2.13). Table 7.2 shows the results of this MTT assay.

Table 7.2. Results of HSM Derivatives on MTT Assay

Horse Salivary Mucin Derivative	**LD_{50} (µg/ml)**	**Concentration (µg/ml)**	**% Cell Viability**
Crude HSM	Curve did not converge	71.88	98.85
HSM V_0	737		
HSM V_i	~986.1		
HSM Muc19	59.79		

LD_{50} values were calculated for HSM V_0, HSM V_i, and HSM Muc19 but not for crude HSM. For crude horse saliva, the percentage cell viability quoted was at the nearest concentration to the crude HSM IC_{50} value (crude HSM IC_{50}: 51.32µg/ml). Crude HSM showed good percentage cell viability (at 71.88µg/ml there was a 98.85% cell viability). The mucin-rich low

molecular weight fraction eluted from a Sepharose 4B column showed the highest LD_{50} value (HSM V_i LD_{50}: ~986.1µg/ml) followed by the void volume eluted from the Sepharose 4B column (HSM V_0 LD_{50}: 737µg/ml). The lowest LD_{50} value was shown by HSM Muc19 (HSM Muc19 LD_{50}: 59.79µg/ml).

7.2 Discussion

7.2.1 Purification and Treatment of HSM

This part of our study looks at the possibility of using HSM derivatives as an alternative to human mucin. HSM was chosen as an alternative to human saliva due to the presence of large polymeric Muc19 in horse saliva (Rousseau et al., 2008). Horse saliva is comprised of over 99% water (Alexander, 1966). It contains more chloride and calcium and less bicarbonate and sodium than ruminants. This gives horse saliva the characteristics of carnivora and omnivora (Alexander et al., 1970; Stick et al., 1981). Unlike carnivora and omnivora, horse saliva contains almost no digestive enzymes (e.g. amylase is detected at 0.44 enzyme units per ml) suggesting horse saliva does not play an important role in digestion but rather in lubrication (Varloud, 2006). Horse saliva contains less than 10 colony forming units of total bacteria per ml (Varloud, 2006). Adult horses can secrete from 35 – 40L a day (primarily from the parotid salivary gland), with a pH of 8.6 – 9.1 (Meyer et al., 1985; Moeller et al., 2008; Stick et al., 1981). The rate of salivary secretion increases when the horse is stimulated by food intake and mastication (Meyer et al., 1985; Meyer et al., 1986). Horse saliva collected for this study was collected during mastication to ensure maximum sample yield.

Rousseau *et al* (2008) performed proteomic analysis on horse saliva to determine the presence of large polymeric mucins. Rousseau *et al* (2008) collected horse saliva in 8M GuHCl (in the absence of protease inhibitors), adjusted densities to 1.41g/ml by the addition of caesium chloride and 4M GuHCl and ultracentrifuged samples at 40 000rpm for at least 68 hours (at 15^{o}C). Centrifuging at 15^{o}C may have caused degradation to mucin structure. The density gradient ultracentrifugation profile can be seen in Figure 7.6.

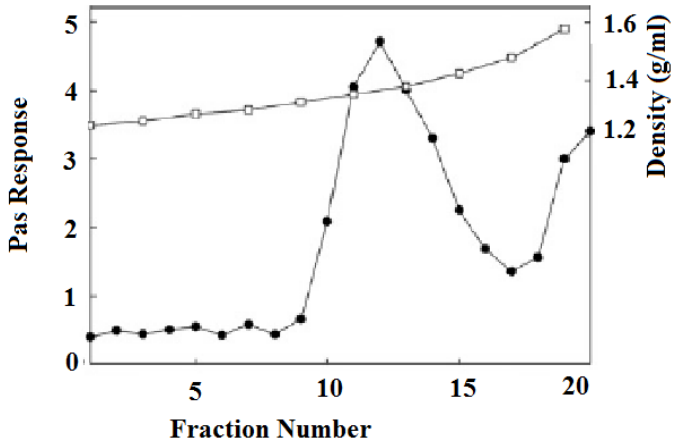

Figure 7.6 Purification of horse mucins from Rousseau et al (2008). Horse saliva collected in 8M GuHCl had their density adjusted to 1.4g/ml with caesium chloride and 4M GuHCl. They were then subjected to an ultracentrifugation for at least 68 hours at 40 000rpm at 15°C. Glycoprotein content was identified using a PAS assay (•) and the densities (□) were recorded on the secondary axis. Fractions 10 – 16 were pooled and collected for proteomic analysis.

Glycoprotein rich samples were then pooled, reduced, carboxymethylated, digested with trypsin, dialysed against water and freeze dried (Rousseau et al., 2008). When we compare our ultracentrifugation profile (Figure 7.2) with the profile of Rousseau *et al* (2008) there is a major difference. The profile of Rousseau *et al* (2008) HSM ultracentrifugation shows a distinct PAS positive peak from fractions 10 – 16, whereas our ultracentrifugation profile (Figure 7.2) did not show a distinct peak. The difference may be explained by the methods chosen. Our method differed in that we ultracentrifuged the HSM V_0 fraction, and where we divided our samples into 9 fractions, Rousseau *et al* (2008) fractioned their samples into 20. Mucins were then identified using tandem mass spectrometry on a quadropole-time-of-flight micromass spectrometer. Rousseau *et al* (2008) showed that horse saliva contains a mixture of two polymeric mucins namely, Muc5b and Muc19.

Our laboratory has previously eluted human saliva through gel filtration (Sepharose 2B) with 0.2M NaCl: 0.02% sodium azide (Peacocke et al., 2012). Figure 7.1 shows the Sepharose 4B profile of HSM eluted with the same buffer i.e. 0.2 M NaCl: 0.02% sodium azide. The protein and glycoprotein profile of HSM eluted Sepharose 4B column showed similarities to human salivary mucin eluted on the same column (Peacocke et al., 2012) with respect to the presence of two distinguishable mucin-rich peaks (designated V_0 and V_i respectively). Figure 7.1 shows two glycoprotein rich peaks denoting two sizes of mucins present. The proteins were small enough to be eluted just after the V_i. The separation between the HSM V_0 and V_i was a lot

closer than the Sepharose 4B separation of PSM V_0 and V_i (Figure 5.3). Aliquots of the Sepharose 4B V_0 from Figure 7.1 was analysed on a slot blot. This method to identify fractions with Muc19 only contrasted with section 5.1.1.3 for PSM V_0 Muc19. This was due to limited availability of horse saliva. Each fraction was then subjected to slot blot analysis using human antibodies raised to Muc5b and horse antibodies raised to Muc19 (Figure 7.3, see Appendix for dilutions). The few fractions that did contain Muc19 were collected and dialysed against 3 changes of distilled water for 6 hours each, then freeze dried for further investigation. When we compare the Muc19 slot blot analysis of HSM (Figure 7.3) and PSM (Figure 5.4) we can see that there is stronger MUC19 expression in PSM V_0 (Figure 5.4).

SDS-PAGE gel electrophoresis could not be performed on HSM derivatives as samples were used entirely for the replicate rounds of pseudoviral and MTT assays. Palm *et al* (2016) ran crude pooled saliva (centrifuged at 470g for 5 mins to remove debris) from 15 healthy horses on a 6% SDS-PAGE gel and stained with Coomassie brilliant blue (CBB). CBB binds to proteins by heteropolar and hydrophobic interactions with basic amino acids (Georgiou et al., 2008). CBB staining of crude horse saliva showed a smearing effect typical of mucins with protein bands present at ~440kDa (Palm et al., 2016). Western blot revealed the presence of IgA and to a lesser extent IgG (Palm et al., 2016). Sousa-Pereira *et al* (2015) ran crude saliva (centrifuged at 12 000g for 10 mins at 4^{o}C to remove debris) on an 8 – 16% gradient polyacrylamide gel and stained with a modified CBB to enhance protein detection (Candiano et al., 2004). They found multiple protein bands from <5 – 250kDa and identified 103 protein families through liquid chromatography–mass spectrometry (Sousa-Pereira et al., 2015). Among the protein families found was Latherin (which aids mastication), Cas (zinc metalloenzymes that convert carbon dioxide to bicarbonate), Casein (protein family of phosphoproteins) and CRISP3 (a protein with antimicrobial properties) (Haendler et al., 1999; McDonald et al., 2009; Sousa-Pereira et al., 2015; Tashian, 1989).

7.2.2 HSM Inhibits HIV-1 *in vitro*

All HSM derivatives (crude HSM, HSM V_0, HSM V_i and Muc19) showed HIV inhibition. Figure 7.5 shows the inhibition curves of HSM on HIV-1 inhibition *in vitro* and Table 7.1 shows the IC_{50} values based upon the level of deviation of the points from the modelled inhibition curve. Crude HSM showed the best inhibition (IC_{50}: 51.32µg/ml, see Table 7.1) but the 95% confidence intervals (6.060 to 434.7µg/ml, see Table 7.1) were too wide for this result to be reliable. The next best inhibition came from the large molecular weight fraction eluted from a Sepharose 4B column (HSM V_0 IC_{50}: 76.35µg/ml, see Table 7.1). This data was more

reliable as there were tighter confidence intervals (HSM V_0 95% confidence interval: 40.27 to 144.8µg/ml, see Table 7.1) indicating the this was a true effect of inhibition. The low molecular weight fraction eluted from the Sepharose 4B column showed inhibition but had the highest IC_{50} value of the HSM derivatives (HSM V_i IC_{50}: 841.8µg/ml, see Table 7.1). Peacocke et al (2012) showed both the high and low molecular weight fraction (MUC5B and MUC7 respectively) eluted from a Sepharose 4B column inhibited pseudoviral HIV-1 subtype C Du422.1 infection in vitro with MUC5B showing marginally better inhibition (Peacocke, 2011). While HSM V_0 did show the better inhibition in our studies the key difference in our samples is that HSM V_0 contains a mixture of Muc5b and Muc19 (Rousseau et al., 2008) and when separated, HSM Muc19 on its own showed an almost 100% reduction in HIV-1 inhibition (HSM Muc19 IC_{50}: 131.9µg/ml, see Table 7.1). This data suggests that the combination of HSM Muc5b and Muc19 is more efficient but further experiments are required to assess the action of HSM Muc5b on HIV-1 as separation of Muc5b and Muc19 in this study proved problematic (data not shown). When we compare the best and most reliable HIV-1 inhibitor from the HSM derivatives i.e. HSM V_0 (IC_{50}: 76.35µg/ml, see Table 7.1) we can see that it's IC_{50} value is over 45 times higher than PGM V_0 (IC_{50}: 1.668µg/ml, see Table 4.1), over three times higher than DTT treated PSM V_0 (IC_{50}: 20.79µg/ml, see Table 5.1) and over eight times higher than PCM V_0 (IC_{50}: 8.974µg/ml, see Table 6.1). This shows that our HSM derivatives have the lowest inhibitive potential from the mucin sources in our study.

7.2.3 Toxicity of HSM Derivatives

To assess the validity of our inhibition data, HSM derivatives were run on an MTT assay to determine if the HSM derivatives were toxic to the TZM-bl target cells. LD_{50} values were calculated for all but the crude HSM samples. For crude HSM cell viability was quoted that was at a concentration close to crude HSM IC_{50} (IC_{50}: 51.32µg/ml (see Table 7.1), percentage cell viability: 98.85% at 71.88µg/ml (see Table 7.2)). Crude HSM showed good percentage cell viability so the corresponding IC_{50} was deemed reliable (crude HSM IC_{50}: 51.32µg/ml, see Table 7.1). The LD_{50} value for HSM V_0 (HSM V_0 LD_{50}: 737µg/ml, see Table 7.2) was over 9 times the corresponding IC_{50} value (HSM V_0 IC_{50}: 76.35µg/ml, see Table 7.1), indicating that HSM V_0 inhibition data could be trusted. HSM V_i showed a high LD_{50} (HSM V_i LD_{50}: ~986.1µg/ml, see Table 7.2) but when compared to its corresponding IC_{50} (HSM V_i IC_{50}: 841.8µg/ml, see Table 7.1) value it could be seen that HSM V_i inhibitory effect may not be reliable. The LD_{50} value for HSM Muc19 (HSM Muc19 LD_{50}: 59.79µg/ml, see Table 7.2) was under 50% of the corresponding IC_{50} (HSM Muc19 IC_{50}: 131.9µg/ml, see Table 7.1) which is

a clear indication that the HSM Muc19 inhibitory data could not be trusted, as the mucin was toxic and killed the target cells before pseudoviral HIV-1 could infect target cells and promote luciferase expression.

While horse saliva has big mucins (i.e. Muc19 and Muc5b), it does not inhibit HIV-1 as effectively as its pig counterpart or PGM. After our first findings of HSM V_0 not being better than PSM V_0, it was decided that their components would not undergo DTT or trypsin treatment. The effect DTT and trypsin would have on HSM and its effect on HIV-1 is a subject for further studies. The high IC_{50} values seen in HSM derivatives (when compared to PGM, PSM and PCM data), as well as saliva's low viscosity compared to PGM and PCM, excluded horse saliva from mucin-derived gel analysis. One explanation for HSM having high IC_{50} values and lower cell survival may be due to the preparation, as HSM only underwent one round of density ultracentrifugation. This may have not been enough to fully eliminate contaminating and/or harmful proteins. Further studies are required to assess the effect of better purification of HSM and its effect on HIV *in vitro*.

CHAPTER 8: THE ANALYSIS OF MUCIN DERIVED GELS ON HIV-1 *IN VITRO*

Our study has shown the anti-HIV-1 potential of PGM, PSM, PCM and HSM *in vitro*. The next step was to construct a gel from the most abundant and effective sources (i.e. purified PGM and purified PCM). We then measured the ability of pig gastric and cervico-vaginal mucin-derived gels to inhibit HIV-1 entry into a model target cell line, TZM-bl (Montefiori, 2009).

8.1 Results

8.1.1 Investigation of Gel Solutions on Pseudoviral Assay

To create the gels, mucins were combined with solutions based on research done by Allen *et al* (1976) and Owen *et al* (1999). Four solutions were constructed in distilled water. These solutions were gel solution 1 (0.02M potassium acetate), gel solution 2 (0.2M potassium chloride), gel solution 3 (0.002% (w/v) sodium azide) and gel solution 4 which was a vaginal fluid simulant (0.351% sodium chloride, 0.14% potassium hydroxide, 0.0222% calcium hydroxide, 0.0018% bovine serum albumin, 0.2% lactic acid, 0.1% acetic acid, 0.016% glycerol, 0.04% urea and 0.5% glucose). All gels were adjusted to neutral pH to successfully use them on *in vitro* assays. The gel solutions were first tested on a pseudoviral assay and MTT assay in the absence of mucins to assess the solutions' inhibitory potential and toxicity respectively, before the addition of mucins. Figure 8.1 shows the log dose response curves of solutions without mucins on the pseudoviral assay.

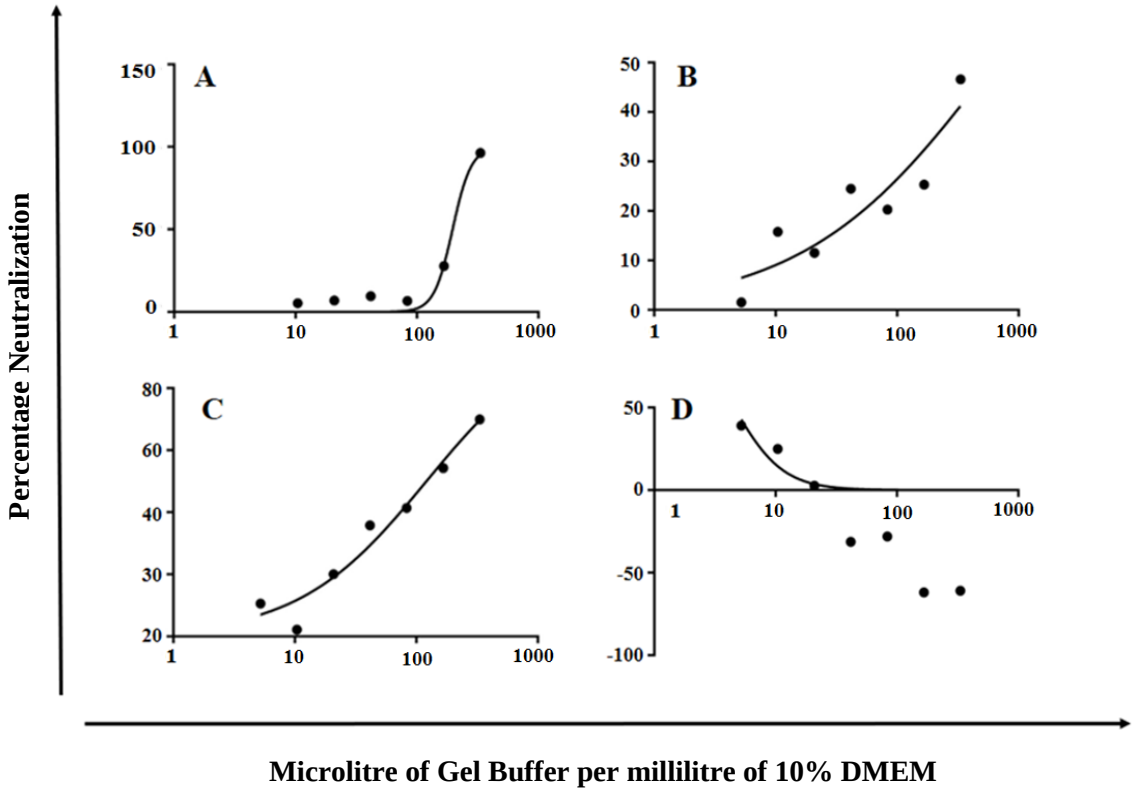

Figure 8.1 Log dose response curves of gel solutions. A, gel solution 1: 0.02M potassium acetate; B, gel solution 2: 0.2M potassium chloride; C, gel solution 3: 0.002% (w/v) sodium azide, and D, gel solution 4: 0.351% sodium chloride, 0.14% potassium hydroxide, 0.0222% calcium hydroxide, 0.0018% bovine serum albumin, 0.2% lactic acid, 0.1% acetic acid, 0.016% glycerol, 0.04% urea and 0.5% glucose.

Figure 8.1 shows the effect gel solutions had on HIV-1 inhibition before the addition of mucins to rule out that the inhibitory effects recorded were not due to the solution. Reliability of the dose response curves can be assessed visually by how close the points of the curve lie to the solid line, which corresponds to the best model of an inhibition curve. Gel solution 1 (Figure 8.1 A) and gel solution 4 (Figure 8.1 D) showed substantial deviation for the modelled inhibition curve. Gel solution 4 also had a negative slope, which is the opposite of what we expect to see from our dose response curves. One interpretation of this is that with increasing concentration there was increased infection over and above the positive control (HIV-1 and TZM-bl cells alone). This may need to be confirmed in further investigations. Gel solution 2 (Figure 8.1 B) and 3 (Figure 8.1C) showed good adherence to the solid line. Table 8.1 shows

the calculated 95% confidence interval of the IC_{50} values based upon the level of deviation of the points from the modelled inhibition curve and the LD_{50} values from the MTT assay.

Table 8.1 Results of Gel Solutions on Pseudoviral Assay and MTT Assay

Component	**Pseudoviral Assay**		**MTT Assay**
	IC_{50} (µg/ml)	**95% Confidence Intervals (µg/ml)**	**LD_{50} (µg/ml)**
Gel Solution 1	No Inhibition		0.01128
Gel Solution 2	1.207	1.161 to 1.256	0.08
Gel Solution 3	No Inhibition		0.01
Gel Solution 4	4.544	0.3454 to 59.79	302.3

Gel solutions 1 and 3 showed no inhibition on the pseudoviral assay and showed low LD_{50} values (gel solution 1 LD_{50}: 0.01128µg/ml; gel solution 3 LD_{50}: 0.01µg/ml). This indicates that gel solutions 1 and 3 in the absence of mucins have a toxic effect on the TZM-bl cell line. Gel solution 2 had a low IC_{50} (IC_{50}: 1.207µg/ml) and tight 95% confidence intervals (95% confidence intervals: 1.161 to 1.256 µg/ml) but showed toxicity as it showed a very low LD_{50} (0.08µg/ml). Gel solution 4 showed a low IC_{50} (IC_{50}: 4.544µg/ml) but exhibited wide 95% confidence intervals (0.3454 to 59.79µg/ml). Gel solution 4 did show a high LD_{50} (302.3µg/ml). Figure 8.2 shows the log dose repose curves of these assays.

8.1.2 Investigation of Mucin-Derived Gels on Pseudoviral Assay

The next step was to combine mucins with the gel solutions and run them on pseudoviral and MTT assays. Mucins were dissolved with gel solutions (see Appendix Table 2.) at a ratio of 30mg of mucin in 1 ml of solution.

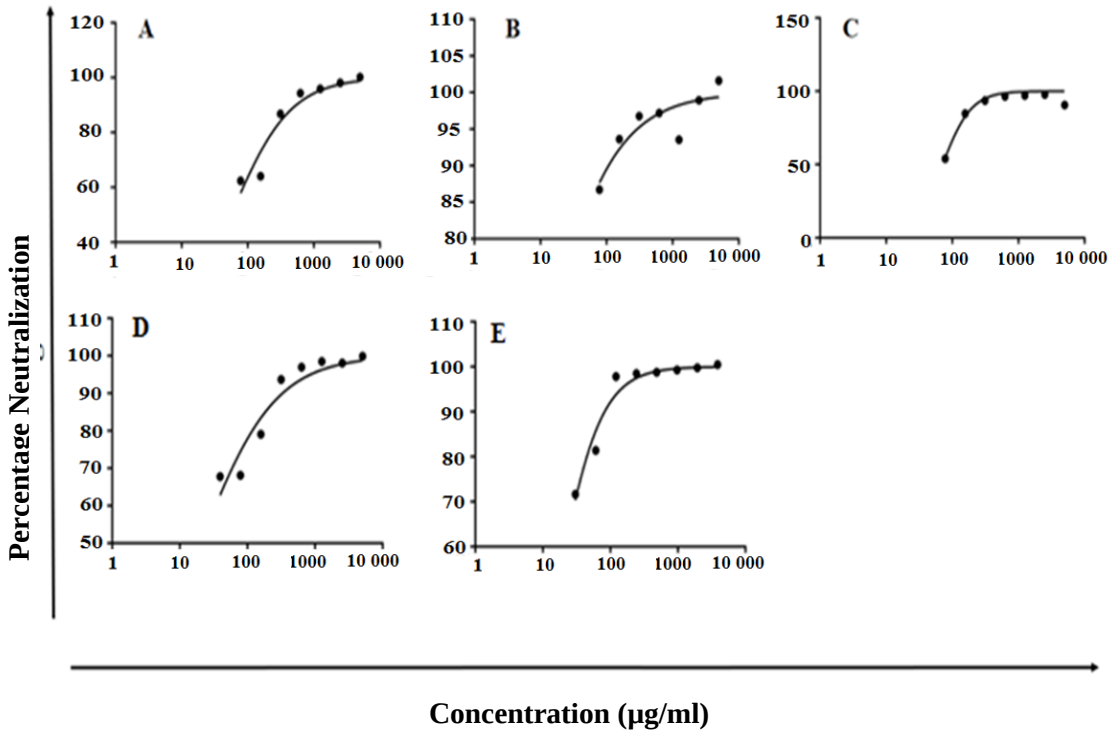

Figure 8.2 Log dose response curve of mucin-derived gels. A, PGM in gel solution 1: 0.02M potassium acetate; B, PGM in gel solution 2: 0.2M potassium chloride; C, PGM in gel solution 3: 0.002% (w/v) sodium azide; D, PGM in gel solution 4: 0.351% sodium chloride, 0.14% potassium hydroxide, 0.0222% calcium hydroxide, 0.0018% bovine serum albumin, 0.2% lactic acid, 0.1% acetic acid, 0.016% glycerol, 0.04% urea and 0.5% glucose and E, PCM in gel solution 4: 0.351% sodium chloride, 0.14% potassium hydroxide, 0.0222% calcium hydroxide, 0.0018% bovine serum albumin, 0.2% lactic acid, 0.1% acetic acid, 0.016% glycerol, 0.04% urea and 0.5% glucose.

All points for mucin derived gels lay close to the solid line that corresponds to the best model of an inhibition curve. This indicated that the data for all mucin-derived gels were reliable. Table 8.2 shows the calculated 95% confidence intervals of the IC_{50} values based upon the level of deviation of the points from the modelled inhibition curve as well as calculated LD_{50} values from the MTT assay.

Table 8.2 Showing the Pseudoviral Assay IC_{50}'s and MTT Assay Percentage Cell Viabilities of Mucin Derived Gels

Component	**Pseudoviral Assay**		**MTT Assay**		
	IC_{50} (µg/ml)	**95% Confidence Intervals (µg/ml)**	**LD_{50} (µg/ml)**	**Concentration (µg/ml)**	**% Cell Viability**
PGM in Gel Solution 1	56.19	31.00 to 101.9	Curve did not converge	140.63	84.62
PGM in Gel Solution 2	5.701	0.3401 to 95.57	134 845		
PGM in Gel Solution 3	71.10	54.01 to 93.59	~17 204		
PGM in Gel Solution 4	20.23	9.566 to 42.76	525.4		
PCM in Gel Solution 4	248.9	234.9 to 263.8	2 088		

Inhibition was shown in all pig mucin-derived gels on the pseudoviral assay. PCM was combined with gel solution 4 only due to limited PCM sample yield. PGM in gel solution 2 showed the best inhibition (IC_{50}: 5.701µg/ml) but had a wide 95% confidence interval (0.3401 to 95.57µg/ml) indicating that we cannot assess the true inhibitory effect of PGM in gel solution 2. PGM in gel solution 4 showed the second-best inhibition (IC_{50}: 20.23µg/ml) and a tight 95% confidence interval (9.566 to 42.76µg/ml). PGM in gel solution 4 had a high LD_{50} (525.4µg/ml) and this indicated the inhibition data as being reliable. PCM in gel solution 4 showed the highest IC_{50} (IC_{50}: 248.9µg/ml) from all the mucin gels and had a high LD_{50} (2 088µg/ml).

8.1.3 Probing of the Mucus Gel Mesh to Determine Structural Arrangement and Tracking of Fluorescently Labelled HIV

Following the results of section 8.1.1 PGM in gel solution 4 was assessed to be the best inhibitor of HIV-1 *in vitro* and thus progressed to further investigation. Initial studies have been performed by the Lai laboratory on PGM in gel solution 4 and it showed the virus was retarded at pH 4 rather than at pH 7. Real trapping/immobilization of the pseudovirus was not seen with either condition. The PEG-coated beads were slowed substantially, perhaps to a comparable extent as similar sized but typically muco-sticky carboxylated latex beads. These experiments are currently being repeated and further assessed. As these experiments are time consuming the repeat data will not be ready by the time of submission of this manuscript.

8.2 Discussion

8.2.1 The Inhibition of HIV-1 by Mucin-Derived Gels

The final part of my study investigates the effect of mucin-derived gels on HIV-1 *in vitro*. To our knowledge this is the first time that pig mucins have been used in the context of an anti-HIV-1 gel *in vitro*. The difficulty of working with gels on the pseudoviral assay is the gel blocking media and cell interactions. This problem was alleviated through serial dilution.

In 1976, Allen *et al* published a paper describing how glycoproteins form a gel *in vivo* while being semi-permeable to proteolytic enzymes. They performed viscosity studies at varying concentrations on PGM in three solutions namely, 0.2M potassium chloride 0.02% sodium azide; 0.02M potassium acetate buffer, pH 5.5 (Allen et al., 1976). From the PGM in solution data Allen *et al* (1976) determined PGM's effective hydrodynamic volume, and showed PGM concentration above 20 – 25mg/ml resulted in gel formation and the average glycoprotein concentration found in stomachs is ~30 – 40mg/ml.

Using the results of Allen *et al* (1976) we constructed our first set of gels from the most abundant available source, namely purified PGM. PGM was diluted at 30mg/ml with the same solutions (gel solution 1: 0.02M potassium acetate; gel solution 2: 0.2M potassium chloride; gel solution 3: 0.02% sodium azide). In the absence of pig mucins, gel solutions 1 and 3 showed no inhibition, where gel solution 2 did inhibit HIV-1 (gel solution 2 IC_{50}: 1.207µg/ml, see Table 8.1) but it had a very low LD_{50} (0.08µg/ml, see Table 8.1) which indicates that the low inhibition may have been due to the solution being toxic to the target cells, allowing less cells to produce luciferase.

Addition of pig mucins brought about inhibition in the presence of all solutions. PGM in gel solution 2 gave the lowest IC_{50} (gel solution 2 IC_{50}: 5.701µg/ml, see Table 8.2) and despite having a high LD_{50} (gel solution 2 LD_{50}: 134 845µg/ml, see Table 8.2) gel solution 2 had a very wide 95% confidence interval indicating that in this study the true inhibitory effect cannot be determined. The next lowest IC_{50} was shown by PGM in gel solution 1 (PGM in gel solution 1 IC_{50}: 56.19µg/ml, see Table 8.2) and then PGM in gel solution 3 (PGM in gel solution 3 IC_{50}: 71.10µg/ml, see Table 8.2) with tight 95% confidence intervals (PGM in gel solution 1 95% confidence interval: 31.00 to 101.9µg/ml; PGM in gel solution 3 95% confidence interval: 54.01 to 93.59µg/ml, see Table 8.2). PGM in gel solution 1 showed good percentage cell viability (at 140.63µg/ml there was 84.62% cell viability, see Table 8.2) and PGM in gel

solution 3 had a high LD_{50} indicating that both the gels were not toxic to the TZM-bl cell lines and that our IC_{50} data can be trusted.

Previous research into the anti-viral effect of PGM involved testing commercial PGM mixed with a basal lamina gel matrix (Lieleg et al., 2012). Lieleg *et al* (2012) used a 1% (weight/volume) mucin in gel solution and tested it against HPV (on a HeLa cell line), Influenza H1N1 strain (on a MDCK cell line) and MCV (on an A549 cell line). They reported their data in terms of percentage infected cells, and for HPV: ~5.6% infection; Influenza H1N1: ~1.2% and finally for MCV: ~3.2%. Percentage infected cells data were not shown for our samples in this thesis due to the large volume of data calculated, but percentage infected cells and percentage neutralization data were used to calculate the IC_{50} values. Our data showed comparative results for two PGM in gel solutions (PGM in gel solution 2: 3.23% infected cells and PGM in gel solution 3: 6.47% infected cells (data not shown)) and PGM in gel solution 1 showed over two-fold percentage infected cells (PGM in gel solution 1: 13.25% (data not shown)). It is important to note one large difference between the studies, is the solution added. Lieleg *et al* (2012) used a basal lamina matrigel that is a subtype of extracellular matrix, whereas this part of our study used biochemical gels to see if neutralization was possible. Despite using biochemical i.e. non-physiological solutions, we showed good inhibition and proved that our mucins were ready for the next stage of gel research.

The successful results of this study thus far prompted us to find a solution to be added to our pig mucins that mimicked the cervico-vaginal mucus make up. The solution chosen was developed by Owen and Katz (1999) to imitate the fluid produced in the human vagina. They reviewed literature on human vaginal secretions, considering interactions with therapeutic, prophylactic and contraceptive products, including pH. Owen and Katz (1999) formulated that in 1L of vaginal fluid simulant (pH 4.2) there were: 3.51g NaCl, 1.4g KOH, 0.222g $Ca(OH)_2$, 0.018g bovine serum albumin, 2g lactic acid, 1g acetic acid, 0.16g glycerol, 0.4g of urea and 5g glucose.

The simulated vaginal fluid (gel solution 4) on its own showed inhibition of HIV-1 in the neutralization assay (gel solution IC_{50}: 4.544µg/ml, see Table 8.1) and despite having a high LD_{50} (gel solution 4 LD_{50}: 302.3µg/ml, see Table 8.1) it had a wide 95% confidence interval (0.3454 to 59.79µg/ml, see Table 8.1). This indicated that the true HIV-1 inhibitory effect of gel solution 4 was unreliable. After the addition of PGM to gel solution 4, the IC_{50} (20.23µg/ml, see Table 8.2) was higher than gel solution 4 alone but had a narrower 95% confidence interval

(9.566 to 42.76µg/ml, see Table 8.2) showing more reliability of inhibition data. PGM in gel solution 4 also had a high LD_{50} (525.4µg/ml, see Table 8.2) indicating that the inhibition data was not influenced by toxicity. PCM addition to Gel Solution 4 gave a higher than 12-fold IC_{50} (248.9µg/ml, see Table 8.2), very tight 95% confidence interval (PCM in gel solution 4 95% confidence interval: 234.9 to 263.8µg/ml, see Table 8.2) and a high LD_{50} value (PCM in gel solution 4 LD_{50}: 2 088µg/ml, see Table 8.2). PGM in gel solution 4 displayed a higher IC_{50} (20.23µg/ml, see Table 8.2) than PGM alone (1.668µg/ml, see Table 4.1). This lowering of inhibition may be due to the gel solution components masking or diluting the full inhibitory potential of PGM.

When the mucins in gel solution 4 data was compared to the Lieleg *et al* (2012) study, our 1% mucin derived gels displayed percentage infections like HPV penetration of PGM in matrigel (~5.6%). At 1% PGM in Gel Solution 4, there is 6.33% (data not shown) infection and the corresponding PCM in Gel Solution 4 allowed 5.96% infection (data not shown). Future studies may be to combine our PGM and PCM with matrigel as a direct comparison to Lieleg *et al* (2012) on our neutralization assay.

When comparing our PGM derivatives and anti-HIV-1 mucin-derived gels to candidate microbicides, we see varying results. Microbicide gel studies are mostly tested on animal models and animal studies were outside the scope of this project but may be covered in future projects. The subsequent studies mentioned all tested compounds diluted with media (PBS or DMEM) against HIV-1 in *in vitro* assays like the pseudoviral assay used in this study unless otherwise stated.

Tao *et al* (2007) assessed the ability of sodium rutin sulphate, a sulphated rutin enhanced from the natural flavonol glycoside rutin, to inhibit HIV-1 subtype B. They measured inhibition on a TZM-bl cell luciferase gene reporter assay like our assay and a p24 ELISA assay. They found that sodium rutin sulphate had an IC_{50} of 11.99µg/ml (Tao et al., 2007). This IC_{50} value is almost half of our PGM in gel solution 4 (IC_{50}: 20.23µg/ml, see Table 8.2) and 20 times lower than PCM in gel solution 4 (IC_{50}: 248.9µg/ml, see Table 8.2). PGM V_0 (IC_{50}: 1.668µg/ml, see Table 4.1) and PCM V_0 (IC_{50}: 8.974µg/ml, see Table 6.1) showed marginally better inhibition than sodium rutin sulphate (IC_{50}: 11.99µg/ml). O'Keefe *et al* (2009) assessed the ability of plant produced Griffithsin to inhibit HIV-1 Subtype C Du156.12 on TZM-bl cells in a pseudovirus-based neutralization assay like the one used in our study. Griffithsin showed a very low IC_{50} value (IC_{50}: <0.003µg/ml), and inhibited HIV-1better than all our PGM

derivatives and mucin-derived gels (O'Keefe et al., 2009). One advantage PGM derivatives or mucin-derived gels have over plant produced Griffithsin is that mucins form part of the innate immune system and may enhance vaginal protection against HIV-1. Alcami *et al* (2014) tested 5-Hydroxytyrosol, a natural compound that has been shown to possess biochemical activity, against HIV integrase and gp41 (Lee-Huang et al., 2007a, 2007b). They used a luciferase reporter gene assay (like the one we used to assess inhibition) with pseudoviral HIV-1 subtypes A, C, D, E and F on pre-activated peripheral blood mononuclear cells. They showed that 5-Hydroxytyrosol had IC_{50} values from 4.62 to 9.25µg/ml across all HIV-1 subtypes (Alcami et al., 2014). Our PGM (IC_{50}: 20.23µg/ml, see Table 8.2) and PCM (IC_{50}: 248.9µg/ml, see Table 8.2) derived gels had higher IC_{50} values, while our PCM V_0 IC_{50} (IC_{50}: 8.974µg/ml, see Table 6.1) lay within the range of the 5-Hydroxytyrosol IC_{50} values but our PGM V_0 on its own, showed better inhibition with a lower IC_{50} (IC_{50}: 1.668µg/ml (see Table 4.1); 5-Hydroxytyrosol IC_{50}: 4.62 to 9.25µg/ml). Pasetto *et al* (2014) used a novel way to test the anti-HIV-1 microbicide activity of the plant flavonoid, Myricetin (not as a gel) on a dual chamber model. In previous studies, researchers have shown Myricetin to possess antibacterial, anti-viral, anti-inflammatory and antioxidant properties (Basso et al., 2005; Comalada et al., 2005; Di Stasi et al., 2002; Havsteen, 1983; Kandaswami et al., 1994; Mehla et al., 2011; Yu et al., 2007). The Dual Chamber Model consisted of a HeLa cell lined apical chamber and a TZM-bl lined basal chamber. The two chambers were separated by a permeable membrane. Both chambers were immersed in cell media and the apical chamber was laid with Myricetin and HIV-1_{BaL} subtype B for 24 hours. Thereafter, the basal TZM-bl cells were tested on a Luciferase assay (Pasetto et al., 2014). They found Myricetin had an IC_{50} of 6.21µg/ml which was lower than our mucin derived gels but over 3.5 times higher than our large mucin fraction of PGM eluted off a Sepharose 2B column (PGM V_0 IC_{50}: 1.668µg/ml, see Table 4.1). Styczynski *et al* (2015) assessed the HIV-1 inhibitory potential of copper (II) phthalocyanine sulphate on a TZM-bl luciferase gene reporter assay. They chose a copper compound as copper has previously been shown to have antibacterial, anti-viral and anti-fungal properties (Borkow et al., 2004, 2005; Coyle et al., 2004). They measured the inhibitory potential of copper (II) phthalocyanine sulphate against pseudoviral HIV-1 subtype B (Styczynski et al., 2015). They found copper (II) phthalocyanine sulphate to have an IC_{50} of 65µg/ml which is over three times higher than our PGM in gel solution 4 (20.23µg/ml, see Table 8.2), over seven times higher than our PCM V_0 (IC_{50}: 8.974µg/ml, see Table 6.1) and over almost forty times higher than PGM V_0 (1.668µg/ml, see Table 4.1). A summary of these comparisons can be seen in Table 8.3.

Table 8.3 Comparison of IC_{50} Data from Our Mucin-Derived Gels and Best Inhibitors Versus Other Microbicidal Candidates

Study	Anti-HIV-1 Candidate	Virus and Cell Line Tested On	IC_{50} (µg/ml)
Our Study	PGM V_0 (Muc5ac and Muc6)	HIV-1 Subtype C Du422.1 on TZM-bl cells	1.668
	PCM V_0	HIV-1 Subtype C Du422.1 on TZM-bl cells	8.974
	PGM in gel solution 4	HIV-1 Subtype C Du422.1 on TZM-bl cells	20.23
	PCM in gel solution 4	HIV-1 Subtype C Du422.1 on TZM-bl cells	248.9
Tao *et al* (2007)	Sodium rutin sulphate	HIV-1_{BAL} Subtype B on TZM-bl cells	11.99
O'Keefe *et al* (2009)	Plant produced Griffithsin	HIV-1 Subtype C Du156.12 on TZM-bl cells	<0.003
Alcami *et al* (2014)	5-Hydroxytyrosol	HIV-1 Subtypes A, C, D, E, F on pre-activated peripheral blood mononuclear cells	4.62 – 9.25
Pasetto *et al* (2014)	Myricetin	HIV- 1_{BAL} Subtype B on TZM-bl cells	6.21
Styczynski *et al* (2015)	Copper (II) phthalocyanine sulfate	HIV-1_{BAL} Subtype B on TZM-bl cells	65

8.2.2 Structural Arrangement and HIV Particle Tracking of PGM in Simulated Vaginal Fluid

The next stage of our study was to determine the structural arrangement and track fluorescently labelled HIV particles through our PGM in gel solution 4. Aliquots of lyophilized PGM were shipped to our collaborator in North Carolina (Associate Professor Sam Lai, University of North Carolina Eshelman School of Pharmacy, Division of Molecular Pharmaceutics) to construct and add simulated vaginal fluid to our PGM and run on his assay.

Our results showed that virus particles were slowed at lower pH (pH 4). Migration of PEG-coated beads was retarded and the pore size experiments showed comparable magnitude of the carboxylated latex beads. This suggests that our PGM in Gel Solution 4 doesn't form a rigid matrix, but rather a soft gel most likely due to mucin entanglement effects. These results suggest our reconstituted mucins don't exhibit the same mucin-mucin end links or cross links

compared to native mucins. The assay did demonstrate that our reconstituted mucins provide some level of barrier properties.

Pig gastric mucus has previously undergone particle tracking to determine the microrheology of the mucus (Georgiades et al., 2014). Researchers collected PGM in non-chaotrophic conditions and purified them by CsCl density gradient ultracentrifugation. While they tested for Muc5ac, they did not mention testing for the presence of Muc6 so it is possible that the results are not for just Muc5ac alone, but in combination with Muc6. Using carboxyl-activated polystyrene microspheres, microrheology experiments revealed that PGM self-assembles, forming a viscoelastic solution at high mucin concentration (Georgiades et al., 2014). It was also noted that not only did gelation occur in PGM at low pH but there was a hundred-fold increase in the elastic shear modulus (Georgiades et al., 2014). Forming a gel at low pH is important to the protection of gastric epithelia from auto-digestion (Hong et al., 2005). This corresponds with our PGM in gel solution 4 data which shows better retardation at a lower gel forming pH (pH 4).

From our data, it can be seen our best HIV-1 inhibiting mucin derivatives (PGM V_0 and PCM V_0), as well as PGM in gel solution 4 are comparable to other microbicidal candidates and in some cases, better (see table 8.3). If the PGM in Gel Solution 4 were to progress to an anti-HIV-1 vaginal gel, the ability to only retard HIV movement (*in vitro*) at pH 4 may be advantageous with respect to the human cervico-vaginal environment. In 2009, Lai et al performed experiments on normal human cervico-vaginal mucus (CVM) that contained healthy lactobacillus-dominated vaginal flora, had inhibited HIV infection a 100-fold better than HIV diffusion through water (Lai et al., 2009). They hypothesized that the normal CVM lactobacilli continuously produced lactic acid thus lowering the pH to 4, and removed the overall negative charge present on the surface of HIV without membrane lysis. During sexual intercourse, semen temporarily neutralizes CVM (to pH 6 – 7) and this neutral pH allows HIV to maintain its native surface charge and diffusion is only slowed down 15-fold. They hypothesized, if a mechanism could be developed that maintained an acidic pH for CVM and hence a high lactic acid content during sexual intercourse, it would provide effective protection for the vagina and penis by trapping HIV before infection can occur (Lai et al., 2009). While our PGM in Gel Solution 4 has been shown to inhibit HIV at pH 4 and contains lactic acid, further experiments are needed to see if our gel can neutralize HIV infected semen, testing *in vivo* non-human primate models as well as to determine the effect on vaginal flora. The best way to test the gel at full concentration would be in an animal model but this lies outside the scope of this study

and may be assessed in future studies. Further studies would also seek to understand the mechanism of mucin specific HIV-1 inhibition by stepwise de-glycosylation to assess the role of glycan groups, as well as, changing the charge of different mucin glycoforms, to see if inhibition changes. Thus far, our data shows that the large molecular weight fraction of PGM eluted from a Sepharose 2B column is our best inhibitor and purified PGM in gel solution 4 is our best anti-HIV-1 gel.

CHAPTER 9: CONCLUSION

Human Immunodeficiency Virus/Acquired Immune Deficiency Syndrome (HIV/AIDS) still presents a global problem with 1.2 million deaths worldwide reported in 2014. Two million new infections were also reported globally. Sub-Saharan Africa is hardest hit by this epidemic and South Africa not only had the highest number of people living with HIV, but also an increase in unsafe sexual practices like no condom use. One possible way to curb the spread of new infections (via the vaginal route of infection), even in the absence of condoms, would be through a microbicide. A vaginal microbicide is a topical gel that, in theory, could be applied to the vagina protecting women from sexual transmission of HIV. Thus far, there has been no success in constructing effective and safe microbicides. Previous anti-HIV gels have disrupted cellular and microbial membranes and altered the pore size of genital mucus coating. The need for a safe and effective HIV-1 preventative gel could not be greater.

This study aimed to prove that mucins derived from animal sources were as effective at inhibiting HIV-1 as human mucins from saliva, breast-milk and cervical plug mucins. This is particularly important for the future direction of this research because we envisage requiring large amounts of material for the development of a vaginal gel that would further fortify epithelial linings subjected to shear and possible tear during sexual activity, increasing the risk of transmission. Human material, although available, requires negotiation and when donated, is usually in small amounts that may need to be pooled to obtain sufficient yield of mucin. Animal material is easily available from local abattoirs and nearby farms.

Our laboratory performs work on mucins, the glycoproteins that gives mucus its gel properties. Previously our laboratory showed mucins from human breast milk (MUC1 and MUC4), cervical mucus plugs and saliva inhibit HIV-1 *in vitro*. After the success of these projects there was a need to source a more abundant supply of mucins to continue HIV research, and this study assesses two animal models, namely, pig (sourced from gastric, saliva and cervico-vaginal) and horse (saliva). Mucus from these sources were purified by a combination of density gradient ultracentrifugation and size exclusion column chromatography. Samples were then treated with either DTT or trypsin and then all derivatives were tested on an *in vitro* pseudoviral HIV-1 subtype C neutralization assay and results were used to calculate the half maximal inhibitory concentration also known as IC_{50}.

Almost all the mucin derivatives from both sources inhibited HIV-1 in vitro, where the Sepharose 2B void volumes of PGM (PGM V_0 IC_{50}: 1.668µg/ml) and PCM (PCM V_0 IC_{50}:

8.974µg/ml) gave the best IC_{50}'s. Purified pig gastric and cervico-vaginal mucins then progressed to the anti-HIV-1 gel phase of this study, where mucins were combined with either 0.02M potassium acetate (gel solution 1); 0.2M potassium chloride (gel solution 2); 0.02% (w/v) sodium azide (gel solution 3) or a simulated vaginal fluid (gel solution 4). The most reliable and effective inhibition was seen in PGM coupled with gel solution 4, it also gave good cell viability in a toxicity assay. This combination of PGM in gel solution 4 was sent to collaborators at the University of North Carolina to be run on a virion particle tracking assay and the results showed successful inhibition at low pH and nanoparticles also revealed the soft structure of our gel is due to mucin entanglement effects. It has been previously shown that at low pH PGM gelation occurs as well as a hundred-fold increase in the elastic shear modulus (Georgiades et al., 2014). Forming a gel at low pH is important to the protection of gastric epithelia from auto-digestion (Hong et al., 2005).

This study had the objective of finding an anti-HIV-1 mucin source that could be made into a gel that was abundant and effective *in vitro* and those endpoints were met, but further studies are needed to assess safety and efficacy in a non-human primate model as well as monitoring how the gel affects the vaginal flora. There is also a need to see how the gel reacts to HIV positive semen as pH is also an issue and it would be important to neutralize the pH raising ability of semen. The long-term goal of this study is to have our PGM-based anti-HIV-1 gel progress to a safe and effective microbicide. Microbicide gels have recently been adding anti-retroviral drugs and this should also be investigated as it may heighten the inhibitive properties.

APPENDIX

1 Buffers

All buffers that required a specific pH were adjusted with either HCl or NaOH and measured on a Basic Crison 20 pH meter (Alella, Spain).

1.1 Collection Buffer 1

1) 10mM Na_2HPO_4
2) 6M GuHCl
3) 10mM EDTA
4) 1mM PMSF (dissolved in 1ml of pure ethanol)
5) 5mM NEM

The above reagents were dissolved in 500ml distilled water, then pH adjusted to 6.5 with 1M HCl and 1M NaOH. This was then made up to 1L with distilled water.

1.2 Collection Buffer 2/Column Chromatography Elution Buffer

1) 11.69g NaCl
2) 0.2g NaN_3

The above reagents were dissolved in 1L distilled water.

1.3 Ultracentrifugation Buffer

1) 10mM Na_2HPO_4
2) 4M GuHCl
3) 10mM EDTA
4) 1mM PMSF (dissolved in ± 2ml of pure ethanol)
5) 5mM NEM

The above reagents were dissolved in 500ml distilled water, then pH adjusted to pH6.5 with 1M HCl and 1M NaOH. This was then made up to 1L with distilled water.

1.4 5% DMEM

1) 2.5ml heat inactivated FBS
2) 1% NEAA
3) 0.25ml of 200x PenStrep
4) 0.5ml of 100x L-glutamine

5) 25mM HEPES
6) 4500mg/L glucose

These reagents were made up in 50ml centrifuge tubes.

1.5 10% DMEM

1) 5ml heat inactivated FBS
2) 1% NEAA
3) 0.25ml of 200x PenStrep
4) 0.5ml of 100x L-glutamine
5) 25mM HEPES
6) 4500mg/L glucose

These reagents were made up in 50ml centrifuge tubes.

1.6. Gradient (4 – 20%) Sodium Dodecyl Sulfate-Polyacrylamide Gel Electrophoresis (SDS-PAGE) Gel Buffers:

1.6.1. 30% Bis/Acrylamide

1) 30g Acrylamide
2) 0.8g Bis

The above reagents were made up to 100ml, with distilled water.

1.6.2. Running gel buffer

1) 0.75M Tris
2) 0.2% SDS

The above reagents were made up to 100ml, with distilled water. The pH was adjusted to pH8.8 with 1M HCl and 1M NaOH.

1.6.3. Spacer gel Buffer

1) 0.25M Tris
2) 0.2% SDS

The above reagents were made up to 100ml, with distilled water. The pH was adjusted to pH6.8 with 1M HCl and 1M NaOH.

1.6.4. Tank Buffer

1) 0.025M Tris
2) 0.19M Glycine

3) 0.1% SDS

The above reagents were made up to 5L, with distilled water. The pH was adjusted to pH8.8 with 1M HCl and 1M NaOH.

1.6.5. Sample Application Buffer

1) 2% SDS
2) 10ml Glycerol
3) 0.01% Bromophenol Blue

The above reagents were made up to 100ml, with distilled water.

2. Ammonium Persulphate (AMPS)

1) 80mg/ml AMPS
2) Made up in distilled water just before gel application.

3. Gradient (4 – 20%) SDS-PAGE Gels

3.1. 4% running gel

1) 30% Bis/Acrylamide
2) 1.5ml Tris-Buffer, pH8.8 + 0.1% SDS
3) 3.7ml distilled water
4) 30µl AMPS
5) 5µl TEMED

3.2. 20% running gel

1) 30% Bis/Acrylamide
2) 1.5ml Tris-Buffer, pH8.8 + 0.1% SDS
3) 0.5ml distilled water
4) 30µl AMPS
5) 5µl TEMED

3.3. 3% stacking gel

1) 30% Bis/Acrylamide
2) 2.80ml spacer gel buffer
3) 73µl AMPS
4) 5µl TEMED

4. Periodic acid Schiff (PAS) gel staining

4.1. Schiff's reagent

1) 1g pararosaniline hydrochloride dissolved in 200ml boiling distilled water, with constant stirring.
2) Solution cooled to 50°C on bench and 20ml 1M HCl added.
3) Cooled to 25°C and added 1g potassium metabisulphite and left in the dark for 12-24 hours.
4) Added 2g activated charcoal, mixed for 1 minute and filtered.
5) Stored at 4°C in the dark.

4.2. 50% ethanol

1) 50ml ethanol
2) 50ml distilled water

4.3. 0.1% periodic acid and 3% acetic acid

1) 1ml 50% solution of periodic acid
2) 99ml 3% acetic acid

4.4. 0.1% SDS

1) 0.1g SDS
2) 100ml distilled water

5. Periodic acid Schiff (PAS) assay for *in vitro* glycoprotein detection

5.1. Schiff's reagent

1) 10g pararosaniline chloride dissolved in 1L boiling distilled water, with constant stirring
2) Solution cooled to 50°C on bench and 200 ml 1M HCl added.
3) 3g activated charcoal added, mixed for 5 – 60 mins and filtered to remove charcoal
4) Step 3 was repeated and then stored at room temperature in a dark bottle.

5.2. Periodic acid solution

1) 7% acetic acid
2) 20µl of 50% periodic acid

5.3. Decolourised Schiff's reagent

1) 100mg sodium metabisulphite
2) 6ml Schiff's reagent
3) Incubated at 37°C until colourless
4) Prepared fresh for every assay

6. BIO-RAD assay for *in vitro* protein detection

1) One part BIO-RAD dye reagent added to 4 parts distilled water.

7. Saline-Sodium Citrate (SSC)

1) A stock solution of 20x SSC was prepared by making up 176g sodium chloride and 88.2g tri-sodium citrate in 1L of distilled water and adjusting to pH7.
2) To make a 4x SSC solution, a 1 in 4 dilution of 20x SSC solution was made with distilled water.

Table 1. Western Blot Primary and Secondary Antibody Dilutions

Mucin	Animal the Primary Antibody was Raised	Species the Primary Antibody was raised against	Primary Antibody Dilution	Animal the Secondary Antibody was raised in	Species the Secondary Antibody was raised against	Secondary Antibody Dilution
MUC5AC	Rabbit	Human	1:5000	Goat	Rabbit	1:5000
MUC5B	Rabbit	Human	1:2000	Goat	Rabbit	1:5000
MUC6	Rabbit	Human	1:1000	Goat	Rabbit	1:5000
MUC7	Mouse	Human	1:2000	Goat	Mouse	1:5000
Muc19	Rabbit	Horse	1:1000	Goat	Rabbit	1:5000

Table 2. Showing components of each Mucin-derived gel

Gel Solution No.	Components		Based on research by
1	0.02M K acetate		(Allen et al., 1976)
2	0.2M KCl		(Allen et al., 1976)
3	0.02% (w/v) Na Azide		(Allen et al., 1976)
4	Composition (in distilled water)	Grams per Litre	(Marques et al., 2011)
	sodium chloride	3.51	
	potassium hydroxide	1.40	
	calcium hydroxide	0.222	
	bovine serum albumin (BSA)	0.018	
	lactic acid	2.00	
	acetic acid	1.00	
	glycerol	0.16	
	urea	0.40	
	glucose	5.00	

All gels were ~pH7.0 – 7.2 to successfully work in the *in vitro* assays.

REFERENCES

[Internet], G. (2017). MUC12 mucin 12, cell surface associated [Homo sapiens (human)] from Bethesda (MD): National Library of Medicine (US), National Center for Biotechnology Information https://www.ncbi.nlm.nih.gov/gene/10071

Ajioka, Y., Allison, L., & Jass, J. (1996). Significance of MUC1 and MUC2 mucin expression in colorectal cancer. *Journal of clinical pathology, 49*(7), 560-564.

Alcami, J., Bedoya, L.-M., Obregón, P., Beltran, M., Gomez-Acebo, E., Auñón, D., & Capa, L. (2014). Antiviral Activity of 5-Hydroxytyrosol, a Microbicidal Candidate against HIV-1 Transmission. *AIDS research and human retroviruses, 30*, A240-A240.

Aldunate, M., Tyssen, D., Johnson, A., Zakir, T., Sonza, S., Moench, T., Cone, R., & Tachedjian, G. (2013). Vaginal concentrations of lactic acid potently inactivate HIV. *J Antimicrob Chemother, 68*(9), 2015-2025. doi:10.1093/jac/dkt156

Alexander, F. (1966). A study of parotid salivation in the horse. *J Physiol, 184*(3), 646.

Alexander, F., & Hickson, J. (1970). The salivary and pancreatic secretions of the horse. *Physiology of Digestion and Metabolism in the Ruminant*, 375-389.

Alexander, R., & Mestecky, J. (2007). Neutralizing antibodies in mucosal secretions: IgG or IgA? *Current HIV research, 5*(6), 588-593.

Allen, A. (1978). Structure of gastrointestinal mucus glycoproteins and the viscous and gel-forming properties of mucus. *British medical bulletin, 34*(1), 28.

Allen, A. (1981a). Structure and function of gastrointestinal mucus. In L. R. Johnson (Ed.), *Physiology of the gastrointestinal tract* (Vol. 1st Edition, pp. 617-619). New York, N.Y.: Raven Press.

Allen, A. (1981b). The structure and function of gastrointestinal mucus in gastrointestinal mucosal protection. *William & Wilkins Co., Baltimore*, 245-259.

Allen, A., Cunliffe, W., Pearson, J., Sellers, L., & Ward, R. (1983). Studies on gastrointestinal mucus. *Scandinavian journal of gastroenterology. Supplement, 93*, 101-113.

Allen, A., Pain, R. H., & Robson, T. R. (1976). Model for the structure of the gastric mucous gel.

Alliston, C., Patterson, T., & Ulberg, L. (1958). Crystallization patterns of cervical mucus as related to estrus in beef cattle. *Journal of animal science, 17*(2), 322-325.

Ambort, D., van der Post, S., Johansson M E , V., MacKenzie, J., Thomsson, E., Krengel, U., & Hansson G , C. (2011). Function of the CysD domain of the gel-forming MUC2 mucin. *Biochem J, 436*(Pt 1), 61-70. doi:10.1042/bj20102066

Amornkul, P. N., Karita, E., Kamali, A., Rida, W. N., Sanders, E. J., Lakhi, S., Price, M. A., Kilembe, W., Cormier, E., & Anzala, O. (2013). Disease progression by infecting HIV-1 subtype in a seroconverter cohort in sub-Saharan Africa. *Aids, 27*(17), 2775-2786.

Amsden, B. (1998). Solute diffusion within hydrogels. Mechanisms and models. *Macromolecules, 31*(23), 8382-8395.

Amsden, B. (1999). An obstruction-scaling model for diffusion in homogeneous hydrogels. *Macromolecules, 32*(3), 874-879.

Andersch-Björkman, Y., Thomsson, K. A., Larsson, J. M. H., Ekerhovd, E., & Hansson, G. C. (2007). Large scale identification of proteins, mucins, and their O-glycosylation in the endocervical mucus during the menstrual cycle. *Molecular & Cellular Proteomics, 6*(4), 708-716.

Anderson, D. J., Politch, J. A., Nadolski, A. M., Blaskewicz, C. D., Pudney, J., & Mayer, K. H. (2010). Targeting Trojan Horse leukocytes for HIV prevention. *AIDS (London, England), 24*(2), 163.

Andrianifahanana, M., Moniaux, N., Schmied, B. M., Ringel, J., Friess, H., Hollingsworth, M. A., Büchler, M. W., Aubert, J.-P., & Batra, S. K. (2001). Mucin (MUC) gene expression in human pancreatic adenocarcinoma and chronic pancreatitis a potential role of MUC4 as a tumor marker of diagnostic significance. *Clinical Cancer Research, 7*(12), 4033-4040.

Apgar, J., Tseng, Y., Fedorov, E., Herwig, M. B., Almo, S. C., & Wirtz, D. (2000). Multiple-particle tracking measurements of heterogeneities in solutions of actin filaments and actin bundles. *Biophysical Journal, 79*(2), 1095-1106.

Apostolopoulos, V., Pietersz, G. A., Tsibanis, A., Tsikkinis, A., Drakaki, H., Loveland, B. E., Piddlesden, S. J., Plebanski, M., Pouniotis, D. S., & Alexis, M. N. (2006). Pilot phase III immunotherapy study in early-stage breast cancer patients using oxidized mannan-MUC1 [ISRCTN71711835]. *Breast Cancer Research, 8*(3), 1.

Ariën, K. K., Jespers, V., & Vanham, G. (2011). HIV sexual transmission and microbicides. *Reviews in medical virology, 21*(2), 110-133.

Arul, G., Moorghen, M., Myerscough, N., Alderson, D., Spicer, R., & Corfield, A. (2000). Mucin gene expression in Barrett's oesophagus: an in situ hybridisation and immunohistochemical study. *Gut, 47*(6), 753-761.

Aubert, J.-P., Kim, Y. S., & Real, F. X. (1994). Altered expression of MUC2, MUC4, and MUC5 mucin genes in pancreas tissues and cancer cell lines. *Gastroenterology, 106*(1O), i4-1091.

Audie, J., Janin, A., Porchet, N., Copin, M., Gosselin, B., & Aubert, J. (1993). Expression of human mucin genes in respiratory, digestive, and reproductive tracts ascertained by in situ hybridization. *Journal of Histochemistry & Cytochemistry, 41*(10), 1479-1485.

Azuma, A., & Schechter, M. S. (2017). Treatment of Cystic Fibrosis and Other Rare Lung Diseases: Springer.

Baeten, J. M., Chohan, B., Lavreys, L., Chohan, V., McClelland, R. S., Certain, L., Mandaliya, K., Jaoko, W., & Julie, O. (2007). HIV-1 subtype D infection is associated with faster disease progression than subtype A in spite of similar plasma HIV-1 loads. *Journal of Infectious Diseases, 195*(8), 1177-1180.

Baggaley, R. F., White, R. G., & Boily, M.-C. (2010). HIV transmission risk through anal intercourse: systematic review, meta-analysis and implications for HIV prevention. *International journal of epidemiology*, dyq057.

Balagué, C., Audié, J.-P., Porchet, N., & Real, F. X. (1995). In situ hybridization shows distinct patterns of mucin gene expression in normal, benign, and malignant pancreas tissues. *Gastroenterology, 109*(3), 953-964.

Ball, S. C., Abraha, A., Collins, K. R., Marozsan, A. J., Baird, H., Quiñones-Mateu, M. E., Penn-Nicholson, A., Murray, M., Richard, N., & Lobritz, M. (2003). Comparing the ex vivo fitness of CCR5-tropic human immunodeficiency virus type 1 isolates of subtypes B and C. *Journal of virology, 77*(2), 1021-1038.

Banerjee, R., & Puniyani, R. (2000). Effects of clove oil-phospholipid mixtures on rheology of gum tragacanth–possible application for surfactant action on mucus gel simulants. *Bio-medical materials and engineering, 10*(3, 4), 189-197.

Banerjee, R. P., R.R. (1999). Effect of eucalyptus oil added surfactants on the rheology of mucus gel simulants. *Applied Rheology, 9*, 254-261.

Baños-Lara, M. D. R., Piao, B., & Guerrero-Plata, A. (2015). Differential mucin expression by respiratory syncytial virus and human metapneumovirus infection in human epithelial cells. *Mediators of inflammation, 2015*.

Bansil, R., Celli, J. P., Hardcastle, J. M., & Turner, B. S. (2013). The influence of mucus microstructure and rheology in Helicobacter pylori infection. *Frontiers in immunology, 4*.

Bansil, R., Stanley, E., & LaMont, J. T. (1995). Mucin biophysics. *Annu Rev Physiol, 57*(1), 635-657.

Bansil, R., & Turner, B. S. (2006). Mucin structure, aggregation, physiological functions and biomedical applications. *Current Opinion in Colloid & Interface Science, 11*(2), 164-170.

Bara, J., Gautier, R., Mouradian, P., Decaens, C., & Daher, N. (1991). Oncofetal mucin Ml epitope family: characterization and expression during colonic carcinogenesis. *International journal of cancer, 47*(2), 304-310.

Bartman, A. E., Buisine, M. P., Aubert, J. P., Niehans, G. A., Toribara, N. W., Kim, Y. S., Kelly, E. J., Crabtree, J. E., & Ho, S. B. (1998). The MUC6 secretory mucin gene is expressed in a wide variety of epithelial tissues. *The Journal of pathology, 186*(4), 398-405.

Bartman, A. E., Serson, S. J., Ewing, S. L., Niehans, G. A., Wiehr, C. L., Evans, M. K., & Ho, S. B. (1999). Aberrant expression of MUC5AC and MUC6 gastric mucin genes in colorectal polyps. *International journal of cancer, 80*(2), 210-218.

Basso, L. A., Silva, L. H. P. d., Fett-Neto, A. G., Azevedo Junior, W. F. d., Moreira, Í. d. S., Palma, M. S., Calixto, J. B., Astolfi Filho, S., Santos, R. R. d., & Soares, M. B. P. (2005). The use of biodiversity as source of new chemical entities against defined molecular targets for treatment of malaria, tuberculosis, and T-cell mediated diseases: a review. *Memórias do Instituto Oswaldo Cruz, 100*(6), 475-506.

Bast, R., Badgwell, D., Lu, Z., Marquez, R., Rosen, D., Liu, J., Baggerly, K., Atkinson, E., Skates, S., & Zhang, Z. (2005). New tumor markers: CA125 and beyond. *International Journal of Gynecological Cancer, 15*(s3), 274-281.

Bergey, E., Gu, M., Collins, A., Bradway, S., & Levine, M. (1993a). Modulation of herpes simplex virus type 1 replication by human salivary secretions. *Oral Microbiol Immunol, 8*(2), 89-93.

Bergey, E. J., Cho, M.-I., Blumberg, B. M., Hammarskjöld, M.-L., Rekosh, D., Epstein, L. G., & Levine, M. J. (1994). Interaction of HIV-1 and human salivary mucins. *JAIDS Journal of Acquired Immune Deficiency Syndromes, 7*(10), 995-1002.

Bergey, E. J., Cho, M.-I., Hammarskjöld, M.-L., Rekosh, D., Levine, M. J., Blumberg, B. M., & Epstein, L. G. (1993b). Aggregation of human immunodeficiency virus type 1 by

human salivary secretions. *Critical Reviews in Oral Biology & Medicine, 4*(3), 467-474.

Berry, M., Ellingham, R., & Corfield, A. (2004). Human preocular mucins reflect changes in surface physiology. *British journal of ophthalmology, 88*(3), 377-383.

Betteridge, K., & Raeside, J. (1962). Investigation of cervical mucus as an indicator of ovarian activity in pigs. *Journal of reproduction and fertility, 3*(3), 410-421.

Bhargava, A. K., Woitach, J. T., Davidson, E. A., & Bhavanandan, V. P. (1990). Cloning and cDNA sequence of a bovine submaxillary gland mucin-like protein containing two distinct domains. *Proceedings of the National Academy of Sciences, 87*(17), 6798-6802.

Bing, L., RAYMENT, S. A., GYURKO, C., Oppenheim, F., OFFNER, G. D., & TROXLER, R. F. (2000). The recombinant N-terminal region of human salivary mucin MG2 (MUC7) contains a binding domain for oral Streptococci and exhibits candidacidal activity. *Biochemical Journal, 345*(3), 557-564.

Blalock, T. D., Spurr-Michaud, S. J., Tisdale, A. S., Heimer, S. R., Gilmore, M. S., Ramesh, V., & Gipson, I. K. (2007). Functions of MUC16 in corneal epithelial cells. *Investigative ophthalmology & visual science, 48*(10), 4509-4518.

Blank, M., Klussmann, E., Krüger-Krasagakes, S., Schmitt-Gräff, A., Stolte, M., Bornhoeft, G., Stein, H., Xing, P. X., McKenzie, I. F., & Verstijnen, C. P. (1994). Expression of MUC2-mucin in colorectal adenomas and carcinomas of different histological types. *International journal of cancer, 59*(3), 301-306.

Blixt-Johansen, G., Ek, A.-C., Ganowiak, W., Granérus, A.-K., Von Schenck, H., Unosson, M., & Wiesel, K. (1992). Improvement of oral mucosa with mucin containing artificial saliva in geriatric patients. *Archives of gerontology and geriatrics, 14*(2), 193-201.

Bobek, L., Tsai, H., Biesbrock, A. R., & Levine, M. J. (1993a). Molecular cloning, sequence, and specificity of expression of the gene encoding the low molecular weight human salivary mucin (MUC7). *Journal of Biological Chemistry, 268*(27), 20563-20569.

Bobek, L. A., Liu, J., Sait, S. N., Shows, T. B., Bobek, Y. A., & Levine, M. J. (1996). Structure and chromosomal localization of the human salivary mucin gene, MUC7. *Genomics, 31*(3), 277-282.

Bobek, L. A., Tsai, H., Biesbrock, A. R., & Levine, M. J. (1993b). Molecular cloning, sequence, and specificity of expression of the gene encoding the low molecular weight human salivary mucin (MUC7). *J Biol Chem, 268*(27), 20563-20569.

Boily, M. C., Baggaley, R. F., Wang, L., Masse, B., White, R. G., Hayes, R. J., & Alary, M. (2009). Heterosexual risk of HIV-1 infection per sexual act: systematic review and meta-analysis of observational studies. *Lancet Infect Dis, 9*(2), 118-129. doi:10.1016/s1473-3099(09)70021-0

Borkow, G., & Gabbay, J. (2004). Putting copper into action: copper-impregnated products with potent biocidal activities. *The FASEB journal, 18*(14), 1728-1730.

Borkow, G., & Gabbay, J. (2005). Copper as a biocidal tool. *Current medicinal chemistry, 12*(18), 2163-2175.

Brayman, M., Thathiah, A., & Carson, D. D. (2004). MUC1: a multifunctional cell surface component of reproductive tissue epithelia. *Reproductive Biology and Endocrinology, 2*(1), 1.

Brenchley, J., & Douek, D. (2008). HIV infection and the gastrointestinal immune system. *Mucosal immunology, 1*(1), 23-30.

Buisine, M.-P., Devisme, L., Degand, P., Dieu, M.-C., Gosselin, B., Copin, M.-C., Aubert, J.-P., & Porchet, N. (2000). Developmental mucin gene expression in the gastroduodenal tract and accessory digestive glands. II. Duodenum and liver, gallbladder, and pancreas. *Journal of Histochemistry & Cytochemistry, 48*(12), 1667-1676.

Buisine, M.-P., Janin, A., Maunoury, V., Audie, J.-P., Delescaut, M.-P., Copin, M., Colombel, J.-F., Degand, P., Aubert, J.-P., & Porchet, N. (1996). Aberrant expression of a human mucin gene (MUC5AC) in rectosigmoid villous adenoma. *Gastroenterology, 110*(1), 84-91.

Buisine, M., Desreumaux, P., Leteurtre, E., Copin, M., Colombel, J., Porchet, N., & Aubert, J. (2001). Mucin gene expression in intestinal epithelial cells in Crohn's disease. *Gut, 49*(4), 544-551.

Buisine, M. P., Desreumaux, P., Debailleul, V., Gambiez, L., Geboes, K., Ectors, N., Delescaut, M. P., Degand, P., Aubert, J. P., & Colombel, J. F. (1999). Abnormalities in mucin gene expression in Crohn's disease. *Inflammatory bowel diseases, 5*(1), 24-32.

Buonaguro, L., Tornesello, M., & Buonaguro, F. (2007). Human immunodeficiency virus type 1 subtype distribution in the worldwide epidemic: pathogenetic and therapeutic implications. *Journal of virology, 81*(19), 10209-10219.

Burdick, M. D., Harris, A., Reid, C. J., Iwamura, T., & Hollingsworth, M. A. (1997). Oligosaccharides expressed on MUC1 produced by pancreatic and colon tumor cell lines. *Journal of Biological Chemistry, 272*(39), 24198-24202.

Byrd, J. C., Yan, P., Sternberg, L., Yunker, C. K., Scheiman, J. M., & Bresalier, R. S. (1997). Aberrant expression of gland-type gastric mucin in the surface epithelium of Helicobacter pylori-infected patients. *Gastroenterology, 113*(2), 455-464.

Cameron, I. L., Kent, J. E., Philo, R., Barnes, C. J., & Hardman, W. E. (2006). Numerical distribution of lymphoid nodules in the human sigmoid colon, rectosigmoidal junction, rectum, and anal canal. *Clinical Anatomy, 19*(2), 164-170.

Campbell, E. M., Perez, O., Melar, M., & Hope, T. J. (2007). Labeling HIV-1 virions with two fluorescent proteins allows identification of virions that have productively entered the target cell. *Virology, 360*(2), 286-293.

Candiano, G., Bruschi, M., Musante, L., Santucci, L., Ghiggeri, G. M., Carnemolla, B., Orecchia, P., Zardi, L., & Righetti, P. G. (2004). Blue silver: a very sensitive colloidal Coomassie G-250 staining for proteome analysis. *Electrophoresis, 25*(9), 1327-1333.

Carlstedt, I., Herrmann, A., Hovenberg, H., Lindell, G., Nordman, H., Wickström, C., & Davies, J. (1995). 'Soluble'and 'insoluble'mucins—identification of distinct populations. *Biochemical Society Transactions, 23*(4), 845-851.

Carlstedt, I., Lindgren, H., & Sheehan, J. (1983a). The macromolecular structure of human cervical-mucus glycoproteins. Studies on fragments obtained after reduction of disulphide bridges and after subsequent trypsin digestion. *Biochemical Journal, 213*(2), 427-435.

Carlstedt, I., Lindgren, H., Sheehan, J., Ulmsten, U., & Wingerup, L. (1983b). Isolation and characterization of human cervical-mucus glycoproteins. *Biochemical Journal, 211*(1), 13-22.

Carlstedt, I., & Sheehan, J. (1983c). Macromolecular architecture and hydrodynamic properties of human cervical mucins. *Biorheology, 21*(1-2), 225-233.

Carlstedt, I., Sheehan, J., Ulmsten, U., & Wingerup, L. (1982). Isolation and purification of the mucin component of human cervical mucus *Mucus in Health and Disease—II* (pp. 273-275): Springer.

Carlstedt, I., & Sheehan, J. K. (1984). Macromolecular properties and polymeric structure of mucus glycoproteins. *Mucus and mucosa, 109*, 157-172.

Carraway, K. L., Ramsauer, V. P., Haq, B., & Carothers Carraway, C. A. (2003). Cell signaling through membrane mucins. *Bioessays, 25*(1), 66-71.

Chantler, E. (2012). *Mucus in Health and Disease—II* (Vol. 144): Springer Science & Business Media.

Chauhan, S. C., Singh, A. P., Ruiz, F., Johansson, S. L., Jain, M., Smith, L. M., Moniaux, N., & Batra, S. K. (2006). Aberrant expression of MUC4 in ovarian carcinoma: diagnostic significance alone and in combination with MUC1 and MUC16 (CA125). *Modern Pathology, 19*(10), 1386-1394.

Chen, Y., Zhao, Y. H., Kalaslavadi, T. B., Hamati, E., Nehrke, K., Le, A. D., Ann, D. K., & Wu, R. (2004). Genome-wide search and identification of a novel gel-forming mucin MUC19/Muc19 in glandular tissues. *American journal of respiratory cell and molecular biology, 30*(2), 155-165.

Church, J. A. (2008). Semen-Derived Amyloid Fibrils Drastically Enhance HIV Infection. *Pediatrics, 122*(Supplement 4), S227-S227.

Cole, A. M., & Cole, A. L. (2008). Antimicrobial Polypeptides are Key Anti-HIV-1 Effector Molecules of Cervicovaginal Host Defense. *American Journal of Reproductive Immunology, 59*(1), 27-34.

Collins, K. B., Patterson, B. K., Naus, G. J., Landers, D. V., & Gupta, P. (2000). Development of an in vitro organ culture model to study transmission of HIV-1 in the female genital tract. *Nature medicine, 6*(4), 475-479.

Colville, T. P., & Bassert, J. M. (2008). Clinical Anatomy and Physiology for Veterinary Technicians (2nd ed., pp. 568): C. V. Mosby.

Comalada, M., Camuesco, D., Sierra, S., Ballester, I., Xaus, J., Gálvez, J., & Zarzuelo, A. (2005). In vivo quercitrin anti-inflammatory effect involves release of quercetin, which inhibits inflammation through down-regulation of the NF-κB pathway. *European journal of immunology, 35*(2), 584-592.

Compton, S. J., & Jones, C. G. (1985). Mechanism of dye response and interference in the Bradford protein assay. *Analytical biochemistry, 151*(2), 369-374.

Cone, R. A. (2009). Barrier properties of mucus. *Advanced drug delivery reviews, 61*(2), 75-85.

Copin, M., Buisine, M., Devisme, L., Leroy, X., Escande, F., Gosselin, B., Aubert, J., & Porchet, N. (2001). Normal respiratory mucosa, precursor lesions and lung carcinomas: differential expression of human mucin genes. *Frontiers in bioscience: a journal and virtual library, 6*, D1264-1275.

Corrales, R., Galarreta, D., Herreras, J., Calonge, M., & Chaves, F. (2003). [Normal human conjunctival epithelium expresses MUC13, MUC15, MUC16 and MUC17 mucin genes]. *Archivos de la Sociedad Espanola de Oftalmologia, 78*(7), 375-381.

Cost, M., Dezzutti, C. S., Clark, M. R., Friend, D. R., Akil, A., & Rohan, L. C. (2012). Characterization of UC781-tenofovir combination gel products for HIV-1 infection prevention in an ex vivo ectocervical model. *Antimicrobial agents and chemotherapy, 56*(6), 3058-3066.

Coyle, B., Kinsella, P., McCann, M., Devereux, M., O'Connor, R., Clynes, M., & Kavanagh, K. (2004). Induction of apoptosis in yeast and mammalian cells by exposure to 1, 10-phenanthroline metal complexes. *Toxicology in Vitro, 18*(1), 63-70.

Crawley, S. C., Gum, J. R., Hicks, J. W., Pratt, W. S., Aubert, J.-P., Swallow, D. M., & Kim, Y. S. (1999). Genomic organization and structure of the 3′ region of human MUC3: alternative splicing predicts membrane-bound and soluble forms of the mucin. *Biochemical and biophysical research communications, 263*(3), 728-736.

Creeth, J., & Denborough, M. (1970). The use of equilibrium-density-gradient methods for the preparation and characterization of blood-group-specific glycoproteins. *Biochem. J, 117*, 879-891.

Cu, Y., & Saltzman, W. M. (2008). Controlled surface modification with poly (ethylene) glycol enhances diffusion of PLGA nanoparticles in human cervical mucus. *Molecular pharmaceutics, 6*(1), 173-181.

Culp, D. J., Latchney, L. R., Fallon, M. A., Denny, P. A., Denny, P. C., Couwenhoven, R. I., & Chuang, S. (2004). The gene encoding mouse Muc19: cDNA, genomic organization and relationship to Smgc. *Physiol Genomics, 19*(3), 303-318. doi:10.1152/physiolgenomics.00161.2004

Davies, J. R., Herrmann, A., Russell, W., Svitacheva, N., Wickström, C., & Carlstedt, I. (2002). Respiratory tract mucins: structure and expression patterns. *Mucus Hypersecretion in Respiratory Disease*, 76-88.

Davies, J. R., Hovenberg, H. W., Linden, C.-J., Howard, R., Richardson, P. S., Sheehan, J. K., & Carlstedt, I. (1996). Mucins in airway secretions from healthy and chronic bronchitic subjects. *Biochemical Journal, 313*(2), 431-439.

Dawes, C. (1972). Circadian rhythms in human salivary flow rate and composition. *J Physiol, 220*(3), 529-545.

Dawson, M., Wirtz, D., & Hanes, J. (2003). Enhanced viscoelasticity of human cystic fibrotic sputum correlates with increasing microheterogeneity in particle transport. *Journal of Biological Chemistry, 278*(50), 50393-50401.

De Bolós, C., Garrido, M., & Real, F. X. (1995). MUC6 apomucin shows a distinct normal tissue distribution that correlates with Lewis antigen expression in the human stomach. *Gastroenterology, 109*(3), 723-734.

Desseyn, J.-L., Aubert, J.-P., Porchet, N., & Laine, A. (2000). Evolution of the large secreted gel-forming mucins. *Molecular Biology and Evolution, 17*(8), 1175-1184.

Desseyn, J.-L., Aubert, J.-P., Van Seuningen, I., Porchet, N., & Laine, A. (1997a). Genomic Organization of the 3′ Region of the Human Mucin GeneMUC5B. *Journal of Biological Chemistry, 272*(27), 16873-16883.

Desseyn, J.-L., Buisine, M.-P., Porchet, N., Aubert, J.-P., Degand, P., & Laine, A. (1998a). Evolutionary history of the 11p15 human mucin gene family. *Journal of molecular evolution, 46*(1), 102-106.

Desseyn, J.-L., Buisine, M.-P., Porchet, N., Aubert, J.-P., & Laine, A. (1998b). Genomic Organization of the Human Mucin GeneMUC5B cDNA andgenomic sequences upstream of the large central exon. *Journal of Biological Chemistry, 273*(46), 30157-30164.

Desseyn, J.-L., Guyonnet-Dupérat, V., Porchet, N., Aubert, J.-P., & Laine, A. (1997b). Human mucin gene MUC5B, the 10.7-kb large central exon encodes various alternate subdomains resulting in a super-repeat structural evidence for a 11p15. 5 gene family. *Journal of Biological Chemistry, 272*(6), 3168-3178.

Devine, P. L., & McKenzie, I. F. (1992). Mucins: structure, function, and associations with malignancy. *Bioessays, 14*(9), 619-625.

Di Stasi, L., Oliveira, G., Carvalhaes, M., Queiroz-Junior, M., Tien, O., Kakinami, S., & Reis, M. (2002). Medicinal plants popularly used in the Brazilian Tropical Atlantic Forest. *Fitoterapia, 73*(1), 69-91.

Doggett, E. G., Lanham, M., Wilcher, R., Gafos, M., Karim, Q. A., & Heise, L. (2015). Optimizing HIV prevention for women: a review of evidence from microbicide studies and considerations for gender-sensitive microbicide introduction. *Journal of the International AIDS Society, 18*(1).

Dohrman, A., Tsuda, T., Escudier, E., Cardone, M., Jany, B., Gum, J., Kim, Y., & Basbaum, C. (1994). Distribution of lysozyme and mucin (MUC2 and MUC3) mRNA in human bronchus. *Experimental lung research, 20*(4), 367-380.

Doncel, G. F., Anderson, S., & Zalenskaya, I. (2014). Role of Semen in Modulating the Female Genital Tract Microenvironment–Implications for HIV Transmission. *American Journal of Reproductive Immunology, 71*(6), 564-574.

Doncel, G. F., & Clark, M. R. (2010). Preclinical evaluation of anti-HIV microbicide products: new models and biomarkers. *Antiviral research, 88,* S10-S18.

Dong, Y., Walsh, M. D., Cummings, M. C., Wright, R. G., Khoo, S. K., Parsons, P. G., & McGuckin, M. A. (1997). Expression of MUC1 and MUC2 mucins in epithelial ovarian tumours. *The Journal of pathology, 183*(3), 311-317.

Dubray, G., & Bezard, G. (1982). A highly sensitive periodic acid-silver stain for 1, 2-diol groups of glycoproteins and polysaccharides in polyacrylamide gels. *Analytical biochemistry, 119*(2), 325-329.

Duperat, V. G., Audie, J.-P., Debailleul, V., Laine, A., Buisine, M.-P., Galiegue-Zouitina, S., Pigny, P., Degand, P., Aubert, J., & Porchet, N. (1995). Characterization of the human mucin gene MUC5AC: a consensus cysteine-rich domain for 11p15 mucin genes? *Biochemical Journal, 305*(1), 211-219.

Duxbury, A., Thakker, N., & Wastell, D. (1989). A double-blind cross-over trial of a mucin-containing artificial saliva. *British dental journal, 166*(4), 115-120.

Eckhardt, A. E., Timpte, C. S., DeLuca, A. W., & Hill, R. L. (1997). The complete cDNA sequence and structural polymorphism of the polypeptide chain of porcine submaxillary mucin. *Journal of Biological Chemistry, 272*(52), 33204-33210.

Erickson, A. M., Henry, B. I., Murray, J. M., Klasse, P. J., & Angstmann, C. N. (2015). Predicting First Traversal Times for Virions and Nanoparticles in Mucus with Slowed Diffusion. *Biophysical Journal, 109*(1), 164-172.

Escande, F., Porchet, N., Aubert, J.-P., & Buisine, M.-P. (2002). The mouse Muc5b mucin gene: cDNA and genomic structures, chromosomal localization and expression. *Biochemical Journal, 363*(3), 589-598.

Escande, F., Porchet, N., Bernigaud, A., Petitprez, D., Aubert, J.-P., & Buisine, M.-P. (2004). The mouse secreted gel-forming mucin gene cluster. *Biochimica et Biophysica Acta (BBA)-Gene Structure and Expression, 1676*(3), 240-250.

Evans, D., Pye, G., Bramley, R., Clark, A., Dyson, T., & Hardcastle, J. (1988). Measurement of gastrointestinal pH profiles in normal ambulant human subjects. *Gut, 29*(8), 1035-1041.

Fang, X., Mou, Y., Huang, Z., Li, Y., Han, L., Zhang, Y., Feng, Y., Chen, Y., Jiang, X., Zhao, W., Sun, X., Xiong, Z., Yang, L., Liu, H., Fan, D., Mao, L., Ren, L., Liu, C.,

Wang, J., Li, K., Wang, G., Yang, S., Lai, L., Zhang, G., Li, Y., Wang, J., Bolund, L., Yang, H., Wang, J., Feng, S., Li, S., & Du, Y. (2012). The sequence and analysis of a Chinese pig genome. *Gigascience, 1*(1), 16. doi:10.1186/2047-217x-1-16

Ferrari, M., Fornasiero, M. C., & Isetta, A. M. (1990). MTT colorimetric assay for testing macrophage cytotoxic activity in vitro. *J Immunol Methods, 131*(2), 165-172.

Fichorova, R. N., Desai, P. J., Gibson, F. C., & Genco, C. A. (2001). Distinct proinflammatory host responses to Neisseria gonorrhoeae infection in immortalized human cervical and vaginal epithelial cells. *Infection and immunity, 69*(9), 5840-5848.

Folks, T. M., Powell, D., Lightfoote, M., Koenig, S., Fauci, A. S., Benn, S., Rabson, A., Daugherty, D., Gendelman, H. E., & Hoggan, M. D. (1986). Biological and biochemical characterization of a cloned Leu-3-cell surviving infection with the acquired immune deficiency syndrome retrovirus. *Journal of Experimental Medicine, 164*(1), 280-290.

Fotopoulos, G., Harari, A., Michetti, P., Trono, D., Pantaleo, G., & Kraehenbuhl, J.-P. (2002). Transepithelial transport of HIV-1 by M cells is receptor-mediated. *Proceedings of the National Academy of Sciences, 99*(14), 9410-9414.

Fox, M., Lahbib, F., Pratt, W., Attwood, J., Gum, J., Kim, Y., & Swallow, D. (1992). Regional localization of the intestinal mucin gene MUC3 to chromosome 7q22. *Annals of human genetics, 56*(4), 281-287.

Fultz, P. (1986). Components of saliva inactivate human immunodeficiency virus. *The Lancet, 328*(8517), 1215.

Gendler, S. J. (2001). MUC1, the renaissance molecule. *Journal of mammary gland biology and neoplasia, 6*(3), 339-353.

Gendler, S. J., Lancaster, C. A., Taylor-Papadimitriou, J., Duhig, T., Peat, N., Burchell, J., Pemberton, L., Lalani, E. N., & Wilson, D. (1990). Molecular cloning and expression of human tumor-associated polymorphic epithelial mucin. *Journal of Biological Chemistry, 265*(25), 15286-15293.

Gendler, S. J., & Spicer, A. (1995). Epithelial mucin genes. *Annu Rev Physiol, 57*(1), 607-634.

GeneCards. MUC22 Gene - GeneCards | MUC22 Protein | MUC22 Antibody. Available from Weizmann Institute of Science Human Gene Database Retrieved 10 October 2017 http://www.genecards.org/cgi-bin/carddisp.pl?gene=MUC22

Georgiades, P., Pudney, P. D., Thornton, D. J., & Waigh, T. A. (2014). Particle tracking microrheology of purified gastrointestinal mucins. *Biopolymers, 101*(4), 366-377.

Georgiou, C. D., Grintzalis, K., Zervoudakis, G., & Papapostolou, I. (2008). Mechanism of Coomassie brilliant blue G-250 binding to proteins: a hydrophobic assay for nanogram quantities of proteins. *Anal Bioanal Chem, 391*(1), 391-403. doi:10.1007/s00216-008-1996-x

Gipson, I., Spurr-Michaud, S., Tisdale, A., Kublin, C., Cintron, C., & Keutmann, H. (1995). Stratified squamous epithelia produce mucin-like glycoproteins. *Tissue and Cell, 27*(4), 397-404.

Gipson, I. K. (2001). 1. Abstract 2. Introduction 3. Biochemical and Structural Properties of Cervical Mucins 4. Localization of Mucin mRNA in Human Reproductive Tract Epithelia 4.1. Secreted Gel-forming Mucins 4.2. Membrane-spanning Mucins. *Frontiers in Bioscience, 6*, d1245-1255.

Gipson, I. K., Blalock, T., Tisdale, A., Spurr-Michaud, S., Allcorn, S., Stavreus-Evers, A., & Gemzell, K. (2008). MUC16 is lost from the uterodome (pinopode) surface of the receptive human endometrium: in vitro evidence that MUC16 is a barrier to trophoblast adherence. *Biology of reproduction, 78*(1), 134-142.

Gipson, I. K., Ho, S. B., Spurr-Michaud, S. J., Tisdale, A. S., Zhan, Q., Torlakovic, E., Pudney, J., Anderson, D. J., Toribara, N. W., & Hill, J., 3rd. (1997a). Mucin genes expressed by human female reproductive tract epithelia. *Biology of reproduction, 56*(4), 999-1011.

Gipson, I. K., Hori, Y., & Argüeso, P. (2004). Character of ocular surface mucins and their alteration in dry eye disease. *The ocular surface, 2*(2), 131-148.

Gipson, I. K., & Inatomi, T. (1997b). Mucin genes expressed by the ocular surface epithelium. *Progress in Retinal and eye research, 16*(1), 81-98.

Gipson, I. K., Moccia, R., Spurr-Michaud, S., Argüeso, P., Gargiulo, A. R., Hill, J. A., Offner, G. D., & Keutmann, H. T. (2001). The amount of MUC5B mucin in cervical mucus peaks at midcycle. *Journal of Clinical Endocrinology & Metabolism, 86*(2), 594-600.

Gipson, I. K., Spurr-Michaud, S., Moccia, R., Zhan, Q., Toribara, N., Ho, S. B., Gargiulo, A. R., & Hill, J. A. (1999). MUC4 and MUC5B transcripts are the prevalent mucin messenger ribonucleic acids of the human endocervix. *Biology of reproduction, 60*(1), 58-64.

Girling, A., Bartkova, J., Burchell, J., Gendler, S., Gillett, C., & Taylor-Papadimitriou, J. (1989). A core protein epitope of the polymorphic epithelial mucin detected by the

monoclonal antibody SM-3 is selectively exposed in a range of primary carcinomas. *International Journal of Cancer, 43*(6), 1072-1076.

Gordon, M., De Oliveira, T., Bishop, K., Coovadia, H., Madurai, L., Engelbrecht, S., van Rensburg, E. J., Mosam, A., Smith, A., & Cassol, S. (2003). Molecular characteristics of human immunodeficiency virus type 1 subtype C viruses from KwaZulu-Natal, South Africa: implications for vaccine and antiretroviral control strategies. *Journal of virology, 77*(4), 2587-2599.

Graham, R. A., Burchell, J. M., & Taylor-Papadimitriou, J. (1996). The polymorphic epithelial mucin: potential as an immunogen for a cancer vaccine. *Cancer Immunology, Immunotherapy, 42*(2), 71-80.

Groenen, M. A., Archibald, A. L., Uenishi, H., Tuggle, C. K., Takeuchi, Y., Rothschild, M. F., Rogel-Gaillard, C., Park, C., Milan, D., Megens, H. J., Li, S., Larkin, D. M., Kim, H., Frantz, L. A., Caccamo, M., Ahn, H., Aken, B. L., Anselmo, A., Anthon, C., Auvil, L., Badaoui, B., Beattie, C. W., Bendixen, C., Berman, D., Blecha, F., Blomberg, J., Bolund, L., Bosse, M., Botti, S., Bujie, Z., Bystrom, M., Capitanu, B., Carvalho-Silva, D., Chardon, P., Chen, C., Cheng, R., Choi, S. H., Chow, W., Clark, R. C., Clee, C., Crooijmans, R. P., Dawson, H. D., Dehais, P., De Sapio, F., Dibbits, B., Drou, N., Du, Z. Q., Eversole, K., Fadista, J., Fairley, S., Faraut, T., Faulkner, G. J., Fowler, K. E., Fredholm, M., Fritz, E., Gilbert, J. G., Giuffra, E., Gorodkin, J., Griffin, D. K., Harrow, J. L., Hayward, A., Howe, K., Hu, Z. L., Humphray, S. J., Hunt, T., Hornshoj, H., Jeon, J. T., Jern, P., Jones, M., Jurka, J., Kanamori, H., Kapetanovic, R., Kim, J., Kim, J. H., Kim, K. W., Kim, T. H., Larson, G., Lee, K., Lee, K. T., Leggett, R., Lewin, H. A., Li, Y., Liu, W., Loveland, J. E., Lu, Y., Lunney, J. K., Ma, J., Madsen, O., Mann, K., Matthews, L., McLaren, S., Morozumi, T., Murtaugh, M. P., Narayan, J., Nguyen, D. T., Ni, P., Oh, S. J., Onteru, S., Panitz, F., Park, E. W., Park, H. S., Pascal, G., Paudel, Y., Perez-Enciso, M., Ramirez-Gonzalez, R., Reecy, J. M., Rodriguez-Zas, S., Rohrer, G. A., Rund, L., Sang, Y., Schachtschneider, K., Schraiber, J. G., Schwartz, J., Scobie, L., Scott, C., Searle, S., Servin, B., Southey, B. R., Sperber, G., Stadler, P., Sweedler, J. V., Tafer, H., Thomsen, B., Wali, R., Wang, J., Wang, J., White, S., Xu, X., Yerle, M., Zhang, G., Zhang, J., Zhang, J., Zhao, S., Rogers, J., Churcher, C., & Schook, L. B. (2012). Analyses of pig genomes provide insight into porcine demography and evolution. *nature, 491*(7424), 393-398. doi:10.1038/nature11622

Gross, M., Guyonnet-Duperat, V., Porchet, N., Bernheim, A., Aubert, J., & Nguyen, V. (1991). *Mucin 4 (MUC4) gene: regional assignment (3q29) and RFLP analysis.* Paper presented at the Annales de genetique.

Gum, J., Hicks, J., Toribara, N., Rothe, E., Lagace, R., & Kim, Y. (1992). The human MUC2 intestinal mucin has cysteine-rich subdomains located both upstream and downstream of its central repetitive region. *Journal of Biological Chemistry, 267*(30), 21375-21383.

Gum, J., Hicks, J. W., Toribara, N. W., Siddiki, B., & Kim, Y. S. (1994). Molecular cloning of human intestinal mucin (MUC2) cDNA. Identification of the amino terminus and overall sequence similarity to prepro-von Willebrand factor. *Journal of Biological Chemistry, 269*(4), 2440-2446.

Gum, J. R., Byrd, J., Hicks, J. W., Toribara, N., Lamport, D., & Kim, Y. (1989). Molecular cloning of human intestinal mucin cDNAs. Sequence analysis and evidence for genetic polymorphism. *Journal of Biological Chemistry, 264*(11), 6480-6487.

Gum, J. R., Crawley, S. C., Hicks, J. W., Szymkowski, D. E., & Kim, Y. S. (2002). MUC17, a novel membrane-tethered mucin. *Biochemical and biophysical research communications, 291*(3), 466-475.

Gum, J. R., Hicks, J. W., Swallow, D. M., Lagace, R. L., Byrd, J. C., Lamport, D. T., Siddiki, B., & Kim, Y. S. (1990). Molecular cloning of cDNAs derived from a novel human intestinal mucin gene. *Biochemical and biophysical research communications, 171*(1), 407-415.

Gurney, K. B., Elliott, J., Nassanian, H., Song, C., Soilleux, E., McGowan, I., Anton, P. A., & Lee, B. (2005). Binding and transfer of human immunodeficiency virus by DC-SIGN+ cells in human rectal mucosa. *Journal of virology, 79*(9), 5762-5773.

Gururaja, T. L., Ramasubbu, N., Venugopalan, P., Reddy, M. S., Ramalingam, K., & Levine, M. J. (1998). Structural features of the human salivary mucin, MUC7. *Glycoconjugate journal, 15*(5), 457-467.

Haase, A. T. (2005). Perils at mucosal front lines for HIV and SIV and their hosts. *Nature Reviews Immunology, 5*(10), 783-792.

Haase, A. T. (2011). Early events in sexual transmission of HIV and SIV and opportunities for interventions. *Annual review of medicine, 62*, 127-139.

Habte, H. H., De Beer, C., Lotz, Z. E., Roux, P., & Mall, A. S. (2010). Anti-HIV-1 activity of salivary MUC5B and MUC7 mucins from HIV patients with different CD4 counts. *Virology journal, 7*(1), 1.

Habte, H. H., De Beer, C., Lotz, Z. E., Tyler, M. G., Schoeman, L., Kahn, D., & Mall, A. S. (2008). The inhibition of the Human Immunodeficiency Virus type 1 activity by crude and purified human pregnancy plug mucus and mucins in an inhibition assay. *Virol J, 5*, 59.

Habte, H. H., Kotwal, G. J., Lotz, Z. E., Tyler, M. G., Abrahams, M., Rodriques, J., Kahn, D., & Mall, A. S. (2007). Antiviral activity of purified human breast milk mucin. *Neonatology, 92*(2), 96-104.

Habte, H. H., Mall, A. S., De Beer, C., Lotz, Z. E., & Kahn, D. (2006). The role of crude human saliva and purified salivary MUC5B and MUC7 mucins in the inhibition of Human Immunodeficiency Virus type 1 in an inhibition assay. *Virology journal, 3*(1), 1.

Haendler, B., Toda, I., Sullivan, D. A., & Schleuning, W. D. (1999). Expression of transcripts for cysteine-rich secretory proteins (CRISPs) in the murine lacrimal gland. *Journal of cellular physiology, 178*(3), 371-378.

Hafez, E. S. E., & Hafez, B. (2013). *Reproduction in farm animals*: John Wiley & Sons.

Handra-Luca, A., Lamas, G., Bertrand, J.-C., & Fouret, P. (2005). MUC1, MUC2, MUC4, and MUC5AC expression in salivary gland mucoepidermoid carcinoma: diagnostic and prognostic implications. *The American journal of surgical pathology, 29*(7), 881-889.

Hanisch, F. G., Chai, W., Rosankiewicz, J. R., Lawson, A. M., Stoll, M. S., & Feizi, T. (1993). Core-typing of O-linked glycans from human gastric mucins. *European journal of biochemistry, 217*(2), 645-655.

Harding, S. E. (1984). An analysis of the heterogeneity of mucins. No evidence for a self-association. *Biochemical Journal, 219*(3), 1061-1064.

Hardt, M., Witkowska, H. E., Webb, S., Thomas, L. R., Dixon, S. E., Hall, S. C., & Fisher, S. J. (2005). Assessing the effects of diurnal variation on the composition of human parotid saliva: quantitative analysis of native peptides using iTRAQ reagents. *Anal Chem, 77*(15), 4947-4954. doi:10.1021/ac050161r

Hart, E. A., Caccamo, M., Harrow, J. L., Humphray, S. J., Gilbert, J. G., Trevanion, S., Hubbard, T., Rogers, J., & Rothschild, M. F. (2007). Lessons learned from the initial sequencing of the pig genome: comparative analysis of an 8 Mb region of pig chromosome 17. *Genome biology, 8*(8), 1.

Hattrup, C. L., & Gendler, S. J. (2008). Structure and function of the cell surface (tethered) mucins. *Annu. Rev. Physiol., 70*, 431-457.

Havsteen, B. (1983). Flavonoids, a class of natural products of high pharmacological potency. *Biochemical pharmacology, 32*(7), 1141-1148.

Haynes, N. (1971). Changes in pig cervical mucus in relation to the oestrous cycle. *Journal of reproduction and fertility, 27*(2), 211-218.

Health, N. D. o. (2015). *National Department of Health, The National Antenatal Sentinel HIV prevalence Survey, South Africa, 2013*.

Hemelaar, J., Gouws, E., Ghys, P. D., & Osmanov, S. (2006). Global and regional distribution of HIV-1 genetic subtypes and recombinants in 2004. *Aids, 20*(16), W13-W23.

Higgins, J. P., & Green, S. (2011). *Cochrane handbook for systematic reviews of interventions* (Vol. 4): John Wiley & Sons.

Higuchi, T., Orita, T., Nakanishi, S., Katsuya, K., Watanabe, H., Yamasaki, Y., Waga, I., Nanayama, T., Yamamoto, Y., & Munger, W. (2004). Molecular cloning, genomic structure, and expression analysis of MUC20, a novel mucin protein, up-regulated in injured kidney. *Journal of Biological Chemistry, 279*(3), 1968-1979.

Hirbod, T., & Broliden, K. (2007). Mucosal immune responses in the genital tract of HIV-1-exposed uninfected women. *Journal of internal medicine, 262*(1), 44-58.

Hladik, F., & Hope, T. J. (2009). HIV infection of the genital mucosa in women. *Current HIV/AIDS Reports, 6*(1), 20-28.

Ho, S. B., Niehans, G. A., Lyftogt, C., Yan, P. S., Cherwitz, D. L., Gum, E. T., Dahiya, R., & Kim, Y. S. (1993). Heterogeneity of mucin gene expression in normal and neoplastic tissues. *Cancer Research, 53*(3), 641-651.

Ho, S. B., Shekels, L. L., Toribara, N. W., Kim, Y. S., Lyftogt, C., Cherwitz, D. L., & Niehans, G. A. (1995). Mucin gene expression in normal, preneoplastic, and neoplastic human gastric epithelium. *Cancer Research, 55*(12), 2681-2690.

Hodges, R. R., & Dartt, D. A. (2013). Tear film mucins: front line defenders of the ocular surface; comparison with airway and gastrointestinal tract mucins. *Experimental eye research, 117*, 62-78.

Hollingsworth, M. A., & Swanson, B. J. (2004). Mucins in cancer: protection and control of the cell surface. *Nature Reviews Cancer, 4*(1), 45-60.

Hong, Z., Chasan, B., Bansil, R., Turner, B. S., Bhaskar, K. R., & Afdhal, N. H. (2005). Atomic force microscopy reveals aggregation of gastric mucin at low pH. *Biomacromolecules, 6*(6), 3458-3466.

Hori, Y., Spurr-Michaud, S., Russo, C. L., Argüeso, P., & Gipson, I. K. (2004). Differential regulation of membrane-associated mucins in the human ocular surface epithelium. *Investigative ophthalmology & visual science, 45*(1), 114-122.

Huang, J., Che, M.-I., Huang, Y.-T., Shyu, M.-K., Huang, Y.-M., Wu, Y.-M., Lin, W.-C., Huang, P.-H., Liang, J.-T., & Lee, P.-H. (2009). Overexpression of MUC15 activates extracellular signal-regulated kinase 1/2 and promotes the oncogenic potential of human colon cancer cells. *Carcinogenesis, 30*(8), 1452-1458.

Hughes, O., Perkins, A., Frier, M., Wastie, M., Denton, G., Price, M., Denley, H., & Bishop, M. (2001). Imaging for staging bladder cancer: a clinical study of intravenous 111indium-labelled anti-MUC1 mucin monoclonal antibody C595. *BJU international, 87*(1), 39-46.

Idris, N., & Carraway, K. L. (1999). Sialomucin complex (Muc4) expression in the rat female reproductive tract. *Biology of reproduction, 61*(6), 1431-1438.

Inatomi, T., Spurr-Michaud, S., Tisdale, A. S., Zhan, Q., Feldman, S. T., & Gipson, I. K. (1996). Expression of secretory mucin genes by human conjunctival epithelia. *Investigative ophthalmology & visual science, 37*(8), 1684-1692.

Itoh, Y., Kamata-Sakurai, M., Denda-Nagai, K., Nagai, S., Tsuiji, M., Ishii-Schrade, K., Okada, K., Goto, A., Fukayama, M., & Irimura, T. (2008). Identification and expression of human epiglycanin/MUC21: a novel transmembrane mucin. *Glycobiology, 18*(1), 74-83.

Jentoft, N. (1990). Why are proteins O-glycosylated? *Trends in biochemical sciences, 15*(8), 291-294.

Jin, F., Jansson, J., Law, M., Prestage, G. P., Zablotska, I., Imrie, J. C., Kippax, S. C., Kaldor, J. M., Grulich, A. E., & Wilson, D. P. (2010). Per-contact probability of HIV transmission in homosexual men in Sydney in the era of HAART. *Aids, 24*(6), 907-913. doi:10.1097/QAD.0b013e3283372d90

Jumblatt, M. M., McKenzie, R. W., Steele, P. S., Emberts, C. G., & Jumblatt, J. E. (2003). MUC7 expression in the human lacrimal gland and conjunctiva. *Cornea, 22*(1), 41-45.

Juusola, J., & Ballantyne, J. (2005). Multiplex mRNA profiling for the identification of body fluids. *Forensic Science International, 152*(1), 1-12.

Kaleebu, P., French, N., Mahe, C., Yirrell, D., Watera, C., Lyagoba, F., Nakiyingi, J., Rutebemberwa, A., Morgan, D., & Weber, J. (2002). Effect of human immunodeficiency virus (HIV) type 1 envelope subtypes A and D on disease

progression in a large cohort of HIV-1—positive persons in Uganda. *Journal of Infectious Diseases, 185*(9), 1244-1250.

Kandaswami, C., & Middleton Jr, E. (1994). Free radical scavenging and antioxidant activity of plant flavonoids *Free radicals in diagnostic medicine* (pp. 351-376): Springer.

Karim, Q. A., Karim, S. S. A., Frohlich, J. A., Grobler, A. C., Baxter, C., Mansoor, L. E., Kharsany, A. B., Sibeko, S., Mlisana, K. P., & Omar, Z. (2010). Effectiveness and safety of tenofovir gel, an antiretroviral microbicide, for the prevention of HIV infection in women. *Science, 329*(5996), 1168-1174.

Karim, S. S. A., & Baxter, C. (2012). Overview of microbicides for the prevention of human immunodeficiency virus. *Best Pract Res Clin Obstet Gynaecol, 26*(4), 427-439. doi:10.1016/j.bpobgyn.2012.01.010

Karlsson, N., Nordman, H., Karlsson, H., Carlstedt, I., & Hansson, G. (1997). Glycosylation differences between pig gastric mucin populations: a comparative study of the neutral oligosaccharides using mass spectrometry. *Biochem. J, 326*, 911-917.

Keele, B. F., Van Heuverswyn, F., Li, Y., Bailes, E., Takehisa, J., Santiago, M. L., Bibollet-Ruche, F., Chen, Y., Wain, L. V., & Liegeois, F. (2006). Chimpanzee reservoirs of pandemic and nonpandemic HIV-1. *Science, 313*(5786), 523-526.

Keicho, N., Ohashi, J., Tamiya, G., Nakata, K., Taguchi, Y., Azuma, A., Ohishi, N., Emi, M., Park, M. H., & Inoko, H. (2000). Fine localization of a major disease-susceptibility locus for diffuse panbronchiolitis. *The American Journal of Human Genetics, 66*(2), 501-507.

Kerschner, J. E. (2007). Mucin gene expression in human middle ear epithelium. *The Laryngoscope, 117*(9), 1666-1676.

Kerschner, J. E., Khampang, P., Erbe, C. B., Kolker, A., & Cioffi, J. A. (2009). Mucin gene 19 (MUC19) expression and response to inflammatory cytokines in middle ear epithelium. *Glycoconjugate journal, 26*(9), 1275-1284.

Khorrami, A. M., Choudhury, A., Andrianifahanana, M., Varshney, G. C., Bhattacharyya, S. N., Hollingsworth, M. A., Kaufman, B., & Batra, S. K. (2002). Purification and characterization of a human pancreatic adenocarcinoma mucin. *Journal of biochemistry, 131*(1), 21-29.

Kim, C.-h., Kim, H. J., Song, K. S., Seong, J.-k., Kim, K.-s., Lee, J.-g., & Yoon, J.-h. (2005). MUC8 as a ciliated cell marker in human nasal epithelium. *Acta oto-laryngologica, 125*(1), 76-81.

Kim, G. E., Bae, H. I., Park, H. U., Kuan, S. F., Crawley, S. C., Ho, J. J., & Kim, Y. S. (2002). Aberrant expression of MUC5AC and MUC6 gastric mucins and sialyl Tn antigen in intraepithelial neoplasms of the pancreas. *Gastroenterology*, *123*(4), 1052-1060.

Kim, Y. S., Gum Jr, J., & Brockhausen, I. (1996). Mucin glycoproteins in neoplasia. *Glycoconjugate journal*, *13*(5), 693-707.

Kirkham, S., Kolsum, U., Rousseau, K., Singh, D., Vestbo, J., & Thornton, D. J. (2008). MUC5B is the major mucin in the gel phase of sputum in chronic obstructive pulmonary disease. *American journal of respiratory and critical care medicine*, *178*(10), 1033-1039.

Kirkham, S., Sheehan, J. K., Knight, D., Richardson, P. S., & Thornton, D. J. (2002). Heterogeneity of airways mucus: variations in the amounts and glycoforms of the major oligomeric mucins MUC5AC and MUC5B. *Biochemical Journal*, *361*(3), 537-546.

Kiwanuka, N., Laeyendecker, O., Robb, M., Kigozi, G., Arroyo, M., McCutchan, F., Eller, L. A., Eller, M., Makumbi, F., & Birx, D. (2008). Effect of human immunodeficiency virus Type 1 (HIV-1) subtype on disease progression in persons from Rakai, Uganda, with incident HIV-1 infection. *Journal of Infectious Diseases*, *197*(5), 707-713.

Klasse, P. J. (2012). The molecular basis of HIV entry. *Cellular microbiology*, *14*(8), 1183-1192.

Kocer, B., McKolanis, J., & Soran, A. (2006). Humoral immune response to MUC5AC in patients with colorectal polyps and colorectal carcinoma. *BMC gastroenterology*, *6*(1), 1.

Kocer, B., Soran, A., Erdogan, S., Karabeyoglu, M., Yildirim, O., Eroglu, A., Bozkurt, B., & Cengiz, O. (2002). Expression of MUC5AC in colorectal carcinoma and relationship with prognosis. *Pathology international*, *52*(7), 470-477.

Koh, D. Q., & Koh, G. H. (2007). The use of salivary biomarkers in occupational and environmental medicine. *Occup Environ Med*, *64*(3), 202-210. doi:10.1136/oem.2006.026567

Korber, B., Muldoon, M., Theiler, J., Gao, F., Gupta, R., Lapedes, A., Hahn, B., Wolinsky, S., & Bhattacharya, T. (2000). Timing the ancestor of the HIV-1 pandemic strains. *Science*, *288*(5472), 1789-1796.

Laemmli, U. K. (1970). Cleavage of structural proteins during the assembly of the head of bacteriophage T4. *nature*, *227*, 680-685.

Lai, S. K., Hida, K., Shukair, S., Wang, Y. Y., Figueiredo, A., Cone, R., Hope, T. J., & Hanes, J. (2009). Human immunodeficiency virus type 1 is trapped by acidic but not by neutralized human cervicovaginal mucus. *J Virol, 83*(21), 11196-11200. doi:10.1128/JVI.01899-08

Lai, S. K., O'Hanlon, D. E., Harrold, S., Man, S. T., Wang, Y. Y., Cone, R., & Hanes, J. (2007). Rapid transport of large polymeric nanoparticles in fresh undiluted human mucus. *Proc Natl Acad Sci U S A, 104*(5), 1482-1487. doi:10.1073/pnas.0608611104

Lai, S. K., Wang, Y.-Y., Hida, K., Cone, R., & Hanes, J. (2010a). Nanoparticles reveal that human cervicovaginal mucus is riddled with pores larger than viruses. *Proceedings of the National Academy of Sciences, 107*(2), 598-603.

Lai, S. K., Wang, Y. Y., Hida, K., Cone, R., & Hanes, J. (2010b). Nanoparticles reveal that human cervicovaginal mucus is riddled with pores larger than viruses. *Proc Natl Acad Sci U S A, 107*(2), 598-603. doi:10.1073/pnas.0911748107

Lamblin, G., Degroote, S., Perini, J.-M., Delmotte, P., Scharfman, A., Davril, M., Lo-Guidice, J.-M., Houdret, N., Dumur, V., & Klein, A. (2001). Human airway mucin glycosylation: a combinatory of carbohydrate determinants which vary in cystic fibrosis. *Glycoconjugate journal, 18*(9), 661-684.

Lan, M. S., Batra, S. K., Qi, W. N., Metzgar, R. S., & Hollingsworth, M. (1990). Cloning and sequencing of a human pancreatic tumor mucin cDNA. *Journal of Biological Chemistry, 265*(25), 15294-15299.

Lancaster, C. A., Peat, N., Duhig, T., Wilson, D., Taylor-Papadimitriou, J., & Gendler, S. J. (1990). Structure and expression of the human polymorphic epithelial mucin gene: an expressed VNTR unit. *Biochemical and biophysical research communications, 173*(3), 1019-1029.

Lapenta, C., Boirivant, M., Marini, M., Santini, S. M., Logozzi, M., Viora, M., Belardelli, F., & Fais, S. (1999). Human intestinal lamina propria lymphocytes are naturally permissive to HIV-1 infection. *European journal of immunology, 29*(4), 1202-1208.

Lee-Huang, S., Huang, P. L., Zhang, D., Lee, J. W., Bao, J., Sun, Y., Chang, Y.-T., Zhang, J., & Huang, P. L. (2007a). Discovery of small-molecule HIV-1 fusion and integrase inhibitors oleuropein and hydroxytyrosol: Part I. Integrase inhibition. *Biochemical and biophysical research communications, 354*(4), 872-878.

Lee-Huang, S., Huang, P. L., Zhang, D., Lee, J. W., Bao, J., Sun, Y., Chang, Y.-T., Zhang, J., & Huang, P. L. (2007b). Discovery of small-molecule HIV-1 fusion and integrase

inhibitors oleuropein and hydroxytyrosol: Part II. Integrase inhibition. *Biochemical and biophysical research communications, 354*(4), 879-884.

Lee, M. J., Lee, H. S., Kim, W. H., Choi, Y., & Yang, M. (2003). Expression of mucins and cytokeratins in primary carcinomas of the digestive system. *Modern Pathology, 16*(5), 403-410.

Lehmann, J. M., Riethmüller, G., & Johnson, J. P. (1989). MUC18, a marker of tumor progression in human melanoma, shows sequence similarity to the neural cell adhesion molecules of the immunoglobulin superfamily. *Proceedings of the National Academy of Sciences, 86*(24), 9891-9895.

Leikauf, G. D., Borchers, M. T., Prows, D. R., & Simpson, L. G. (2002). Mucin apoprotein expression in COPD. *CHEST Journal, 121*(5_suppl), 166S-182S.

Levanon, K., Ng, V., Piao, H.-Y., Zhang, Y., Chang, M. C., Roh, M. H., Kindelberger, D. W., Hirsch, M. S., Crum, C. P., & Marto, J. A. (2010). Primary ex vivo cultures of human fallopian tube epithelium as a model for serous ovarian carcinogenesis. *Oncogene, 29*(8), 1103-1113.

Levy, J. A. (2007). *HIV and the Pathogenesis of AIDS*: ASM press Washington, DC.

Li, G., Zhang, H., Lü, J., Hou, P., Zhou, Y., Ma, X., & Wang, H. (2005). Variable number of tandem repeats polymorphism of MUC20 is associated with the progression of IgA nephropathy. *Zhonghua yi xue za zhi, 85*(19), 1333-1338.

Li, S., Intini, G., & Bobek, L. A. (2006). Modulation of MUC7 mucin expression by exogenous factors in airway cells in vitro and in vivo. *American journal of respiratory cell and molecular biology, 35*(1), 95-102.

Lieleg, O., Lieleg, C., Bloom, J., Buck, C. B., & Ribbeck, K. (2012). Mucin biopolymers as broad-spectrum antiviral agents. *Biomacromolecules, 13*(6), 1724-1732.

Ligtenberg, M., Vos, H., Gennissen, A., & Hilkens, J. (1990). Episialin, a carcinoma-associated mucin, is generated by a polymorphic gene encoding splice variants with alternative amino termini. *Journal of Biological Chemistry, 265*(10), 5573-5578.

Lihana, R. W., Ssemwanga, D., Abimiku, A. l., & Ndembi, N. (2012). Update on HIV-1 diversity in Africa: a decade in review. *AIDS Rev, 14*, 83-100.

Linden, S., Sutton, P., Karlsson, N., Korolik, V., & McGuckin, M. (2008). Mucins in the mucosal barrier to infection. *Mucosal immunology, 1*(3), 183-197.

Liu, B., Offner, G. D., Nunes, D. P., Oppenheim, F. G., & Troxler, R. F. (1998). MUC4 is a major component of salivary mucin MG1 secreted by the human submandibular gland. *Biochemical and biophysical research communications, 250*(3), 757-761.

Liu, B., Rayment, S., Oppenheim, F. G., & Troxler, R. F. (1999). Isolation of human salivary mucin MG2 by a novel method and characterization of its interactions with oral bacteria. *Archives of biochemistry and biophysics*, *364*(2), 286-293.

Llinares, K., Escande, F., Aubert, S., Buisine, M.-P., De Bolos, C., Batra, S. K., Gosselin, B., Aubert, J.-P., Porchet, N., & Copin, M.-C. (2004). Diagnostic value of MUC4 immunostaining in distinguishing epithelial mesothelioma and lung adenocarcinoma. *Modern Pathology*, *17*(2), 150-157.

Mall, A. (1984). *Physical and Chemical Changes in the Porcine Gastric Mucus in the Normal and Ulcerated States.* (Master of Science), University of Cape Town.

Mall, A. (2008). Analysis of mucins: role in laboratory diagnosis. *Journal of clinical pathology*, *61*(9), 1018-1024.

Mall, A., Fourie, J., McLeod, H., Muschol, A., Campbell, J., & Hickman, R. (1991). Administration of sucralfate prolongs survival of animals with experimental peptic ulceration. *The American journal of medicine*, *91*(2), S37-S42.

Mall, A., Hickman, R., Terblanche, J., & Kahn, D. (1997a). The pig as an ulcer model. *Gastroenterology*, *113*(1), 366-367.

Mall, A., McLeod, H., Dent, D., & Hickman, R. (1992). Gastric cancer mucins as clinical markers. *Gut*, *33*(12), 1681-1681.

Mall, A., McLeod, H. A., Hickman, R., Kahn, D., & Dent, D. M. (1999). Fragmentation pattern of mucins in normal and diseased gastric mucosae: a glycoprotein fractionates with gastric mucins purified from mucosal scrapings of cancer and peptic ulcer patients. *Digestion*, *60*(3), 216-226.

Mall, A., Merrifield, E., Fourie, J., McLeod, H., & Hickman, R. (1997b). Alterations in porcine gastric mucin during the development of experimental ulceration. *Digestion*, *58*(2), 138-146.

Mall, A. S., Hutton, D. A., Coan, R. M., Sellers, L. A., & Allen, A. (1988). Gastric mucins: different size of subunit according to reducing conditions: Portland Press Limited.

Mall, A. S., Sellers, L. A., & Allen, A. (1987). Purification of pig duodenal mucus glycoprotein from protein and nucleic acid: Portland Press Limited.

Mall, A. S., Suleman, N., Taylor, K., Kidd, M., Tyler, M., Lotz, Z., Hickman, R., & Kahn, D. (2004). The relationship of a Helicobacter heilmannii infection to the mucosal changes in abattoir and laboratory pig stomach. *Surgery today*, *34*(11), 943-949.

Mall, A. S., Tyler, M. G., Ho, S. B., Krige, J. E., Kahn, D., Spearman, W., Myer, L., & Govender, D. (2010). The expression of MUC mucin in cholangiocarcinoma. *Pathol Res Pract, 206*(12), 805-809. doi:10.1016/j.prp.2010.08.004

Malmberg, E. K., Pelaseyed, T., Petersson, Å. C., Seidler, U. E., De Jonge, H., Riordan, J. R., & Hansson, G. C. (2008). The C-terminus of the transmembrane mucin MUC17 binds to the scaffold protein PDZK1 that stably localizes it to the enterocyte apical membrane in the small intestine. *Biochemical Journal, 410*(2), 283-289.

Manage, A., & Petrikovics, I. (2013). Confidence limit calculation for antidotal potency ratio derived from lethal dose 50. *World J Methodol, 3*(1), 7-10. doi:10.5662/wjm.v3.i1.7

Marques, M. R., Loebenberg, R., & Almukainzi, M. (2011). Simulated biological fluids with possible application in dissolution testing. *Dissolution Technol, 18*(3), 15-28.

Masaki, Y., Oka, M., Ogura, Y., Ueno, T., Nishihara, K., Tangoku, A., Takahashi, M., Yamamoto, M., & Irimura, T. (1998). Sialylated MUC1 mucin expression in normal pancreas, benign pancreatic lesions, and pancreatic ductal adenocarcinoma. *Hepato-gastroenterology, 46*(28), 2240-2245.

Matsuzaka, Y., Tounai, K., Denda, A., Tomizawa, M., Makino, S., Okamoto, K., Keicho, N., Oka, A., Kulski, J. K., & Tamiya, G. (2002). Identification of novel candidate genes in the diffuse panbronchiolitis critical region of the class I human MHC. *Immunogenetics, 54*(5), 301-309.

McDonald, R. E., Fleming, R. I., Beeley, J. G., Bovell, D. L., Lu, J. R., Zhao, X., Cooper, A., & Kennedy, M. W. (2009). Latherin: a surfactant protein of horse sweat and saliva. *PLoS One, 4*(5), e5726.

Mehla, R., Bivalkar-Mehla, S., & Chauhan, A. (2011). A flavonoid, luteolin, cripples HIV-1 by abrogation of tat function. *PLoS One, 6*(11), e27915.

Meng, G., Wei, X., Wu, X., Sellers, M. T., Decker, J. M., Moldoveanu, Z., Orenstein, J. M., Graham, M. F., Kappes, J. C., & Mestecky, J. (2002). Primary intestinal epithelial cells selectively transfer R5 HIV-1 to CCR5+ cells. *Nature medicine, 8*(2), 150-156.

Mesquita, P. M., Cheshenko, N., Wilson, S. S., Mhatre, M., Guzman, E., Fakioglu, E., Keller, M. J., & Herold, B. C. (2009). Disruption of tight junctions by cellulose sulfate facilitates HIV infection: model of microbicide safety. *Journal of Infectious Diseases, 200*(4), 599-608.

Mestecky, J., Lamm, M. E., Ogra, P. L., Strober, W., Bienenstock, J., McGhee, J. R., & Mayer, L. (2005). *Mucosal immunology*: Academic Press.

Meurens, F., Summerfield, A., Nauwynck, H., Saif, L., & Gerdts, V. (2012). The pig: a model for human infectious diseases. *Trends in microbiology, 20*(1), 50-57.

Meyer, H., Coenen, M., & Gurer, C. (1985). Investigations of saliva production and chewing in horses fed various feeds. *Proc of 9th ENPS, East Lansing MI*.

Meyer, H., Coenen, M., & Probst, D. (1986). Digestive physiology of the horse. 14. Mixing of saliva with feed and passage through the esophagus of horses. *Journal of Animal Physiology and Animal Nutrition, 56*, 171-183.

Milman, H. A. (2006). Toxicology of the Pancreas SAGE Publications Sage CA: Los Angeles, CA.

Moeller, B. A., McCall, C. A., Silverman, S. J., & McElhenney, W. H. (2008). Estimation of saliva production in crib-biting and normal horses. *Journal of Equine Veterinary Science, 28*(2), 85-90.

Moniaux, N., Andrianifahanana, M., Brand, R., & Batra, S. K. (2004). Multiple roles of mucins in pancreatic cancer, a lethal and challenging malignancy. *British journal of cancer, 91*(9), 1633-1638.

Moniaux, N., Chaturvedi, P., Varshney, G. C., Meza, J. L., Rodriguez-Sierra, J. F., Aubert, J., & Batra, S. K. (2007). Human MUC4 mucin induces ultra-structural changes and tumorigenicity in pancreatic cancer cells. *Br J Cancer, 97*(3), 345-357. doi:10.1038/sj.bjc.6603868

Moniaux, N., Escande, F., Batra, S. K., Porchet, N., Laine, A., & Aubert, J. P. (2000). Alternative splicing generates a family of putative secreted and membrane-associated MUC4 mucins. *European journal of biochemistry, 267*(14), 4536-4544.

Moniaux, N., Junker, W. M., Singh, A. P., Jones, A. M., & Batra, S. K. (2006). Characterization of Human Mucin MUC17 complete coding sequence and organization. *Journal of Biological Chemistry, 281*(33), 23676-23685.

Moniaux, N., Nollet, S., Porchet, N., Degand, P., Laine, A., & Aubert, J.-P. (1999). Complete sequence of the human mucin MUC4: a putative cell membrane-associated mucin. *Biochemical Journal, 338*(2), 325-333.

Montefiori, D. C. (2009). Measuring HIV neutralization in a luciferase reporter gene assay *HIV Protocols* (pp. 395-405): Springer.

Mthembu, Y., Lotz, Z., Tyler, M., de Beer, C., Rodrigues, J., Schoeman, L., & Mall, A. S. (2014). Purified human breast milk MUC1 and MUC4 inhibit human immunodeficiency virus. *Neonatology, 105*(3), 211-217. doi:10.1159/000357201

Nagashunmugam, T., Malamud, D., Davis, C., Abrams, W. R., & Friedman, H. M. (1998). Human submandibular saliva inhibits human immunodeficiency virus type 1 infection by displacing envelope glycoprotein gp120 from the virus. *Journal of Infectious Diseases, 178*(6), 1635-1641.

Neilson, J. R., John, G. C., Carr, J. K., Lewis, P., Kreiss, J. K., Jackson, S., Nduati, R. W., Mbori-Ngacha, D., Panteleeff, D. D., & Bodrug, S. (1999). Subtypes of human immunodeficiency virus type 1 and disease stage among women in Nairobi, Kenya. *Journal of virology, 73*(5), 4393-4403.

Network, M. T. (2011). MTN Statement on Decision to Discontinue Use of Tenofovir Gel in VOICE, a Major HIV Prevention Study in Women. Retrieved from http://www.mtnstopshiv.org/node/3909

Newton, J., Jordan, N., Oliver, L., Strugala, V., Pearson, J., James, O., & Allen, A. (1998). Helicobacter pylori in vivo causes structural changes in the adherent gastric mucus layer but barrier thickness is not compromised. *Gut, 43*(4), 470-475.

Nordman, H., Davies, J., Herrmann, A., Karlsson, N., Hansson, G., & Carlstedt, I. (1997). Mucus glycoproteins from pig gastric mucosa: identification of different mucin populations from the surface epithelium. *Biochem. J, 326*, 903-910.

Nordman, H., Davies, J., Lindell, G., De Bolos, C., Real, F., & Carlstedt, I. (2002). Gastric MUC5AC and MUC6 are large oligomeric mucins that differ in size, glycosylation and tissue distribution. *Biochem. J, 364*, 191-200.

Nordman, H., Davies, J. R., & Carlstedt, I. (1998). Mucus glycoproteins from pig gastric mucosa: different mucins are produced by the surface epithelium and the glands. *Biochemical Journal, 331*(3), 687-694.

Novitsky, V., Wang, R., Bussmann, H., Lockman, S., Baum, M., Shapiro, R., Thior, I., Wester, C., Wester, C. W., & Ogwu, A. (2010). HIV-1 subtype C-infected individuals maintaining high viral load as potential targets for the “test-and-treat” approach to reduce HIV transmission. *PLoS One, 5*(4), e10148.

Nunn, K. L., Wang, Y.-Y., Harit, D., Humphrys, M. S., Ma, B., Cone, R., Ravel, J., & Lai, S. K. (2015). Enhanced trapping of HIV-1 by human cervicovaginal mucus is associated with Lactobacillus crispatus-dominant microbiota. *MBio, 6*(5), e01084-01015.

Nyamweya, S., Hegedus, A., Jaye, A., Rowland-Jones, S., Flanagan, K. L., & Macallan, D. C. (2013). Comparing HIV-1 and HIV-2 infection: Lessons for viral immunopathogenesis. *Reviews in medical virology, 23*(4), 221-240.

O'Keefe, B. R., Vojdani, F., Buffa, V., Shattock, R. J., Montefiori, D. C., Bakke, J., Mirsalis, J., d'Andrea, A.-L., Hume, S. D., & Bratcher, B. (2009). Scaleable manufacture of HIV-1 entry inhibitor griffithsin and validation of its safety and efficacy as a topical microbicide component. *Proceedings of the National Academy of Sciences, 106*(15), 6099-6104.

Ogata, S., Uehara, H., Chen, A., & Itzkowitz, S. (1992). Mucin gene expression in colonic tissues and cell lines. *Cancer Research, 52*(21), 5971-5978.

Olmsted, S. S., Khanna, K. V., Ng, E. M., Whitten, S. T., Johnson, O. N., Markham, R. B., Cone, R. A., & Moench, T. R. (2005). Low pH immobilizes and kills human leukocytes and prevents transmission of cell-associated HIV in a mouse model. *BMC infectious diseases, 5*(1), 1.

Olmsted, S. S., Padgett, J. L., Yudin, A. I., Whaley, K. J., Moench, T. R., & Cone, R. A. (2001). Diffusion of macromolecules and virus-like particles in human cervical mucus. *Biophysical Journal, 81*(4), 1930-1937.

Orlando, R. C. (1991). Esophageal epithelial defense against acid injury. *Journal of clinical gastroenterology, 13*, S6.

Owen, D. H., & Katz, D. F. (1999). A vaginal fluid simulant. *Contraception, 59*(2), 91-95.

Owens, S. R., Chiosea, S. I., & Kuan, S.-F. (2008). Selective expression of gastric mucin MUC6 in colonic sessile serrated adenoma but not in hyperplastic polyp aids in morphological diagnosis of serrated polyps. *Modern Pathology, 21*(6), 660-669.

Packer, L. M., Williams, S. J., Callaghan, S., Gotley, D. C., & McGuckin, M. A. (2004). Expression of the cell surface mucin gene family in adenocarcinomas. *International journal of oncology, 25*(4), 1119-1126.

Pallesen, L. T., Berglund, L., Rasmussen, L. K., Petersen, T. E., & Rasmussen, J. T. (2002). Isolation and characterization of MUC15, a novel cell membrane-associated mucin. *European journal of biochemistry, 269*(11), 2755-2763.

Pallesen, L. T., Pedersen, L. R. L., Petersen, T. E., Knudsen, C. R., & Rasmussen, J. T. (2008). Characterization of human mucin (MUC15) and identification of ovine and caprine orthologs. *Journal of dairy science, 91*(12), 4477-4483.

Palm, A.-K. E., Wattle, O., Lundström, T., & Wattrang, E. (2016). Secretory immunoglobulin A and immunoglobulin G in horse saliva. *Veterinary Immunology and Immunopathology, 180*, 59-65.

Parham, P. (2014). *The immune system*: Garland Science.

Park, S. Y., Roh, S. J., Kim, Y. N., Kim, S. Z., Park, H. S., Jang, K. Y., Chung, M. J., Kang, M. J., Lee, D. G., & Moon, W. S. (2009). Expression of MUC1, MUC2, MUC5AC and MUC6 in cholangiocarcinoma: prognostic impact. *Oncology reports, 22*(3), 649.

Pasetto, S., Pardi, V., & Murata, R. M. (2014). Anti-HIV-1 activity of flavonoid myricetin on HIV-1 infection in a dual-chamber in vitro model. *PLoS One, 9*(12), e115323.

Paszkiewiczgadek, A., Gindzienski, A., & Porowska, H. (1995). The use of preparative polyacrylamide gel electrophoresis and electroelution for purification of mucus glycoproteins. *Analytical biochemistry, 226*(2), 263-267.

Peacocke, J. (2011). *The Role of Crude Salivary Mucus and Its Purified Mucins MUC5B and MUC7 In The Inhibition Of The Human Immunodeficiency Virus Type 1.* (Master of Science in Medicine (Surgery)), University of Cape Town, Cape Town, Western Cape Province, South Africa.

Peacocke, J., Lotz, Z., de Beer, C., Roux, P., & Mall, A. S. (2012). The role of crude saliva and purified salivary mucins in the inhibition of the Human Immunodeficiency Virus type 1. *Virology journal, 9*(1), 1-9.

Pearson, J. P., Allen, A., & Parry, S. (1981). A 70000-molecular-weight protein isolated from purified pig gastric mucus glycoprotein by reduction of disulphide bridges and its implication in the polymeric structure. *Biochem. J, 197*, 155-162.

Peat, N., Gendler, S. J., Lalani, E.-N., Duhig, T., & Taylor-Papadimitriou, J. (1992). Tissue-specific expression of a human polymorphic epithelial mucin (MUC1) in transgenic mice. *Cancer Research, 52*(7), 1954-1960.

Perez-Vilar, J., Eckhardt, A. E., & Hill, R. L. (1996). Porcine submaxillary mucin forms disulfide-bonded dimers between its carboxyl-terminal domains. *Journal of Biological Chemistry, 271*(16), 9845-9850.

Perez-Vilar, J., & Hill, R. L. (1999). The structure and assembly of secreted mucins. *Journal of Biological Chemistry, 274*(45), 31751-31754.

Perez-Vilar, J., & Mabolo, R. (2007). Gel-forming mucins. Notions from in vitro studies. *Histol Histopathol, 22*(4), 455-464.

Piazza, R., Buzzaccaro, S., Secchi, E., & Parola, A. (2012). What buoyancy really is. A generalized Archimedes' principle for sedimentation and ultracentrifugation. *Soft Matter, 8*(27), 7112-7115.

Pigny, P., Guyonnet-Duperat, V., Hill, A. S., Pratt, W. S., Galiegue-Zouitina, S., d'Hooge, M. C., Laine, A., Van-Seuningen, I., Degand, P., & Gum, J. R. (1996). Human mucin

genes assigned to 11p15. 5: identification and organization of a cluster of genes. *Genomics, 38*(3), 340-352.

Pinkus, G. S., & Kurtin, P. J. (1985). Epithelial membrane antigen—a diagnostic discriminant in surgical pathology: immunohistochemical profile in epithelial, mesenchymal, and hematopoietic neoplasms using paraffin sections and monoclonal antibodies. *Human pathology, 16*(9), 929-940.

Piras, M., Hand, A. R., & Piludu, M. (2011). Electron microscopic immunogold localization of salivary mucin MUC5B in human buccal and palatal glands. *Acta histochemica, 113*(8), 844-847.

Polge, C. (1965). Symposium on Infertility [Abridged]. *Proceedings of the Royal Society of Medicine, 58*(11 Pt 1), 907.

Porchet, N., Pigny, P., Buisine, M.-P., Debailleul, V., Degand, P., Laine, A., & Aubert, J.-P. (1995). Human mucin genes: genomic organization and expression of MUC4, MUC5AC and MUC5B. *Biochemical Society Transactions, 23*(4), 800-805.

Porchet, N., Van Cong, N., Dufosse, J., Audie, J., Guyonnet-Duperat, V., Gross, M., Denis, C., Degand, P., Bernheim, A., & Aubert, J. (1991). Molecular cloning and chromosomal localization of a novel human tracheo-bronchial mucin cDNA containing tandemly repeated sequences of 48 base pairs. *Biochemical and biophysical research communications, 175*(2), 414-422.

Pozzolini, M., Scarfì, S., Benatti, U., & Giovine, M. (2003). Interference in MTT cell viability assay in activated macrophage cell line. *Analytical biochemistry, 313*(2), 338-341.

Pratt, W. S., Crawley, S., Hicks, J., Ho, J., Nash, M., Kim, Y. S., Gum, J. R., & Swallow, D. M. (2000). Multiple transcripts of MUC3: evidence for two genes, MUC3A and MUC3B. *Biochemical and biophysical research communications, 275*(3), 916-923.

Rachagani, S., Torres, M. P., Moniaux, N., & Batra, S. K. (2009). Current status of mucins in the diagnosis and therapy of cancer. *Biofactors, 35*(6), 509-527.

Raeside, J. (1963). Urinary oestrogen excretion in the pig at oestrus and during the oestrous cycle. *Journal of reproduction and fertility, 6*(3), 421-426.

Rakha, E. A., Boyce, R. W., El-Rehim, D. A., Kurien, T., Green, A. R., Paish, E. C., Robertson, J. F., & Ellis, I. O. (2005). Expression of mucins (MUC1, MUC2, MUC3, MUC4, MUC5AC and MUC6) and their prognostic significance in human breast cancer. *Modern Pathology, 18*(10), 1295-1304.

Ramsey, K. A., Rushton, Z. L., & Ehre, C. (2016). Mucin Agarose Gel Electrophoresis: Western Blotting for High-molecular-weight Glycoproteins. *Journal of visualized experiments: JoVE*(112).

Raynal, B. D., Hardingham, T. E., Sheehan, J. K., & Thornton, D. J. (2003). Calcium-dependent protein interactions in MUC5B provide reversible cross-links in salivary mucus. *Journal of Biological Chemistry, 278*(31), 28703-28710.

Rees, W., & Turnberg, L. (1982). Mechanisms of gastric mucosal protection: a role for the 'mucus-bicarbonate'barrier. *Clinical Science, 62*(4), 343-348.

Reid, C. J., Gould, S., & Harris, A. (1997). Developmental expression of mucin genes in the human respiratory tract. *American journal of respiratory cell and molecular biology, 17*(5), 592-598.

Reis, C. A., David, L., Carvalho, F., Mandel, U., de Bolós, C., Mirgorodskaya, E., Clausen, H., & Sobrinho-Simões, M. (2000). Immunohistochemical study of the expression of MUC6 mucin and co-expression of other secreted mucins (MUC5AC and MUC2) in human gastric carcinomas. *Journal of Histochemistry & Cytochemistry, 48*(3), 377-388.

Reis, C. A., David, L., Correa, P., Carneiro, F., de Bolós, C., Garcia, E., Mandel, U., Clausen, H., & Sobrinho-Simões, M. (1999). Intestinal metaplasia of human stomach displays distinct patterns of mucin (MUC1, MUC2, MUC5AC, and MUC6) expression. *Cancer Research, 59*(5), 1003-1007.

Retz, M., Lehmann, J., Röder, C., Plötz, B., Harder, J., Eggers, J., Pauluschke, J., Kalthoff, H., & Stöckle, M. (1998). Differential mucin MUC7 gene expression in invasive bladder carcinoma in contrast to uniform MUC1 and MUC2 gene expression in both normal urothelium and bladder carcinoma. *Cancer Research, 58*(24), 5662-5666.

Ringel, J., & Löhr, M. (2003). The MUC gene family: their role in diagnosis and early detection of pancreatic cancer. *Molecular cancer, 2*(1), 1.

Rose, M. C., & Gendler, S. J. (1997). Airway mucin genes and gene products *Airway mucus: basic mechanisms and clinical perspectives* (pp. 41-66): Springer.

Rose, M. C., & Voynow, J. A. (2006). Respiratory tract mucin genes and mucin glycoproteins in health and disease. *Physiological reviews, 86*(1), 245-278.

Rousseau, K., Kirkham, S., Johnson, L., Fitzpatrick, B., Howard, M., Adams, E. J., Rogers, D. F., Knight, D., Clegg, P., & Thornton, D. J. (2008). Proteomic analysis of polymeric salivary mucins: no evidence for MUC19 in human saliva. *Biochemical Journal, 413*(3), 545-552.

Russo, C. L., Spurr-Michaud, S., Tisdale, A., Pudney, J., Anderson, D., & Gipson, I. K. (2006). Mucin gene expression in human male urogenital tract epithelia. *Human Reproduction, 21*(11), 2783-2793.

Sadler, J. E. (1998). Biochemistry and genetics of von Willebrand factor. *Annual review of biochemistry, 67*(1), 395-424.

Salvi, G., De Los Rios, P., & Vendruscolo, M. (2005). Effective interactions between chaotropic agents and proteins. *Proteins: Structure, Function, and Bioinformatics, 61*(3), 492-499.

Sandberg, T., Blom, H., & Caldwell, K. D. (2009). Potential use of mucins as biomaterial coatings. I. Fractionation, characterization, and model adsorption of bovine, porcine, and human mucins. *Journal of Biomedical Materials Research Part A, 91*(3), 762-772.

Sasaki, M., Nakanuma, Y., Ho, S. B., & Kim, Y. S. (1998). Cholangiocarcinomas arising in cirrhosis and combined hepatocellular-cholangiocellular carcinomas share apomucin profiles. *American journal of clinical pathology, 109*(3), 302-308.

Schömig, V. J., Käsdorf, B. T., Scholz, C., Bidmon, K., Lieleg, O., & Berensmeier, S. (2016). An optimized purification process for porcine gastric mucin with preservation of its native functional properties. *RSC Advances, 6*(50), 44932-44943.

Seong, J.-K., Koo, J. S., Lee, W. J., Kim, H.-N., Park, J.-Y., Song, K. S., Hong, J. H., & Yoon, J.-H. (2002). Upregulation of MUC8 and downregulation of MUC5AC by inflammatory mediators in human nasal polyps and cultured nasal epithelium. *Acta oto-laryngologica, 122*(4), 401-407.

Sharma, P., Dudus, L., Nielsen, P. A., Clausen, H., Yankaskas, J. R., Hollingsworth, M. A., & Engelhardt, J. F. (1998). MUC5B and MUC7 are differentially expressed in mucous and serous cells of submucosal glands in human bronchial airways. *American journal of respiratory cell and molecular biology, 19*(1), 30-37.

Sheehan, J. K., Brazeau, C., Kutay, S., Pigeon, H., Kirkham, S., Howard, M., & Thornton, D. J. (2000). Physical characterization of the MUC5AC mucin: a highly oligomeric glycoprotein whether isolated from cell culture or in vivo from respiratory mucous secretions. *Biochemical Journal, 347*(1), 37-44.

Sheehan, J. K., Howard, M., Richardson, P. S., Longwill, T., & Thornton, D. J. (1999). Physical characterization of a low-charge glycoform of the MUC5B mucin comprising the gel-phase of an asthmatic respiratory mucous plug. *Biochemical Journal, 338*(2), 507-513.

Sheehan, J. K., Kirkham, S., Howard, M., Woodman, P., Kutay, S., Brazeau, C., Buckley, J., & Thornton, D. J. (2004). Identification of Molecular Intermediates in the Assembly Pathway of the MUC5AC Mucin. *Journal of Biological Chemistry, 279*(15), 15698-15705. doi:10.1074/jbc.M313241200

Sheehan, J. K., Richardson, P. S., Fung, D., Howard, M., & Thornton, D. J. (1995). Analysis of respiratory mucus glycoproteins in asthma: a detailed study from a patient who died in status asthmaticus. *American journal of respiratory cell and molecular biology, 13*(6), 748-756.

Shen, H., Hu, Y., & Saltzman, W. (2006). DNA diffusion in mucus: effect of size, topology of DNAs, and transfection reagents. *Biophysical Journal, 91*(2), 639-644.

Shi, L. (2000). Biomimetic surfaces of biomaterials using mucin-type glycoproteins. *Trends in Glycoscience and Glycotechnology, 12*(66), 229-240.

Shi, L., Ardehali, R., Caldwell, K. D., & Valint, P. (2000a). Mucin coating on polymeric material surfaces to suppress bacterial adhesion. *Colloids and Surfaces B: Biointerfaces, 17*(4), 229-239.

Shi, L., & Caldwell, K. D. (2000b). Mucin adsorption to hydrophobic surfaces. *Journal of colloid and interface science, 224*(2), 372-381.

Shorgen, R., Gerken, T., & Jentoft, N. (1989). Role of glycosylation on the conformation and chain dimensions of O-linked glycoproteins: light-scattering studies of OSM. *Biochemistry, 28*, 5525-5536.

Siddiqui, J., Abe, M., Hayes, D., Shani, E., Yunis, E., & Kufe, D. (1988). Isolation and sequencing of a cDNA coding for the human DF3 breast carcinoma-associated antigen. *Proceedings of the National Academy of Sciences, 85*(7), 2320-2323.

Singh, A. P., Chaturvedi, P., & Batra, S. K. (2007). Emerging roles of MUC4 in cancer: a novel target for diagnosis and therapy. *Cancer Research, 67*(2), 433-436.

Śliwka, L., Wiktorska, K., Suchocki, P., Milczarek, M., Mielczarek, S., Lubelska, K., Cierpiał, T., Łyżwa, P., Kiełbasiński, P., Jaromin, A., Flis, A., & Chilmonczyk, Z. (2016). The Comparison of MTT and CVS Assays for the Assessment of Anticancer Agent Interactions. *PLoS One, 11*(5). doi:10.1371/journal.pone.0155772

Sousa-Pereira, P., Cova, M., Abrantes, J., Ferreira, R., Trindade, F., Barros, A., Gomes, P., Colaço, B., Amado, F., & Esteves, P. J. (2015). Cross-species comparison of mammalian saliva using an LC–MALDI based proteomic approach. *Proteomics, 15*(9), 1598-1607.

Spurr-Michaud, S., Argüeso, P., & Gipson, I. (2007). Assay of mucins in human tear fluid. *Experimental eye research, 84*(5), 939-950.

Stein, Z. A. (1990). HIV prevention: the need for methods women can use. *American Journal of Public Health, 80*(4), 460-462.

Stick, J., Robinson, N., & Krehbiel, J. (1981). Acid-base and electrolyte alterations associated with salivary loss in the pony. *American journal of veterinary research, 42*(5), 733-737.

Styczynski, A. R., Anwar, K. N., Sultana, H., Ghanem, A., Lurain, N., Chua, A., Ghassemi, M., & Novak, R. M. (2015). In vitro antiretroviral activity and in vivo toxicity of the potential topical microbicide copper phthalocyanine sulfate. *Virology journal, 12*(1), 132.

Suh, J., Dawson, M., & Hanes, J. (2005). Real-time multiple-particle tracking: applications to drug and gene delivery. *Advanced drug delivery reviews, 57*(1), 63-78.

Swallow, D., Gendler, S., Griffiths, B., Kearney, A., Povey, S., Sheer, D., Palmer, R., & Taylor-Papadimitriou, J. (1987a). The hypervariable gene locus PUM, which codes for the tumour associated epithelial mucins, is located on chromosome 1, within the region 1g21–24. *Annals of human genetics, 51*(4), 289-294.

Swallow, D. M., Gendler, S., Griffiths, B., Corney, G., Taylor-Papadimitriou, J., & Bramwell, M. E. (1987b). The human tumour-associated epithelial mucins are coded by an expressed hypervariable gene locus PUM. *nature, 328*(6125), 82-84.

Swartz, M. J., Batra, S. K., Varshney, G. C., Hollingsworth, M. A., Yeo, C. J., Cameron, J. L., Wilentz, R. E., Hruban, R. H., & Argani, P. (2002). MUC4 expression increases progressively in pancreatic intraepithelial neoplasia. *American journal of clinical pathology, 117*(5), 791-796.

Takeuchi, K., Yagawa, M., Ishinaga, H., Kishioka, C., Harada, T., & Majima, Y. (2003). Mucin gene expression in the effusions of otitis media with effusion. *International journal of pediatric otorhinolaryngology, 67*(1), 53-58.

Tao, J., Hu, Q., Yang, J., Li, R., Li, X., Lu, C., Chen, C., Wang, L., Shattock, R., & Ben, K. (2007). In vitro anti-HIV and-HSV activity and safety of sodium rutin sulfate as a microbicide candidate. *Antiviral research, 75*(3), 227-233.

Tashian, R. E. (1989). The carbonic anhydrases: widening perspectives on their evolution, expression and function. *Bioessays, 10*(6), 186-192.

Taylor-Papadimitriou, J., Burchell, J. M., Plunkett, T., Graham, R., Correa, I., Miles, D., & Smith, M. (2002). MUC1 and the immunobiology of cancer. *Journal of mammary gland biology and neoplasia, 7*(2), 209-221.

Taylor, B. S., Sobieszczyk, M. E., McCutchan, F. E., & Hammer, S. M. (2008). The challenge of HIV-1 subtype diversity. *N Engl J Med, 358*(15), 1590-1602. doi:10.1056/NEJMra0706737

Temann, U.-A., Prasad, B., Gallup, M. W., Basbaum, C., Ho, S. B., Flavell, R. A., & Rankin, J. A. (1997). A novel role for murine IL-4 in vivo: induction of MUC5AC gene expression and mucin hypersecretion. *American journal of respiratory cell and molecular biology, 16*(4), 471-478.

Terada, T., Ohta, T., Sasaki, M., Nakanuma, Y., & Kim, Y. S. (1996). Expression of MUC apomucins in normal pancreas and pancreatic tumours. *The Journal of pathology, 180*(2), 160-165.

Thornton, D., Davies, J., Kraayenbrink, M., Richardson, P., Sheehan, J., & Carlstedt, I. (1990). Mucus glycoproteins from 'normal'human tracheobronchial secretion. *Biochemical Journal, 265*(1), 179-186.

Thornton, D. J., Carlstedt, I., Howard, M., Devine, P. L., Price, M. R., & Sheehan, J. K. (1996). Respiratory mucins: identification of core proteins and glycoforms. *Biochemical Journal, 316*(3), 967-975.

Thornton, D. J., Howard, M., Khan, N., & Sheehan, J. K. (1997). Identification of Two Glycoforms of the MUC5B Mucin in Human Respiratory Mucus Evidence For a Cysteine-rich Sequence Repeated Within The Molecule. *Journal of Biological Chemistry, 272*(14), 9561-9566.

Thornton, D. J., Khan, N., Mehrotra, R., Howard, M., Sheehan, J. K., Veerman, E., & Packer, N. H. (1999). Salivary mucin MG1 is comprised almost entirely of different glycosylated forms of the MUC5B gene product. *Glycobiology, 9*(3), 293-302.

Thornton, D. J., Rousseau, K., & McGuckin, M. A. (2008). Structure and function of the polymeric mucins in airways mucus. *Annu Rev Physiol, 70*, 459-486. doi:10.1146/annurev.physiol.70.113006.100702

Thornton, D. J., & Sheehan, J. K. (2004). From mucins to mucus: toward a more coherent understanding of this essential barrier. *Proc Am Thorac Soc, 1*(1), 54-61. doi:10.1513/pats.2306016

Tian, P., Brandl, M., & Mandrell, R. (2005). Porcine gastric mucin binds to recombinant norovirus particles and competitively inhibits their binding to histo-blood group antigens and Caco-2 cells. *Letters in applied microbiology, 41*(4), 315-320.

Toribara, N., Roberton, A., Ho, S., Kuo, W., Gum, E., Hicks, J., Gum, J., Byrd, J., Siddiki, B., & Kim, Y. (1993). Human gastric mucin. Identification of a unique species by expression cloning. *Journal of Biological Chemistry, 268*(8), 5879-5885.

Toribara, N. W., Gum Jr, J. R., Culhane, P. J., Lagace, R. E., Hicks, J. W., Petersen, G. M., & Kim, Y. S. (1991). MUC-2 human small intestinal mucin gene structure. Repeated arrays and polymorphism. *Journal of Clinical Investigation, 88*(3), 1005.

Toribara, N. W., Ho, S. B., Gum, E., Gum, J. R., Lau, P., & Kim, Y. S. (1997). The carboxyl-terminal sequence of the human secretory mucin, MUC6 analysis of the primary amino acid sequence. *Journal of Biological Chemistry, 272*(26), 16398-16403.

Touloumi, G., Pantazis, N., Pillay, D., Paraskevis, D., Chaix, M.-L., Bucher, H. C., Kücherer, C., Zangerle, R., Kran, A.-M. B., & Porter, K. (2013). Impact of HIV-1 subtype on CD4 count at HIV seroconversion, rate of decline, and viral load set point in European seroconverter cohorts. *Clinical Infectious Diseases, 56*(6), 888-897.

Trevan, J. W. (1927). The error of determination of toxicity. *Proceedings of the Royal Society of London. Series B, Containing Papers of a Biological Character, 101*(712), 483-514.

Tsutsumida, H., Goto, M., Kitajima, S., Kubota, I., Hirotsu, Y., Wakimoto, J., Batra, S. K., Imai, K., & Yonezawa, S. (2007). MUC4 expression correlates with poor prognosis in small-sized lung adenocarcinoma. *Lung cancer, 55*(2), 195-203.

Turner, B., Bhaskar, K., Hadzopoulou-Cladaras, M., Specian, R., & LaMont, J. (1995). Isolation and characterization of cDNA clones encoding pig gastric mucin. *Biochemical Journal, 308*(1), 89-96.

Tytgat, K., Swallow, D., Van Klinken, B., Büller, H., Einerhand, A., & Dekker, J. (1995). Unpredictable behaviour of mucins in SDS/polyacrylamide-gel electrophoresis. *Biochemical Journal, 310*(Pt 3), 1053.

Tytgat, K. M., Büller, H. A., Opdam, F. J., Kim, Y. S., Einerhand, A. W., & Dekker, J. (1994). Biosynthesis of human colonic mucin: Muc2 is the prominent secretory mucin. *Gastroenterology, 107*(5), 1352-1363.

Tytgat, K. M., Opdam, F. J., Einerhand, A. W., Büller, H. A., & Dekker, J. (1996). MUC2 is the prominent colonic mucin expressed in ulcerative colitis. *Gut, 38*(4), 554-563.

Ullery, J. C., Livingston, N., & Abou-Shabanah, E. H. (1959). The Mucous Fern Phenomenon In The Cervical And Nasal Smears: A Review And Current Concept Of Arborization. *Obstetrical & gynecological survey*, *14*(1), 1-25.

UNAIDS. (2013). *Global Report 2012: UNAIDS Report on the Global AIDS Epidemic*. Retrieved from http://www.unaids.org/sites/default/files/media_asset/20121120_UNAIDS_Global_Report_2012_with_annexes_en_1.pdf

UNAIDS. (2014). *The Gap Report*. Retrieved from http://files.unaids.org/en/media/unaids/contentassets/documents/unaidspublication/2014/UNAIDS_Gap_report_en.pdf

UNAIDS. (2015). AIDS by the numbers. *World AIDS Day 2015.* Retrieved from http://www.unaids.org/sites/default/files/media_asset/AIDS_by_the_numbers_2015_en.pdf

Utsunomiya, T., Yonezawa, S., Sakamoto, H., Kitamura, H., Hokita, S., Aiko, T., Tanaka, S., Irimura, T., Kim, Y. S., & Sato, E. (1998). Expression of MUC1 and MUC2 mucins in gastric carcinomas: its relationship with the prognosis of the patients. *Clinical cancer research*, *4*(11), 2605-2614.

Van Klinken, B., Dekker, J., Buller, H., & Einerhand, A. (1995). Mucin gene structure and expression: protection vs. adhesion. *American Journal of Physiology-Gastrointestinal and Liver Physiology*, *269*(5), G613-G627.

Van Kooij, R., Kathmann, G. A., & Kramer, M. (1983). Secretory piece and plasma proteins in human cervical mucus during the cycle. *Journal of reproduction and fertility*, *68*(1), 63-68.

Vandenhaute, B., Buisine, M.-P., Debailleul, V., Clément, B., Moniaux, N., Dieu, M.-C., Degand, P., Porchet, N., & Aubert, J.-P. (1997). Mucin gene expression in biliary epithelial cells. *Journal of hepatology*, *27*(6), 1057-1066.

Varloud, M. (2006). Activité amylolytique des secretions salivaires. *Implication des Micro-Organismes de l'Estomac dans la Digestion de l'Amidon par le Cheval. Thesis presented to the National Agricultural Institute of Paris-Grignon*, 62-68.

Veerman, E. C., Van Den Keijbus, P., Nazmi, K., Vos, W., Van Der Wal, J., Bloemena, E., Bolscher, J., & Amerongen, A. N. (2003). Distinct localization of MUC5B glycoforms in the human salivary glands. *Glycobiology*, *13*(5), 363-366.

Venegas, M. F., Navas, E. L., Gaffney, R. A., Duncan, J. L., Anderson, B. E., & Schaeffer, A. J. (1995). Binding of type 1-piliated Escherichia coli to vaginal mucus. *Infection and immunity, 63*(2), 416-422.

Vinall, L. E., Pratt, W. S., & Swallow, D. M. (2000). Detection of mucin gene polymorphism. *Glycoprotein Methods and Protocols: The Mucins*, 337-350.

Voelker, R. (2006). Anti-HIV microbicide efforts press on. *JAMA, 296*(7), 753-755.

Walsh, M. D., Young, J. P., Leggett, B. A., Williams, S. H., Jass, J. R., & McGuckin, M. A. (2007). The MUC13 cell surface mucin is highly expressed by human colorectal carcinomas. *Human pathology, 38*(6), 883-892.

Whembolua, G.-L. S., Granger, D. A., Singer, S., Kivlighan, K. T., & Marguin, J. A. (2006). Bacteria in the oral mucosa and its effects on the measurement of cortisol, dehydroepiandrosterone, and testosterone in saliva. *Hormones and Behavior, 49*(4), 478-483.

Wickstrom, C., & Carlstedt, I. (2001). N-terminal cleavage of the salivary MUC5B mucin. Analogy with the Van Willebrand propolypeptide? *J Biol Chem, 276*(50), 47116-47121. doi:10.1074/jbc.M106593200

Williams, S. J., McGuckin, M. A., Gotley, D. C., Eyre, H. J., Sutherland, G. R., & Antalis, T. M. (1999a). Two novel mucin genes down-regulated in colorectal cancer identified by differential display. *Cancer Research, 59*(16), 4083-4089.

Williams, S. J., Munster, D. J., Quin, R. J., Gotley, D. C., & McGuckin, M. A. (1999b). The MUC3 gene encodes a transmembrane mucin and is alternatively spliced. *Biochemical and biophysical research communications, 261*(1), 83-89.

Williams, S. J., Wreschner, D. H., Tran, M., Eyre, H. J., Sutherland, G. R., & McGuckin, M. A. (2001). Muc13, a novel human cell surface mucin expressed by epithelial and hemopoietic cells. *Journal of Biological Chemistry, 276*(21), 18327-18336.

Wreschner, D. H., Hareuveni, M., Tsarfaty, I., Smorodinsky, N., Horev, J., Zaretsky, J., Kotkes, P., Weiss, M., Lathe, R., & Dion, A. (1990). Human epithelial tumor antigen cDNA sequences. *European journal of biochemistry, 189*(3), 463-473.

www.proteinatlas.org. Tissue expression of MUC16 - Summary - The Human Protein Atlas. Retrieved from http://www.proteinatlas.org/ENSG00000181143-MUC16/tissue#gene_information

Wykes, M., MacDonald, K., Tran, M., Quin, R., Xing, P., Gendler, S., Hart, D., & McGuckin, M. (2002). MUC1 epithelial mucin (CD227) is expressed by activated dendritic cells. *Journal of leukocyte biology, 72*(4), 692-701.

Ye, S. B., Choi, Y. S., Choi, Y. H., Bae, C. H., Kim, Y. W., Park, S. Y., Song, S. Y., & Kim, Y. D. (2016). Effect of High Glucose on MUC5B Expression in Human Airway Epithelial Cells. *Clin Exp Otorhinolaryngol*. doi:10.21053/ceo.2016.00045

Yin, B. W., & Lloyd, K. O. (2001). Molecular cloning of the CA125 ovarian cancer antigen identification as a new mucin, MUC16. *Journal of Biological Chemistry, 276*(29), 27371-27375.

Yolken, R., Peterson, J., Vonderfecht, S., Fouts, E., Midthun, K., & Newburg, D. (1992). Human milk mucin inhibits rotavirus replication and prevents experimental gastroenteritis. *Journal of Clinical Investigation, 90*(5), 1984.

Yu, D., Chen, Y., Han, J., Zhang, H., Chen, X., Zou, W., Liang, L., Xu, C., & Liu, Z. (2008). MUC19 expression in human ocular surface and lacrimal gland and its alteration in Sjögren syndrome patients. *Experimental eye research, 86*(2), 403-411.

Yu, Y.-B., Miyashiro, H., Nakamura, N., Hattori, M., & Park, J. C. (2007). Effects of triterpenoids and flavonoids isolated from Alnus firma on HIV-1 viral enzymes. *Archives of pharmacal research, 30*(7), 820-826.

Zaretsky, J. Z., & Wreschner, D. H. (2013). *Gel-Forming and Soluble Mucins*.

Zhang, S., Zhang, H. S., Reuter, V. E., Slovin, S. F., Scher, H. I., & Livingston, P. O. (1998). Expression of potential target antigens for immunotherapy on primary and metastatic prostate cancers. *Clinical Cancer Research, 4*(2), 295-302.

Zhang, Z.-Q., Schuler, T., Zupancic, M., Wietgrefe, S., Staskus, K., Reimann, K., Reinhart, T., Rogan, M., Cavert, W., & Miller, C. (1999). Sexual transmission and propagation of SIV and HIV in resting and activated CD4+ T cells. *Science, 286*(5443), 1353-1357.

Zotter, S., Lossnitzer, A., Hageman, P. C., Delemarre, J., Hilkens, J., & Hilgers, J. (1987). Immunohistochemical localization of the epithelial marker MAM-6 in invasive malignancies and highly dysplastic adenomas of the large intestine. *Laboratory investigation; a journal of technical methods and pathology, 57*(2), 193-199.